ATTACHMENT H

Kevin Weight

From: marilyn milum <marilynmilum@yahoo.com>
Sent: Wednesday, December 6, 2023 7:03 AM
To: Kevin Weight; Helana Ruter
Subject: Fw: 333 N 7th Ave.

Hi Kevin,
The letter below is from one of our brokers we have been using for the last few years representing the property at 333 N 7th Ave.
Please include this for our file concerning the hardship meeting. Thank you.
Sincerely,
Marilyn Milum

Sent from Yahoo Mail for iPhone [mail.onelink.me]

Begin forwarded message:

On Tuesday, December 5, 2023, 1:25 PM, Justin Horwitz <justin.horwitz@svn.com> wrote:

Craig/Marilyn,
Please let this email serve as my insight on the value of the property and particularly how the value has been impacted by the existing structures over the course of 3+ years of attempting to sell your property. Generally speaking, the majority of developers that are willing to pay market pricing for development property are not structured for nor interested in pursuing sites that require historic preservation as part of a planned development. We are finding that most of the development community is interested solely in the land so that they can more freely plan a development with a clearer path to entitlements. We are currently asking $9.2mm for the 2.39 AC site. That is ±$88 PSF on land value which I believe is right in line with the market and I do believe the site would have sold long ago if it weren't for the complexities created by the push for historic preservation. It's hard to specifically gauge how much loss in value will occur if a developer is to incorporate these structures, but at this moment and certainly for the foreseeable future, we are finding that there is not any interested parties at any price.

Justin Horwitz, SIOR | Senior Advisor
SVN Desert Commercial Advisors | AZ O/I CRE Sales Team
5343 N. 16th St., Suite 100 | Phoenix, AZ 85016
Phone 480.425.5518 | Mobile 480.220.2674
justin.horwitz@svn.com | www.svndesertcommercial.com [svndesertcommercial.com]
AZ O/I LinkedIn [linkedin.com]

Kevin Weight

From: marilyn milum <marilynmilum@yahoo.com>
Sent: Thursday, December 7, 2023 10:30 AM
To: Kevin Weight; Helana Ruter
Subject: Another break-in

The police were there again this morning.
Homeless people sleeping in the building.
More wasted resources of Phoenix PD
The police have to clear the property each time and make sure no one is inside, that is a big job. And a dangerous job.
Swat units, canine units and the use of many officers was not meant to be used in this way.
Marilyn

Sent from Yahoo Mail for iPhone [mail.onelink.me]

Kevin Weight

From: marilyn milum <marilynmilum@yahoo.com>
Sent: Wednesday, December 6, 2023 11:14 PM
To: Kevin Weight; Helana Ruter
Subject: Fw: 333 N 7th Ave.

Hi Kevin,
Please add this letter of opinion from one of the primary brokers who has had it listed since 2019.
Than you,
Marilyn Milum

Sent from Yahoo Mail for iPhone [mail.onelink.me]

Begin forwarded message:

On Wednesday, December 6, 2023, 9:35 PM, Paul Borgesen <paul.borgesen@transwestern.com> wrote:

Marilyn,

It is my opinion that potential HP restrictions have kept multiple groups from making an offer on the property as it is not financially feasible to bring the current structure up to code as well as incorporate it into a new development. Most developers are not willing to take on the city or HP try and deal with this potential hurdle. Most groups hear that there may be an interest in the property from HP and that is the end of the conversation about the project. The property is zoned to allow apartments and is surrounded by new apartment development and this in my opinion would be the highest and best use for the land this would also bring you as the seller the highest value.

Paul Borgesen, SIOR
Senior Vice President

Capital Markets | Investment Sales

TRANSWESTERN
2501 E. Camelback Rd, Suite 1

Phoenix, Arizona 85016

Direct: 602.296.6377

Cell: 602.214.9033

transwestern.com [transwestern.com]

From: marilyn milum <marilynmilum@yahoo.com>
Sent: Tuesday, December 5, 2023 1:44 PM
To: Paul Borgesen <paul.borgesen@transwestern.com>
Subject: Fw: 333 N 7th Ave.

Hi Paul ,

Please write us a similar letter and also state we missed that window of opportunities where Justin also told me earlier there may have well been multiple bidders , bidding war if HP buildings did not need to stay and interests rates and building rates were lower , etc

Thank you 🙏

P S this is being used in our hardship hearing and they wanted a statement of this sort for

An argument in addition to what you had provided previously.

Sent from Yahoo Mail for iPhone [mail.onelink.me]

Begin forwarded message:

On Tuesday, December 5, 2023, 1:25 PM, Justin Horwitz <justin.horwitz@svn.com> wrote:

> Craig/Marilyn,
> Please let this email serve as my insight on the value of the property and particularly how the value has been impacted by the existing structures over the course of 3+ years of attempting to sell your property. Generally speaking, the majority of developers that are willing to pay market pricing for development property are not structured for nor interested in pursuing sites that require historic preservation as part of a planned development. We are finding that most of the development community is interested solely in the land so that they can more freely plan a development with a clearer path to entitlements. We are currently asking $9.2mm for the 2.39 AC site. That is ±$88 PSF on land value which I believe is right in line with the market and I do believe the site would have sold long ago if it weren't for the complexities created by the push for historic preservation. It's hard to specifically gauge how much loss in value will occur if a developer is to incorporate these structures, but at this moment and certainly for the foreseeable future, we are finding that there is not any interested parties at any price.
>
> **Justin Horwitz, SIOR** | Senior Advisor
> **SVN Desert Commercial Advisors | AZ O/I CRE Sales Team**

5343 N. 16th St., Suite 100 | Phoenix, AZ 85016
Phone 480.425.5518 | Mobile 480.220.2674
justin.horwitz@svn.com | www.svndesertcommercial.com [svndesertcommercial.com]
AZ O/I LinkedIn [linkedin.com]

Kevin Weight

From: marilyn milum <marilynmilum@yahoo.com>
Sent: Thursday, December 7, 2023 1:26 AM
To: Kevin Weight; Helana Ruter
Subject: 333 N 7th ave

Kevin,
You may wonder why two different brokers letters.
The two brokers have been working since 2019 on trying to sell our property on &th ave.
Justin is still at SVN and Paul has chosen to change companies but they are still co-listing since the two had it listed at the one compant when they were associates.
You are possibly wondering why I am up so late my husband just left to check on the property on 7th since we are have had tresspassers coming in at night sleepng, and making messes,very hazadous.
After multiple breakends we secured the building further and he needs to check if the barriers we used are working or weather they are down, meaning they got in again.
Marilyn

Kevin Weight

From: marilyn milum <marilynmilum@yahoo.com>
Sent: Thursday, December 7, 2023 9:08 PM
To: Kevin Weight; Helana Ruter; marilyn milum
Subject: Invoice for one year

Please note that this is just for one year in which we extended it it for as long as we were under contract with the developer which was in the purchase agreement.
We have a different carrier now and at this moment I cannot locate our invoice.

Kevin Weight

From: marilyn milum <marilynmilum@yahoo.com>
Sent: Thursday, December 7, 2023 9:15 PM
To: Kevin Weight; Helana Ruter
Subject: insurance and taxes

I have been trying to download our tax amounts we have paid for the last two years.
The site has been down.
It is public knowledge so I will say when I looked up a few days ago it was a little over $40,000.00 and has been that amout approx., for the last two years.

Burns & Wilcox

150 Burns & Wilcox Center
14631 N. Scottsdale Road
Scottsdale, AZ 85254

Insurance Quote

Date:	Monday, June 13, 2022
Agency:	NEATE DUPEY INSURANCE GROUP
Attn:	ANDY DUPEY
Insured:	MILUM TEXTILE SERVICES, INC
Application / Policy:	APP80562253

We are pleased to submit our **QUOTE** for the above captioned insured. Please review this **QUOTE** carefully as coverage offered may be **DIFFERENT** than the coverage requested.

Proposed Policy Period:	6/14/2022 - 6/14/2023
Insurance Carrier:	MT VERNON SPECIALTY INSURANCE COMPANY
Line of Business:	PACKAGE

Price Breakout:	
Premium:	$ 16,687.00
Carrier Policy Fee:	
Carrier Inspection Fee:	
Brokerage Fee:	$ 1,700.00
State Tax:	$ 551.61
Stamping Fee:	$ 36.77
Total Due:	**$ 18,975.38**

Agency Commission: 15.00%

Additional Subjectivities Required for Binding:

**FEES ARE FULLY EARNED

*BROKER FEE WILL BE ADDED TO ANY A/P ENDORSEMENT OR AUDIT

We appreciate the opportunity and look forward from hearing from you. Please call or e-mail us if you have any questions.

Melinda Lampson
Burns & Wilcox

Sent from Yahoo Mail for iPhone [mail.onelink.me]

Kevin Weight

From: marilyn milum <marilynmilum@yahoo.com>
Sent: Thursday, December 7, 2023 11:11 PM
To: Kevin Weight; Helana Ruter
Subject: comments about 333N 7th ave

To:marilyn milum
Thu, Dec 7 at 11:06 PM
Kevin,

Please include this in the files. Thank you.

In case you are wondering why there are two different companies with our brokers, Justin and Paul were associates at the same firm before Paul went to work for a different firm. Both of these gentlemen have worked very hard to represent us and are still working on the listing. They have reported to us during the last several years their obstacles in selling our property that have been mainly the "Historical Preservation" ("HP") problem we have with the City that prevents successful sales efforts. Non one wants to buy such a property, which has been confirmed repeatedly by our brokers' many sales contacts.

Both have told us repeatedly that buyers are not interested in dealing with HP. We have also have had extensive feedback that it would be cost prohibitive to even try to save these structures.

We can no longer maintain them. It has caused a huge burden financially on us not to mention what is has done to us mentally and physically and our quality of life. We are septuagenarians that want to retire and the property is our retirement fund. My husband is ill and this is not equitable for us to bear the burden and expense of this property. It has been debilitating. We can no longer deal with these costs after four years of determined sales efforts. To impose such a mandate on two individuals is criminal or at least unconstitutional. We feel like someone has stolen our property and we have to bear the burden of paying a ransom for it as well as in the interim maintaining the property for the thieves.

Property taxes, Insurance, utilities, and to maintain such as broken windows, kicked in doors, trash, feces, graffiti, and our precious time.

Prop 207 was a clear indication that the citizens in Arizona do not want this abuse by government officials.

I hate to be so blunt, but that is now how we are feeling . We have earnestly tried to work with the City, we are in the fifth year of this tyrany and we are tired of all the red tape and emotional, physical, financial abuse we have been dealt by the city and it is truly time for the City to release this terrible burden. We feel the City has gone too far.

We are asking for fairness and justice. We also think there are political schemes behind this to stop more contemporary development rather than just to save a "priceless" building. There is no significant historic value to preserve, it is simply a manipulation and political effort by primarily a very small number of people who want to limit the density.

We have been damaged. These are dilapidated buildings that have outlived their use.

We believe this mandate has enough severe impact to our rights that it warrants compensation. The whole idea of "historic" is so subjective. The City should bear the cost and pay for it if they want a museum.
Instead the City wants to give rich developers, taxpayers money at their whim and when the taxpayer will probably never see the inside of these buildings they want to keep. I s that fair and equitable?
The City is on record telling us over and over do not pursue a demo permit , it will be turned down and told us they would not let the buildings go.

These are decaying buildings that need to be torn down for useful housing.

Since it has gotten cold now, the homeless are trespassing causing the SWAT teams, the canine teams and multiple officers (a dozen or more, yesterday), more today. Every time a break in occurs, we call the police they have to search the property and clear it. What a horrible use of our police resources. This is inviting criminal activity downtown. These officers could lose their lives going into the dilapidated buildings to search nooks and corners, closets, all room by room. These intruders are scared inside the building and could react with violence towards our City's finest.

Our freedom has been taken from us.

All of this has occurred because a very small number of people have a whim for saving these junky, old buildings with no modern times commercial, viable use.

Please help resolve these serious matters in the near future well before October by when these issues would be five years with out resolution.

A solution will also help our efforts to sell the property which has been substantially slowed by other substantially more complex matters than HP considerations for a building that does not seem to meet any realistic HP concerns compared to other HP properties.

We have reviewed the check lists requested and feel like most of these requests i.e., getting itemized construction costs to restore the 100 year old property are burdensome and are not applicable to the site. We never plan on using the property for another commercial laundry and to get an itemized costs would be so expensive and unrealistic it assumed these request would be for much smaller projects. To do what you are requesting would be a hardship and speaking with a contractor undoable.

It would be 10's of thousands of dollars and a waste of the contractors time and ours.

The contractors would not take us seriously.

Thank you.

Sincerely,

Marilyn Milum

Kevin Weight

From: marilyn milum <marilynmilum@yahoo.com>
Sent: Friday, December 8, 2023 8:50 AM
To: Kevin Weight; Helana Ruter
Subject: Property Taxes, Utilities, maintanence , insurance

Good morning Kevin,

TO add to file please
WE have calclated between $ in excess of 100,000 a year saving the property for PHOENIX

Multiple insurance companies turned us down for insuranc

Insuring an empty building is risky and to keeping this place up is simply unsastainable for us

In the last couple of weeks we have turned off utilities

Aps we beleive has left one meter on by mistake.

We need to call them to turn off the last meter

METROWEST
DAILY NEWS

NEWS

Historic riding ring collapses in Ashland

Rob Haneisen/Daily News staff

Published 11:01 p.m. ET Jan. 29, 2011 | **Updated 1:50 a.m. ET Jan. 30, 2011**

A massive outdoor riding ring, one of only four of its kind in the country and a local historic landmark, collapsed yesterday afternoon after years of decay and weighed down by several feet of recent snow.

The building off Olive Street was brought to the site in 1975 by Bill Sibson, 59, who disassembled the 60- by 120-foot building at the old Waseeka Farm on Chestnut Street with the help of family and friends. In 1979, he put it back together at his mother's Gleanmoura Farm, which means Mary's Glen in Gaelic.

The building had rare German lamella roof architecture, which gave the appearance of criss-crossed arches 25 feet above the riding floor. That structure held the roof up without needing any poles or beams in the center of the floor, which made it a perfect riding ring for horse lessons.

The building was first constructed around 1920 as a birthday gift for a daughter in the Powers family at Waseeka Farm, Sibson said.

Elegant in appearance at the height of its use, what remained yesterday was a pancaked heap of timbers and boards.

"I was walking my dog, and I heard a loud crack, and I saw it collapse," said Rory Warren, who lives on Clinton Street in Hopkinton and was one of the people who helped Sibson assemble the ring decades ago. "It's in seven sections, and it just came down like dominoes."

Warren and Sibson said snow stacked on the roof was definitely the reason for yesterday's collapse around 2:15 p.m., although the structure was in rough shape and had already started to lean before this winter.

Ashland Fire Lt. David Iarussi said neighbors heard the collapse and called police and fire departments. No one was in or near the building when it fell, and a huge cloud of dust flew up.

"It's the loss of a historic structure," Iarussi said.

Warren recalled the intricacy of the diamond-patterned roof and the simplicity of its white pine-board design, which allowed for interchangeable parts.

"Now it's gone - just a pile of wood on the ground," Warren said.

When the family disassembled the old ring in 1975, every bolt, nut and shingle, plus the lamella planks, were stored in garages and barns - trucked over from Chestnut Street in the family station wagon - until they could be painstakingly put back together.

"We had to cat's-paw every nail out of it," Sibson said.

Sibson said he thinks the other three lamella buildings in the country were made into aircraft hangars.

"I knew that it was going to go ... but I didn't think it would crush so flat," Sibson said.

Sibson said he hopes the town will let him salvage some of the lamella boards this spring so he can one day build a small cabin with the historic pieces.

(Rob Haneisen can be reached at rhaneis@cnc.com or 508-626-3882.)

Kevin Weight

From: marilyn milum <marilynmilum@yahoo.com>
Sent: Thursday, December 21, 2023 12:30 AM
To: Helana Ruter; Kevin Weight
Subject: A little more complicated Lamella

https://www.google.com/gasearch?q=lamella%20roof%20collapses&tbm=&shem=rime&source=sh/x/gs/m2/5#fpstate=ive&vld=cid:2426b60c,vid:YsJqJKtrwlk,st:0 [google.com]

Sent from Yahoo Mail for iPhone [mail.onelink.me]

Kevin Weight

From: marilyn milum <marilynmilum@yahoo.com>
Sent: Thursday, December 21, 2023 12:40 AM
To: Helana Ruter; Kevin Weight
Subject: Complicated

Politically I'm not sure the Lamella enthusiast
Would be as supportive if they knew Zollinger was part of the Nazi party . Is the public going to be accepting of the Nazi link with the Nazi example of superior engineering…?
https://www.youtube.com/watch?v=YsJqJKtrwlk [youtube.com]

Sent from Yahoo Mail for iPhone [mail.onelink.me]

Kevin Weight

From: marilyn milum <marilynmilum@yahoo.com>
Sent: Thursday, December 28, 2023 3:48 PM
To: Helana Ruter; Kevin Weight
Subject: Roof collapse

Not sure if I sent this one

ancy, so likely not too critical unless a whole series of these are breaking.

Is this in snow country? Maybe some unbalanced load caused flex failures.

LaminatedTimber (Materials) 22 Nov 19 16:07

Wooden lamella roofs were known for not handling unbalanced roof loadings and there were many, many failures and collapses. Some lamella roofs are doing fine. I know of at least five in Wisconsin that have been performing fine for 80 or so years. A school gym was built in Fargo, ND in the 1960s with solid wooden lamella and it collapse within months of completion. The guy who sat at my desk before me bid it as a glued laminated timber radial rib dome and when told it would go to lamella he "warned" the general contractor about problems. Hate to say "I told you so" but that's what happened. Luckily there were no injuries in the collapse.

I cannot help with your design and repair method.

Lamella is a real groovy looking type of material. The historical and iconic Brown Derby in LA has a lamella roof.

Andreas

McSEpllc (Structural) 24 Dec 19 00:18

The lamella roof was developed and patented by Friedrich Zollinger after WWI as a way to address the housing shortage (it uses about 46% of the lumber compared to the previous wood construction techniques used in Germany.

Sent from Yahoo Mail for iPhone [mail.onelink.me]

Justin Horwitz - SVN
Paul Borgesen - Transwestern
5343 N. 16th St. #100
Phoenix, AZ 85016

Helena Ruter
City of Phoenix Historic Preservation Officer
200 W. Washington St.
Phoenix, AZ 85003

Dear Ms. Ruter,

On behalf of Paul Borgesen, Senior Vice President with Transwestern, and myself, Justin Horwitz, Senior Advisor with SVN, please accept this letter in relation to the Milum Textile property located at 333 N 7th Ave, Phoenix, AZ 85007.

Paul and I are commercial real estate agents with substantial experience selling development properties particularly in Downtown Phoenix. In April 2020, we began actively listing the subject property for sale and to this point, we have been unsuccessful in solidifying a buyer for the property. Throughout the course of our listing, the subject property has received good interest from prospective buyers. However, following initial conversation with various zoning attorneys, the overwhelming majority of prospective buyers do not pursue the purchase of the property due to concerns over multiple City of Phoenix interests in historical preservation of several major structures. This has presented a number of challenges, but a few of the main issues are as follows:

1. The process is relatively more complex. Incorporating historical structures on any site adds multiple layers of processes to the design, planning, and zoning stages that eliminates a number of quality developers. The majority of developers we have presented the site to ultimately are not equipped to handle an abnormal development process or do not have an interest in taking on the risk given the amount of unpredictable expenses in the pre-development and construction phases. Simply put, our experience has been that most developers want a “cookie cutter” site that allows them to repeat their typical planning, zoning, design, and construction processes. This site does not allow for that with historical structures in place.
2. Historical structures in their current location dramatically hinder design capabilities and limit a developers ability to maximize density in its planned development. This directly impacts the ultimate price they are willing to pay for the property.
3. Retaining the structures creates liability that adds significant costs to a project making it infeasible. The existing structures are quite old and have had years of industrial wear and tear placed on them. Again placing more unpredictability and liability into a project than any prospective buyer has been willing to take on.
4. Items 1-3 listed above are primarily addressing the items of contention solely from a redevelopment perspective. We have also spent countless hours over these last few years attempting to identify end users that have an interest in retaining and using the existing structures. While we have had groups acknowledge the unique elements of the structures and have a vision for an end use, the estimated costs of renovations steer groups away from pursuing a purchase of the property. To be more specific, we had a licensed general contractor walk the property and while we could not get a specific bid, we were provided with a rough estimate upwards of $10MM to simply bring the building up to code. This was purely contemplating the

costs to bring the building up to current code (i.e. remove and replace the existing complex utility system, replace the electrical system, treat any asbestos due to the age of the structure, sure up the roof system that requires significant inspection to even understand its current condition, redesign and replace the entire HVAC system, and address general ADA items just to name a few). Again, this is only to bring the building to code in a “vanilla shell” condition and does not include the cost to customize the interior layout for an end user.

The main purpose of this letter is to attempt to identify how much the property is worth as raw land with all structures demolished as opposed to its value with various structures historically preserved. This proves to be a rather difficult task. While we have contemplated comparable sales for land sites in the immediate area (please see Exhibit “A” - Comparable Sales enclosed), it’s virtually impossible to identify a value for the property with structures in place. As mentioned above, in over three years of tireless efforts to find a buyer, we have come up empty handed. One could argue that there is no buyer in the foreseeable future for this property at any price given the significant cost of improvements due to the issues listed above. Alternatively, as it pertains to the potential value of the land with all structures demolished, we have identified seven comparable sites based on location, land size, and/or intended use for the property. The sales comparables range from $111 PSF to $316 PSF on land value only. The average of the seven comparable sales is $201 PSF. Relative to the subject property, one could argue that without any historically preserved structures, the land’s value is upwards of $21MM for the 2.39 AC of land. Our current asking price for the property is $9.2MM with no qualified parties pursuing at this price. We do however have a number of groups that have indicated a high level of interest in the property if the owner of the property can deliver the property with either a demo permit for the entirety of the site or with all structures fully demolished.

In closing and as mentioned above, without any prospective buyers to currently reference, it is difficult for Paul or I to determine the value of the property with historically preserved structures in place. However, it is safe to assume that the loss in value to the property would be significant relative to the comparable sales in the area.

Please feel free to reach out should you have any questions.

Sincerely,

Justin Horwitz

Paul Borgesen

Exhibit "A" - Comparable Sales

Site	Land Size	Sale Price/ Land PSF	Sale Date	Notes
520 S. 5th St. Phoenix, AZ 85004	2.56 AC	$17,300,000 $155 PSF	12/8/23	Existing parking lots; Covered land purchase.
840 N. Central Ave. Phoenix, AZ 85004	1.11 AC	$10,500,000 $217 PSF	12/8/23	Part of assemblage.
343 E. Lincoln St. Phoenix, AZ 85004	1.00 AC	$8,643,000 $198 PSF	10/2/23	Future use for Phoenix Suns/Mercury.
114 E. Portland St. Phoenix, AZ 85004	0.64 AC	$8,820,000 $316 PSF	2/2023	Future development site.
510 E. Lincoln St. Phoenix, AZ 85004	1.60 AC	$9,500,000 $136 PSF	1/5/23	Future development site.
601 N. Central Ave. Phoenix, AZ 85004	1.83 AC	$22,000,000 $275 PSF	3/2/22	Future development site.
362 N. 3rd Ave. Phoenix, AZ 85003	0.76 AC	$3,700,000 $111 PSF	12/29/21	Future development site
AVERAGES		**$201 PSF**		

From: marilyn milum <marilynmilum@yahoo.com>
Sent: Monday, January 8, 2024 2:22 PM
To: Kevin Weight; Helana Ruter
Subject: Important information

Please add this to our HP file and please make available to HP commission and city council members.

We feel like the city of Phoenix has not done their due diligence in insisting on keeping structures when they know virtually nothing about their safety.

This is very risky.
Sincerely,
Marilyn Milum

Sent from Yahoo Mail for iPhone [mail.onelink.me]

Kevin Weight

From: marilyn milum <marilynmilum@yahoo.com>
Sent: Monday, January 8, 2024 2:17 PM
To: Kevin Weight; Helana Ruter; Roger Strassburg
Subject: Sensitivity analysis of Kiewitt-Lamella reticulated domes due to member loss - ScienceDirect

https://urldefense.com/v3/__https://www.sciencedirect.com/science/article/abs/pii/S0143974X21004983__;!!LkjWUF49MRd51_ry!YS_y5Q2hnymJZQY8-OEQ-SbJIQ36tP5gb5x5whpMIF5Upyv_9NY1x9eMw_Z-NMfaAnWPo1FVyLmapJpS4ssrj66u9Lqs-Q$

Sent from my iPhone

ScienceDirect

Journal of Constructional Steel Research
Volume 188, January 2022, 107016

Sensitivity analysis of Kiewitt-Lamella reticulated domes due to member loss

Zubin Zhang, Ruiyi Gu, Haiqin Wang

Show more

Share Cite

https://doi.org/10.1016/j.jcsr.2021.107016
Get rights and content

Abstract

In this paper, the sensitivity analysis of Kiewitt-Lamella (K-L) reticulated domes with different parameters is carried out. The sensitivity of the dome due to gradual and sudden member loss is analyzed in both static and dynamic aspects, which will clarify the distribution rule of the member sensitivity and provide a reference for future study on the K-L reticulated dome. The results show that the member sensitivity of the K-L reticulated dome with different design parameters has similar regularities. For the members in the same ring, the sensitivity of the latitudinal members is larger than that of the diagonal members. For the members in different rings, the sensitivity of the inner ring members is larger than that of the outer ring members. In addition, the static analysis shows that the latitudinal members closer to the radial members are more sensitive than those apart from the radial members, and the diagonal members paralleling to the radial members are more sensitive than the unparallel ones. The dynamic analysis shows that the K-L reticulated dome will experience a local internal force redistribution after a member's sudden loss and finally reach a stable equilibrium state on the new load transfer path without overall progressive collapse. According to the research results, a better scheme for strengthening the structure is proposed: increasing the cross-section of sensitive members is more effective in improving the structural stability than important components.

Introduction

The single-layer reticulated dome is usually used as the supporting structure for the roof of large cylindrical storage tanks in the petrochemical industry. With the development of the storage tank roof to a large span, the single-form reticulated dome used in realistic projects has been restricted. For example, a great many members of the Lamella reticulated dome are gathered at the apex, and the structure of the node is complicated, so some members must be properly removed, which changes the force transfer path and then adversely affects the overall structural strength. In addition, for the Kiewitt reticulated dome, the number of nodes in the outermost ring increases as the span increases, and the difficulty of construction also increases. Combining these two types of reticulated domes to form a Kiewitt-

Lamella (K-L for short) composite single-layer reticulated dome can effectively solve the above-mentioned problem for the large-span single reticulated dome [1,2].

At present, scholars worldwide have conducted many kinds of research on Kiewitt reticulated domes and Lamella reticulated domes, and there are also many studies on structure sensitivity. Gao *et al.* [3] discussed the problems of redundancy related to the Alternate path method, and the sensitivity of the Kiewitt single-layer reticulated dome was explored. Han *et al.* [4] evaluated the redundancy and progressive collapse performance of the large-span Lamella single-layer and double-layer domes based on the ultimate bearing capacities in both the original and damaged status. Sebastian [5] and Chen *et al.* [6] proposed the sensitivity index based on the internal force responses of members to identify sensitive members, which plays an important role in evaluating structural safety and reliability. However, the research on K-L reticulated domes needs to be strengthened, especially the sensitivity analysis of them. It plays an important role in determining the context of the system, optimizing algorithms, reliability evaluation of system performance, and structural redundancy research [7,8]. In fact, sensitivity analysis is a major prerequisite in the establishment of structural optimization, reliability evaluation, and parameter identification [9]. However, there are many members in single-layer reticulated shells, and the effects of different members on the elastoplastic stability of the structure are often different, and it has been proven that the failure of some critical members may lead to the progressive collapse of the space structure [[10], [11], [12]]. Therefore, the elastoplastic stability of the K-L reticulated dome on the member sensitivity is worth studying.

In realistic construction, collapse accidents of space structures have occurred around the world. For example, in 2004, due to the perforation of the ceiling in the terminal of the Charles de Lego Airport, the critical metal connecting members could not continue to bear the weight, and eventually collapsed. In 2014, South Korea continued to snow for many days, and the final snow load reached 0.9kN/m^2, which far exceeded the design load value. A space structure that does not consider this effect may collapse suddenly due to partial damage caused by the failure of a member without significant deformation in advance. If a member loses stability, it will inevitably affect other members connected to it. Therefore, the stability of a specific member cannot be analyzed in isolation, and the interaction of other members should be comprehensively considered and determined from the overall structural analysis [13]. Pandey et al. [8] proposed a redundancy assessment method based on sensitivity analysis. In this method, the response of the structure under design load is used as the research object, the member loss is used as the analysis parameter, and the member sensitivity and the structural redundancy are quantified theoretically with a numerical method. Subsequently, on this basis, the Japanese Society of Steel Construction considered the buckling of a single member, and made this redundancy assessment method further suitable for large-span space structures [14]. In recent years, Shekasheband et al. [15] divided the member loss into gradual and sudden loss, and carried out a numerical investigation into the static and dynamic response of tensegrity systems in the event of gradual and sudden member loss.

Therefore, in this paper, the sensitivity analysis of large-span reticulated dome due to member loss refers to the above method. One member is removed each time, and the static and dynamic response of the domes in the event of gradual or sudden member loss is investigated. The response and characteristics of the studied structures include the load-deflection response in static analysis and displacement-time history of the structures in the dynamic analyses. In addition, an effective measure for improving structural stability is discussed, which will provide a reference scheme for the designers.

Section snippets

Analysis model

Take one of the K-L reticulated domes as an example to illustrate the analysis model. As shown in Fig. 1(a), the span is 60m, the rise-to-span ratio is 1/4, the symmetrical sectors are 8, and the frequencies are 12 (Kiewitt: Lamella is 9:3).

For rings from the inside to the outside, they are marked as the first to the twelfth ring. Since the members are directly in contact with the top skin and need to bear the bending moment, it is appropriate to use I-beams but not steel circular pipes [16]. …

Sensitivity analyses of the K-L reticulated dome due to gradual member loss

A unique K-L reticulated dome can be determined when the span, the rise-to-span ratio, the number of rings, the symmetrical sectors, and the frequency ratio are determined. Currently, most of the large-span K-L reticulated domes are 12 rings. Therefore, the sensitivity analysis of the K-L reticulated dome with 12 rings is carried out, and both geometric and material nonlinearities analyses are performed to obtain the ultimate bearing capacity. Considering the influence of latitudinal members…

Sensitivity analyses of the K-L reticulated dome due to sudden member loss

The previous part discussed the static load-bearing capacity of the dome in the event of gradual member loss. Practically, when losing a member in the structure which is under load, energy stored in this member is released, and this induces a state of transient vibration in the structure. In order to compare the response of the damaged dome caused by the sudden member loss, this section introduces the results of the dynamic analysis. The K-L reticulated dome, which with 60m spans, 1/4…

Distribution and influence of sensitive members and important members

According to the previous analysis, the sensitivity of the members in different areas is different. In this paper, the sensitive member is defined as the member with a sensitivity larger than 5%, and the important member is defined as the member with a negative sensitivity. The important member loss can contain or block continuous structural damage. The sensitive members and the important members are shown in red and blue, respectively, as shown in Fig. 18.

It verifies that the sensitive members …

Conclusion and discussion

In this paper, a numerical investigation into the static and dynamic response of the K-L reticulated domes in the event of gradual and sudden member loss is carried out. The results of this study are used to obtain certain conclusions regarding the sensitivity of the K-L reticulated domes to member loss. In addition, the distribution of sensitive members and important members is distinguished, and a more economical structural reinforcement scheme is proposed and verified according to this rule, …

Funding

This research did not receive any specific grant from funding agencies in the public, commercial, or not-for-profit sectors.…

Declaration of Competing Interest

The authors declare that they have no known competing financial interests or personal relationships that could have appeared to influence the work reported in this paper.…

Recommended articles

References (22)

Y. Chen *et al.*
Effective insights into the geometric stability of symmetric skeletal structures under symmetric variations
Int. J. Solids Struct. (2015)

F. Piroglu *et al.*
Partial collapses experienced for a steel space truss roof structure induced by ice ponds
Eng. Fail. Anal. (2016)

B. Shekastehband *et al.*
Sensitivity analysis of tensegrity systems due to member loss
J. Constr. Steel Res. (2011)

W. Li *et al.*
Static stability analysis of a reticulated shell with a roofing system
Eng. Struct. (2019)

L.M. Tian *et al.*
Progressive collapse resistance of single-layer latticed domes subjected to non-uniform snow loads
J. Constr. Steel Res. (2021)

C.L. Zhang *et al.*
Effect of unsymmetrical loading distribution to the stability of single-layer latticed domes
J. Chongqing Jianzhu Univ. (2014)

D.C. Li
Static Stability and Local Failure Sensitivity Analysis of Kiewitt-Lamella Single Layer Reticulated Shells
(2019)

J. Cai *et al.*
Static stability analysis of Kiewitt-Lamella single-layer reticulated shells

F. Gao *et al.*
Sensitivity analysis on load carrying capacity of K6 single-layer reticulated domes to member failure
Architect. Struct. Design (2009)

Q.H. Han *et al.*
Progressive collapse analysis of large-span reticulated domes
Int. J. Steel. Struct. (2014)

View more references

Cited by (2)

Sensitivity of post-buckling behaviour of single layer reticulated shells to loading and member imperfections ↗

2022, Structural Stability Research Council Conference 2022, Held in conjunction with NASCC: The Steel Conference

Application of Sensitivity Analysis to Progressive Collapse Resistance of Planar Truss Structures ↗

2022, Applied Sciences (Switzerland)

View full text

Fire Prevention & Protection

Reading A Building: More Roof Size-Up

When reading a building, do you include the roof in your size-up, and if so, what are you thinking about? To assist with this question, let's consider some important factors that are worthy of your consideration.

10.4.2004

By John W. Mittendorf

When reading a building, do you include the roof in your size-up, and if so, what are you thinking about? To assist with this question, let's consider some important factors that are worthy of your consideration. Obviously, some factors will be dependent on the type of roof construction in your particular area, however, West Coast roofs and East Coast roofs have a lot in common in both construction methods and styles.

Open Web Bar Joist

Open web bar joist (or metal deck) roofs are the commercial roof of choice in the Midwest and Eastern portions of the country and are primarily steel truss construction underneath a metal decking (Q decking). The metal decking is covered by built-up layers of insulation material, tar, and composition. As steel loses it's strength around 1,000 degrees, such roofs have a quick failure rate with minimal warning, and suppression personnel should be aware of these hazards. However, another more subtle hazard is that fire can propagate between the metal base and the composition covering, enhancing the spread of fire with minimal visible warning signs.

Older Truss Roofs

These roofs are found anywhere in the country and on various types and sizes of commercial buildings primarily constructed during the 1800s until the 1950s – until the introduction of the flat roof with its numerous variations. The older truss roofs were normally constructed with a "large" size of wooden truss members, 1 x 6-inch sheathing as a roof base/covering, and can be found in numerous styles as follows:

Bridge Truss: This type is recognizable by it's characteristic sloping sides, ends, and flat top.

Gable Truss: This type is also identified by it's gable or peaked roof design.
Parallel Chord Truss: This roof looks similar to other types of flat roofs but can be found on older buildings and is constructed from a "large" size of truss members (compared to newer lightweight truss members).

Lamella: Although this roof can be similar in external appearance to other types of arch roofs, it is significantly different as it was constructed in an egg crate – geometric or diamond-patterned – design. This roof can be found on gymnasiums, recreational buildings, large supermarkets, etc.

Tied Truss: This arched roof uses metal tie rods to give lateral support to the walls of the building. Tie rods with turnbuckles are used below each arch member (as there is no bottom chord) to ensure that the arches do not push the exterior walls outward. With this mind, it is easy to see if fire exposes metal tie rods in this type of roof, a collapse of the building is more than a possibility. Hint: If you are ever inside a building and observe this type of roof construction, make a mental note for future reference as it may save your life!

Bowstring Truss: Most firefighters are familiar with the "bowstring truss" roof as numerous fire service writers have appropriately written on the hazards of this common roof. Interestingly, whether you are a firefighter on the East or West coast (or anywhere in between), you will likely have this roof in your municipality. It is constructed of "large-size" wooden members (Note: most wooden members used in these older truss roofs were "rough-cut" or full size lumber and used steel plates and bolts for connectors) with 1 x 6-inch sheathing roof decking. Multiple firefighter deaths attributed to this specific roof have cautioned firefighters to assume a defensive position if a working fire is encountered.

John W. Mittendorf joined the Los Angeles City (CA) Fire Department (LAFD) in 1963, rising to the rank of captain II, task force commander. In 1981, he was promoted to battalion chief and in the year following became the commander of the In-Service Training Section. In 1993, he retired from LAFD after 30 years of service. Mittendorf has been a member of the National Fire Protection Research Foundation on Engineered Lightweight Construction Technical Advisory Committee. He has provided training programs for the National Fire

Academy in Emmitsburg, Maryland; the University of California at Los Angeles; and the British Fire Academy at Morton-in-Marsh, England. He is a member of the editorial advisory board of Fire Engineering *and author of the books* Truck Company Operations *(Fire Engineering, 1998) and* Facing the Promotional Interview *(Fire Engineering, 2003).*

Share

Tags **Building Construction** **John Mittendorf** **Migration**

RELATED POSTS

Podcast: Back Step Boys: Joe Jardin and Frank Leeb

Sprinkler System Failure Floods Elevator at WA Senior Housing Complex

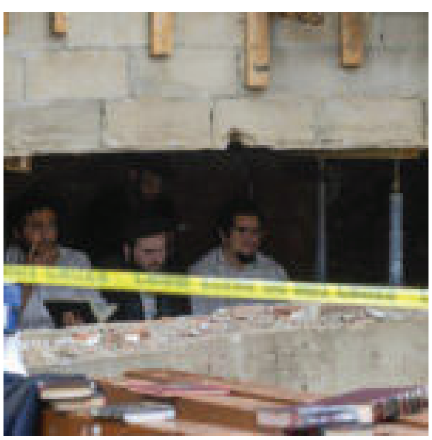

NYC Officials: Illegal Tunnel Under Synagogue Destabilized Nearby Buildings

From: marilyn milum
To: Helana Ruter
Subject: Failures of Lamella
Date: Thursday, January 25, 2024 11:15:43 AM
Attachments: image.png

A lot of the integrity is no longer there, not up to US safety standards.

11:13

roofs [1]. In 1925, the idea spread to America as well [3].

1.2 Previous Roof Failures

Due to the curve of the lamella roof, these structures are susceptible to failure from high wind loads. In 1926, hurricane winds caused the destruction of two lamella buildings in

Florida with one roof being torn off completely and deposited upside-down a few hundred feet away [1, 7].

Lamella roof construction was principally in use from its introduction by Zollinger up until the 1940s, with construction mostly halted because of wind failures. Engineers at the time used a wind load of 10 psf on the vertical projection for normal wind areas and 37.5 psf for high-wind regions. The latter wind pressure correlated with a 130 mph wind speed, the highest measured in that era [1].

In modern times, the wind loads on a curved roof are better known thanks to modern wind tunnel testing and computer simulations. It is now known that wind flowing over a curved roof creates uplift (similar to an aircraft wing), not simply a uniform horizontal curved roof creates uplift (similar to an aircraft wing), not simply a uniform horizontal load on the vertical projection. This creates a very different loading condition than the horizontal load which could potentially explain the failures of some lamella roofs in the first half of the 1900s.

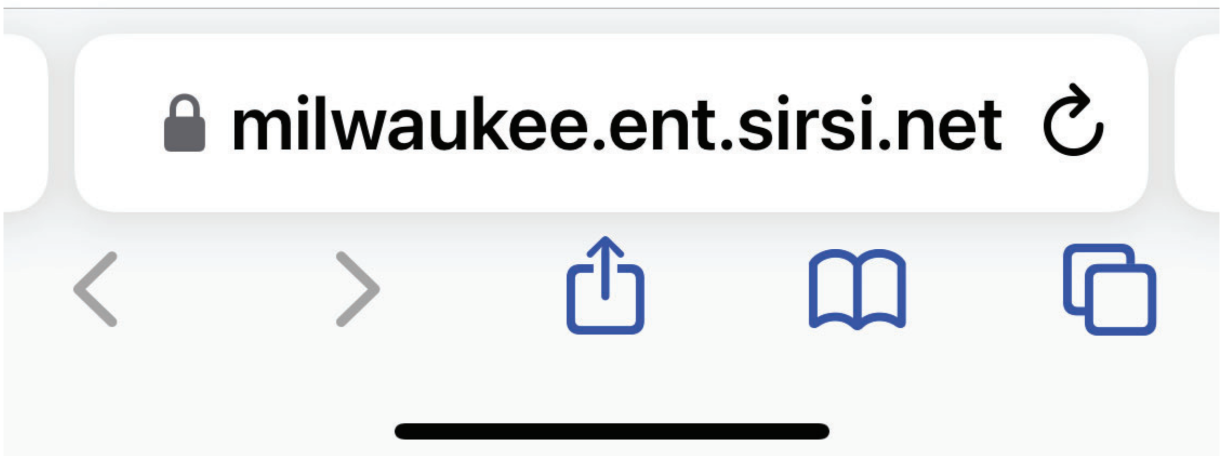

[Sent from Yahoo Mail for iPhone [mail.onelink.me]]()


11:57
Fwd: Photos 5
AA
Thank you.
Got it.
Cool.
Delete
Archive
Move
Reply
More

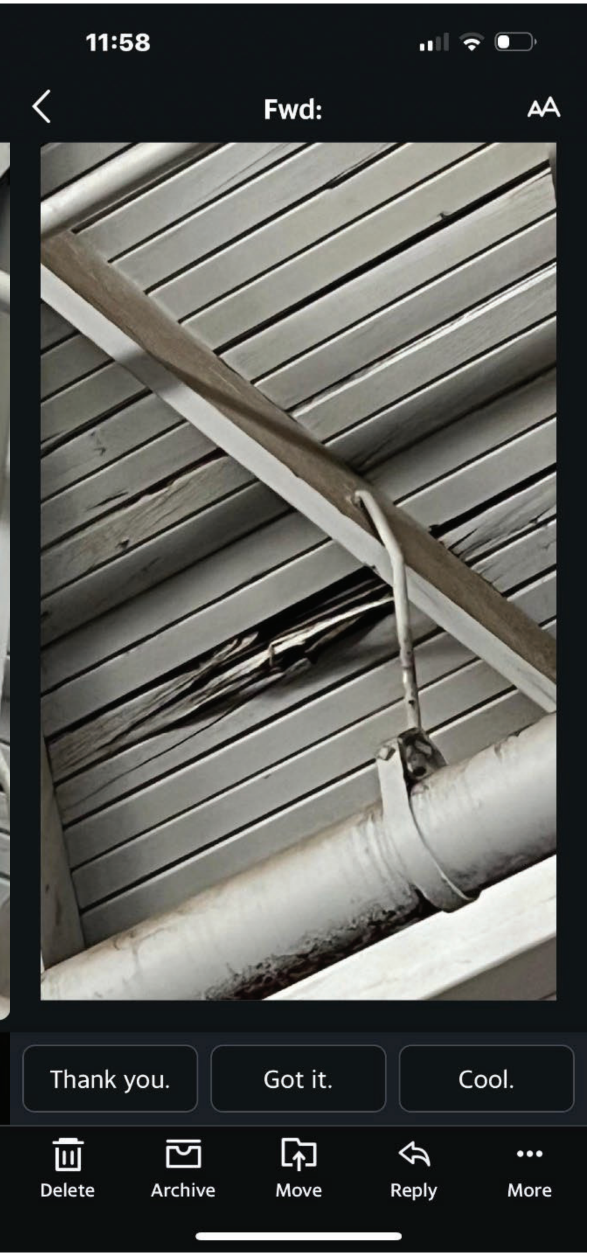
11:58
Fwd:
AA
Thank you.
Got it.
Cool.
Delete
Archive
Move
Reply
More

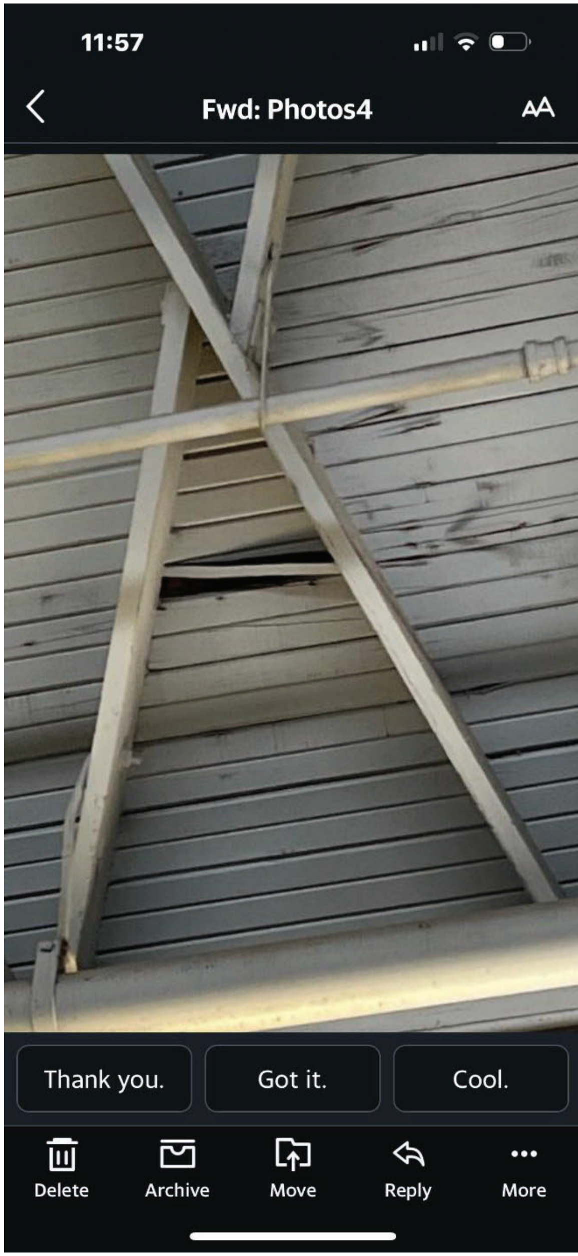
11:57
Fwd: Photos4
AA
Thank you.
Got it.
Cool.
Delete
Archive
Move
Reply
More


11:58
Fwd: Photos 5
AA
Today at 5:51PM
Thank you.
Got it.
Cool.
Delete
Archive
Move
Reply
More

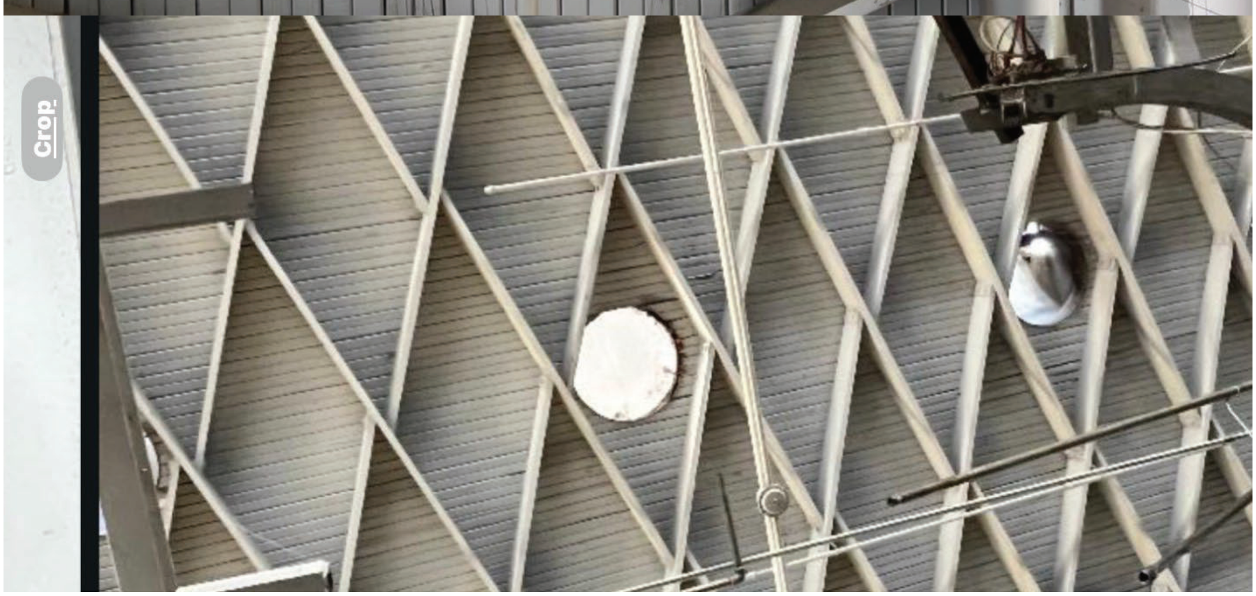
Crop

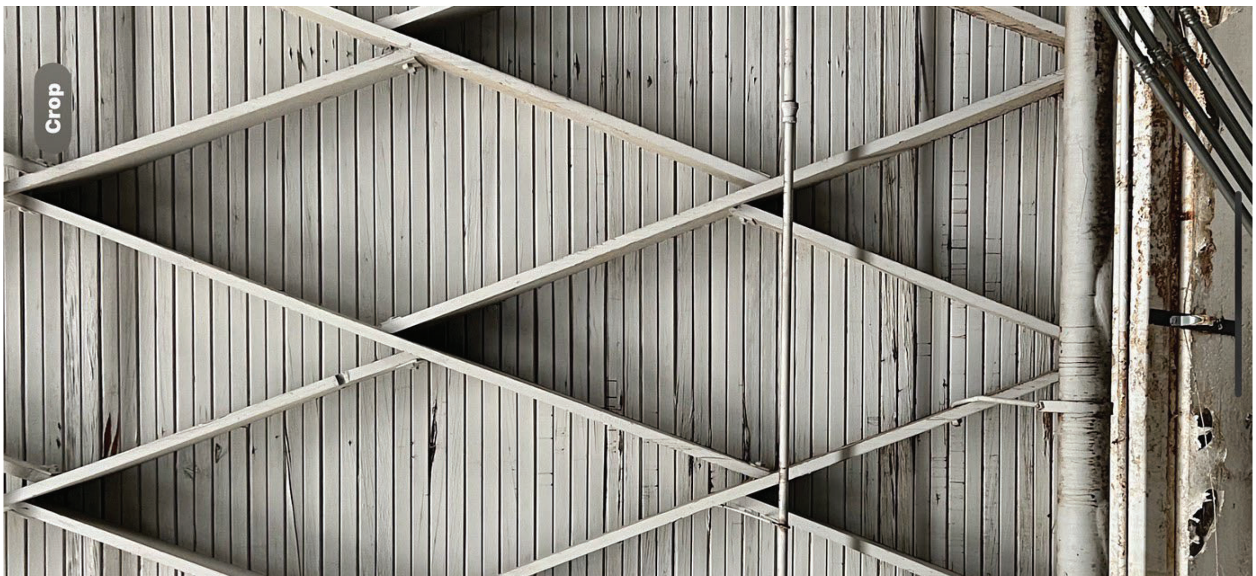
Crop

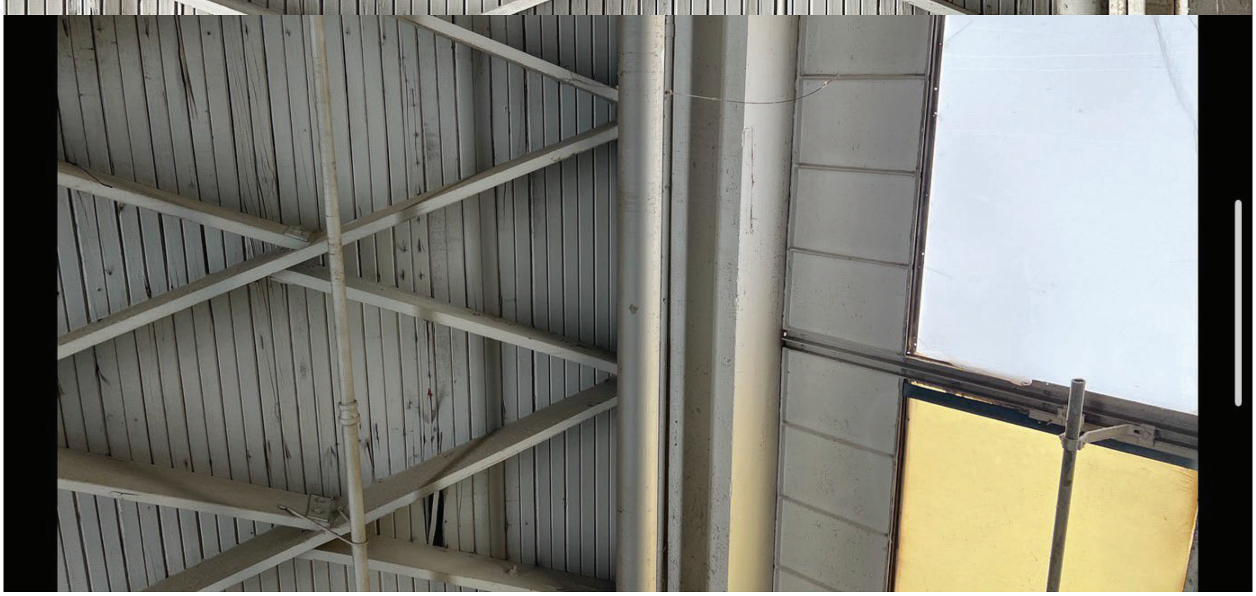


Crop


Crop


Crop


Crop

ScienceDirect

Engineering Structures
Volume 188, 1 June 2019, Pages 111-120

Identification of critical members for progressive collapse analysis of single-layer latticed domes

Shen Yan [a] [b], Xianzhong Zhao [b], Kim J.R. Rasmussen [a], Hao Zhang [a]

Show more

Share Cite

https://doi.org/10.1016/j.engstruct.2019.03.027
Get rights and content

Highlights

- Distribution of critical member in different single-layer dome types is investigated.
- Method is proposed to identify critical members based on collapse mechanism of domes.
- Proposed identification method performs excellent compared to the other two methods.
- Methods are proposed to increase progressive collapse resistance of single-layer dome.

Abstract

This paper presents a method to identify the critical member in a single-layer latticed dome, which in the context of progressive collapse is defined as the member whose removal causes the most severe damage. The distribution of critical members in four typical types of single-layer latticed domes, including the Kiewit dome, the Ribbed dome, the Schwedler dome and the Lamella dome, is investigated through a comprehensive Alternate Path analysis scheme composed of hundreds of individual dynamic nonlinear analyses. The Alternate Path analyses also confirm the progressive collapse mechanism of single-layer latticed domes, i.e., the nodal snap-through buckling at either end of the initially removed member. On this basis, a critical member identification method is established, using an index that implicitly estimates the relative vulnerability to node buckling following the removal of a member to determine the criticality of this member. This method along with two other methods, using either static axial force or free vibration response, are evaluated via comparison against the nonlinear dynamic Alternate Path analysis results, and this proposed method shows a beyond-compare accuracy. Furthermore, based on the established understanding of the progressive collapse mechanism and the factors influencing the node buckling resistance, three methods for increasing the progressive collapse resistance of single-layer latticed domes are presented.

Introduction

Structural domes have a long history in the built environment as an important design feature of many famous structures around the world. Since the days of Ancient Rome, permanent structures roofed with domes made from natural stones, bricks and concrete (found in ancient buildings in several countries) have been constructed [1], and continual improvements have been made in constructing and analysing these types of domes, even in the new millennium [2], [3], [4]. Starting from the last century, various forms of single-layer latticed domes built with steel become popular because they are capable of achieving larger span, and have been widely used for buildings with large-span roofing, such as sports stadiums and exhibition centres. For their efficient and safe design, extensive studies have been conducted to investigate the static and dynamic stability [5], [6], the earthquake resistance [7], [8] and the optimum topological design [9], [10] of dome structures. However, the progressive collapse of single-layer latticed domes remains an area in need of research. Since the collapse of the World Trade Centre towers in 2001, a substantial body of research has been carried out on the progressive collapse of frame structures [11], [12] and, more recently, certain types of roof structures, mainly truss-type roofs [13], [14], [15], [16], while research on single-layer latticed domes is very limited. Zhao et al. [17] conducted progressive collapse tests on two single-layer latticed Kiewitt domes, showing the collapse of a dome can be caused merely by the loss of a single critical member. This demonstrates a need for further investigation of current analysis and design methods for single-layer latticed domes.

The Alternate Path (AP) Method, in which a load-carrying element is removed to evaluate the structural capacity in resisting local damage, is arguably the most appropriate and widely accepted method for studying the structural progressive collapse performance. The previously mentioned tests by Zhao et al. [17] and the tests by Xu et al. [18] on two single-layer latticed domes, a Kiewit-Lamella dome and a geodesic dome, were carried out following the concept of the AP method. Han et al. [19] numerically employed the AP method to investigate the collapse resistance of a Schwedler Monoclinal dome subject to the loss of several members or nodes. When applying AP method to a structure constructed with many members, an important issue to be addressed is how to identify the critical members (sometimes referred to as the sensitive members), i.e., the members whose removal cause the most severe damage. Accurately identifying the critical members ensures the most dangerous collapse scenarios are taken into account, and also helps to reduce the computational cost. The current guidelines for progressive collapse design of frame structures [20], [21] stipulate that, critical members of a building include the columns at corners, as well as columns located at the middle of both the long side and the short side of the building.

However, thus far there is no such codified recommendation for single-layer latticed domes, and therefore an efficient method for identifying the critical members in single-layer latticed domes, the types of which are numerous and the geometry of which can be complicated, is of significant interest. Some researchers recommended FE-based methods [18], [19], [22], in which, to evaluate the criticality of a dome member, the structural response of the remaining structure following the removal of this member is obtained through static linear or nonlinear FE analysis, and is compared with that of the intact structure. Analysis is performed on each member in the dome, and the critical members are identified as those whose initial failure cause the most severe reduction of structural performance. Such methods are accurate in terms of finding the critical members, but cannot be considered as an efficient strategy for selection of removed member in the AP method because they are, in actuality, static AP method themselves. An attractive method for identifying the critical members should require no or just one simple analysis of the structure. Xu [23] studied several single-layer Kiewit domes, and suggested that the critical members were in lines with members having the most pronounced response, with respect to the fundamental vibration mode, in an eigenvalue vibration analysis of the intact dome. This selection criterion, although very simple, is not established on account of the failure mechanism under progressive collapse and thus, as will be shown later in this study, has a poor accuracy.

This paper presents a method to identify the most critical members in a single-layer latticed dome on the basis of the progressive collapse mechanism. In the tests by Zhao et al. [17], nodal snap-through buckling at either end of the initially removed member, referred to as "node buckling" in this present study, was regarded as the collapse mechanism for the tested Kiewit dome models. This conclusion is first examined for other types of single-layer latticed domes as well as Kiewit domes with different geometries through an extensive nonlinear dynamic AP analysis, which also extends the pool of the experimental results, providing an overview of the critical member distribution in different types of single-layer latticed domes. The critical member identification method is then proposed, using an index that implicitly estimates the relative vulnerability to node buckling following the removal of a member to determine the criticality of this member. This method along with two other methods, using either static axial force or free vibration response as identification index, are evaluated via comparison against the nonlinear dynamic AP analysis results. Furthermore, based on the established understanding of the progressive collapse mechanism and the factors influencing the node buckling resistance, several methods for increasing the progressive collapse resistance of single-layer latticed domes are suggested.

Section snippets

Prototype structure

In order to gain a comprehensive understanding of the distribution of the critical members, four single-layer latticed domes being the most common types, i.e., a Kiewit dome, a Ribbed dome, a Schwedler dome and a Lamella dome, are investigated by means of nonlinear dynamic AP analysis.

The Kiewit dome as shown in Fig. 1a has a constant span of 40 m, which is a moderate span for single-layer latticed domes. The rise-span ratio affects the stability characteristic of the dome and thus can have…

Criticality index based on node buckling

On the basis of the progressive collapse mechanism, a method for identifying the most critical members in a single-layer latticed dome is proposed in this section. Fig. 5 illustrates a schematic diagram of a node undergoing snap-through buckling. Subjected to a vertical point load, the end node of the removed member remains connected to the adjoining members. For an intact latticed dome, its in-plane and out-of-plane stiffness can be approximated by converting the latticed dome into an…

Application of criticality index in determining critical members

For the prototype Kiewit dome, the criticality indices of all members are determined using Eqs. (6), (7), (8), (9), (10). Table 1 shows the results. It is observed that among all 44 members, those ranking in the top 10% in terms of criticality index are all the most critical members determined by the nonlinear dynamic AP analysis, and those ranking in the top 20% almost cover all the members in the first two criticality grades. Therefore, the proposed criticality index shows an appreciable…

Methods for increasing the progressive collapse resistance of single-layer latticed domes

The progressive collapse resistance of a single-layer latticed dome is limited by the collapse load of the most critical members. Therefore, by reducing the criticality indices of these members, the progressive collapse resistance of the dome can be improved. This is achievable through the following methods.

The first is to enhance dome members. Once the most critical members are identified, a higher overall progressive collapse resistance of the dome can be achieved by enhancing these members…

Conclusion

This paper presents a method to identify the most critical members for progressive collapse analysis and design of single-layer latticed domes. A comprehensive finite-element Alternate Path analysis is performed on four typical types of single-layer latticed domes, i.e., the Kiewit dome, the Ribbed dome, the Schwedler dome and the Lamella dome, demonstrating that the nodal snap-through buckling at either end of the initially removed member is the major progressive collapse mechanism. On this…

Acknowledgement

The work presented in this paper was funded by the National Natural Science Foundation of China (Grands No. 51678432 and No. 51708417).…

Research data for this article

Data not available / Data will be made available on request

Further information on research data

References (23)

H.J. Cowan
A history of masonry and concrete domes in building construction
Build Environ (1977)

E. Hamed *et al.*
Time-dependent and thermal behaviour of spherical shallow concrete domes
Eng Struct (2009)

M. Brocato *et al.*
A new type of stone dome based on Abeille’s bond
Int J Solids Struct (2012)

A. López *et al.*
Direct evaluation of the buckling loads of semi-rigidly jointed single-layer latticed domes under symmetric loading
Eng Struct (2007)

F. Fan *et al.*
Elasto-plastic stability of single-layer reticulated shells

Thin Walled Struct (2010)

M.P. Saka
Optimum topological design of geometrically nonlinear single layer latticed domes using coupled genetic algorithm
Comput Struct (2007)

J.N. Richardson *et al.*
Coupled form-finding and grid optimization approach for single layer grid shells
Eng Struct (2013)

B.I. Song *et al.*
Progressive collapse testing and analysis of a steel frame building
J Constr Steel Res (2014)

K. Khandelwal *et al.*
Progressive collapse analysis of seismically designed steel braced frames
J Constr Steel Res (2009)

X. Zhao *et al.*
Experimental study on progressive collapse-resistant behavior of planar trusses
Eng Struct (2017)

View more references

Cited by (20)

Collapse-resisting mechanism and damage propagation pattern of suspended-domes following sudden cable loss
2024, Journal of Constructional Steel Research

Show abstract

A state-of-the-art review of progressive collapse research and guidelines for single-layer lattice shell structures
2023, Structures

Show abstract

System-reliability-based disaster resilience analysis: Framework and applications to structural systems
2022, Structural Safety

> *Citation Excerpt :*
> …However, when the structural system becomes highly sophisticated and local damage or an element failure plays a critical role in the structural collapse, cascading failure mechanisms need to be considered. On the other hand, various redundancy indices considering the effects of cascading failures have also been developed [63–69]. The methods perform dynamic analyses during which damaged elements are removed to simulate load redistributions.…

Show abstract

Elasto-plastic buckling behaviour of aluminium alloy single-layer cylindrical reticulated shells with gusset joints

2021, Engineering Structures

> *Citation Excerpt :*
>
> …Therefore, the elasto-plastic buckling behaviour of reticulated shells should be investigated exhaustively. Existing research observations indicate that the main parameters that influence the elasto-plastic buckling behaviour of reticulated shells include the shell type, span, rise-to-span ratio, load distribution, member section, support condition, member curvature, initial geometric imperfection, material property, and joint stiffness [3,13–21]. The influence of other parameters on the buckling capacity can be understood intuitively.…

Show abstract

Experimental and numerical study on cable breakage equivalent force in cable-stayed structures consisting of low-relaxation seven-wire steel strands

2020, Structures

> *Citation Excerpt :*
>
> …However, a data acquisition frequency of 0.5 kHz was used and the location of data acquisition was also close to the strand breakage location. In the published results [5,9,10,12–16], there is a discrepancy between the assumed CBEF(t) related to different cable-stayed structures and also its duration. On the other hand, none of these simple assumptions have been verified.…

Show abstract

Behaviour of H-section purlin connections in resisting progressive collapse of roofs

2019, Engineering Structures

> *Citation Excerpt :*
>
> …The last several decades have witnessed plenty of progressive collapse incidents of building structures, leading to a growing interest in this disproportional failure phenomenon among academic and engineering communities. As a result, a great number of studies have been conducted to investigate the progressive collapse resistance of multi-storey frame structures [1–3] and, more recently, roof structures [4–6]. Among the various types of roof structures, trusses have received the most attention in the research of progressive collapse.…

Show abstract

View all citing articles on Scopus

View full text

Modular steel lamella roofs by Hugo Junkers

A lightweight structure from the 1920s

Bibliographic Data | Preview | Full text (€) | References

Add to Favorites

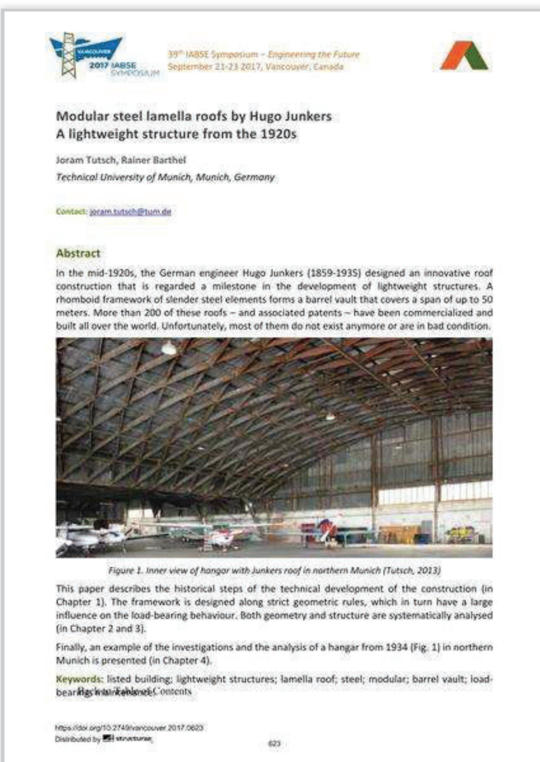
39th IABSE Symposium – *Engineering the Future*
September 21-23 2017, Vancouver, Canada

Modular steel lamella roofs by Hugo Junkers
A lightweight structure from the 1920s

Joram Tutsch, Rainer Barthel
Technical University of Munich, Munich, Germany

Contact: joram.tutsch@tum.de

Abstract

In the mid-1920s, the German engineer Hugo Junkers (1859-1935) designed an innovative roof construction that is regarded a milestone in the development of lightweight structures. A rhomboid framework of slender steel elements forms a barrel vault that covers a span of up to 50 meters. More than 200 of these roofs – and associated patents – have been commercialized and built all over the world. Unfortunately, most of them do not exist anymore or are in bad condition.

Figure 1. Inner view of hangar with Junkers roof in northern Munich (Tutsch, 2013)

This paper describes the historical steps of the technical development of the construction (in Chapter 1). The framework is designed along strict geometric rules, which in turn have a large influence on the load-bearing behaviour. Both geometry and structure are systematically analysed (in Chapter 2 and 3).

Finally, an example of the investigations and the analysis of a hangar from 1934 (Fig. 1) in northern Munich is presented (in Chapter 4).

Keywords: listed building; lightweight structures; lamella roof; steel; modular; barrel vault; load-bearing behaviour

https://doi.org/10.2749/vancouver.2017.0623
Distributed by structurae

623

Author(s): Joram Tutsch, Rainer Barthel

Presented at IABSE Symposium: *Engineering the Future*, Vancouver, Canada, 21-23 September 2017, published in Engineering the Future, pp. 623-630

DOI: 10.2749/vancouver.2017.0623

Price: **€ 25.00** incl. VAT for PDF document

ADD TO CART

Download preview file (PDF) 0.27 MB

In the mid-1920s, the German engineer Hugo Junkers (1859-1935) designed an innovative roof construction that is regarded a milestone in the development of lightweight structures. A rhomboid framewo...

Read more

Bibliographic Details

Author(s): Joram Tutsch (Technical University of Munich, Munich, Germany)
Rainer Barthel (Technical University of Munich, Munich, Germany)

Medium: conference paper

Language(s): English

Conference: IABSE Symposium: *Engineering the Future*, Vancouver, Canada, 21-23 September 2017

Published in: Engineering the Future

Page(s): 623-630 **Total no. of pages:** 8

Year: 2017

DOI: 10.2749/vancouver.2017.0623

Abstract: In the mid-1920s, the German engineer Hugo Junkers (1859-1935) designed an innovative roof construction that is regarded a milestone in the development of lightweight structures. A rhomboid framework of slender steel elements forms a barrel vault that covers a span of up to 50 meters. More than 200 of these roofs – and associated patents – have been commercialized and built all over the world. Unfortunately, most of them do not exist anymore or are in bad condition.

Figure 1. Inner view of hangar with Junkers roof in northern Munich (Tutsch, 2013)

This paper describes the historical steps of the technical development of the construction (in Chapter 1). The framework is designed along strict geometric rules, which in turn have a large influence on the load-bearing behaviour. Both geometry and structure are systematically analysed (in Chapter 2 and 3).

Finally, an example of the investigations and the analysis of a hangar from 1934 (Fig. 1) in northern Munich is presented (in Chapter 4).

Keywords:

steel listed building lightweight structures lamella roof modular

barrel vault load-bearing kmtaoinTtaebnlaenocfe.Contents *buildings*

MDPI

Article

The Geometry of Timber Lamella Vaults: Prototype Analysis

Milica Petrović [1,*], Isidora Ilić [1], Svetislav Mijatović [2] and Nenad Šekularac [1,*]

[1] Faculty of Architecture, University of Belgrade, 11000 Belgrade, Serbia
[2] Faculty of Physics, University of Belgrade, 11000 Belgrade, Serbia
* Correspondence: milica.petrovic@arh.bg.ac.rs (M.P.); nenad.sekularac@arh.bg.ac.rs (N.Š.)

Abstract: This paper presents timber lamella structures applied to the circular cylinder surface when all lamellae axes intersect at the nodes. To achieve the uniformity of all elements in this structure, the geometry of the structure must be carefully designed. The main methods for the research are graphical and numerical methods for geometric design and a prototype construction for a specific geometric pattern. The methods are discussed for their ease of replication, as well as the possibility of reinterpretation on other surfaces, while the prototype design and construction give insight into the process from design to execution. The combination of these methods allows for a thorough analysis of the geometry for lamella structures. The analysis shows that geometrical design must begin from the whole to the lamella, and that the number of element types in the structure depends on the disposition of the elements and the angle of the pattern. The discussion shows the advantages and limitations of the proposed methods, while the conclusions give the guidelines for the implementation of lamella structures into new design projects.

Keywords: right circular cylinder; parametric equations; graphical method; timber structures

check for updates

Citation: Petrović, M.; Ilić, I.; Mijatović, S.; Šekularac, N. The Geometry of Timber Lamella Vaults: Prototype Analysis. *Buildings* **2022**, *12*, 1653. https://doi.org/10.3390/buildings12101653

Academic Editor: Reinhard Brandner

Received: 3 September 2022
Accepted: 8 October 2022
Published: 11 October 2022

1. Introduction

Lamella structures are spatial structures in a diamond pattern formed by ribs called lamellae [1]. They are usually classified as braced structures—vaults and domes [1,2]. This paper will present timber lamella vaults when the diamond pattern of lamellae is applied to a circular cylinder surface. Contemporary tendencies in architecture, following the sustainable development trend, have led architects to think about the return to natural materials and the reduction of pollution created by the construction industry. The advantages of historical timber structures are being examined for possible modification and application in contemporary architectural practice. Lamella structures have stood out because of their aesthetics, economy and ease of construction.

1.1. Literature Review

The design of the Zollinger roof structure made an impact on the construction industry after World War I. The *roof of modernism* [3] was designed by the architect Friedrich Zollinger and patented in 1921 [4]. When invited to the City Council meeting for the rebuilding of Merseburg, Germany at the end of 1918, the architect Zollinger had an idea of how to design a simple construction model for new houses. The loadbearing elements of the house would be made out of cast-in-place concrete, and the innovative roof structure would be constructed out of timber lamellae, easily prefabricated and assembled even by untrained workers. The diamond pattern of the structure, reinforced with decking, required no additional structural elements, making it cost-efficient compared to traditional roofs. The analysis of material consumption showed that traditional roofs require twice as much material per square meter of the floor plan as the Zollinger roof. The section of this timber lamella structure shows that the roof shape is a segmental arch consisting of two circular segments. This form provides additional volume, so two floors could have been placed under the roof as shown in Figure 1 [5].

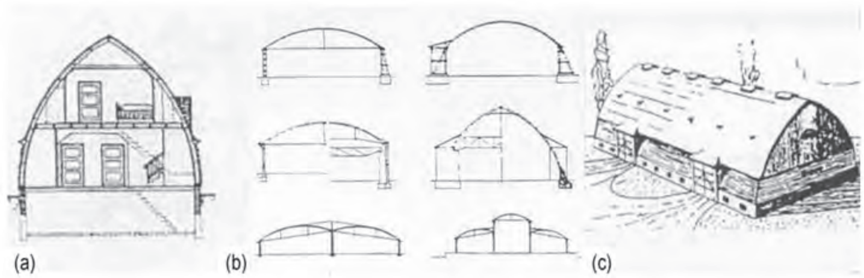

Figure 1. Lamella roofs for (**a**) housing, (**b**) halls and (**c**) barns [5].

The roof is constructed out of timber lamellae with variable cross-section and the upper edge was shaped to follow the arch of the roof. Lamellae were all uniform in shape and size. Two types of lamellae were applied, based on the roof span. The dimensions of the first type were width/height/length = b/h/L = 2.5/15/190 cm and the second were b/h/L = 5/30/150 cm (Figure 2) [6]. When the need for production halls with large spans increased, so did the cross-section of the lamellae, which showed great deflections right after the construction [7]. Other architects started experimenting with the change of disposition and the doubling of the lamellae [7,8], but soon new types of lamella structures were designed, using steel elements and purlins as reinforcement [7,9].

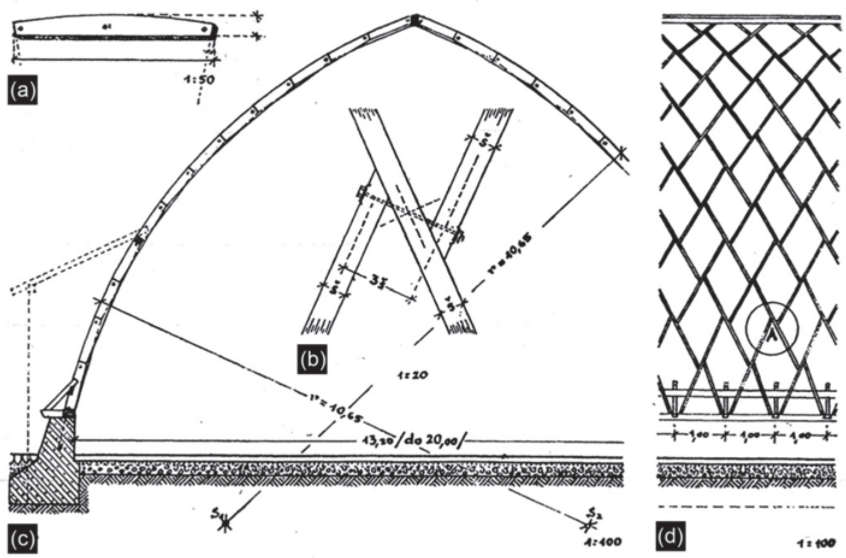

Figure 2. Zollinger lamella roof design: (**a**) lamella detail with dimensions, (**b**) joints of lamellae, (**c**) transverse section and (**d**) longitudinal section of the roof for housing [6].

The geometry of the first lamella roofs was half of a circular cylinder surface or its segment, in the span to rise ratio between 1:2 (semicircle) to 1:8 (flat arch) [10]. Later, the diamond pattern was applied to the spherical surface for dome structures and to this day, examples on free-form geometries can be found. Lamella structures were built all over the world, from timber to concrete, all following the geometry of a cylinder [7,9–11]. Other types of geometries were too complex to calculate without a computer. If the geometry is symmetrical on both axes, the number of equations is smaller, and the calculation is simpler [10]. With the use of computer software, new lamella structures on free-form geometries were erected.

The aesthetics and expressiveness of the diamond pattern have made lamella structures the primary choice for large-span objects where the structure remains visible. The advantage of lamella structures is the uniformity of the elements—the lamellae and their joints, which lead to the ease of production and assembly, the speed of erection and the minimised cost of the overall structure regarding the volume it covers. In order to preserve its advantages, it is necessary to find a suitable geometrical pattern for the lamellae axes to be applied to a circular cylinder surface. Throughout the years, several solutions were designed in timber and steel. The original structure, the Zollinger roof, was made out of timber planks placed vertically to the floor. Each lamella is twice the size of the diamond, and they are connected interchangeably, one in the middle of the other [1]. Three lamellae intersect at the node, with one central and two connecting lamellae shown in Figure 2. They are spaced apart for three widths of the lamella to mount the bolts [12]. This spacing also allows for the lamellae to be placed vertically and to follow the curve of the vault. The length of lamellae in steel lamella structures by engineers Emil M. Hünnebeck and Hugo Junkers is the size of the diamond, which allows them to put the connecting lamellae closer and to still follow the vaulted surface [13]. In these structures, the lamellae are rotated or translated in the horizontal plane to have all uniform elements and to follow the envelope of the cylinder, as presented in Figure 3. This creates an eccentricity at the node, resulting in the moment around the vertical lamella axis for the dominant axial forces in the structure.

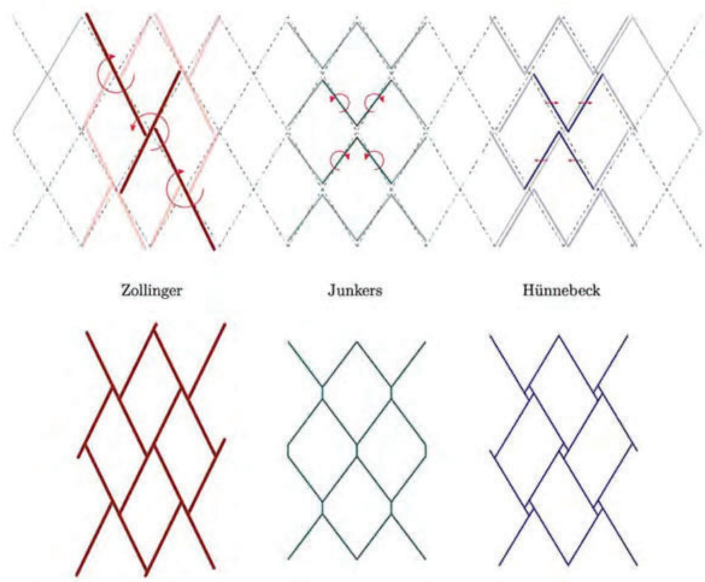

Figure 3. Diagrams showing three types of lamella vaults and the rotation/translation of the lamellae (**up**) with different types of nodes (**down**) [13].

Recent developments in lamella structures have shown the possibility to apply the diamond pattern on a number of forms using contemporary tools. Authors research regularities in different geometries trying to find the best structural pattern and the construction strategy for timber structures [14–16]. In recent years, a development in lamella structures was presented through workshops, experiments and built objects such as TIJ Bird Observatory [17–19].

1.2. The Aim of the Study

This paper discusses the geometry of timber lamella vaults. The design and position of the lamellae on the cylindrical surface have to be precisely defined in order to maintain the diamond pattern and the uniformity of the elements. The focus of this research is the lamella structure where all lamellae axes intersect at the node to avoid eccentricity (Figure 4). This will create a problem of rotation of lamellae in relation to the cylindrical surface, which is analysed and presented in this paper. The aim of this study is to better understand the geometry of lamella structures to be easily modified and adapted for use in contemporary structures. The idea is to comprehend the regularities of the geometrical design for cylindrical surfaces for the purpose of interpretation on other surfaces.

Figure 4. Diagram showing the node with one central lamella and two connecting lamellae when lamellae axes intersect.

The methods applied in this paper are the graphical method, the numerical method and prototype design. The graphical method presented in this paper is a novel approach, not found in the literature. The authors used different software to find the best possible solution for the geometric design of the lamellae axes. To expand the analysis, and to precisely define the geometry of the axes, a numerical method was applied. The authors presented a new method for defining the geometry of the axes and compared it to the method presented by Tutsch [13]. The prototype design was derived from result comparison of the graphical and numerical method. This prototype shows the level of uniformity of the elements and the time needed for prefabrication and construction. The erection of the prototype followed the instructions presented by Hosseinzadeh [10] since no other authors describe the method of erection.

The discussion includes all three approaches for the geometrical analysis and presentation of timber lamella vaults: (1) the graphical method, (2) the numerical method and (3) the physical model. The conclusions of this research affirm the aim of the study and open new questions for further research.

2. The Geometrical Design Methods

To obtain the precise geometry of the lamellae, the research was carried out using graphical and numerical methods. The main criterion is that the uniformity of the elements needs to be preserved since this is one of the main advantages of lamella structures.

The chosen geometry for the lamella vault is a cylinder surface. The cylinder type is a right circular cylinder, consisting of two of the same parallel bases the shape of a circle. The envelope of a cylinder is a perpendicular surface with all the same and parallel lines equal to the height of the cylinder, which is the vertical distance between the two bases.

The original lamella structure, the Zollinger roof, was designed as two circular cylinder surface segments of the same radius that meet along the ridge. Cylinder surface segments were also used for other types of buildings, such as halls and barns [5,7,9,11].

2.1. The Graphical Method

2.1.1. Connecting of the Arched Lamellae

The first iteration for the geometrical design of the lamella structure using the graphical method was based on the analysis of the lamella joint. The observed joint is a modification of the original joint for a Zollinger roof. In this joint, the axes of the lamellae intersect at the node, reducing the eccentricity. The three lamellae at the node are connected using steel plates bolted to the lamellae [20]. The research conducted by engineers Scheer and Purnomo at TU Berlin has shown a layout of the lamella structure, with a span of 21.5 m, a length of 21 m, an arch rise of 6.2 m and arch segments for the angle 120° [21]. The presented layout was used to design one lamella as a starting point for the geometry of the structure. Lamellae were connected one to another, forming an arch in one direction. The other direction of the lamellae was obtained by the rotation of the arch for 120°. The idea was for all lamellae to be vertical to the floor plane, that is, for the arches to move translationally and to form the vaulted structure.

This design process turned out to be wrong because the lamellae cannot be placed vertically and intersect at the node at the same time. When all the arches made from lamellae are in place, it can be observed that the node of the lamellae is not where it should be placed—each lamella should be connected to the middle of the lamella from the other direction. Figure 5 shows the details A, B and C with respect to the structure. Detail A shows the only position where it is possible to place a lamella vertically to the floor plane and that is the ridge of the vault. Detail B shows the slight distance of the lamella from the middle of the other one, at 1/4 of the arch, while detail C shows the greatest deviation of one lamella to the middle of the other, observed at the point of support of the structure.

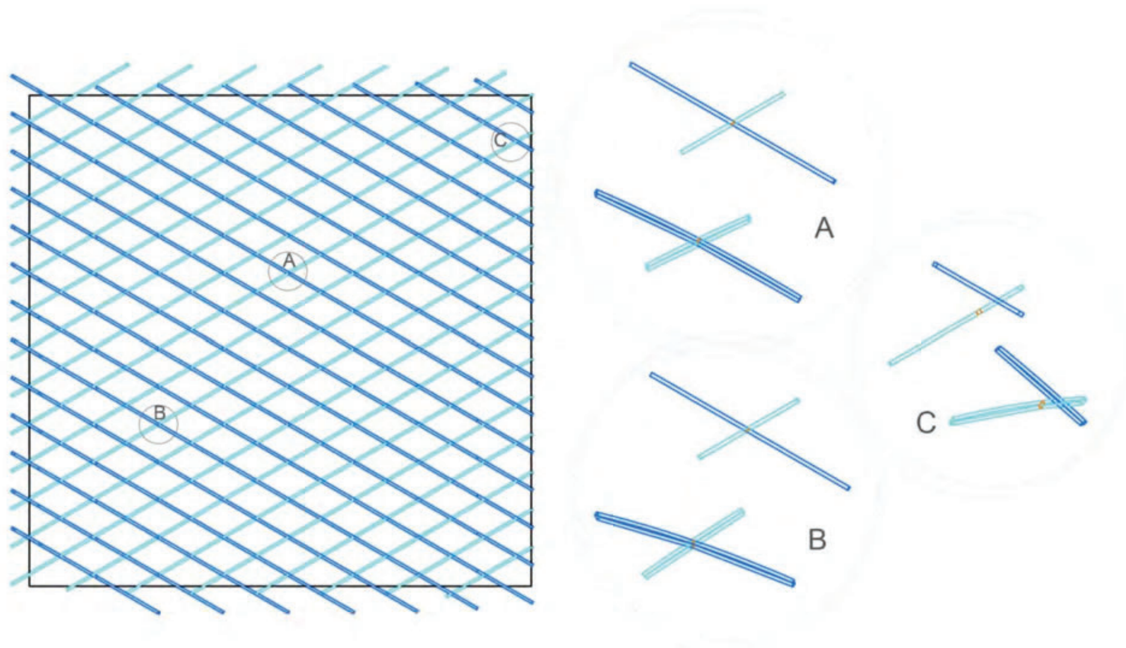

Figure 5. The plan and details of the lamella vault for the graphical method of connecting the lamellae in an arch with details A, B and C showing the misplacement of the connecting lamellae in the node.

The conclusion is that lamella structures cannot be designed starting from an individual element to the whole assembly because the ends of connecting lamellae do not meet at the middle of the central lamella. It is necessary to start with the whole to obtain a more accurate geometry of the lamellae. Vertical sections through the circular cylinder give an ellipse in the section, which cannot give uniform lamellae.

2.1.2. Projection of the Pattern to the Cylinder Surface

The second iteration was led by the idea that the fastest and simplest way of obtaining the diamond pattern structure on a cylinder surface is to project the pattern to the cylinder surface in software for 3D design, such as Rhino [22]. The half-radius of the base circle for the cylinder was r = 12.4 m and the length of the cylinder was l = 21 m. The arch segment had a span of a = 21.5 m and a rise of f = 6.2 m, giving the length of the arch a_1 = 26 m. The network was made with angles of 60° and 120°, the length of the cylinder surface l = 21 m and the width equal to the length of the arch segment of the cylinder a_1 = 26 m. The proportions of the cylinder were obtained from the layout by Scheer and Purnomo [21]. When the network is projected onto the cylinder the disposition of lamellae is obtained. This process is shown in Figure 6, which shows the detail of the structure with different lengths of lamellae from support to the ridge.

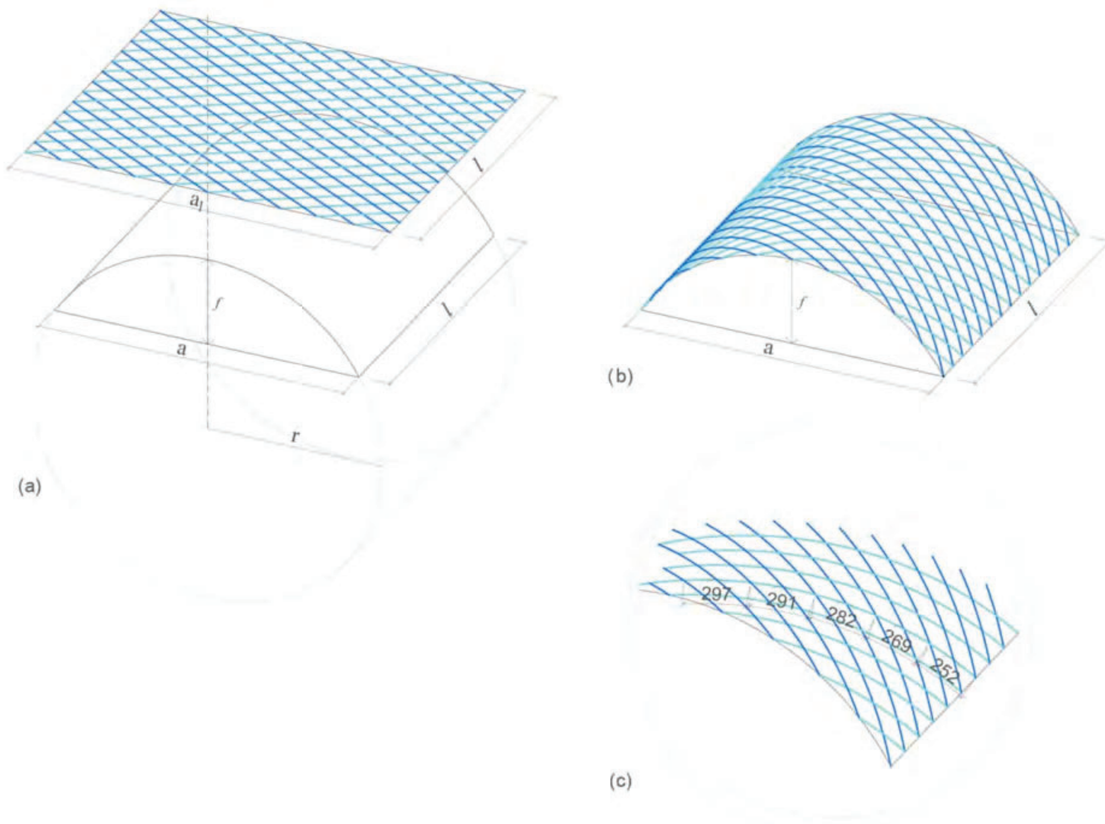

Figure 6. The axonometric view and detail of the lamella vault for the graphical method of projection of the diamond pattern to the cylinder surface: (**a**) the projection plane and the cylinder surface for projection, (**b**) the axis of the lamellae lying on the cylinder surface, (**c**) detail of the lamellae axes showing their different lengths.

This process of geometrical design has many advantages. It is easily understandable, so it is easy to replicate and apply to any surface. It is not time-consuming, nor it is necessary to always apply the same diamond pattern with angles of 60° and 120°, allowing more design freedom. The lamellae are vertical to the floor plane and intersect at the node, creating a continuous surface for placement of any roof tiling. The only problem is the different lengths of the lamellae, which is why this design does not fulfil the main criteria of the uniform elements. On the other hand, each horizontal segment of the vault has the same lamellae with the same joints, thus making sets of uniform elements. From the ridge to the supports, the length of the lamellae decreases and the angle of the bevelling increases. This structure could be easily prefabricated using a CNC machine for the shaping of the lamellae, in order to decrease the time for their production. If steel plates are used for the joints, a large number of different sets would not be economical to make. However, there are lamella structures constructed like this, such as the ice rink structure in Toronto from 2019 with T-section joints [23].

2.1.3. Division of Cylinder Surface to Equal Parts

The third iteration for the geometric design was also led starting from the whole to the elements with the aim for the lamellae of the same geometric characteristics to have uniform elements and to fulfil the main criteria. Based on the layout presented by Scheer and Purnomo [21], a segment of the cylinder surface was divided into equal parts, radially into 20 segments and longitudinally at every 0.75 m to obtain all the nodes of the lamellae. Lamellae rest on supports every 1.5 m and the nodes are placed interchangeably as each lamella connects to the middle of the one from the other direction (Figure 7a). The nodes were connected with lines passing two lengths of the diamond to obtain the desired length of the lamellae. Two types of lamellae were obtained, the ones 3 m in length and the ones on the perimeter with a length of 1.5 m. These lamellae axes do not intersect at the nodes, so the connection was simulated by a short line, which presented the joint (Figure 7b). Straight axis lamellae create a structure similar to a folded plate, which was not the idea behind the design. The lamellae needed to have the arched axis that lies on the cylinder surface in order to have all the same lamellae and a uniform surface of the structure.

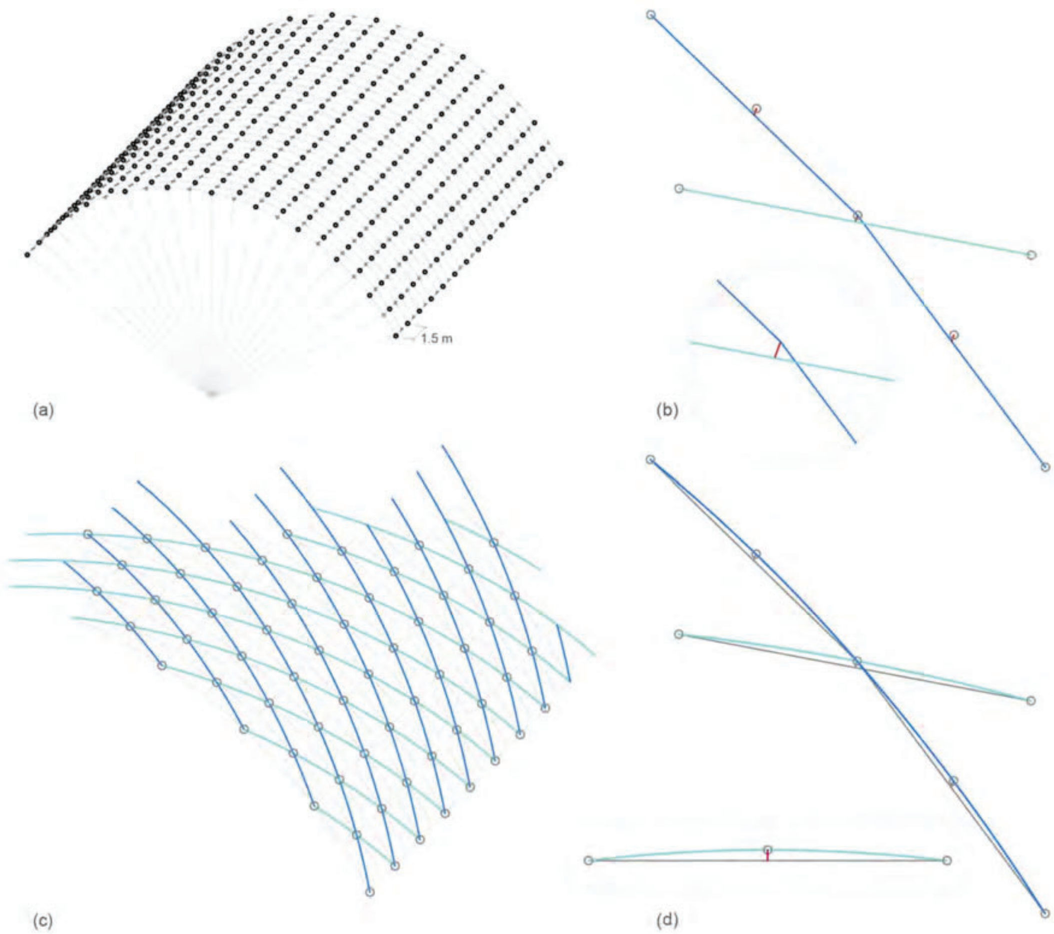

Figure 7. The process of division of cylinder surface to equal parts: (**a**) axonometric view of the lamellae vault with nodes of the lamellae spaced 1.5 m apart, (**b**) detail of each lamellae span and the connections at the nodes, (**c**) segment of a lamellae vault with all arched axes of the lamellae intersecting in the node and (**d**) detail of the arched lamellae defined by the span and rise lines.

The arched axis of the lamellae was designed using the two lines, which defined the plane for each lamella in the structure. The ends of the line connecting the nodes and the top of the line presenting the connection define the arch span and rise (Figure 7d). The most precise geometry is derived this way and the geometrical model fulfils the main criteria. All lamellae have the same geometry and uniform joints, making the production of the elements easy for mass prefabrication.

2.2. The Numerical Method

The geometrical shape that connects all the nodes and divides the cylindrical surface into uniform segments is a helix.

Starting with the parametric equation of a circle [13]

$$x_k = \begin{pmatrix} y \\ z \end{pmatrix} = \begin{pmatrix} R\cos\varphi \\ R\sin\varphi \end{pmatrix} \tag{1}$$

from which the parametric equation for a circular cylinder is obtained

$$x_{kz} = \begin{pmatrix} x \\ y \\ z \end{pmatrix} = \begin{pmatrix} x \\ R\cos\varphi \\ R\sin\varphi \end{pmatrix} \tag{2}$$

the parametric equation of the helix can be derived

$$x_s = \begin{pmatrix} x \\ y \\ z \end{pmatrix} = R\begin{pmatrix} (\varphi - \varphi_0)\tan\beta_s \\ \cos\varphi \\ \sin\varphi \end{pmatrix} \tag{3}$$

with pitch

$$h_s = 2\pi R\tan\beta_s. \tag{4}$$

The angle formed by the lamellae is constant and can be derived from the parameters, i.e., the length of the roof—L, the length of the arch—B, the number of cylinder divisions in the X-direction—*m* and the number of cylinder divisions in the Y-direction—*n*, as shown in Figure 8a, with its equation given as follows:

$$\tan\beta_s = \frac{n \cdot L}{m \cdot B} \tag{5}$$

$$\beta_s = \arctan\frac{n \cdot L}{m \cdot B} \tag{6}$$

The radius of curvature of the helix is

$$R_s = \frac{R}{\cos^2\beta_s} \tag{7}$$

and its arch length is

$$B_s = \frac{B}{\cos\beta_s} \tag{8}$$

deriving the abstract angle of the opening of the helix

$$\alpha_s = \frac{B_s}{R_s} = \frac{B \cdot \cos\beta_s}{R} = \alpha \cdot \cos\beta_s \tag{9}$$

Based on the elements of the lamella roof structures, as presented in Figure 8b, the authors of this paper derive the following parametric equations for the two helixes that form the basic geometry of the lamella roof:

$$x_{s_1} = \begin{pmatrix} x \\ y \\ z \end{pmatrix} = \begin{pmatrix} \frac{h}{\alpha} \cdot \varphi \\ R\cos\left(\varphi + \frac{k_1}{2} \cdot \alpha\right) \\ R\sin\left(\varphi + \frac{k_1}{2} \cdot \alpha\right) \end{pmatrix} \tag{10}$$

$$x_{s_2} = \begin{pmatrix} x \\ y \\ z \end{pmatrix} = \begin{pmatrix} \frac{h}{\alpha} \cdot \varphi \\ R\cos\left(\varphi + \frac{k_2}{2} \cdot \alpha\right) \\ -R\sin\left(\varphi + \frac{k_2}{2} \cdot \alpha\right) \end{pmatrix} \tag{11}$$

-h is the length of the helix for one lamella,

$$h = \frac{L}{m} \tag{12}$$

-α is the angle of the helix needed for one lamella,

$$\alpha = \frac{B}{n} \tag{13}$$

-φ is a variable that defines the segment of the helix (the length of the lamella axis is the angle of 24°);

-k_1 is a coefficient that is an even number;

-k_2 is a coefficient that is an odd number.

Coefficients k_1 and k_2 define the movement of the helixes relative to one another for half of the length of a lamella to get the right geometry for each lamella to connect to the middle of the one from the other direction.

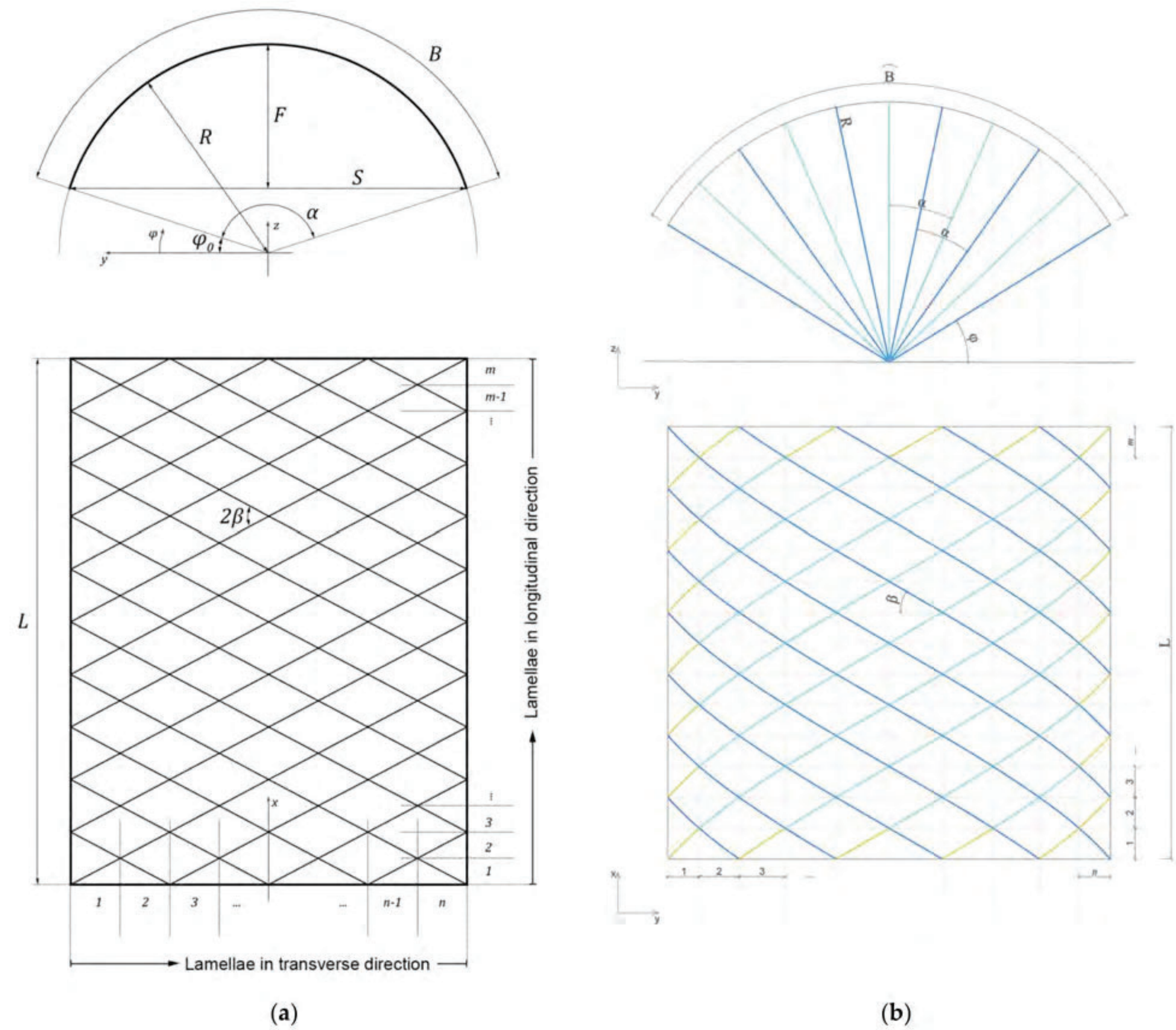

Figure 8. Floor plan and section of the lamella vault for geometrical analysis (**a**) by Tutsch [13]; (**b**) by the authors.

In comparison to the parametric equation of the helix by Tutsch [13], the parametric equations provided by the authors define each lamella axis, taking into account the mutual relation of lamellae. The helix equation by Tutsch defines the helix that follows the segment of the cylinder envelope, not taking into account that the helix from the other direction has to be translated for half of the length of the lamella. The authors define the length of a lamella as a segment of the helix with the variable φ, while the coefficients k_1 and k_2 enable the connection of the lamellae in the middle of the central lamellae. The graphic output of the equations by the authors was developed in Wolfram Mathematica and is presented in Figure 9.

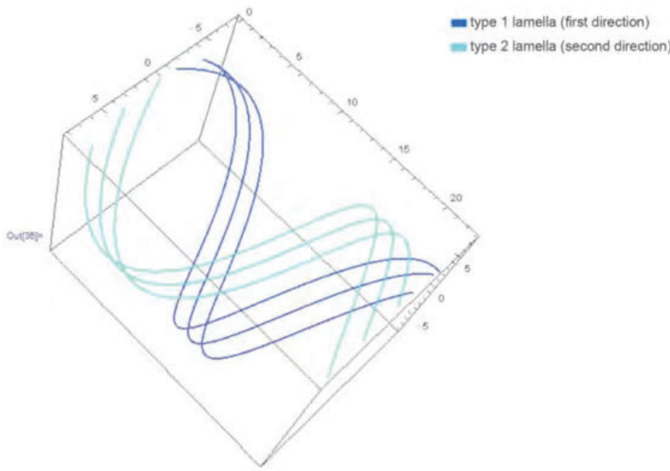

Figure 9. The graphic presentation of the parametric equations for the helixes developed in Wolfram Mathematica. The blue graph shows the helix from one direction and the green one shows the helix from the other, translated for half of the lamella length.

When applying the numerical method for the geometrical design, the conclusion is that even the infinitely small segment of a helix is a spatial curve. This results in lamellae torqued around their longitudinal axes, which complicates the manufacture, see Figure 10a. For lamellae to be manufactured, an idealisation is needed. Each segment of a helix needs to be converted to an arch, as it was shown in the graphical method, in order to define a planar curve for the lamellae manufacture. This leads to a slight rotation of the connecting lamellae in the node, as presented in Figure 10b.

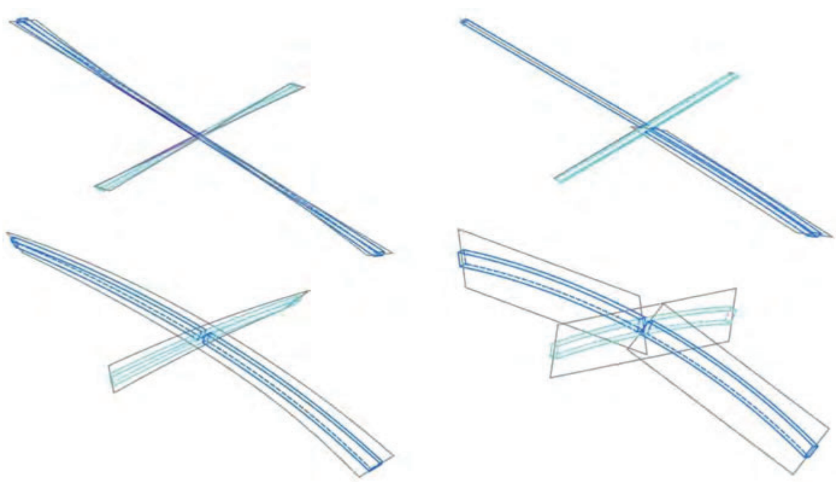

(a) (b)

Figure 10. The axonometric view of the intersection of the lamellae at the node (**a**) showing the lamellae axes following the helix curve obtained by the numerical method, and (**b**) showing vertical axial planes of the lamellae in order to present the rotation at the node obtained by the graphical method.

3. The Physical Model of a Lamella Vault

In architecture, physical models help to solve problems during the design process, working in parallel with drawings, 3D models and construction with materials corresponding to the designed structure [24]. During this process, different aspects of the design can be modified or changed due to the design process on various scales and with a variety of tools. Design problems can be resolved from the level of the node to the structure as a whole. This practice was common in historical constructions when knowledge was acquired by model design and construction and their analysis. This process of constant iterations and relations between designing on a computer and designing a physical model is called complex modelling in contemporary architecture [25]. The hypothesis is that it helps with better observation and learning about the design.

Following the conclusions of the geometry analysis, the prototype was designed from the lamellae with axes as planar arches to be easily manufactured. The axes of the lamellae intersect at the node, eliminating the eccentricity that appeared at the original joint, making this prototype an improvement of the historical lamella structure.

3.1. The Design of the 3D Model

The first step towards the design of a physical model of a timber lamella vault was the design of a 3D model with all the necessary details of the lamellae and their joints. The model was based on the arched lamellae axes obtained by the graphical method presented in Figure 7, since the geometry of the axes provided by the numerical method results in torqued lamellae, see Figure 10a,b. The cross-section was first assigned to the lamella placed vertically to the floor plane and their connecting lamellae in the middle. The ends of the lamellae were bevelled following the vertical axis planes of the lamellae so that the whole cross-section of the connecting lamellae was pressed onto the middle of the central one. The lamellae were then rotated around the axis of the cylinder in order to obtain the whole structure. Thus, all lamellae are the same and all lamellae axes lie in the envelope of the cylinder. Arches along the gables were designed as three-hinged arches. Lamellae pressed onto the gable were cut obliquely by following the vertical plane of the three-hinged arch.

The joints for the lamellae were designed with steel plates bolted to the lamellae. The inspiration was a T-section joint presented in the Timber Construction Manual [26]. This joint is designed using two steel plates welded to each other to form a T-section. The difference between this joint and the applied one is that, in this design, two steel plates were placed on the outside edges of the lamellae and welded to the central steel plate. The T-section joint is placed inside the lamellae and requires additional shaping, as opposed to the applied joint. The supports were designed as point supports following the same design logic as the joints.

The final design is presented in Figures 11 and 12. The 3D model of the structure can be observed in Figure 11, while Figure 12 presents floor plans and sections of the structure, providing information about its dimensions.

3.2. Elements for the Physical Model

The designed structure has a span of 10.75 m, it is 3.1 m high and requires 81 lamellae. Based on the position of the lamellae in the structure, six types can be distinguished. All lamellae have the same radius of curvature because they all lie on the cylinder surface. The length of most lamellae is approximately 3 m, except the ones along the perimeter, which are 1.5 m long (Table 1). Type 1 has a span of 289 cm and it is the most used type in the structure. Type 3 shows the lamellae next to the supports, and type 4 are the lamellae lying on the gable arch. Two special types are types 5 and 6, which lie on the arch and the supports at the same time. The differences between the lamella types are created by the length and the different angles of the bevelling of the ends. The disposition of the lamellae in the diamond pattern with angles 60° and 120° requires this number of types, and it cannot be reduced. The cross-section of the lamellae is width/height = b/h = 6/16 cm.

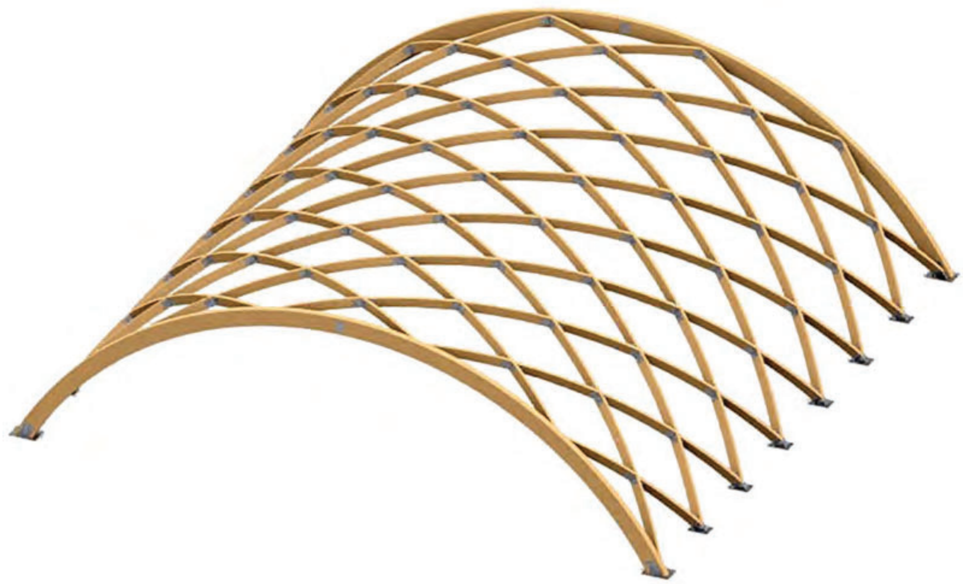

Figure 11. Three-dimensional model of the designed lamella vault.

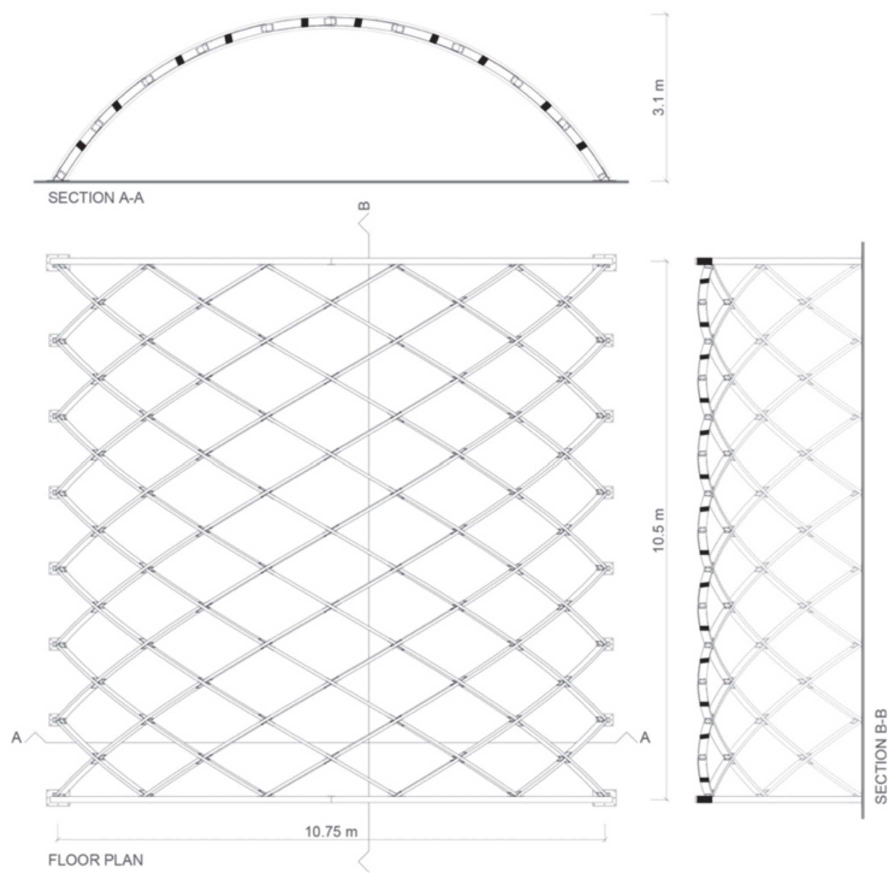

Figure 12. Floor plan and sections of the lamella vault of the physical model.

Table 1. Specification of timber lamellae.

Type		Span of a Lamella [cm]	Number of Lamellae	Total Volume for the Type [m^3]
1	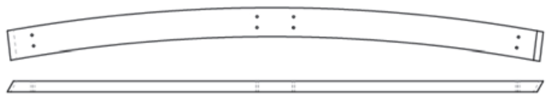	289	33	1.007
2	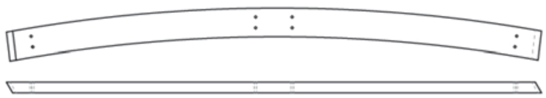	289	24	0.732
3		149.5	12	0.189
4		153	8	0.129
5	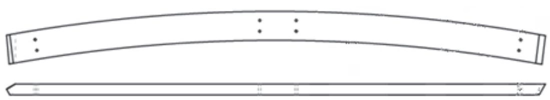	292	2	0.062
6	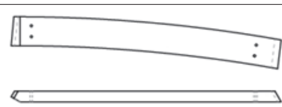	148	2	0.031
			Total:	**2.15**

The structure has six types of joints based on their position inside the structure: two types of lamellae joints, the arch and the lamellae joints, the support joints and two types of arch and lamella support joints. The dimensions of the steel plates depended on the position of the node and its geometry, as well as the position of the bolts according to technical regulations (Table 2). The width of the steel plates was 3 mm for all of the joints, except for the supports made from 5 mm thick steel plates. The used bolts were M12, class 5.6.

The majority of the lamellae belong to types 1 and 2 (Table 1) where the bevelling of the lamellae shows that they are mirrored one in reference to the other. Other types of lamellae are derived from types 1 and 2. The same goes for the joints.

3.3. Construction of the Physical Model

The prefabrication of the elements preceded the construction of the designed timber lamella vault. The base for lamellae was made from an arched glued laminated timber beam, with an arch radius of 844 cm and outer edge length of 630 cm. In order to have 81 lamellae, 35 base arches needed to be made. The gable three-hinged arches were made from four equal arched glued laminated timber beams, with an arch radius of 635 cm and an outer edge length of 680 cm. Steel plate joints were prefabricated in a workshop according to the design, out of 3 mm and 5 mm steel plates with mechanically predrilled holes for bolts. The anchor plates were made from 10 mm thick steel plates.

Table 2. Specification of steel joints.

Type		Number of Joints	Total Volume for the Type [m^3]	Total Weight for the Type [kg]
1	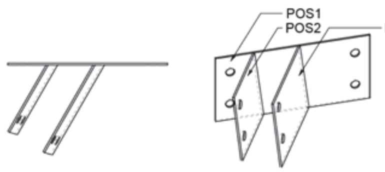	70	0.0132	103.620
2	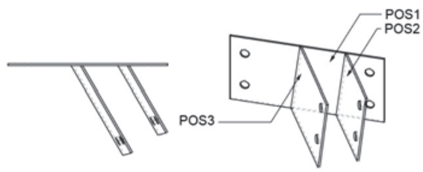	48	0.00904	70.964
3	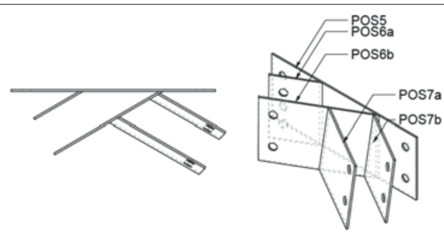	8	0.00249	19.547
4	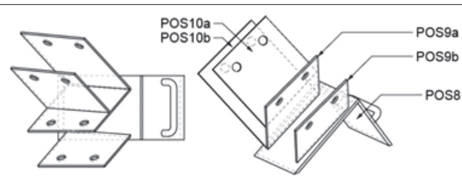	12	0.00391	30.694
5	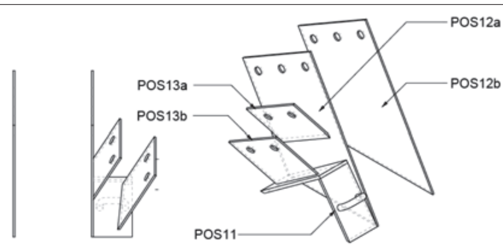	2	0.000855	6.712
6	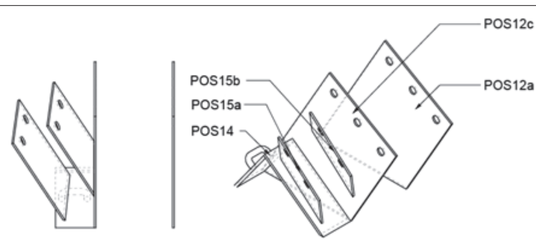	2	0.000855	6.712
			Total:	**238.25**

The construction of the lamella vault started with the placement and levelling of the anchor plates, anchored to the ground with M16 anchor bolts. Support joints were welded to anchor plates at the designed positions to provide a good starting point for mounting timber elements. The shaping and placement of three-hinged arches was the next step. The gable arches were measured and shaped on the ground, connected with steel plates at the hinge, and then lifted and placed into the supports. The positions of the joints for the lamella and the arch were measured and marked. The joints were then mounted to the three-hinged arch. To achieve the stability of the gable arch, the first lamellae needed to be placed near the arch supports, as presented in Figure 13. The construction layout dictated the sequence of the lamellae assembly, starting from one gable to the next, forming one bay at a time in order to check the dimensions and the positions of the lamellae and the joints. The described process of bay-by-bay construction was presented as the best manner of construction for a lamella vault [10].

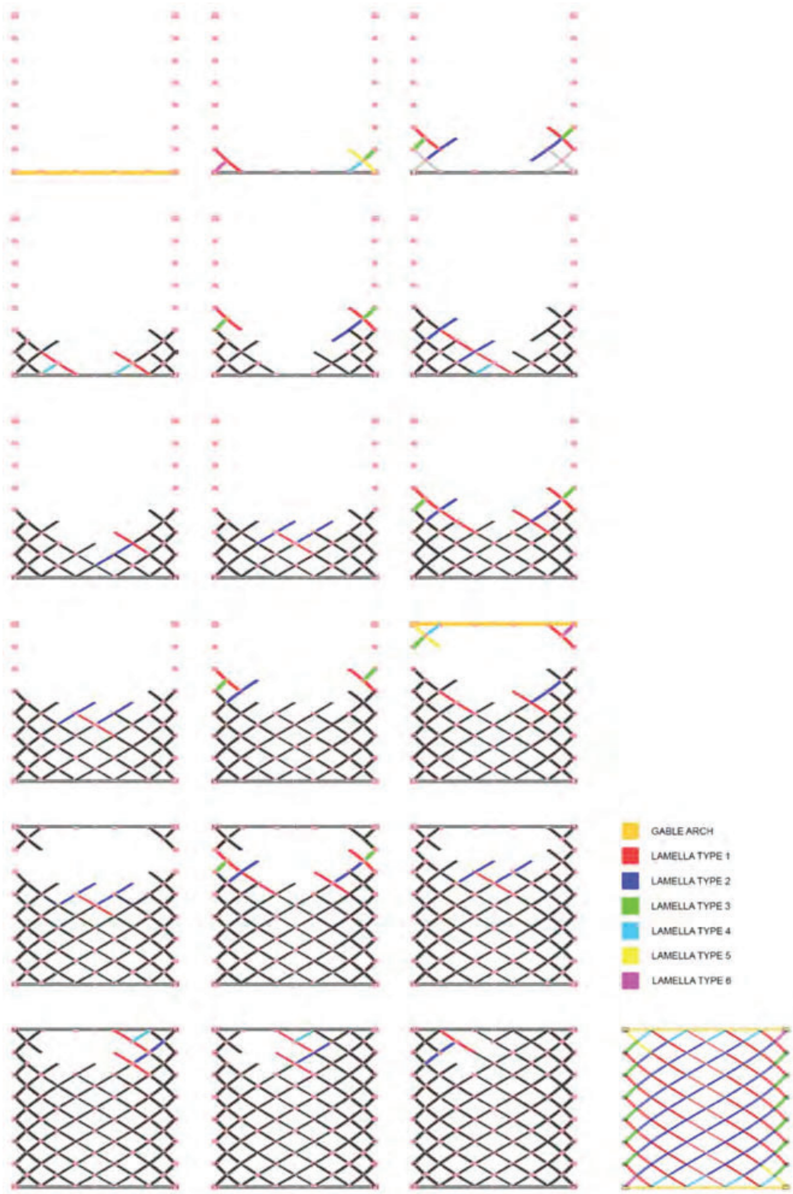

Figure 13. A diagram of the construction process of the physical model.

The base arches for the lamellae were delivered to the building site where they were measured and bevelled according to the specifications. During the construction, it was concluded that the base arches tended to elongate because of high temperatures, so the position of the joints had to be measured according to the triangle between the edge joints and the middle one. The joints were mounted onto the middle of each lamella on the ground. The lamellae would be then placed at the designed position in the structure and controlled by the position of the stings marking the height of the nodes. The lamellae would be temporarily secured with screws until the whole bay was positioned, after which the holes for the bolts would be drilled and the bolts mounted.

At the beginning of the construction, there was a need for additional supports, since the structure was very unstable. With the increase of the bays, the structure began to adapt to the cylinder shape. The larger number of lamellae showed that every other lamella reinforced the previous one and set its position in the structure. This was observed as a successive relief in the construction process right after the construction of the first bay, and it was confirmed after half of the structure was constructed.

The construction experience contributed to a better understanding of the timber lamella vault. Conclusions were drawn regarding the method of assembly and the preparation of the structural elements. This experience also opened questions related to the modification of the structure.

The construction process and the physical model are shown in Figure 14.

Figure 14. Photo of the construction process and the physical model in detail.

4. Discussion

Lamella structures are a specific type of spatial structure primarily because of their diamond pattern. They have the advantage of the uniformity of elements, leading to an economical structure that is easily assembled. This pattern creates an unstable system if no additional structural elements are applied. One of the ways to solve this problem is to form moment connections between lamellae. In order to design a lamella structure, the geometry must be precisely defined.

The original joint has a large moment of eccentricity compared to the other types of joints and the load capacity of the bolts connecting the three lamellae at the node is much smaller [12,26]. Throughout the years, engineers have suggested a modification of the original joint and have designed a joint with all three lamellae axes intersecting at the node, thus eliminating the eccentricity [20,21,26]. The proposed joints are usually designed with steel plates, having a greater loading capacity than the original one. The geometrical design and the prototype presented in this paper are for the lamella structure where all lamellae axes intersect at the node, and the eccentricity is eliminated.

The chosen geometry of the lamella structure in this paper is a lamella vault. The diamond pattern is applied to the envelope of the right circular cylinder. The material of the lamellae is timber, and the joints are formed out of steel plates bolted to the lamellae.

The discussion in this paper is led by the following criteria:

1. The geometry of the structure must provide uniformity of all structural elements.
2. The lamellae must intersect at the nodes to reduce the eccentricity of the joints.
3. The construction must be simple and performed in a short period.
4. The designed structure must be economical.

The criteria are derived from the advantages of historical lamella structures, which must not be damaged by the modification of the structure.

The geometrical design of the lamella vault was approached using the graphical method and the numerical method. The numerical method for geometrical design opens the possibility of easy modification of set parameters. The diamond pattern of the lamellae can be applied to any type of surface by following the methodology shown in Section 2.2. The authors' numerical method presents a further observation of the specific pattern of lamellae and gives the possibility of adaptation, which would include the interchangeability of the original connection—one lamella connects to the middle of the next one from the other direction. The presented parametric equations can also be used for 3D modelling in different software plug-ins, such as Grasshopper for Rhino. This enables the fast and precise design of the geometrical model [15,16,19]. For the physical model, the axis curves of the lamellae would have to be optimised. The parametric definition of the helix, even for an infinitesimal segment, gives a spatial curve, so it is necessary to modify it into a planar curve—an arch that will define the axis of the lamella for the construction. One of the graphical methods has shown this modification. The presented graphical methods have shown two possible approaches to geometric design: (1) from lamella to the whole structure and (2) from the whole to the lamella. The analysis has shown that the right process of design is the second one and both graphical methods that followed this process have proven successful.

The method of pattern projection to the cylinder surface creates a reasonable structure with all vertical lamellae that intersect at the nodes. This geometry does not fulfil the first criteria since there are numerous sets of uniform lamellae, depending on the density of the structural pattern. This could be overcome by the production of lamellae on a CNC machine, thus reducing the prefabrication time. The number of joint sets would be the same as the number of lamellae sets, so a simple joint must be designed to be easily modified for different angles in the structure. If the elements were to be mass-produced, this structure would have complied with all the criteria except the first one.

The method of division of the cylinder surface into equal parts was applied to the design of the physical model of the lamella vault. This method gives a uniform structure with six types of lamellae and the corresponding joints, no matter the density of the pattern since the types of the elements depend on their position in the structure. The differences among lamellae are created because of different angles for bevelling, which also influences the angles in the joints. Types 1 and 2 are mirrored elements, which are the consequence of the diamond pattern and the angles of 60° and 120°. The number of types could be reduced for one if the pattern was created with 90° angles. This proves that the structure fulfils the first two criteria. The only problem with this structure is the rotation of lamellae at the nodes because the axes of the lamellae intersect at the nodes.

In historical lamella structures, the rotation/translation of the lamellae was applied in the horizontal plane to have all lamellae vertical to the floor [13]. This resulted in a variety of joints that had large moments of eccentricity, since the lamellae do not intersect at the nodes, but the criteria for uniform elements was fulfilled. The advantage of Junkers' structure, over the ones of Zollinger and Hünnebeck, was that all the joint elements were the same. In comparison to these structures, the designed joint for the presented physical model has reduced the eccentricity in the node, leaving the axes of lamellae to intersect. On the other hand, the rotation of the lamellae appears in the vertical plane, making a torsional movement around the axis, so they are not vertical in relation to the floor. The rotation of the lamellae at the node is the consequence of the approximation of the arched axis of the lamella corresponding to the helix curve, as presented in Sections 2.1.3 and 2.2. This rotation of the lamellae demands further shaping after the construction is finished, to provide a continuous surface, as it would be for the vertically placed lamellae.

The construction of the physical model for the timber lamella vault with a 10.75 m span and a length of 10.5 m lasted seven days with only three workers. The hypothesis is that five workers would finish the construction in a smaller amount of time, thus also fulfilling the third criterion. The number of workers and the period of construction affect the economy of the structure [27], i.e., the cost of construction is reduced for a small number of workers and the short construction time. In comparison to standardised timber vaults, this structure is not economical because all the elements are specially designed only for this structure, while standardised vaults use mass-produced elements.

The discussion and analysis of the presented geometry of timber lamella vaults still leave an open question for choosing the best way to design a lamella structure, thus giving the designer the possibility to adapt the structure to its needs.

5. Conclusions

The presented research shows the problems of the geometrical design of timber lamella vaults. The diamond pattern of the lamellae is applied to the right circular cylinder envelope with the idea to explore different methodologies for geometrical design that could be replicated on any type of surface. The physical model of the structure has presented problems that emerge during the construction, contributing to the thorough analysis from design to execution.

The conclusions about the geometry of timber lamella vaults are drawn as follows:

- The graphical geometrical design method needs to follow the process of design from the whole to the lamella to obtain the correct geometry with as many possible uniform elements.
- The graphical method following the process of projection of the pattern to the cylinder surface gives various sets of uniform elements—lamellae and the corresponding joints—leaving them vertical to the floor plan. This process is easily replicated and the lamellae pattern is easily modified to meet designers' needs.
- The graphical method of the division of the cylinder surface into equal parts results in the most uniform elements. The lamellae are rotated around their longitudinal axis, so they are not vertical to the floor plan.
- The smallest possible number of element types is five for timber lamella vaults where the axes of lamellae intersect at the nodes. This can be achieved only for the 90° angle between the lamellae, that is, for the square pattern of lamellae.

- The geometrical design approach using the numerical method gives parametric equations that are easily modified in 3D modelling software to meet designers' needs.

The presented geometrical analysis and physical model of a timber lamella vault have shown the adaptability of lamella structures and the possibility to use them in different contemporary architectural projects.

Author Contributions: Conceptualization, M.P.; methodology, M.P. and S.M.; software, S.M.; validation, N.Š.; formal analysis, M.P., I.I. and S.M.; investigation, M.P. and I.I.; resources, M.P.; data curation, M.P., I.I. and S.M.; writing—original draft preparation, M.P.; writing—review and editing, M.P. and N.Š.; visualization, M.P. and I.I.; supervision, N.Š.; project administration, M.P.; funding acquisition, N.Š. All authors have read and agreed to the published version of the manuscript.

Funding: This research received no external funding.

Institutional Review Board Statement: Not applicable.

Informed Consent Statement: Not applicable.

Acknowledgments: This research was supported by LAB—Architectural Engineering Laboratory—Structural Problems of Architectural Buildings in the Faculty of Architecture at the University of Belgrade.

Conflicts of Interest: The authors declare no conflict of interest.

References

1. Lan, T. Space Frame Structures. In *Handbook of Structural Engineering*; Chen, W.F., Ed.; CRC Press: London, UK, 1997; pp. 943–1001.
2. Makowski, Z.S. *Analysis, Design and Construction of Braced Barrel Vaults*; Elsevier: New York, NY, USA, 1985.
3. Programme © Bauhaus Kooperation 2020. Available online: https://www.bauhaus100.com/programme/eventdetails/400/ (accessed on 29 September 2020).
4. Zollinger, F. Space-Enclosing, Flat or Curved Components. German Patent DE387469C, 28 December 1923.
5. Winter, K.; Rug, W. Innovationen im Holzbau—Die Zollinger-Bauweise. *Bautechnik* **1992**, *69*, 190–197.
6. Peulić, Đ. *Konstruktivni Elementi Zgrada*; Croatia Knjiga: Zagreb, Croatia, 2002.
7. Wolf, K. Rautennetze by Emil Hünnebeck—Steel Lamella Roofs of the Interwar Period. In *Iron, Steel and Buildings: The Proceedings of the Seventh Conference of the Construction History Society*; Construction History Society: Cambridge, UK, 2020; pp. 117–128.
8. Tutsch, J. Die Rautennetzwerke von Emil M. Hünnebeck. Lecture, Technische Universität München. 2017. Available online: https://mediatum.ub.tum.de/doc/1380458/982932173316.pdf (accessed on 7 October 2022).
9. Weller, B.; Tasche, M.; Baatz, J. Lamella Roof Constructions by Hugo Junkers. In Proceedings of the International Association for Shell and Spatial Structures (IASS) Symposium, Valencia, Spain, 28 September–2 October 2009; Domingo, A., Lazaro, C., Eds.; Universidad Politecnica de Valencia: Valencia, Spain, 2009; pp. 1611–1621.
10. Hosseinzadeh, H. Analysis of Lamella Structural Systems with Particular Reference to Lamella Barrel Vaults. Master's Thesis, Department of Civil Engineering, University of Surrey, Guildford, UK, 1967.
11. Leslie, T. Laborious and Difficult: The Evolution of Pier Luigi Nervi's Hangar Roofs, 1935–1941. In Proceedings of the 6th International Congress on Construction History, Brussels, Belgium, 9–13 July 2018.
12. Franke, L.; Stahr, A.; Dijoux, C.; Heidenreich, C. How does the Zollinger Node really work? A Structural Experimental Investigation to a Better Understanding of the Nodal Behavior. In Proceedings of the IASS Annual Symposium 2017, Hamburg, Germany, 25–28 September 2017.
13. Tutsch, J.F. Weitgespannte Lamellendächer der Frühen Moderne: Konstruktionsgeschichte, Geometrie und Tragverhalten. Ph.D. Dissertation, Fakultät für Architektur, Technische Universität, München, Germany, 2020.
14. Petrović, M.; Ilić, I. Structural patterns in architecture. In Proceedings of the IASS Anual Symposium 2020/21, Guildford, UK, 23–27 August 2021; pp. 858–864.
15. Löschke, H.; Stahr, A.; Schröder, T.H.; Schmidt-Kleespies, F.; Hallahan, R. Segmentation and assembly atrategy for lamella roof shell structures. In Proceedings of the IASS Anual Symposium 2020/21, Guildford, UK, 23–27 August 2021; pp. 2800–2807.
16. Jin, J.; Han, L.; Chai, H.; Zhang, X.; Yuan, P.F. Digital design and construction of lightweight steel-timber composite gridshell for large span roof. In *Intelligent & Informed, Proceedings of the 24th International Conference of the Association for Computer-Aided Architectural Design Research in Asia (CAADRIA), Wellington, New Zeland, 18 April 2019*; Victoria University of Wellington: Wellington, New Zeland, 2019; Volume 1, pp. 183–192.
17. FLEX. ZolinkR Wave IASS 2015 Amsterdam. Available online: https://vimeo.com/135884817 (accessed on 2 September 2022).
18. Adieste. Digitally Fabricated Lamella Structure. Available online: https://issuu.com/adieste/docs/mp3ad (accessed on 2 September 2022).
19. Pintos, P. Tij Observatory/RAU Architects + RO&AD Architecten. 2019. Available online: https://www.archdaily.com/915456/tij-observatory-ro-and-ad-architecten (accessed on 2 September 2022).

20. Müller, C. *Holzeimbau, Laminated Timber Construction*; Birkhauser: Berlin, Germany, 2000.
21. Scheer, C.; Purnomo, J. Recent Research on Timber Lamella Barrel Vaults. In *Analysis, Design and Construction of Braced Barrel Vaults*; Makowski, Z.S., Ed.; Elsevier: New York, NY, USA, 1985; pp. 406–421.
22. Rhino Software. Available online: https://www.rhino3d.com (accessed on 15 July 2022).
23. BlogTO on Twitter. Available online: https://twitter.com/blogTO/status/1090708821083934722/photo/1 (accessed on 12 August 2022).
24. Stojanović, Đ.V. Adaptivni Principi u Arhitektonskom Projektovanju. Ph.D. Thesis, Faculty of Architecture, University of Belgrade, Beograd, Serbia, 2013.
25. Tamke, M. CITA: Working for and with material performance. *Serb. Archit. J.* **2013**, *5*, 202–226. [CrossRef]
26. Herzog, T.; Natterer, J.; Schweitzer, R.; Volz, M.; Winter, W. *Timber Construction Manual*; Detail: Munich, Germany, 2004.
27. Šekularac, N. Oblikovanje Naborastih Konstrukcija Primenom Drvenih Rešetkastih Nosača. Ph.D. Thesis, Faculty of Architecture, University of Belgrade, Belgrade, Serbia, 2010.

Design and Analysis of

Timber Lamella Segmental Arches

by

Glenn Frazee

A Report Submitted to the Faculty of the

Milwaukee School of Engineering

In Partial Fulfillment of the

Requirements for the Degree of

Master of Science in Structural Engineering

Milwaukee, WI

May 2011

Abstract

A lamella roof offers a unique architectural feature in its interwoven network of timbers. As a roof system, the stiffness created by the interlocking members results in a curved roof that uses less material than a traditional rafter and purlin design. The goal of this paper is for the reader to be able to create a preliminary design of a lamella roof that will be strong enough to withstand the loads stipulated by the most current ASCE 7-10 Minimum Design Loads for Buildings and Other Structures. This design is facilitated by load tables developed by the author using the finite element method and connection tables in compliance with the National Design Specification for Wood Construction 2005 Edition using the Allowable Stress Design (ASD) procedure. In reality, the values used for this preliminary design will give a conservative design that could most likely be lightened with a more in-depth structural analysis. Testing on a steel lamella model shows inconclusive results when compared to those predicted by the load table program developed by the author and should be investigated further.

Acknowledgments

I would like to thank the following people:

Dr. John Zachar for advising me, suggesting the project topic, keeping me on track, providing suggestions and commentary, and generally being a great professor and mentor.

Dr. H. P. Huttelmaier for his role on my committee and teaching me the finite element analysis method, as well as helping me apply it to my project.

Professor Michael McGeen also for his duties as a committee member and helpful input on multiple topics, especially the architectural considerations of lamella design.

H. Kubenik Metals for fabricating and donating a complete lamella arch for proof-of-concept and testing.

Denise Gergetz for her tireless work in finding many obscure texts on lamella construction and engineering.

Tim Warner for his helpful email correspondences and enlightening monograph.

Table of Contents

List of Figures

List of Tables

Nomenclature

Symbols

a = one-half span of arch (von Kármán method only)

A = area

A = vertical reaction (Scofield method only)

b = breadth or thickness of lumber section

B = vertical reaction #2 (Scofield method only, used if reactions are unbalanced)

C_e = exposure factor

C_s = slope factor

C_t = thermal factor

d = dead load (Scofield Method only)

d = depth of lumber section

D = axial thrust in lamella arch

E = Young's modulus (modulus of elasticity)

f = rise of arch (von Kármán method only)

$\tilde{f}$ = beam element forces vector

$\tilde{F}$ = combined forces vector

I = moment of inertia about the X-X axis

$\tilde{k}$ = beam element stiffness matrix

$\tilde{K}$ = combined stiffness matrix

ℓ = length of lamella between top bolt centers

$\ell_{c\text{-}c}$ = center-to-center length of lamella

L_r = construction live load

n = number of lamellas in the span of an arch

p = live load per unit length of horizontal projection (von Kármán method only)

p_g = ground snow load

p_f = flat roof snow load

q = dead load per unit length of arc (von Kármán method only)

r = Rise-to-Span ratio (T/S)

R = radius of curvature of lamella arch

s = snow load (Scofield method only)

s = shift of lamella connection

S = span of lamella arch

S_b = balanced snow load

S_u = unbalanced snow load

S_{xx} = section modulus about the X-X axis

T = rise of lamella arch

$\tilde{u}$ = beam element displacement matrix

$\tilde{U}$ = combined displacement matrix

W = wind load (Scofield method only)

x = distance measured from arch line of symmetry, distance from origin

θ = skew angle (or angle of inclination) of transverse lamella arches

Abbreviations

AISC	American Institute of Steel Construction
ASCE	American Society of Civil Engineers
DL	Dead Load (Gravity Load)
FEA	finite element analysis
LL	Live Load (Gravity Load)
mph	miles per hour
NDS	National Design Specification
plf	pounds per lineal foot
psf	pounds per square foot
SL	Snow Load (Gravity Load)
WL	Wind Load

Glossary

Rise – Height of curved roof from springing points to apex

Span – Clear distance covered by a roof

Springing Point – Hinging point in a two-pinned arch

Thrust – Force on a lamella parallel to its long dimension

1 Introduction

A lamella roof is made up of a series of intersecting skewed arches, each arch made up of smaller individual pieces called lamellas. These skewed arches come together to form a curved roof profile. J. S. Allen puts it well:

> The timber arched roof was made up of relatively short timbers referred to as ‘lamellas’ varying in thickness and depth depending upon the span but identical for any given span. These lamellas are curved on their top edges and beveled at the ends which are radial to the curvature and are bolted together on edge with the curved side uppermost, to form a rhomboid network of framing timbers. In this manner the external surface of the roof takes up the arched form [1].

Figure 1 displays the recently completed Hale County Animal Shelter, a project designed and constructed by the Rural Studio of Auburn University. Easily visible are the individual lamella pieces and the rhomboid patterns they create. The tops are cut to fit the curved profile of the roof. Connection details will be discussed later.

Figure 1 - Hale County Animal Shelter [2].

Figure 2 shows four different configurations for a lamella roof. This paper will focus on the segmental arch, where the profile of the roof follows a segment of a circle rather than a parabola or a gothic arch [3].

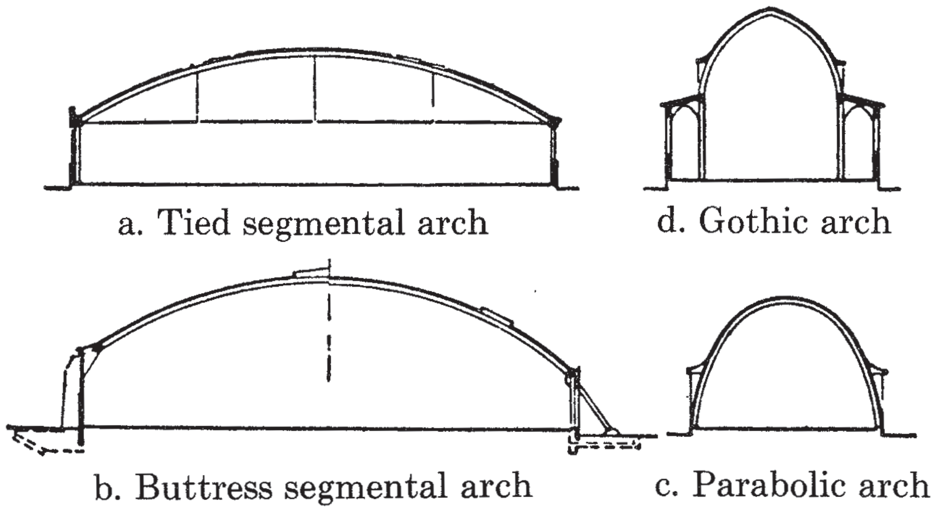

Figure 2 - Types of Lamella Roofs [3].

End support conditions, such as the tied arch or the buttressed arch, account for the resulting horizontal thrust in the springing ends of the arch [4]. While such supports should be taken into consideration in the roof design, it is beyond the scope of this project to delve into the different design calculations pertaining to each.

1.1 History of Lamella Construction

Lamella construction originated from the German architect Friedrich Zollinger (Figure 3) around 1920. Zollinger was appointed Town Building Advisor at Merseburg/Saale in 1918 at a time when Merseburg was experiencing a housing crunch [1].

Figure 3 - Friedrich Zollinger [5].

Because of the new ammonia factories and coal mines, thousands of workers moved to the city for work. Unsurprisingly, no new houses were built during World War I and there was a housing shortage for the new workers [1].

To solve this problem, architects of the time improved upon existing ideas or created new building techniques [5]. Zollinger created the "Zollbau Lamellen Dach" system, which utilized precast concrete panels and gothic arched roofs to create dwellings. He created the Merseburg Building Company which then went on to build over 1,250 apartments. Interestingly, the Zollbau method also encouraged the tenants of these flats to help out with construction and, given the assembly-line nature of the method, this was easy to achieve [1]. The Merseburg Building Company acquired material and land for the "self-help settlers" and also looked after the planning and organization of construction projects [5].

Zollinger applied for and received patents in Germany (1921), Australia (1922), and in the United Kingdom (1923). His patent documents show roofs using gothic arches and "a number of similar curved or straight wood, iron, or reinforced concrete units, bars, or battens" [1]. Figure 4 shows a drawing of a typical house built with the Zollbau method.

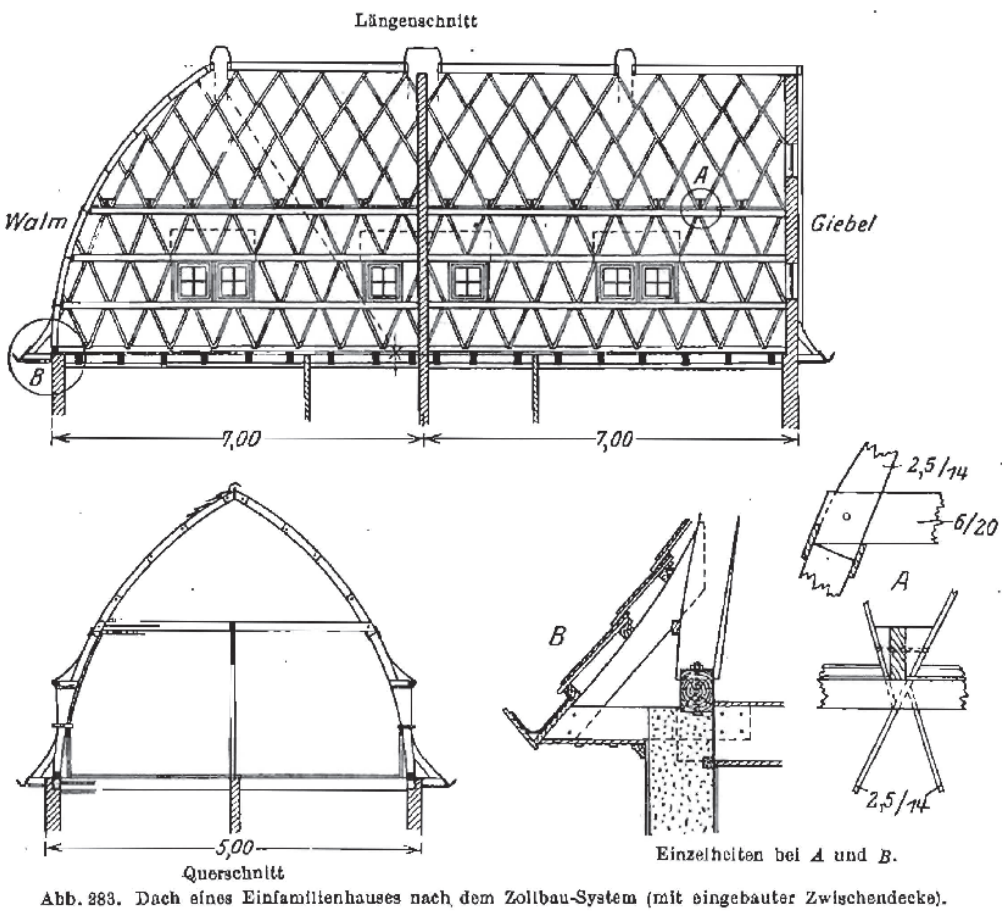

Figure 4 - Lamella Roof Using the Zollbau Method [6].

Over time Zollinger refined his Zollbau method for larger spans, such as for churches, schools, and large halls. The idea caught on in Europe and was used widely for arched roofs [1]. In 1925, the idea spread to America as well [3].

1.2 Previous Roof Failures

Due to the curve of the lamella roof, these structures are susceptible to failure from high wind loads. In 1926, hurricane winds caused the destruction of two lamella buildings in

Florida with one roof being torn off completely and deposited upside-down a few hundred feet away [1, 7].

Lamella roof construction was principally in use from its introduction by Zollinger up until the 1940s, with construction mostly halted because of wind failures. Engineers at the time used a wind load of 10 psf on the vertical projection for normal wind areas and 37.5 psf for high-wind regions. The latter wind pressure correlated with a 130 mph wind speed, the highest measured in that era [1].

In modern times, the wind loads on a curved roof are better known thanks to modern wind tunnel testing and computer simulations. It is now known that wind flowing over a curved roof creates uplift (similar to an aircraft wing), not simply a uniform horizontal load on the vertical projection. This creates a very different loading condition than the horizontal load which could potentially explain the failures of some lamella roofs in the first half of the 1900s.

2 Fabrication of Lamella Pieces

The advantage of the circular segmental lamella arch is that a lamella cut to fit the curve of the arch will fit anywhere on the arch. Because of this, if one creates a template for a lamella on the arch, this same template can be used for every lamella. The only difference is due to the right and left skew of the intersecting arches. Depending on the skew, the bevels on the lamella ends will have to be cut one way or the other. The left- and right-hand lamellas are mirror copies of each other, however. Figure 5 illustrates the difference in the left- and right-handed lamellas in that the bevel angles change direction based on the direction of skew.

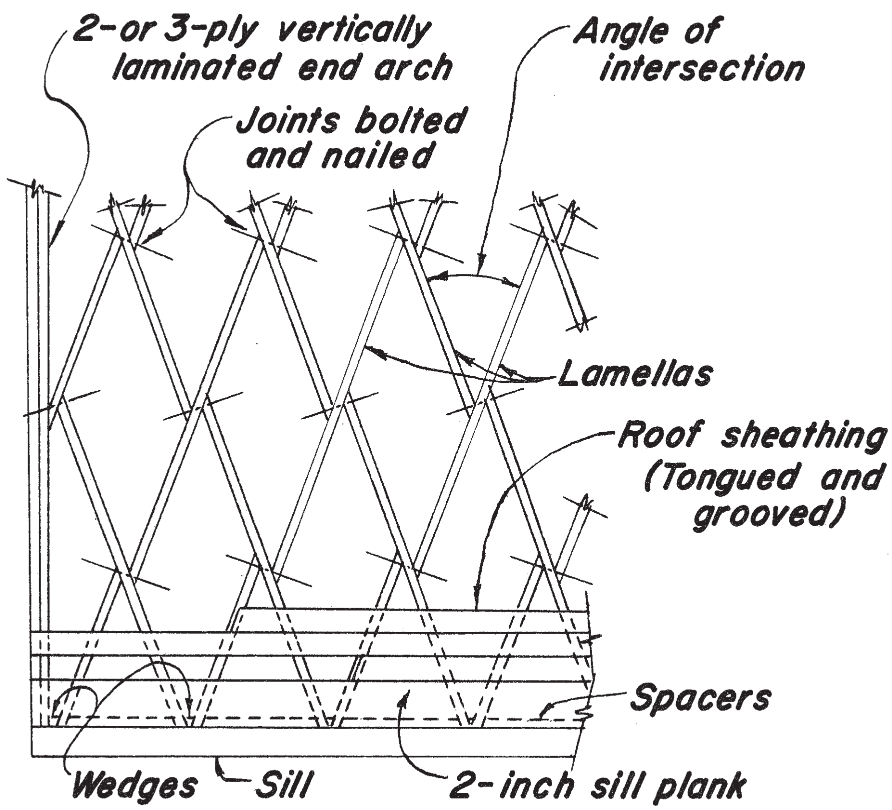

Figure 5 - Lamella Roof Plan View [3].

The designer most likely will know two properties of the arch: its span, *S,* and its rise, *T*. From this information, one can find the radius, *R* [8]:

$$R = \frac{4T^2 + S^2}{8T}. \tag{1}$$

Since the roof arch is circular, skewing the arch results in a lamella arch that follows an elliptical curve [4]. If the radius of the circular roof arch is given by *R* and the skew of the lamella arches is given by θ, the minor axis of the elliptical path the lamella arches follow has a length of *2R* and the length of the major axis would be given by

$$\ell_{major} = \frac{2R}{\cos\theta}. \tag{2}$$

The length of the individual lamella planks is a function of the load capacity of the plank, the curvature of the roof, and the general aesthetics of the roof design. Depending on the loading conditions of the roof, lamella sizes may need to be chosen based off of the load resistance capacity of the board cross-section.

A smaller radius of curvature of the roof limits the length that a lamella plank can reach depending on its depth. A board with a shallower depth will need to be shorter so that cutting out the curvature of the roof on the top of the plank still leaves enough depth on the ends for adequate connection detailing. Figure 6 depicts this relationship.

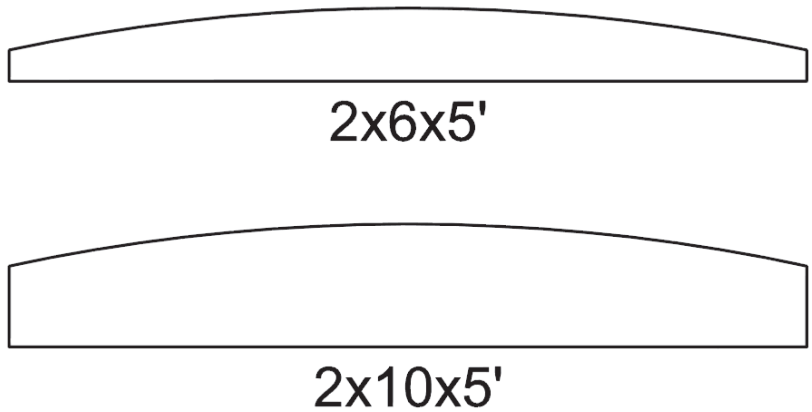

Figure 6 - Lamella Planks with a Radius of Curvature of 12 Feet.

From Figure 6, one can see that the 2x6 plank would not have adequate space on the ends for proper connection detailing while the 2x10 example with the same top radius of curvature would.

Several maximum length tables were developed by the author based on connection detailing considerations. These tables can be found in Appendix B pages 133-142. Section 2.1.1 delves into the connection considerations in more detail.

In designing for aesthetics, having too few boards making up the arch of the lamella roof would appear clunky, boxy, and awkward. Figure 7 illustrates this situation. The inside of the roof appears more angular and harsh and the lamellas themselves are hulking and ungainly. However, this roof uses less lamellas, requiring fewer connections and less labor to install. Also, since the spacing between lamellas increases, the load that each lamella takes on increases, necessitating an increase in size.

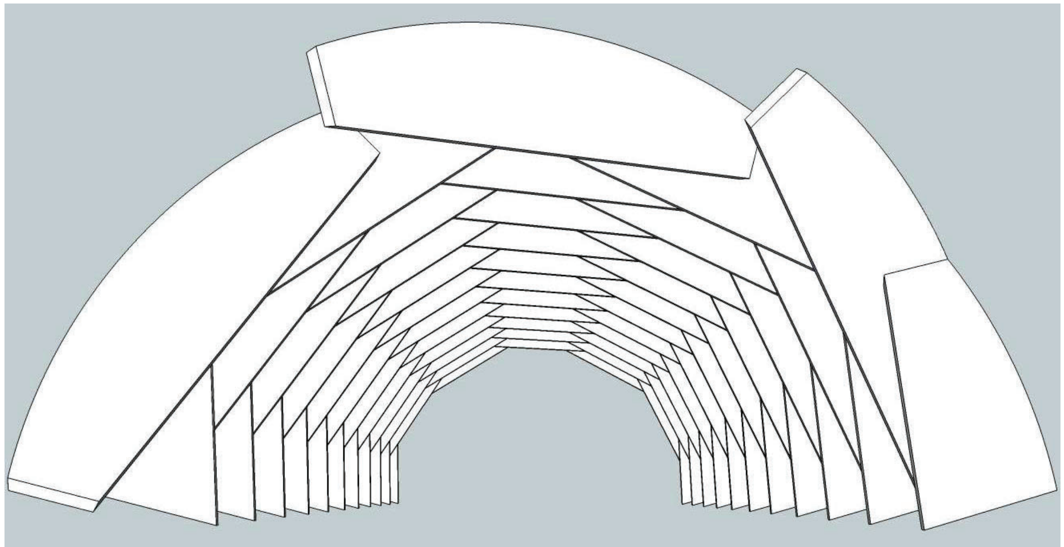

Figure 7 - Three Lamellas Per Arch.

Increasing the number of lamellas per arch makes for a more aesthetically pleasing roof structure. Figure 8 is an image of a lamella roof with nine lamellas per arch. Instead of the roof feeling boxy, the curves are more flowing and the lamellas themselves are more elegant and lithe. Less ceiling space is wasted with the extra depth of the deeper members from Figure 7, resulting in an eye-pleasing ceiling.

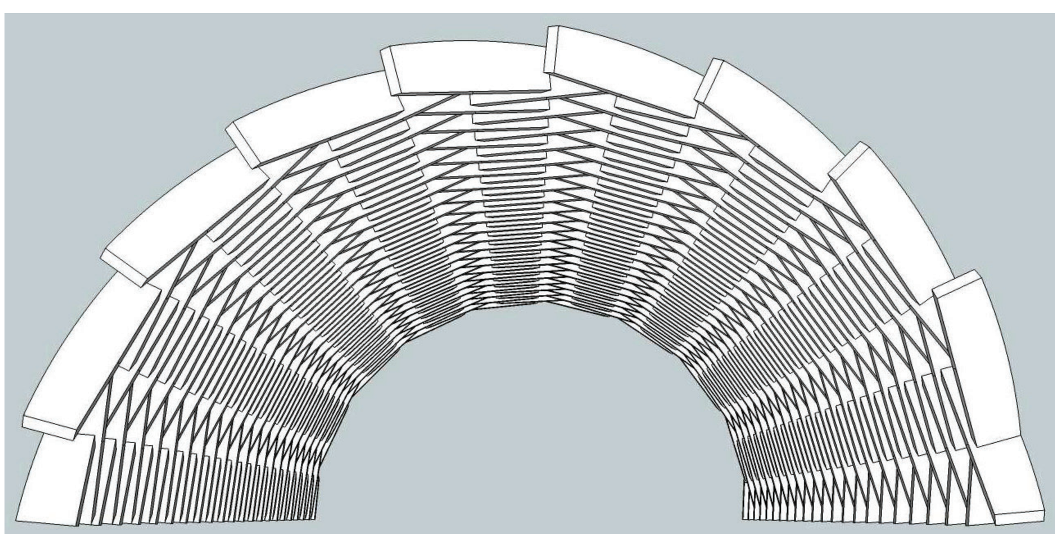

Figure 8 - Nine Lamellas Per Arch.

The number of lamellas per arch is up to the designer, though there is an upward bound on the number of lamellas that can fit into one arch. While having more planks per curve would reduce the spacing between them, resulting in lower loads per lamella which could reduce the necessary cross-section, this trade off may not be cost effective. The trick is finding the right balance between aesthetics and constructability.

2.1 Template Creation

Since the lamellas are essentially modular and can be used anywhere on the roof, creating a cut template is the most efficient means of mass-producing the lamellas. The following sections will further explain the parameters that go into the template creation.

2.1.1 Connection Requirements

Connections in lamella structures are generally handled by bolts or nails or some combination thereof. Depending on the size of the members, specially-made connection plates can also be used [3]. Figure 9 shows the two connection types.

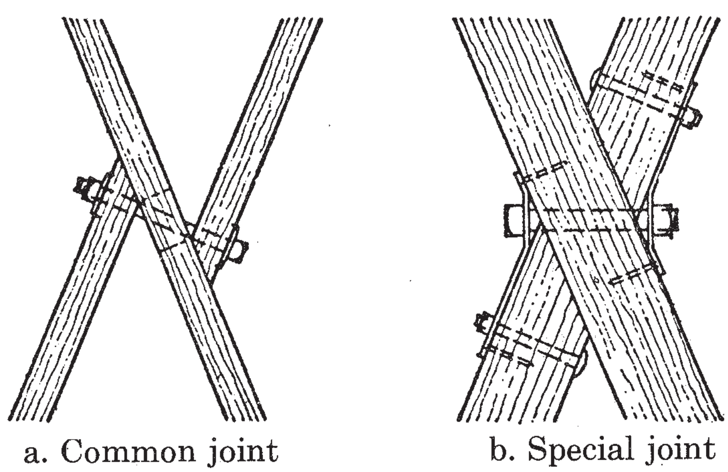

Figure 9 - Example Lamella Connections [3].

Generally, the connection detail labeled “Special joint” in Figure 9 is used for material thicknesses greater than three inches nominal [1]. These allow for the load paths in the lamellas to follow a concentric path which reduces the forces in the connections and the lamellas themselves, as opposed to the eccentric connection of the “Common joint.” Having the connection detail of the “Special joint” simplifies the connection to a simple compression connection [9]. Due to the fact that these types of connections need to be specially fabricated and engineered for each project, their design is beyond the scope of this project.

The National Design Specification for Wood Construction (NDS) specifies certain conditions that must be met for wood connections. The direction of the load path through the connection dictates the edge and end distances as well as bolt spacing. These conditions are tabulated in Tables 11.5.1A, 11.5.1B, 11.5.1C, and 11.5.1D of the NDS 2005 Specification, which are displayed in the Appendix A page 130-131 as well as in the rest of the section. These tables give the distances in a multiple of the connector dowel diameter, *D*.

Table 11.5.1A, shown in Figure 10, dictates the edge distance requirements. Though the primary load path is axial compression, there is still a bit of shear perpendicular to grain that must be accounted for.

Table 11.5.1A Edge Distance Requirements [1,2]

Direction of Loading	Minimum Edge Distance
Parallel to Grain:	
when $\ell/D \leq 6$	1.5D
when $\ell/D > 6$	1.5D or ½ the spacing between rows, whichever is greater
Perpendicular to Grain:[2]	
loaded edge	4D
unloaded edge	1.5D

1. The ℓ/D ratio used to determine the minimum edge distance shall be the lesser of:
   (a) length of fastener in wood main member/D = ℓ_m/D
   (b) total length of fastener in wood side member(s)/D = ℓ_s/D
2. Heavy or medium concentrated loads shall not be suspended below the neutral axis of a single sawn lumber or structural glued laminated timber beam except where mechanical or equivalent reinforcement is provided to resist tension stresses perpendicular to grain (see 3.8.2 and 10.1.3).

Figure 10 - Connection Edge Distance Requirements [10].

The loaded edge (top edge) of the lamella must have an edge distance of 4*D* while the bottom edge must have 1.5*D*. The second part of the parallel to grain consideration does not apply since the ℓ/D ratio will never be greater than six. A 2x member would need a bolt smaller than ¼″ for the ℓ/D ratio to exceed six; however, anything smaller than that would not be used in construction.

Tables 11.5.1B (Figure 11) and 11.5.1C (Figure 12) have two columns for the connection parameters. Choosing a distance from one of the columns instead of the others will affect the Geometry Factor C_Δ, which is a reduction factor used in determining dowel fastener connection strength. In order to make C_Δ equal to one, the minimum edge distances and fastener spacings must all be met.

Table 11.5.1B	**End Distance Requirements**	
	End Distances	
Direction of Loading	Minimum end distance for $C_\Delta = 0.5$	Minimum end distance for $C_\Delta = 1.0$
Perpendicular to Grain	2D	4D
Parallel to Grain, Compression: (fastener bearing away from member end)	2D	4D
Parallel to Grain, Tension: (fastener bearing towards member end)		
for softwoods	3.5D	7D
for hardwoods	2.5D	5D

Figure 11 - Connection End Distance Requirements [10].

Figure 11 displays the minimum end distances to the cut end of the board. Since the primary load on the lamella connections is a perpendicular to grain load through shear and compression parallel to grain from the axial load, the top two rows of the table in Figure 11 govern. While under wind loading there may be some tension developed due to uplift of the roof, this tension force is so much smaller than the compressive force that the connection, properly designed for the compressive load, will most likely be able to resist it anyway.

Table 11.5.1C	**Spacing Requirements for Fasteners in a Row**	
	Spacing	
Direction of Loading	Minimum spacing	Minimum spacing for $C_\Delta = 1.0$
Parallel to Grain	3D	4D
Perpendicular to Grain	3D	Required spacing for attached members

Figure 12 - Connection Spacing for Fasteners in a Row [10].

Understanding what “fasteners in a row” means is seen in Figure 13.

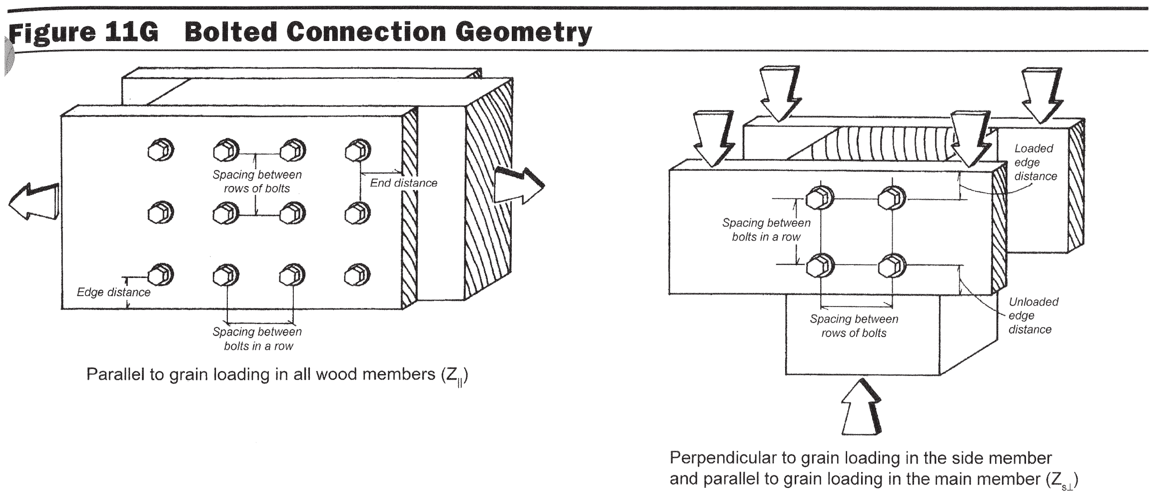

Figure 13 - Diagram of Bolt Spacing [10].

Determining “fasteners in a row” depends on the direction of load. Figure 13 shows how the direction of load changes the designation of spacing between rows and between bolts in a row. Figure 14 then shows the minimum distances for spacing between rows.

Table 11.5.1D Spacing Requirements Between Rows [1,2]

Direction of Loading	Minimum Edge Distance
Parallel to Grain:	1.5D
Perpendicular to Grain:	
when $\ell/D \leq 2$	2.5D
when $2 < \ell/D < 6$	$(5\ell + 10D) / 8$
when $\ell/D \geq 6$	5D

1. The ℓ/D ratio used to determine the minimum edge distance shall be the lesser of:
   (a) length of fastener in wood main member/D = ℓ_m/D
   (b) total length of fastener in wood side member(s)/D = ℓ_s/D
2. The spacing between outer rows of fasteners paralleling the member on a single splife plate shall not exceed 5" (see Figure 11H).

Figure 14 - Connection Spacing Between Rows [10].

Since the orientation of the row changes depending on the load path, one must take the greater of the two spacing conditions. Since the ratio of *ℓ/D* will never exceed six and the next highest spacing is $4D$ from Figure 12, the spacing between bolts in the lamella connection will, at most, be four times the bolt diameter. Whether or not the $2 < \ell/D < 6$ condition from Figure 14 will apply depends on the member thickness and bolt diameter and whether or not its associated minimum spacing will be greater than $4D$. For 2x lumber, this only happens with ¼″ bolts; because of this, using ¼″ bolts will result in having a C_Δ value of 1.0 for all cases.

Combining all of these requirements results in the following two connection details, shown in Figure 15 and Figure 16. One should note that the bolt connection line is at an angle to the perpendicular due to the geometry of the connection.

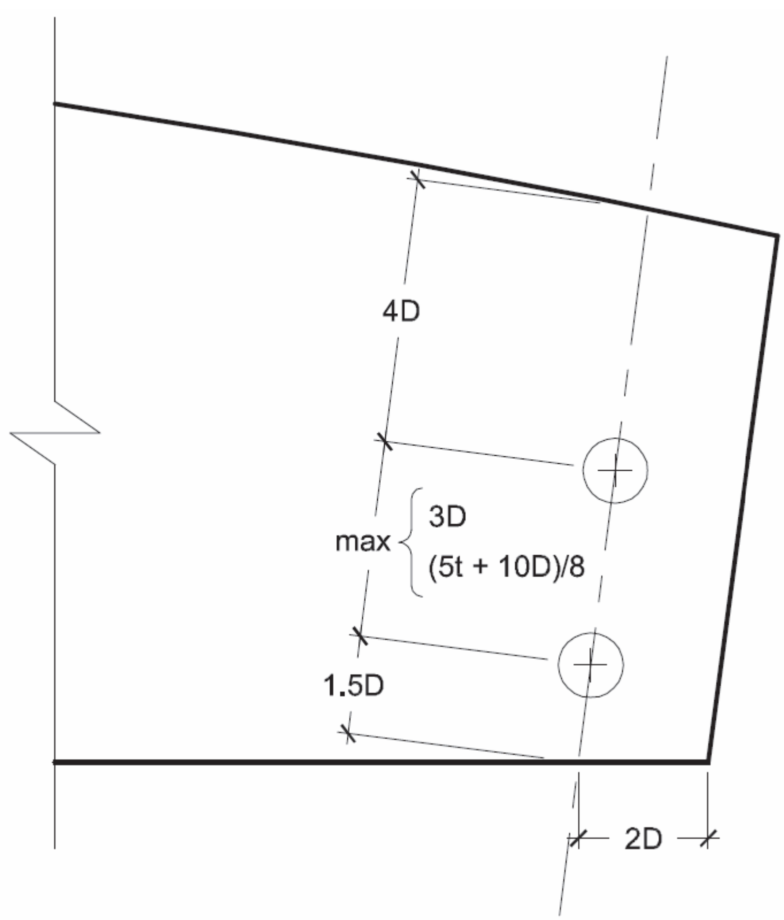

Figure 15 - Connection Detail for C_Δ = 0.5.

In most cases, the end distance requirement of 2*D* is already met or exceeded due to the bevel at the end of the lamella. Even with a bevel cut of 45°, a 2x member will still have about 2″ end distance, taking bolt diameter into consideration, adequate for even 1″ diameter bolts.

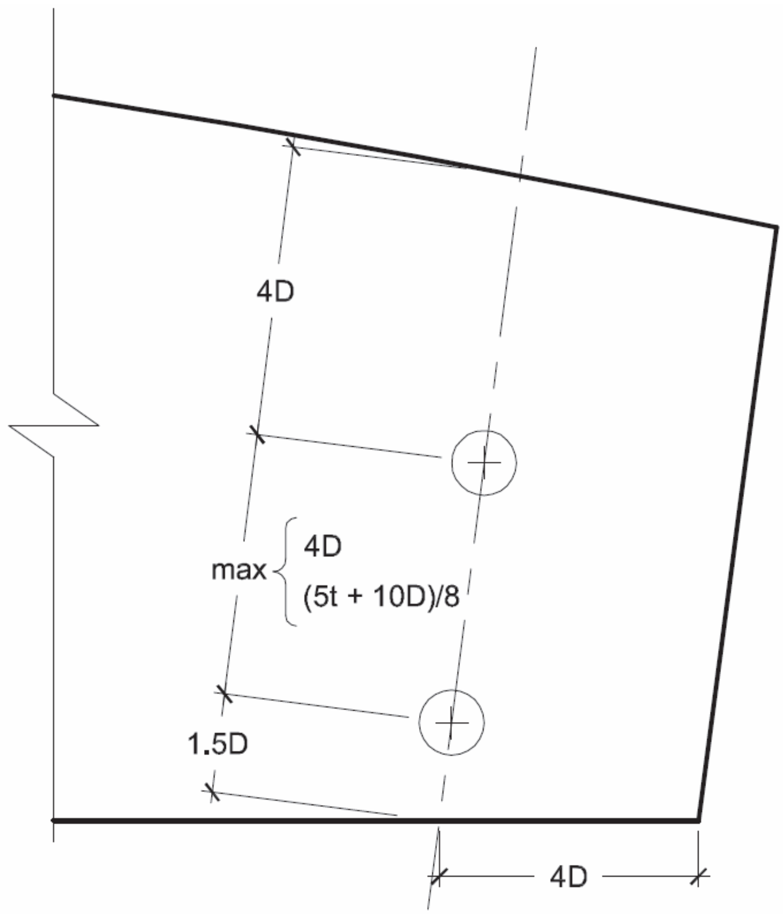

Figure 16 - Connection Detail for C_Δ = 1.0.

One may notice that the end distance requirement of 4*D* changes the geometry of the connection significantly. In order to keep the edge of the bolt on line with the end of the bevel (see Figure 17) and still comply with Figure 16, a 2x member will need bolts with a diameter equal to or smaller than one-half inch. A 3x member could have bolts as large as ⅞″ in diameter and still comply; however, 3x members would use the "Special joint" found in Figure 9 so the spacing found in Figure 15 and Figure 16 do not apply. Because of this, only connections using bolts smaller than those just listed can use a C_Δ value of 1.0.

One should note that although there are only two bolts shown in the connection on Figure 15 and Figure 16, having more than two bolts is perfectly acceptable so long as the minimum spacing and end distances are met.

Also, complying with the connection detail such that $C_\Delta = 1.0$ necessitates increasing the member depth to accommodate the increased spacing or using a shorter lamella while keeping the same radius of curvature on the top.

In order to connect the side lamellas through the continuous lamella, the middle of each lamella must have slotted holes.

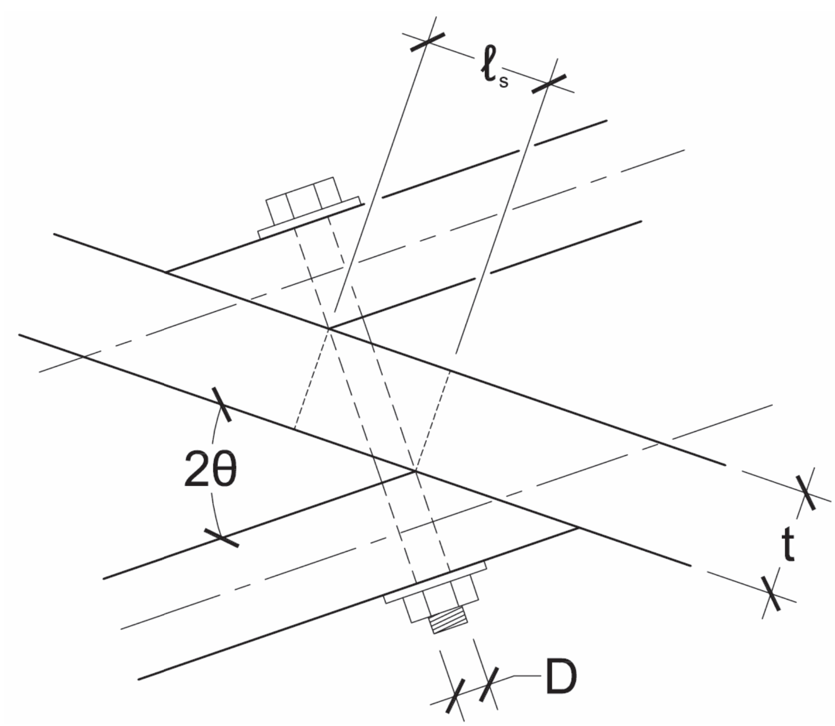

Figure 17 - Connection Slot Plan View.

The slots are located with the same spacing as the bolts. The slot length ℓ_s is

$$\ell_s = t\tan 2\theta + \frac{D}{\cos 2\theta} + 0.25''. \tag{3}$$

In the author's opinion, adding an extra quarter inch to the slot length will allow a little tolerance for fabrication error and make for easier construction.

Since the bolts on the ends can be in two configurations depending on the C_Δ value, so too can the slots. Figure 18 and Figure 19 show both configurations. The same spacing and end distances used on the end bolt connection should be used on the slots.

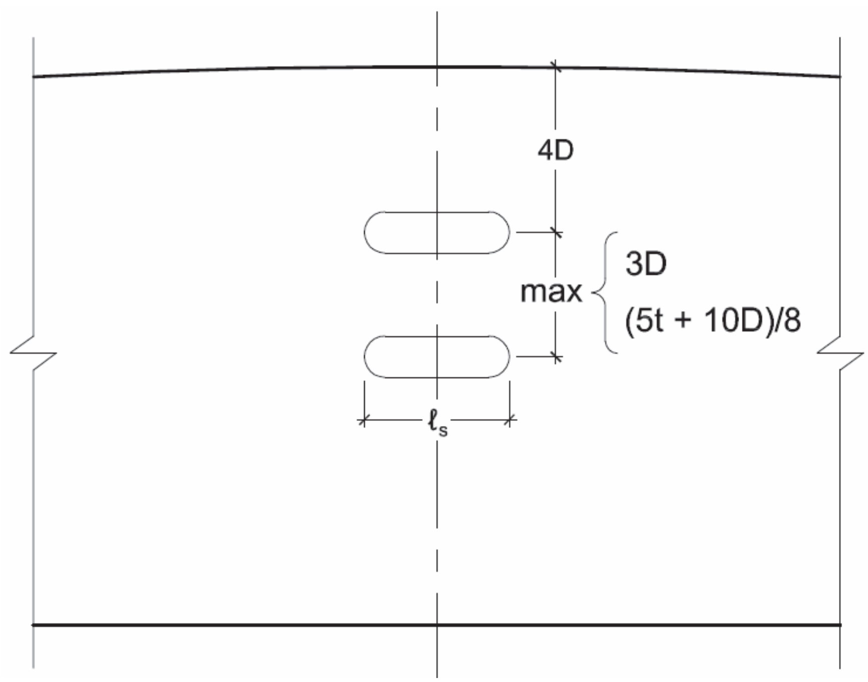

Figure 18 - Connection Slots Elevation View for C_Δ = 0.5.

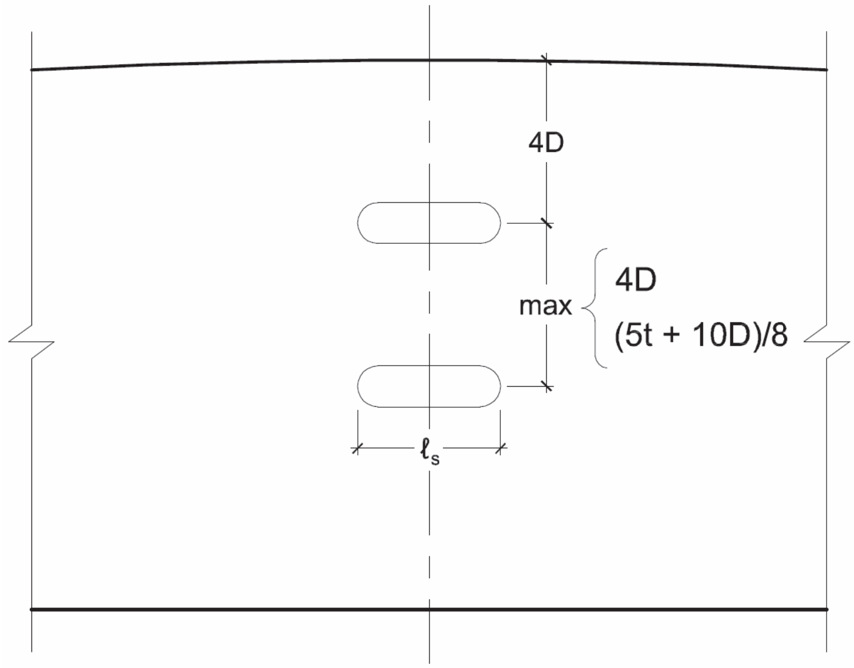

Figure 19 - Connection Slots Elevation View for C_Δ = 1.0.

2.1.2 Actual Lamella Length

The arc of the lamella roof is in itself a chord of a larger circle. Using simple trigonometry, one can find the angle β that this big arc subtends of the circle:

$$\beta = 2\arccos\left(\frac{R-T}{R}\right). \tag{4}$$

Figure 20 depicts this layout.

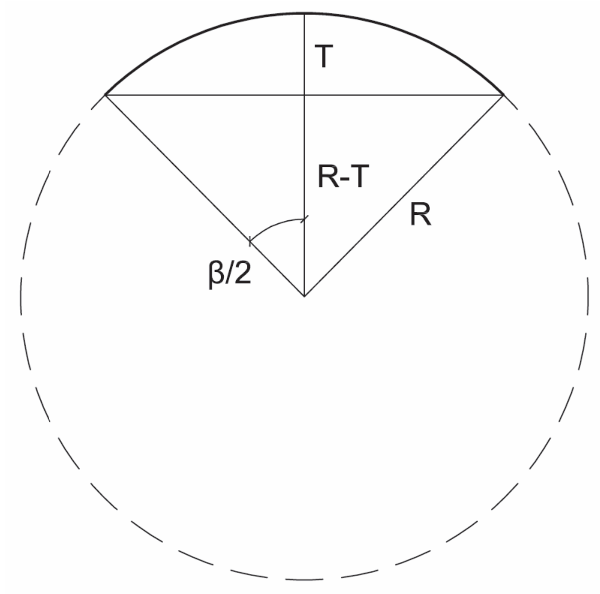

Figure 20 - Roof Arch as a Portion of a Circle.

From there, finding the length of the individual lamellas begins by choosing the number of lamellas, *n*, that the span of the roof arch. After doing so, one then divides the arch into a series of chords. The secant line between the ends of these chords is the center-to-center length of the lamella $\ell_{c\text{-}c}$, as shown in Figure 21.

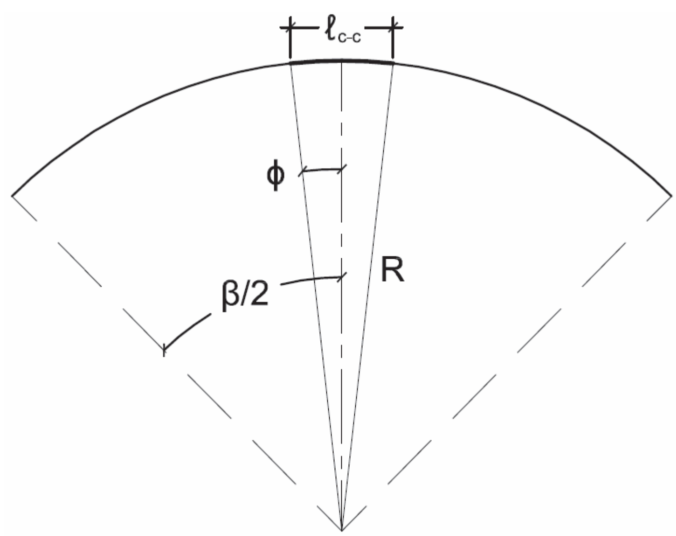

Figure 21 - Lamella as a Portion of the Roof Arch.

This secant line subtends a portion of the arc of the roof where the angle that it subtends is 2ϕ, found by

$$2\phi = \frac{\beta}{n} = \frac{2}{n}\arccos\left(\frac{R-T}{R}\right). \tag{5}$$

The center-to-center length is then found as

$$\ell_{c-c} = 2R\sin\phi. \tag{6}$$

From there, the spacing is simply

$$\text{Spacing} = \ell_{c-c}\tan\theta. \tag{7}$$

Then, the length of the lamella between bolt centerlines is

$$\ell = \frac{\ell_{c-c}}{\cos\theta} = \frac{2R\sin\phi}{\cos\theta}. \tag{8}$$

This length represents the length of the lamella from where its centerline crosses the centerline of the bolts. Combining Equations (7) and (8) results in Table 1.

Table 1 - Spacing of Lamellas with a Given Skew Angle.

Spacing of Lamellas with a Given Skew Angle								
Length	Skew Angle of Lamella Arch [θ] (deg)							
[ℓ] (ft)	19°	19.5°	20°	20.5°	21°	21.5°	22°	22.5°
3.0	0.98	1.00	1.03	1.05	1.08	1.10	1.12	1.15
3.5	1.14	1.17	1.20	1.23	1.25	1.28	1.31	1.34
4.0	1.30	1.34	1.37	1.40	1.43	1.47	1.50	1.53
4.5	1.47	1.50	1.54	1.58	1.61	1.65	1.69	1.72
5.0	1.63	1.67	1.71	1.75	1.79	1.83	1.87	1.91
5.5	1.79	1.84	1.88	1.93	1.97	2.02	2.06	2.10
6.0	1.95	2.00	2.05	2.10	2.15	2.20	2.25	2.30
6.5	2.12	2.17	2.22	2.28	2.33	2.38	2.43	2.49
7.0	2.28	2.34	2.39	2.45	2.51	2.57	2.62	2.68
7.5	2.44	2.50	2.57	2.63	2.69	2.75	2.81	2.87
8.0	2.60	2.67	2.74	2.80	2.87	2.93	3.00	3.06
8.5	2.77	2.84	2.91	2.98	3.05	3.12	3.18	3.25
9.0	2.93	3.00	3.08	3.15	3.23	3.30	3.37	3.44
9.5	3.09	3.17	3.25	3.33	3.40	3.48	3.56	3.64
10.0	3.26	3.34	3.42	3.50	3.58	3.67	3.75	3.83
10.5	3.42	3.50	3.59	3.68	3.76	3.85	3.93	4.02
11.0	3.58	3.67	3.76	3.85	3.94	4.03	4.12	4.21
11.5	3.74	3.84	3.93	4.03	4.12	4.21	4.31	4.40
12.0	3.91	4.01	4.10	4.20	4.30	4.40	4.50	4.59
12.5	4.07	4.17	4.28	4.38	4.48	4.58	4.68	4.78
13.0	4.23	4.34	4.45	4.55	4.66	4.76	4.87	4.97
13.5	4.40	4.51	4.62	4.73	4.84	4.95	5.06	5.17
14.0	4.56	4.67	4.79	4.90	5.02	5.13	5.24	5.36
14.5	4.72	4.84	4.96	5.08	5.20	5.31	5.43	5.55
15.0	4.88	5.01	5.13	5.25	5.38	5.50	5.62	5.74
15.5	5.05	5.17	5.30	5.43	5.55	5.68	5.81	5.93
16.0	5.21	5.34	5.47	5.60	5.73	5.86	5.99	6.12
16.5	5.37	5.51	5.64	5.78	5.91	6.05	6.18	6.31
17.0	5.53	5.67	5.81	5.95	6.09	6.23	6.37	6.51
17.5	5.70	5.84	5.99	6.13	6.27	6.41	6.56	6.70
18.0	5.86	6.01	6.16	6.30	6.45	6.60	6.74	6.89
18.5	6.02	6.18	6.33	6.48	6.63	6.78	6.93	7.08
19.0	6.19	6.34	6.50	6.65	6.81	6.96	7.12	7.27
19.5	6.35	6.51	6.67	6.83	6.99	7.15	7.30	7.46
20.0	6.51	6.68	6.84	7.00	7.17	7.33	7.49	7.65

Figure 22 shows a plan view of this situation while Figure 23 shows a detailed view.

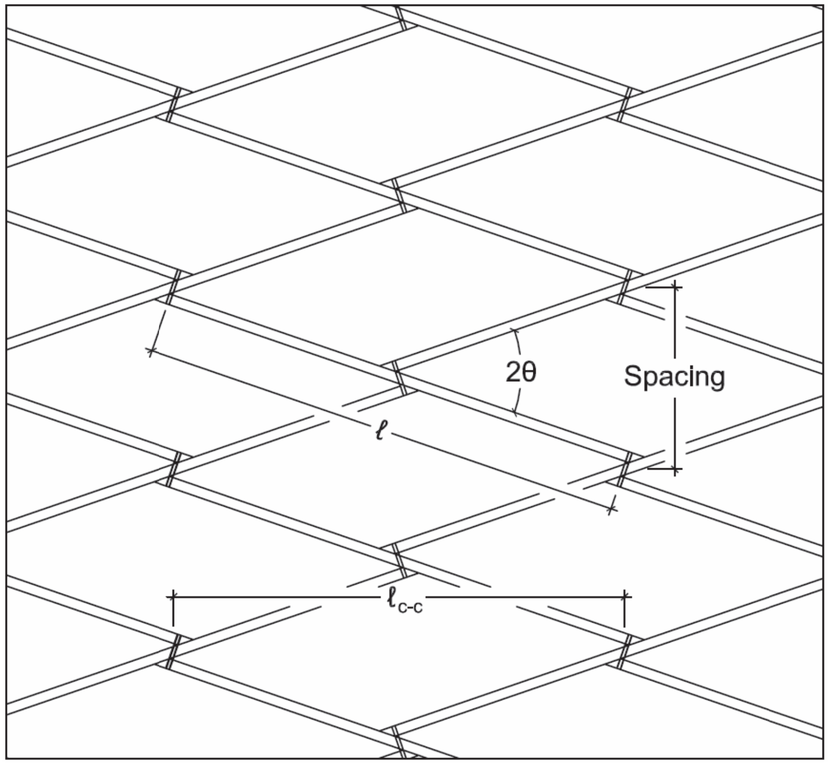

Figure 22 - Lamella Length and Spacing.

Since the lamellas are connected eccentrically, their length must be adjusted to take the eccentricity into account. The center-to-center length of the lamella is found by the designer by using Equation (6) and is used for calculations (see Section 5.2). The additional length is a function of the skew of the lamella arches, the diameter of the bolts, and the thickness of the lamellas themselves.

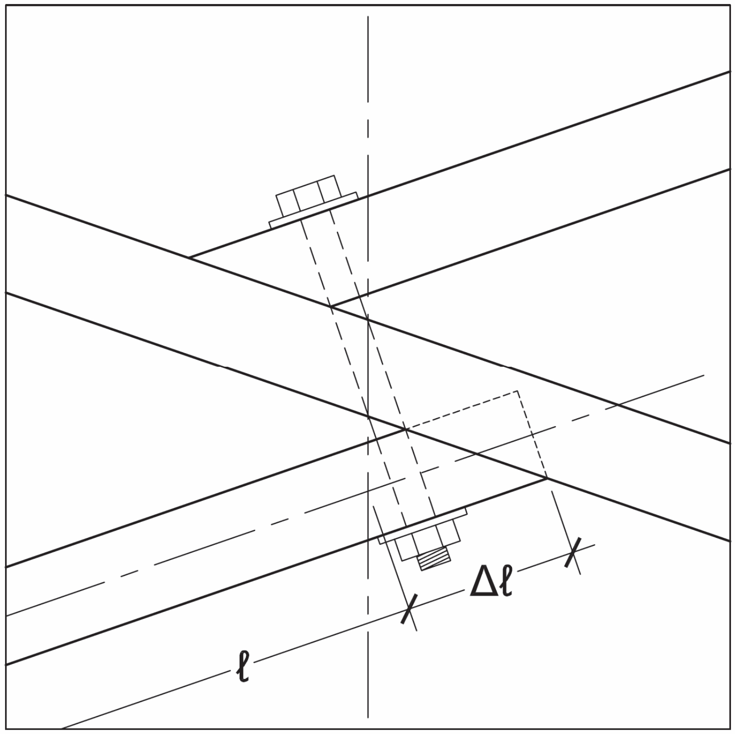

Figure 23 - Additional Length Due to Eccentricity.

This additional length, $\Delta\ell$, can be found through simple trigonometry, though the derivation is somewhat lengthy and thus omitted:

$$\Delta\ell = \frac{1}{2}\left[\frac{t + 2D\tan 2\theta}{2\sin\theta\cos\theta} + \frac{t}{\tan 2\theta}\right]. \tag{9}$$

Then, since this $\Delta\ell$ is added on each end of the lamella, the total lamella length becomes

$$\ell_T = \ell + 2\Delta\ell. \tag{10}$$

Substituting Equations (8) and (9) into Equation (10) yields

$$\ell_T = \frac{2R\sin\phi}{\cos\theta} + \frac{t + 2D\tan 2\theta}{2\sin\theta\cos\theta} + \frac{t}{\tan 2\theta}. \tag{11}$$

Now the lamella subtends an angle $2\phi_T$ in its own skewed plane, similar to Equation (5), where according to Warner [11],

$$\phi_T = \arcsin\left(\frac{\ell_T}{2R}\right). \tag{12}$$

After this, one must find the bevel angles on the ends of the lamellas. There are two that must be found – the radial bevel and the skew bevel. Warner goes through a derivation in his monograph that shows that for typical lamella roofs, where there are sufficient lamellas per arch such that ϕ_T is around or less than 10°, the radial bevel can be approximated to ϕ_T and the skew bevel to 2θ [11]. It should be noted that the bolt holes are also skewed to approximately the same ϕ_T angle. These two bevels are illustrated in Figure 24.

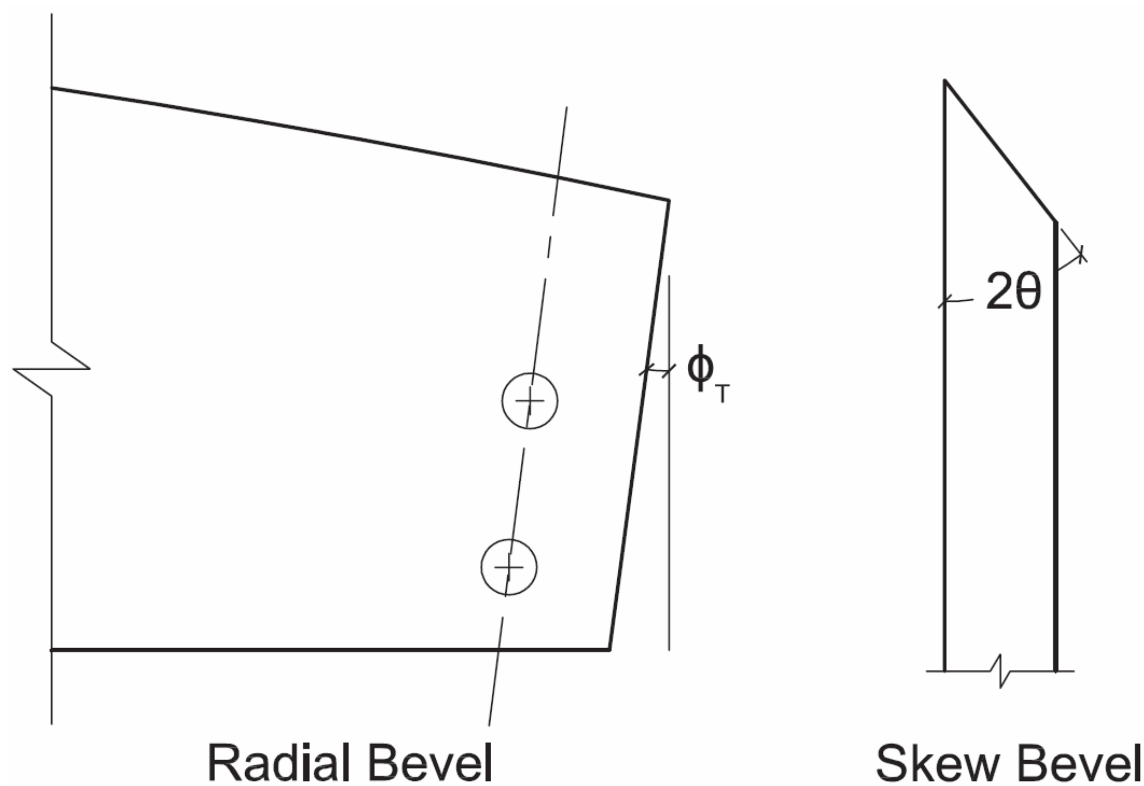

Figure 24 - Lamella End Bevels.

While one could firm down a more exact value for the bevel angles, expecting typical construction power tools to cut an angle to anything more precise than a whole number is impractical. The same holds true for the bolt line skew.

Another factor for constructability considerations is the "shift" of the connection, as illustrated in Figure 25.

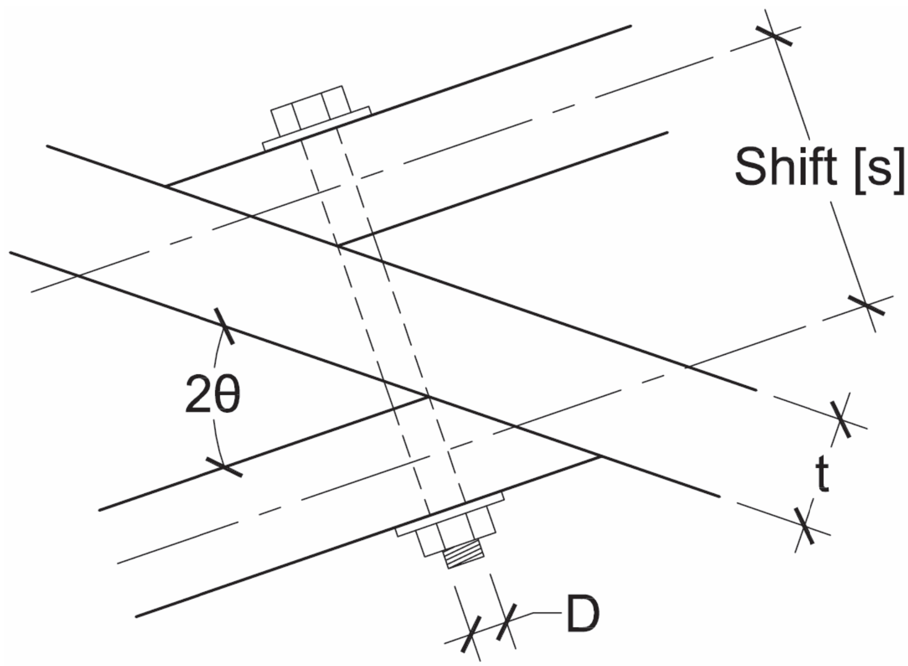

Figure 25 - "Shift" of the Lamella Connection.

The shift is determined by the thickness of the lamella, the skew angle of the lamella arch, and the bolt diameter. From trigonometry, the shift can be found by

$$s = D\tan 2\theta + \frac{t}{\cos 2\theta} + t, \tag{13}$$

or reduced, according to Masani [4], as

$$s = t\left(1 + \sec 2\theta\right) + D\tan 2\theta. \tag{14}$$

This information is easily tabulated as shown in Table 2. Note that this table only applies to 2x lumber with an actual thickness of 1.5 inches.

Table 2 - Lamella Connection Shift.

Shift of Lamellas with a Given Skew Angle [s] (in)								
Bolt Diameter	Skew Angle of Lamella Arch [θ] (deg)							
	19°	19.5°	20°	20.5°	21°	21.5°	22°	22.5°
1/4"	3.60	3.63	3.67	3.70	3.74	3.78	3.83	3.87
5/16"	3.65	3.68	3.72	3.76	3.80	3.84	3.89	3.93
3/8"	3.70	3.73	3.77	3.81	3.86	3.90	3.95	4.00
1/2"	3.79	3.84	3.88	3.92	3.97	4.02	4.07	4.12
5/8"	3.89	3.94	3.98	4.03	4.08	4.13	4.19	4.25
3/4"	3.99	4.04	4.09	4.14	4.19	4.25	4.31	4.37
7/8"	4.09	4.14	4.19	4.25	4.31	4.37	4.43	4.50
1"	4.18	4.24	4.30	4.36	4.42	4.48	4.55	4.62

From here one can determine the length of bolt needed for the connection by adding a thickness of lamella and extra for the nut and washers. An inch to an inch and half extra should suffice. Thus,

$$\ell_{bolt} \geq t\left(2+\sec 2\theta\right)+D\tan 2\theta+\left(\text{extra}\right)=s+t+\left(\text{extra}\right). \tag{15}$$

Obviously the builder would want to choose a length of bolt commonly available by manufacturers.

2.1.3 Top Curve Cut

When looking at a section view of the roof arch, the top curve of the lamella follows the same circular curve as the entire roof. However, since the lamellas themselves are skewed, the curvature on the top is elliptic.

Masani states that the elliptic curve on the top of the lamella can be approximated by a simple circular arc with a radius slightly larger than that of the roof itself [4]. This is probably due to the fact that since the lamella is so short in comparison to the entire curvature of the roof, the minute differences between the elliptic curve and the circular curve will be indistinguishable. In fact, when the author attempted to draw an illustration depicting the difference between the elliptic curve and the circular curve, the difference was so minute that unless he zoomed in very close, it was impossible to differentiate between the two.

This arc would have a span of ℓ_T and a rise of

$$T' = R - \frac{\ell_T}{2\tan\phi_T}, \tag{16}$$

along with a radius of

$$R' = \frac{4(T')^2 + \ell_T^2}{8(T')} = \frac{4\left(R - \frac{\ell_T}{2\tan\phi_T}\right)^2 + \ell_T^2}{8\left(R - \frac{\ell_T}{2\tan\phi_T}\right)}. \tag{17}$$

This arc would have a point of tangency at the midpoint of the lamella at the very top of the plank. The detail for the top curve is shown in Figure 26 (*d* is the depth of the lamella).

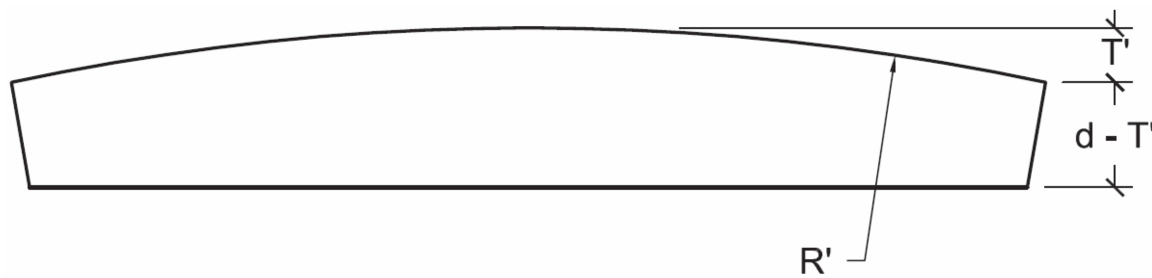

Figure 26 - Top Curvature Cut Detail.

3 Analysis of the Lamella Arch

Analysis of the lamella roof is carried out assuming that it acts like a two-hinged arch [1, 4]. Unfortunately, there exists no closed-form analytical solution for the moments, thrusts, and horizontal reactions of such an arch.

3.1 Arch Approximation Methods

Before the advent of calculators and computerized structural analysis packages, several approximate analytical methods were developed to solve for the forces in a two-hinged arch under a given loading condition. Two of those methods were the von Kármán Method and the Scofield Method. The author has also conducted a computer analysis of the arch using a finite element analysis method, which will also be discussed.

3.1.1 von Kármán Method

Sometime in the late 1930's Theodore von Kármán developed an approximate analysis for the two-hinged arch while working at the California Institute of Technology. His approximation assumes the arch follows a parabolic curve instead of a circular to simplify the derivations. As von Kármán developed this method while in California, it is perhaps not surprising that snow loading is not included; however, he includes radial loads from the structure weight, uniform vertical loads from live loads, and uniform horizontal loads from wind loads [12]. In the following sections, Equations (18) through (52) are taken from or derived from von Kármán's paper [12].

3.1.1.1 Live Load (Uniform Vertical Load)

For live loads, von Kármán replaces the uniform vertical load with a uniform perpendicular load (perpendicular to the curve of the arch along its entire length) and a uniform horizontal load along the vertical section, as depicted in Figure 27.

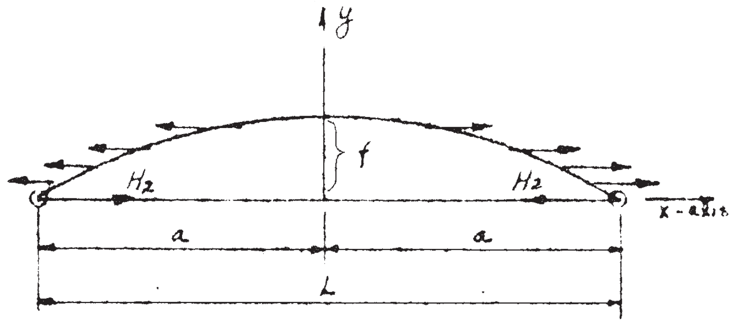

Figure 27 - Live Load Replacement [12].

The vertical reaction from the perpendicular load is

$$V_1 = pR\sin\phi_0 \tag{18}$$

where

$$\sin\phi_0 = \frac{a}{R} \tag{19}$$

so

$$V_1 = pR\left(\frac{a}{R}\right). \tag{20}$$

Since a is half the span, Equation (20) can be rewritten as

$$V_\ell = \frac{pS}{2}, \tag{21}$$

which should come as no surprise as it is the same as one would find through elementary statics from a uniform vertical load on the projected member length.

The horizontal reaction is a combination of the reaction due to the perpendicular load and the uniform vertical load. For this von Kármán writes

$$H_\ell = H_1 + H_2 = pR\cos\phi_0 + \frac{3}{7}pf. \tag{22}$$

Substituting

$$\cos\phi_0 = \frac{R-f}{R}, \tag{23}$$

the total horizontal reaction due to live load becomes

$$H_\ell = pR - \frac{4}{7}pf. \tag{24}$$

After this, the thrust at the springing points can then be approximately found as

$$T_\ell = p\left(R + \frac{3}{7}f\right). \tag{25}$$

The moment equation for the arch is

$$M_\ell = \frac{pf^2}{14}\left(1 - 8\frac{x^2}{a^2} + 7\frac{x^4}{a^4}\right), \tag{26}$$

but since a is half the arch span,

$$M_\ell = \frac{pf^2}{14}\left(1 - 32\frac{x^2}{S^2} + 112\frac{x^4}{S^4}\right). \tag{27}$$

At the center point of the arch the positive moment will be greatest. This is also the spot where x is equal to zero, which simplifies Equation (27) to

$$M_{\ell} = \frac{pf^2}{14}. \tag{28}$$

3.1.1.2 Dead Load (Radial Load)

For this analysis, the dead load q is defined as the load per unit length of the arc. Since the curvature of the arc changes with its distance from the centerpoint, the load on the horizontal projection of the arch also changes. Coincidentally, the dead load can be considered to have a load q plus an additional variably distributed load. This load increases as it gets closer to the springing points of the arch.

Because of this, the total horizontal reaction is the sum of the reaction from the uniform load and the reaction of the variable load:

$$H_d = H_3 + H_4, \tag{29}$$

where

$$H_3 = qR - \frac{4}{7}qf \tag{30}$$

and

$$H_4 = \frac{4}{21}qf. \tag{31}$$

Combining Equations (30) and (31), the equation for the dead load horizontal reaction becomes

$$H_d = qR - \frac{8}{21}qf. \tag{32}$$

Since the additional variably distributed load changes with distance from the center of the arch, the vertical component of the force in the arch also changes. The equation for the vertical component can be expressed as

$$V_{xd} = qx + q\frac{f}{R}\frac{x^3}{3a^2}. \tag{33}$$

At the arch springing points, x equals a, which makes the vertical reaction

$$V_d = qa\left(1 + \frac{f}{3R}\right). \tag{34}$$

Substituting half of the span for a yields

$$V_d = \frac{qS}{2}\left(1 + \frac{f}{3R}\right). \tag{35}$$

The thrust at any point in the arch can be found by

$$T_d = \sqrt{H_d^2 + V_{xd}^2}. \tag{36}$$

One can substitute Equations (32) and (34) for H_d and V_{xd} in the above equations, then solve for the sill thrust by substituting a for x:

$$T_d = q\sqrt{\left(R - \frac{8}{21}f\right)^2 + a^2\left(1 - \frac{f}{3R}\right)^2}, \tag{37}$$

which can be approximated as

$$T_d = q\left(R + \frac{13}{21}f\right). \tag{38}$$

Like the horizontal reaction, the moment due to dead load is also a combination of a uniform load and the variably distributed load:

$$M_d = M_3 + M_4, \tag{39}$$

where

$$M_3 = \frac{qf^2}{14}\left(1 - 8\frac{x^2}{a^2} + 7\frac{x^4}{a^4}\right) \tag{40}$$

and

$$M_4 = \frac{-qf^2}{42}\left(1 - 8\frac{x^2}{a^2} + 7\frac{x^4}{a^4}\right). \tag{41}$$

Combining these results in the dead load moment equation, we have

$$M_d = \frac{qf^2}{21}\left(1 - 8\frac{x^2}{a^2} + 7\frac{x^4}{a^4}\right). \tag{42}$$

Or, since a is half of the arch span,

$$M_d = \frac{qf^2}{21}\left(1 - 32\frac{x^2}{S^2} + 112\frac{x^4}{S^4}\right). \tag{43}$$

Also, the positive moment will be the greatest in the middle of the arch which is where x is equal to zero. At this point, the maximum positive moment is given by:

$$M_d = \frac{qf^2}{21}. \tag{44}$$

Here von Kármán comments that the dead load moment is 2/3 the live load moment with the same load magnitude.

3.1.1.3 *Wind Load (Uniform Vertical Load)*

The wind load acting on the arch is assumed to be a uniformly distributed vertical load w acting on the vertical projection of the arch, as shown in Figure 28.

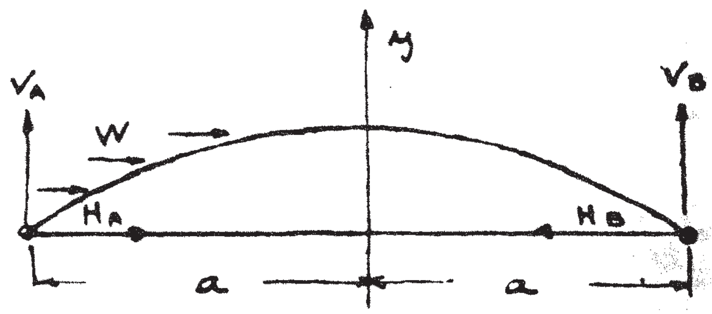

Figure 28 - Wind Load on the Arch [12].

The vertical reactions are equal and opposite and can be found through simple statics. They are:

$$V_A = -V_b = \frac{-wf^2}{4a}. \tag{45}$$

Since a is half of the span, Equation (45) becomes

$$V_A = -V_b = \frac{-wf^2}{2S}. \tag{46}$$

From here, the two horizontal reactions are found to be:

$$H_A = -\frac{5}{7}wf \tag{47}$$

and

$$H_B = \frac{2}{7}wf, \tag{48}$$

with the direction of each horizontal reaction being opposite that of the direction of the wind load, as expected.

The moment equation for the arch changes depending on which side of the arch is being examined. On the windward side of the arch, the moment formula is

$$M_w = \frac{wf^2}{28}\left[-1 - 7\frac{x}{a} + 8\left(\frac{x}{a}\right)^2 - 14\left(\frac{x}{a}\right)^4\right]. \tag{49}$$

If one substitutes half of the span for *a*, it becomes

$$M_w = \frac{wf^2}{28}\left[-1 - 14\frac{x}{S} + 32\left(\frac{x}{S}\right)^2 - 224\left(\frac{x}{S}\right)^4\right]. \tag{50}$$

On the leeward side of the arch, the moment formula is:

$$M_w = \frac{wf^2}{28}\left[-1 - 7\frac{x}{a} + 8\left(\frac{x}{a}\right)^2\right] \tag{51}$$

or

$$M_w = \frac{wf^2}{28}\left[-1 - 14\frac{x}{S} + 32\left(\frac{x}{S}\right)^2\right]. \tag{52}$$

3.1.2 Scofield Method

This method comes from the book *Modern Timber Engineering,* 5th ed. published in 1963 [3]. Scofield appears to partially base his design calculations on the von Kármán method. In this analysis, four primary load patterns are considered: radial loads from the dead weight of the structure, uniform vertical loads from live load, uniform horizontal loads from wind load, and uniform vertical loads on half of the structure from snow drift loads [3]. In the following sections, Equations (53) through (71) are from Scofield [3].

3.1.2.1 Dead Load (Radial Load)

The dead load on an arch acts upon its entire curved length, not just the projected horizontal length. The loading diagram appears in Figure 29.

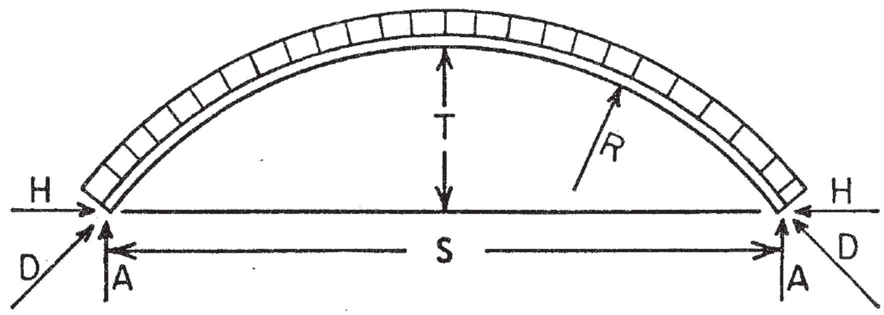

Figure 29 - Dead Load [3].

Scofield lists the following equations to solve for the arch forces:

$$A = 0.5dS\sqrt{1+\frac{16}{3}\left(\frac{T}{S}\right)^2}, \tag{53}$$

$$H = \frac{AS}{2T} - dR, \tag{54}$$

$$D = H\left(\frac{R-T}{R}\right) + \frac{AS}{2R}, \tag{55}$$

and

$$\text{Maximum M} = 0.068dT^2. \tag{56}$$

3.1.2.2 Construction Live Load (Uniform Vertical Load)

The loading for a construction live load, acts on the horizontal projection of the arch, making the vertical reactions easily solved by elementary statics. The loading diagram is shown in Figure 30.

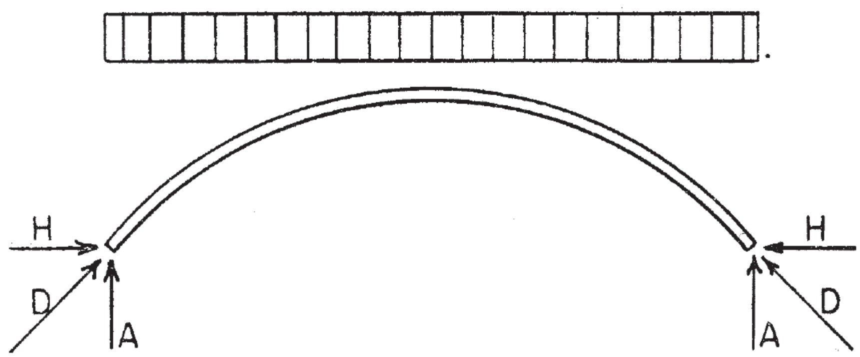

Figure 30 - Construction Live Load [3].

Equations (57) through (59) can be employed to calculate the roof live load forces:

$$A = 0.5 L_r S, \tag{57}$$

$$H = L_r \left(R - 0.57356T \right), \tag{58}$$

and

$$\text{Maximum M} = -0.09092 L_r T^2. \tag{59}$$

The thrust, *D,* is the same as Equation (55) in the radial load case.

3.1.2.3 Snow Drift Load (Uniform Vertical Load on Half of Structure)

Snow is assumed to accumulate on the leeward face of the lamella roof with a uniform weight distribution, as seen in Figure 31.

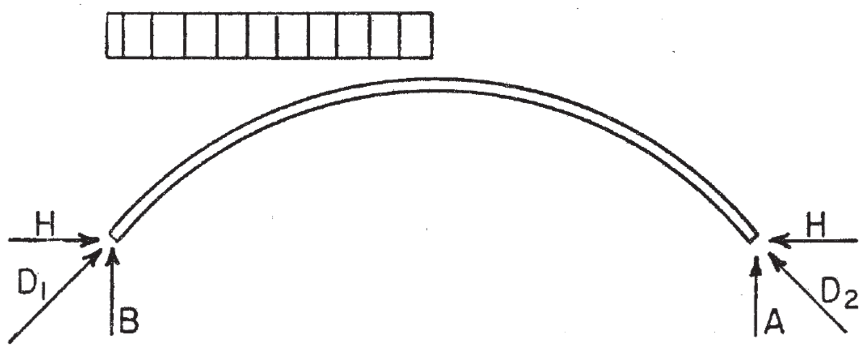

Figure 31 - Snow Drift Load [3].

The unbalanced loading creates unbalanced vertical support conditions, necessitating the addition of reaction *B*. This loading also creates two different thrusts, D_1 and D_2. Equations (60) through (65) are employed to determine the forces for the snow drift load:

$$A = \frac{sS}{8}, \tag{60}$$

$$B = \frac{3sS}{8}, \tag{61}$$

$$H = \frac{s}{2}\left(R - 0.57356T\right), \tag{62}$$

$$D_1 = H\left(\frac{R-T}{R}\right) + \frac{BS}{2R}, \tag{63}$$

$$D_2 = H\left(\frac{R-T}{R}\right) + \frac{AS}{2R}, \tag{64}$$

and

$$\text{Maximum M} = \frac{AS}{2} - HT - R\left(\sqrt{A^2 + H^2} - H\right). \tag{65}$$

3.1.2.4 Wind Load (Uniform Horizontal Load)

Wind is assumed to be uniformly distributed over the rise of the arch with the load projected on the height of the arch, as seen in Figure 32.

Figure 32 - Wind Load [3].

The horizontal load adds different vertical, horizontal, and thrust reactions at each springing point. These forces are:

$$A = -B = \frac{WT^2}{2S}, \tag{66}$$

$$H_1 = \frac{19WT}{64}, \tag{67}$$

$$H_2 = \frac{45WT}{64}, \tag{68}$$

$$D_1 = \frac{WT}{64}\left(13 - \frac{3T}{R}\right), \tag{69}$$

$$D_2 = \frac{WT}{64}\left(45 - \frac{29T}{R}\right), \tag{70}$$

and

$$\text{Maximum M} = 0.154WT^2. \tag{71}$$

3.1.3 Finite Element Method

As stated in Section 4.1, there is no closed-form analytical solution for the forces and reactions in an arch. The only way to truly "solve" for the forces and reactions is to perform a finite element analysis.

Beam elements are the finite elements of choice for this model. They are made up of individual linear elements with end reactions on the local x- and y-axes as well as moment reactions on either end, giving six degrees of freedom per element. Figure 33 depicts this layout.

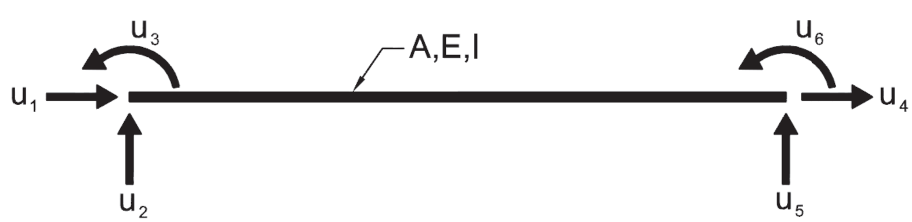

Figure 33 - Beam Element.

The author chose to approximate the lamella arch with 40 beam elements of the same length ℓ, cross-sectional area A, moment of inertia I, and modulus of elasticity E. The beam elements follow the curve of the arch with the nodes falling on the line of the circular arch, creating a series of secant lines. Obviously, the more beam elements used, the closer the analysis will be to the "exact" solution. However, 40 beam elements give a good enough approximation for design purposes.

Gravity loads are placed at the nodes between beam elements. To solve for the end reactions in the arch is a multi-step process. First, one must solve for the displacements of the nodal points [13]:

$$\tilde{U} = \tilde{K}^{-1}\tilde{F}. \tag{72}$$

These matrices have already been reduced to include only the unrestrained degrees of freedom (i.e., the end support conditions were removed). Once the nodal displacements are found, the end support conditions are added back into the $\tilde{U}$ matrix and the $\tilde{K}$ matrix is expanded to include the end stiffnesses. The nodal reactions at the springing ends are then found by [13]:

$$\tilde{F} = \tilde{K}\tilde{U}. \tag{73}$$

However, in order to do this process, one must begin with both the combined stiffness matrix $\tilde{K}$ and the combined force vector $\tilde{F}$. The $\tilde{K}$ matrix is made up of all the stiffness matrices from all the beam elements. The beam element stiffness matrix, $\tilde{k}$, is as follows [14]:

$$\tilde{k} = \begin{bmatrix} \frac{EA}{\ell} & 0 & 0 & \frac{-EA}{\ell} & 0 & 0 \\ 0 & \frac{12EI}{\ell^3} & \frac{6EI}{\ell^2} & 0 & \frac{-12EI}{\ell^3} & \frac{6EI}{\ell^2} \\ 0 & \frac{6EI}{\ell^2} & \frac{4EI}{\ell} & 0 & \frac{-6EI}{\ell^2} & \frac{2EI}{\ell} \\ \frac{-EA}{\ell} & 0 & 0 & \frac{EA}{\ell} & 0 & 0 \\ 0 & \frac{-12EI}{\ell^3} & \frac{-6EI}{\ell^2} & 0 & \frac{12EI}{\ell^3} & \frac{-6EI}{\ell^2} \\ 0 & \frac{6EI}{\ell^2} & \frac{2EI}{\ell} & 0 & \frac{-6EI}{\ell^2} & \frac{4EI}{\ell} \end{bmatrix}. \tag{74}$$

This stiffness matrix only applies when the beam element is oriented so that it runs parallel to the horizon. However, the 40 beam elements that approximate the arch are all rotated to different angles. A generalized image of the rotated beam elements is shown in Figure 34.

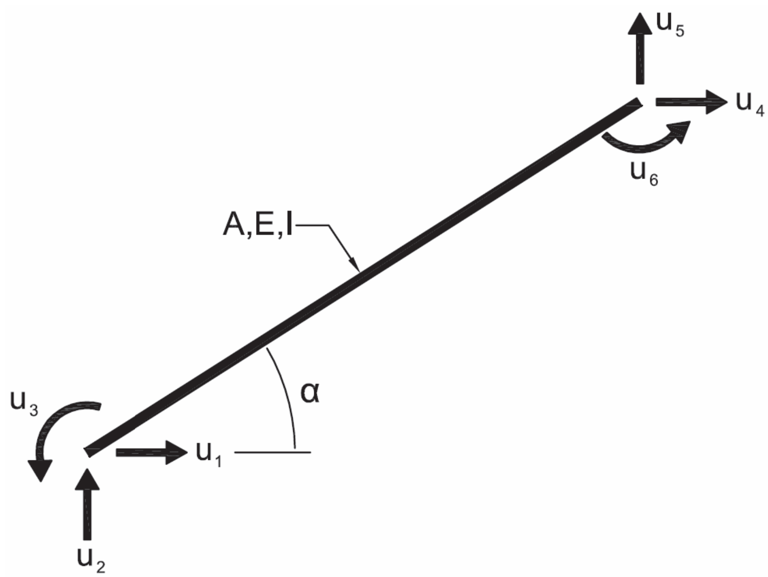

Figure 34 - Rotated Beam Element.

Since the 40 beam elements are all rotated to some degree, the stiffness matrix for each must be changed. To do this, the beam stiffness matrix must be multiplied by a transformation matrix as such [13]:

$$\tilde{k}_{rot} = \tilde{T}^T \tilde{k} \tilde{T}, \tag{75}$$

where

$$T = \begin{bmatrix} \cos\alpha & \sin\alpha & 0 & 0 & 0 & 0 \\ -\sin\alpha & \cos\alpha & 0 & 0 & 0 & 0 \\ 0 & 0 & 1 & 0 & 0 & 0 \\ 0 & 0 & 0 & \cos\alpha & \sin\alpha & 0 \\ 0 & 0 & 0 & -\sin\alpha & \cos\alpha & 0 \\ 0 & 0 & 0 & 0 & 0 & 1 \end{bmatrix}, \tag{76}$$

which gives the stiffness matrix for a beam element rotated to an angle α. This process must be carried out individually for all 40 beam elements in the arch. After that, all of the individual $\tilde{k}_{rot}$ matrices must be combined by aligning corresponding degrees of freedom [13]. This results in a $\tilde{K}$ matrix of size 123 x 123. Obviously, this matrix math is far too cumbersome to do manually, so computer aid is required.

The next part of the process is assembling the forces vector, $\tilde{F}$. As stated before, the uniform loads are converted to nodal loads at each of the nodes between beam elements. The loads are developed for the various load cases as described in the following subsections.

3.1.3.1 Dead Loads

The dead load is a function of the length of the beam elements adjacent to the corresponding node. Simply stated, the dead load acting on the node is the weight per unit length of the beam element (and other structure load assumed to be included with dead load) multiplied by half of the beam element length on either side of the node. If all beam elements are the same length, the nodal loads at every node besides the nodes at the springing points of the arch should be exactly the same. The loads at the springing point nodes should be exactly half of the loads on the rest of the nodes.

3.1.3.2 Live Load

The live load is a function of the horizontal projection of the beam elements around a node. As each beam element has some rotation of angle α, the horizontal component of the beam element is the beam element length multiplied by the cosine of the angle, or

$$\ell_x = \ell \cos \alpha. \tag{77}$$

The live load on a node will then be the product of the uniform vertical load and the sum of half of the horizontal components of the adjacent beam elements. These values will vary depending on the curvature of the arch. If the arch was flat, all of the nodal loads would be the same since the beam element horizontal components would be the same as their lengths.

3.1.3.3 Snow Loads

The loads due to snow come in two varieties: balanced snow loads (S_b) and unbalanced snow loads (S_u) or drift loads. Since the lamella roof is curved, this complicates things slightly in finding the balanced and unbalanced snow loads. To find these loads, section 7.4.3 of the ASCE 7-10 code was used. The code specifies that the loading diagrams for the different curvature cases should be based on Figure 7-3 of the ASCE 7-10 code, which can be found in Appendix C, page 144. The flat roof snow load, p_f, is used to find the sloped roof snow loads and can be found by

$$p_f = 0.7 C_e C_t I_s p_g, \tag{78}$$

where

$C_e =$ Exposure Factor,
$C_t =$ Temperature Factor,
$I_s =$ Importance Factor,
$p_g =$ Ground Snow Load.

To simplify calculations and the generation of load tables, some assumptions were made. The thermal factor C_t is assumed to be 1.2 based on ASCE 7-10, Table 7-3. The assumption is that the lamella roof will be covering an unheated space or one that is open to the air. This may not be true for all cases but will give the worst case for a conservative design. From this thermal factor, the slope factor C_s can be found from the graphs in Figure 35.

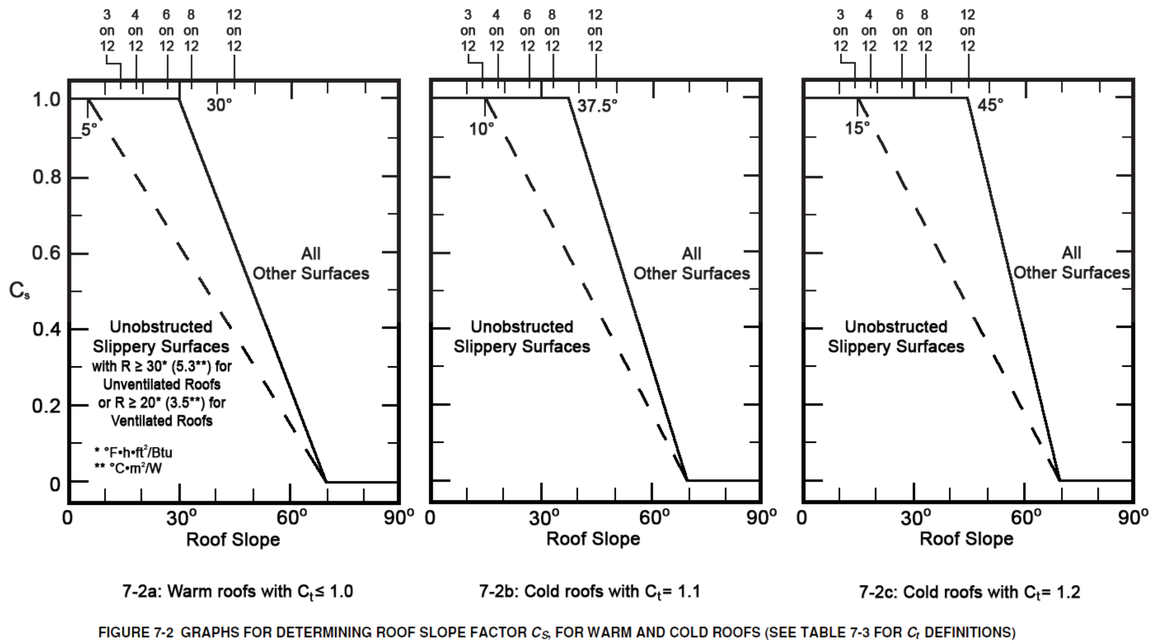

Figure 35 - Graphs for Determining Roof Slope Factor C_s [15].

Since the thermal factor is 1.2, the far right graph in Figure 35 must be used. Also, the roofing surface is assumed to not be an unobstructed slippery surface, demarked by the solid line.

ASCE Figure 7-3 (see Appendix C, page 144) has variables C_s^* and C_s^{**} used for calculations. For Case 1, C_s^* will be equal to 1.0, found by reading the rightmost chart above at an eave slope of 30°. From here, it is easy to see that C_s^{**} for all cases will also be 1.0, since that value is taken at a 30° slope, too. It is also assumed that the lamella roof will not be abutting any other structure so the alternate distribution for Case 2 and Case 3 in ASCE Figure 7-3 need not be used.

ASCE Figure 7-3 also necessitates finding the exposure factor C_e for the roof. This factor is listed in Table 7-2 of the ASCE 7-10 and ranges from 0.7 to 1.2. Here it is assumed that the lamella roof falls under Exposure Category C and that the structure is "Fully Exposed," giving a C_e value of 0.9 (see Appendix C, page 143 for Table 7-2). For the majority of buildings, this C_e value will be a conservative design value.

Using these assumptions, ASCE Figure 7-3 was adjusted by the author to become the Simplified Figure 7-3 found in Appendix C, page 145. The loading patterns from that table are used for snow load calculations.

The Importance Factor I_s for the roof is assumed to be 1.10, which correlates to a building that falls under Risk Category III.

Section 7.3.4 of the ASCE 7-10 also stipulates a Minimum Snow Load for Low-Slope Roofs, p_m. For curved roofs, this occurs when the angle between the springing end and the apex of the roof is less than ten degrees [15]. In order to ignore this case, loads were only calculated for roofs where that angle exceeds ten degrees. It should also be noted that for ground snow loads greater than 20 psf,

$$p_m = (20 \text{ psf}) I_s, \tag{79}$$

which would always be less than the p_f loads for anything over 30 psf.

3.1.3.4 Wind Loads

It should be noted that the wind loads stipulated in ASCE 7-10 are very generalized and most likely far greater than anything the building structure will ever experience. In many cases, lower wind loads can be found by doing wind tunnel testing with a scale model of the building and surrounding area, including other buildings and topological configurations. Since it is unrealistic to perform this analysis for every possible arch configuration, the approximate method from ASCE 7-10 is used.

Wind loads on the lamella roof are based on the Directional Procedure from ASCE 7-10, Chapter 27 [15]. First, one must find the velocity pressure:

$$q_z = 0.00256 K_z K_{zt} K_d V^2 \quad (\text{lb/ft}^2). \tag{80}$$

From this, the design wind pressures can be calculated:

$$p = qGC_p - q_i GC_{pi}. \tag{81}$$

The wind directionality factor, K_d, is given as 0.85 for an arched roof according to Table 26.6-1 in ASCE 7-10 [15]. It is assumed that the lamella structure is on flat ground with no topographic irregularities, so the topographic factor K_{zt} can be set equal to 1.0, as shown in Section 26.8.2 in ASCE 7-10 [15].

For ease of calculation, the building is assumed to be in Exposure Category C, the second-windiest Category. This means that the building is assumed to be in an area of flat, open country or flatlands. The next-windiest is Category D, which assumes conditions like open water and/or similar for over 5,000 feet upwind.

The Exposure Category affects the calculation of K_z, the velocity pressure exposure coefficient, as found by

$$K_z = \max\left[2.01\left(\frac{z}{z_g}\right)^{(2/\alpha)}, 2.01\left(\frac{15}{z_g}\right)^{(2/\alpha)}\right], \tag{82}$$

where z is the height above ground where the pressure is taken and z_g and α are two coefficients found in Table 26.9-1 of ASCE 7-10. For Exposure Category C, they are 900 and 9.5, respectively [15].

The Directional Procedure also specifies finding a Pressure Coefficient C_p for the structure. It specifies two different scenarios for an arched roof: one with the roof springing from an elevated wall and one with the roof springing from ground level. It is assumed that the lamella arch is part of a roof and thus springs from an elevated wall.

The arch acts kind of like the wing of an airplane in that the windward side receives downward pressure while the middle and leeward parts receive uplift. This loading scenario is presented in Figure 36, which graphically depicts that which is shown in ASCE 7-10 Figure 27.4-3. Areas that receive uplift have a negative value for C_p value. The windward and middle portions of the arch have a C_p value that is dependent on r, the ratio of the rise, R to the span, S [15].

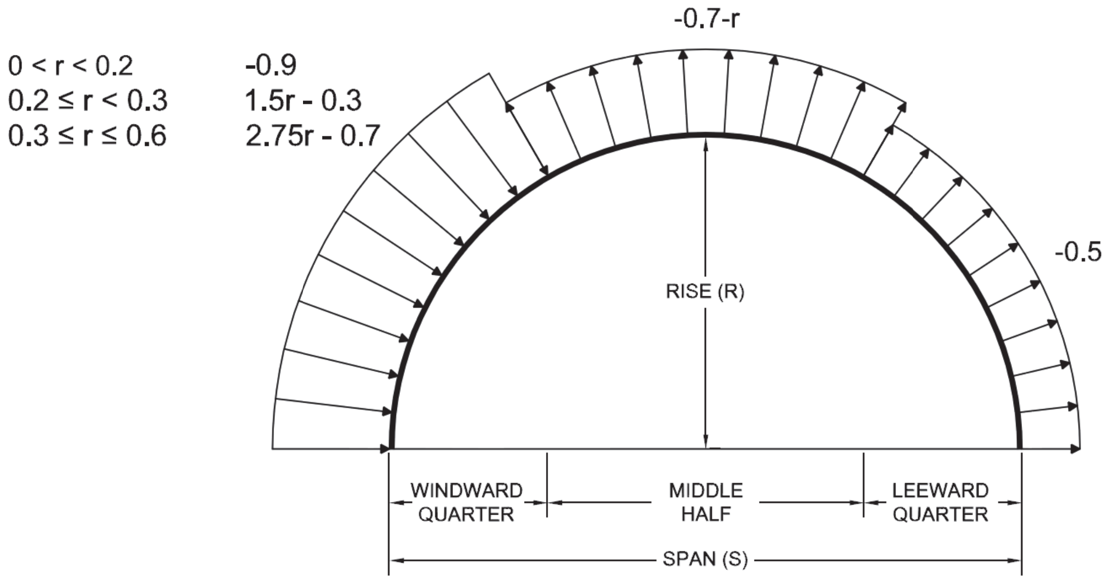

Figure 36 - Pressure Coefficients C_p for Arched Roof [15].

One can easily see the effect of uplift on the middle and leeward portions of the arched roof. It should also be noted that the C_p coefficient for the windward portion changes depending on the Rise-to-Span ratio.

The final necessary piece is the internal pressure coefficient GC_{pi}. It is assumed that the roof will be enclosed as per Section 26.10 in the ASCE 7-10. This gives a GC_{pi} value of ±0.18 according to Table 26.11-1.

It should also be noted that this procedure is only valid for buildings classified as "low-rise," meaning buildings under 60 feet in height. Because of this, the load tables developed by the author do not list rises above this 60-foot limit.

3.2 Comparison of Analysis Methods

The three analysis methods discussed previously will now be compared to see if the von Kármán method or the Scofield method can be used for a close approximation instead of a complicated computer analysis.

The methods were tested using an arch with the following characteristics:

- Risk Category III structure
- 40 ft span
- 10 psf dead load
- 120 mph wind zone (equates to 10 psf for von Kármán/Scofield)
- 30 psf ground snow
- 20 psf construction live load

The loads on the arch were found in intervals for rises between two and twenty feet. Since, in the finite element model, the moment capacity of the arch is dependent on the stiffness, two tables for each loading case were developed. One reflects a flexible arch with the ratio of the moment of inertia to the area (*I/A*) equal to one, and the other a stiff arch with the *I/A* ratio equal to one hundred.

For a comparison to real lumber shapes, a 24x24 sawn lumber member has the greatest *I/A* ratio at about 46. A 2x3 has the smallest *I/A* ratio at about 0.52 but is not a deep enough member to use for lamella construction. Any lumber with at least a 4 inch nominal depth has an *I/A* of at least 1.

In Table 3 through Table 10, the highlighted light grey cells feature values found through the von Kármán or Scofield methods, which are within ten percent of the FEA model values. Also note that entries with a positive percent difference have values higher than those from the FEA model and thus are conservative design values. These values are highlighted in dark gray. Essentially, any highlighted entries would be suitable approximations for the given Rise-to-Span ratio. Dashed entries are greater than 1000% difference.

3.2.1 Dead Loads

The values given by von Kármán and Scofield for the end reactions and arch thrusts are, for the most part, close to those found through the finite element analysis.

Table 3 - Flexible Arch Analyses Comparison for Dead Load.

Dead Load - Flexible Arch								
Rise/Span [r] (-)	von Kármán Method				Scofield Method			
	Vertical Reaction	Horizontal Reaction	Thrust	Moment	Vertical Reaction	Horizontal Reaction	Thrust	Moment
0.050	0.0%	0.3%	0.4%	310.1%	0.0%	0.4%	0.5%	485.6%
0.075	0.0%	0.2%	0.3%	-2.6%	0.0%	0.4%	0.5%	39.1%
0.100	-0.1%	0.1%	0.4%	-18.3%	0.0%	0.4%	0.7%	16.7%
0.125	-0.2%	0.2%	0.6%	-22.9%	0.0%	0.6%	1.0%	10.1%
0.150	-0.4%	0.3%	0.8%	-25.3%	-0.1%	0.8%	1.2%	6.7%
0.175	-0.6%	0.5%	1.0%	-27.1%	-0.1%	1.0%	1.5%	4.1%
0.200	-1.0%	0.8%	1.3%	-28.7%	-0.2%	1.3%	1.6%	1.7%
0.225	-1.6%	1.2%	1.5%	-30.4%	-0.3%	1.5%	1.8%	-0.6%
0.250	-2.2%	1.8%	1.8%	-32.1%	-0.4%	1.8%	1.8%	-3.0%
0.275	-3.0%	2.5%	2.1%	-33.8%	-0.5%	2.0%	1.8%	-5.4%
0.300	-3.9%	3.5%	2.4%	-35.4%	-0.7%	2.3%	1.6%	-7.8%
0.325	-5.0%	4.7%	2.6%	-37.1%	-0.9%	2.6%	1.5%	-10.2%
0.350	-6.2%	6.2%	2.9%	-38.8%	-1.1%	2.9%	1.2%	-12.6%
0.375	-7.5%	8.1%	3.2%	-40.4%	-1.3%	3.2%	0.9%	-15.0%
0.400	-8.9%	10.2%	3.4%	-42.1%	-1.6%	3.6%	0.5%	-17.3%
0.425	-10.3%	12.8%	3.7%	-43.6%	-1.8%	4.0%	0.1%	-19.5%
0.450	-11.9%	15.9%	4.0%	-45.1%	-2.1%	4.4%	-0.4%	-21.7%
0.475	-13.5%	19.5%	4.2%	-46.6%	-2.4%	4.9%	-0.9%	-23.8%
0.500	-15.1%	23.7%	4.5%	-48.0%	-2.7%	5.4%	-1.4%	-25.8%

The values for the von Kármán method are fairly close except for the moment calculation. Since few, if any, arched lamella roofs have such a small *r* ratio, it would be safe to say that the von Kármán method fails for the moment calculation. The values for the Scofield method match very well for all *r* values except for the moment entries, which are within range until the Rise is about one-quarter of the span.

Table 4 - Stiff Arch Analyses Comparison for Dead Load.

Dead Load - Stiff Arch								
Rise/Span [r] (-)	von Kármán Method				Scofield Method			
	Vertical Reaction	Horizontal Reaction	Thrust	Moment	Vertical Reaction	Horizontal Reaction	Thrust	Moment
0.050	0.0%	32.8%	31.3%	-	0.0%	32.9%	31.4%	-
0.075	0.0%	14.6%	13.5%	-	0.0%	14.8%	13.7%	-
0.100	-0.1%	8.3%	7.4%	-	0.0%	8.6%	7.7%	-
0.125	-0.2%	5.4%	4.7%	-	0.0%	5.8%	5.1%	-
0.150	-0.4%	3.9%	3.4%	564.9%	-0.1%	4.4%	3.9%	849.5%
0.175	-0.6%	3.2%	2.8%	72.3%	-0.1%	3.7%	3.2%	146.1%
0.200	-1.0%	2.8%	2.4%	12.3%	-0.2%	3.3%	2.8%	60.4%
0.225	-1.6%	2.8%	2.3%	-8.9%	-0.3%	3.2%	2.6%	30.1%
0.250	-2.2%	3.1%	2.4%	-18.9%	-0.4%	3.1%	2.4%	15.8%
0.275	-3.0%	3.7%	2.5%	-25.7%	-0.5%	3.2%	2.2%	6.1%
0.300	-3.9%	4.5%	2.6%	-30.3%	-0.7%	3.3%	1.9%	-0.4%
0.325	-5.0%	5.6%	2.8%	-33.6%	-0.9%	3.4%	1.6%	-5.2%
0.350	-6.2%	7.0%	3.0%	-36.4%	-1.1%	3.6%	1.3%	-9.2%
0.375	-7.5%	8.7%	3.3%	-38.7%	-1.3%	3.9%	1.0%	-12.5%
0.400	-8.9%	10.8%	3.5%	-40.8%	-1.6%	4.1%	0.5%	-15.5%
0.425	-10.3%	13.4%	3.8%	-42.7%	-1.8%	4.5%	0.1%	-18.2%
0.450	-11.9%	16.4%	4.0%	-44.5%	-2.1%	4.8%	-0.4%	-20.7%
0.475	-13.5%	19.9%	4.2%	-46.1%	-2.4%	5.3%	-0.9%	-23.1%
0.500	-15.1%	24.1%	4.5%	-47.6%	-2.7%	5.8%	-1.4%	-25.2%

Making the arch stiffer lowers the axial thrust in the arch, which in turn lowers the horizontal reaction. For this reason, there is more highlighted in dark gray in Table 4 as compared to Table 3, as the forces are being overestimated.

3.2.2 Live Loads

Surprisingly, the values predicted by the von Kármán and Scofield methods were both very close to the FEA analysis, except for the von Kármán moment. For the flexible arch (Table 5), the values for horizontal reaction were all within 1% of the FEA model. All of the thrust values for each analysis were either within 10% of the FEA model or at least overestimated the thrust for a conservative design.

Table 5 - Flexible Arch Analyses Comparison for Live Load.

Live Load - Flexible Arch						
Rise/Span [r] (-)	von Kármán Method			Scofield Method		
	Horizontal Reaction	Thrust	Moment	Horizontal Reaction	Thrust	Moment
0.050	0.3%	0.4%	101.9%	0.3%	0.4%	157.0%
0.075	0.1%	0.4%	-8.2%	0.1%	0.3%	16.8%
0.100	0.1%	0.6%	-18.2%	0.1%	0.4%	4.1%
0.125	0.1%	1.1%	-20.5%	0.0%	0.5%	1.2%
0.150	0.0%	1.7%	-21.3%	0.0%	0.6%	0.2%
0.175	0.0%	2.6%	-21.6%	0.0%	0.7%	-0.1%
0.200	0.1%	3.8%	-21.6%	0.0%	0.7%	-0.3%
0.225	0.1%	5.3%	-21.6%	0.0%	0.8%	-0.3%
0.250	0.1%	7.1%	-21.6%	0.0%	0.8%	-0.2%
0.275	0.1%	9.2%	-21.5%	0.0%	0.7%	-0.1%
0.300	0.2%	11.6%	-21.4%	0.0%	0.6%	0.1%
0.325	0.2%	14.3%	-21.2%	0.0%	0.5%	0.2%
0.350	0.3%	17.3%	-21.1%	0.0%	0.3%	0.4%
0.375	0.3%	20.6%	-20.9%	0.1%	0.1%	0.7%
0.400	0.4%	24.1%	-20.7%	0.1%	-0.2%	0.9%
0.425	0.5%	27.5%	-20.6%	0.2%	-0.8%	1.1%
0.450	0.7%	30.8%	-20.4%	0.3%	-1.6%	1.4%
0.475	0.8%	33.9%	-20.3%	0.4%	-2.9%	1.5%
0.500	1.0%	36.8%	-20.3%	0.5%	-4.2%	1.5%

Unfortunately, the moments predicted by the von Kármán method were almost all far too low to be acceptable approximations. However, almost all of the moments found in the Scofield method were within the 10% margin, which demonstrates that the Scofield method accurately predicts the forces in a flexible arch for live load.

Similar to the results in Table 4, Table 6 for the stiff arch shows that the forces predicted by the two approximation methods are overestimates.

Table 6 - Stiff Arch Analyses Comparison for Live Load.

Live Load - Stiff Arch						
Rise/Span [r] (-)	von Kármán Method			Scofield Method		
	Horizontal Reaction	Thrust	Moment	Horizontal Reaction	Thrust	Moment
0.050	32.8%	31.3%	-	32.8%	31.3%	-
0.075	14.6%	13.6%	-	14.6%	13.5%	-
0.100	8.2%	7.6%	-	8.2%	7.3%	-
0.125	5.3%	5.2%	-	5.2%	4.6%	-
0.150	3.7%	4.4%	167.2%	3.6%	3.2%	240.1%
0.175	2.7%	4.4%	38.4%	2.7%	2.4%	76.2%
0.200	2.1%	5.0%	7.1%	2.0%	1.9%	36.3%
0.225	1.7%	6.1%	-4.7%	1.6%	1.6%	21.3%
0.250	1.4%	7.7%	-11.3%	1.3%	1.3%	12.9%
0.275	1.2%	9.6%	-14.8%	1.1%	1.1%	8.4%
0.300	1.1%	11.9%	-16.8%	0.9%	0.9%	5.9%
0.325	1.0%	14.5%	-18.0%	0.8%	0.7%	4.3%
0.350	1.0%	17.5%	-18.8%	0.7%	0.4%	3.4%
0.375	0.9%	20.7%	-19.2%	0.7%	0.2%	2.9%
0.400	1.0%	24.2%	-19.4%	0.7%	-0.1%	2.6%
0.425	1.0%	27.6%	-19.5%	0.7%	-0.8%	2.4%
0.450	1.1%	30.9%	-19.6%	0.7%	-1.6%	2.4%
0.475	1.2%	33.9%	-19.6%	0.8%	-2.8%	2.4%
0.500	1.3%	36.9%	-19.7%	0.8%	-4.2%	2.2%

3.2.3 Wind Load

Since the wind loading assumed by the von Kármán and Scofield methods is completely different than the loading dictated by ASCE 7-10, the values for the arch forces are nowhere near those found with the finite element analysis. There is no way one could use the approximation methods for wind loads.

Table 7 - Flexible Arch Analyses Comparison for Wind Load.

Wind Load - Flexible Arch						
Rise/Span [r] (-)	von Kármán Method			Scofield Method		
	Horizontal Reaction	Thrust	Moment	Horizontal Reaction	Thrust	Moment
0.050	-99.5%	-99.5%	-99.6%	-99.5%	-99.5%	-98.1%
0.075	-98.9%	-99.0%	-99.1%	-98.9%	-98.9%	-96.1%
0.100	-98.2%	-98.2%	-98.5%	-98.1%	-98.2%	-93.7%
0.125	-97.3%	-97.3%	-97.9%	-97.2%	-97.3%	-91.1%
0.150	-96.2%	-96.3%	-97.3%	-96.1%	-96.3%	-88.4%
0.175	-95.1%	-95.1%	-96.7%	-94.9%	-95.3%	-85.7%
0.200	-94.0%	-94.0%	-96.1%	-93.7%	-94.3%	-83.1%
0.225	-92.8%	-92.8%	-95.5%	-92.6%	-93.4%	-80.8%
0.250	-91.3%	-90.9%	-95.3%	-91.0%	-91.9%	-79.8%
0.275	-90.2%	-89.6%	-94.9%	-89.9%	-91.0%	-78.1%
0.300	-89.3%	-88.4%	-94.6%	-88.9%	-90.2%	-76.7%
0.325	-88.4%	-87.2%	-94.3%	-88.0%	-89.5%	-75.5%
0.350	-87.7%	-86.1%	-94.1%	-87.2%	-89.0%	-74.7%
0.375	-86.6%	-83.7%	-94.2%	-86.1%	-87.5%	-75.0%
0.400	-86.1%	-82.8%	-94.1%	-85.6%	-87.1%	-74.7%
0.425	-85.8%	-82.0%	-94.1%	-85.3%	-86.9%	-74.6%
0.450	-85.6%	-81.3%	-94.1%	-85.0%	-86.9%	-74.6%
0.475	-85.1%	-78.7%	-94.3%	-84.5%	-85.5%	-75.3%
0.500	-85.0%	-78.2%	-94.3%	-84.4%	-85.6%	-75.6%

Table 8 - Stiff Arch Analyses Comparison for Wind Load.

Wind Load - Stiff Arch						
Rise/Span [r] (-)	von Kármán Method			Scofield Method		
	Horizontal Reaction	Thrust	Moment	Horizontal Reaction	Thrust	Moment
0.050	-99.4%	-99.4%	-97.6%	-99.3%	-99.3%	-89.7%
0.075	-98.8%	-98.8%	-98.4%	-98.7%	-98.8%	-92.9%
0.100	-98.0%	-98.1%	-98.0%	-98.0%	-98.0%	-91.5%
0.125	-97.1%	-97.2%	-97.5%	-97.0%	-97.2%	-89.3%
0.150	-96.1%	-96.2%	-97.0%	-96.0%	-96.2%	-86.9%
0.175	-95.0%	-95.0%	-96.4%	-94.8%	-95.2%	-84.5%
0.200	-93.9%	-93.9%	-95.9%	-93.6%	-94.3%	-82.2%
0.225	-92.7%	-92.7%	-95.4%	-92.4%	-93.3%	-80.0%
0.250	-91.2%	-90.8%	-95.2%	-90.9%	-91.8%	-79.2%
0.275	-90.2%	-89.6%	-94.8%	-89.8%	-90.9%	-77.6%
0.300	-89.2%	-88.3%	-94.5%	-88.8%	-90.2%	-76.3%
0.325	-88.4%	-87.2%	-94.3%	-87.9%	-89.5%	-75.2%
0.350	-87.6%	-86.0%	-94.1%	-87.1%	-88.9%	-74.4%
0.375	-86.5%	-83.7%	-94.2%	-86.0%	-87.4%	-74.9%
0.400	-86.1%	-82.7%	-94.1%	-85.6%	-87.1%	-74.5%
0.425	-85.8%	-81.9%	-94.1%	-85.2%	-86.9%	-74.4%
0.450	-85.5%	-81.2%	-94.1%	-85.0%	-86.8%	-74.5%
0.475	-85.0%	-78.7%	-94.3%	-84.4%	-85.5%	-75.2%
0.500	-85.0%	-78.2%	-94.3%	-84.4%	-85.6%	-75.6%

3.2.4 Snow Drift Load

The loading pattern for snow drifts followed by Scofield is similar to the one stipulated in ASCE 7-10 in that they only affect one half of the arch. After that, the similarities end. ASCE takes into account snow piling and snow slipping due to the roof curvature, whereas Scofield just assumed the drift was a uniform lineal load.

Table 9 - Flexible Arch Analyses Comparison for Snow Drift Load.

Snow Drift Load - Flexible Arch				
Rise/Span [r] (-)	Scofield Method			
	Vertical Reaction	Horizontal Reaction	Thrust	Moment
0.050	8.9%	41.3%	39.6%	2.2%
0.075	8.9%	41.0%	37.4%	3.6%
0.100	8.9%	40.8%	34.9%	5.1%
0.125	8.9%	40.7%	32.4%	6.9%
0.150	2.9%	33.2%	22.7%	1.7%
0.175	-3.1%	24.1%	12.6%	-4.3%
0.200	-6.9%	17.6%	5.7%	-7.5%
0.225	-6.0%	14.0%	3.3%	-7.9%
0.250	-1.9%	12.6%	4.3%	-5.6%
0.275	3.8%	12.7%	7.5%	-2.7%
0.300	11.0%	13.6%	12.5%	0.7%
0.325	19.5%	15.2%	19.1%	4.4%
0.350	30.0%	17.7%	27.8%	7.3%
0.375	33.6%	18.2%	30.5%	8.6%
0.400	36.6%	18.9%	32.7%	8.5%
0.425	38.8%	19.5%	34.3%	8.5%
0.450	39.9%	19.8%	34.5%	8.2%
0.475	40.7%	20.0%	34.5%	6.5%
0.500	41.2%	20.5%	34.1%	5.2%

For the most part the Scofield analysis overestimates the forces in the arch due to drift loading even though the load patterns are different. Unfortunately, it underestimates the moment in a couple of cases for the flexible arch and in about half of the cases for the stiff arch.

Table 10 - Stiff Arch Analyses Comparison for Snow Drift Load.

Snow Drift Load - Stiff Arch				
Rise/Span [r] (-)	Scofield Method			
	Vertical Reaction	Horizontal Reaction	Thrust	Moment
0.050	8.9%	87.0%	80.7%	-31.3%
0.075	8.9%	61.3%	54.0%	-17.1%
0.100	8.9%	52.3%	43.2%	-8.6%
0.125	8.9%	48.0%	37.0%	-3.0%
0.150	2.9%	38.0%	25.2%	-5.0%
0.175	-3.1%	27.4%	14.1%	-9.1%
0.200	-6.9%	20.0%	6.6%	-11.1%
0.225	-6.0%	15.9%	3.9%	-11.0%
0.250	-1.9%	14.1%	4.8%	-8.4%
0.275	3.8%	13.9%	7.8%	-5.2%
0.300	11.0%	14.7%	12.7%	-1.6%
0.325	19.5%	16.1%	19.3%	2.4%
0.350	30.0%	18.5%	27.9%	5.5%
0.375	33.6%	18.9%	30.6%	7.0%
0.400	36.6%	19.5%	32.8%	7.1%
0.425	38.8%	20.1%	34.4%	7.3%
0.450	39.9%	20.3%	34.6%	7.2%
0.475	40.7%	20.5%	34.5%	5.6%
0.500	41.2%	20.9%	34.1%	4.4%

3.3 Effects of Curvature on Arch Forces

Changing the amount of curvature in the arch has a profound effect on the distribution of forces in the arch. An arch with a low rise will, not surprisingly, act more like a straight beam. A half-circle arch will act much differently.

Appendix D displays twenty graphs that show the horizontal reaction, axial force, and moments plotted against the Rise-to-Span ratio for all five load types. The graphs show two lines, one representing the forces on a stiff arch (I/A = 100), and one for a flexible one (I/A = 1). This design is to show how changing the stiffness of the arch changes the force-resisting characteristics of the arch and to give an envelope of acceptable forces. For the most part, the two curves are very similar. In a few cases they differ. A few specific cases are highlighted in the following sections.

The graphs are based on the following arch characteristics:

- 40 foot span
- 10 psf dead load
- 20 psf construction load
- 115 mph wind
- 30 psf ground snow load

Graphs based on different spans and loadings would obviously have different values, but the general shape of the curves would be the same.

3.3.1 Dead Load

The curves on the dead load graphs are, for the most part, very similar. A flexible arch has slightly higher forces for the horizontal reaction, axial force, and negative moment. This difference is more apparent as the Rise-to-Span ratio decreases. However, the positive moment graph shows a large difference between a stiff and flexible arch in the low rise ranges with the stiff arch curve looking like a V, as seen in Figure 37.

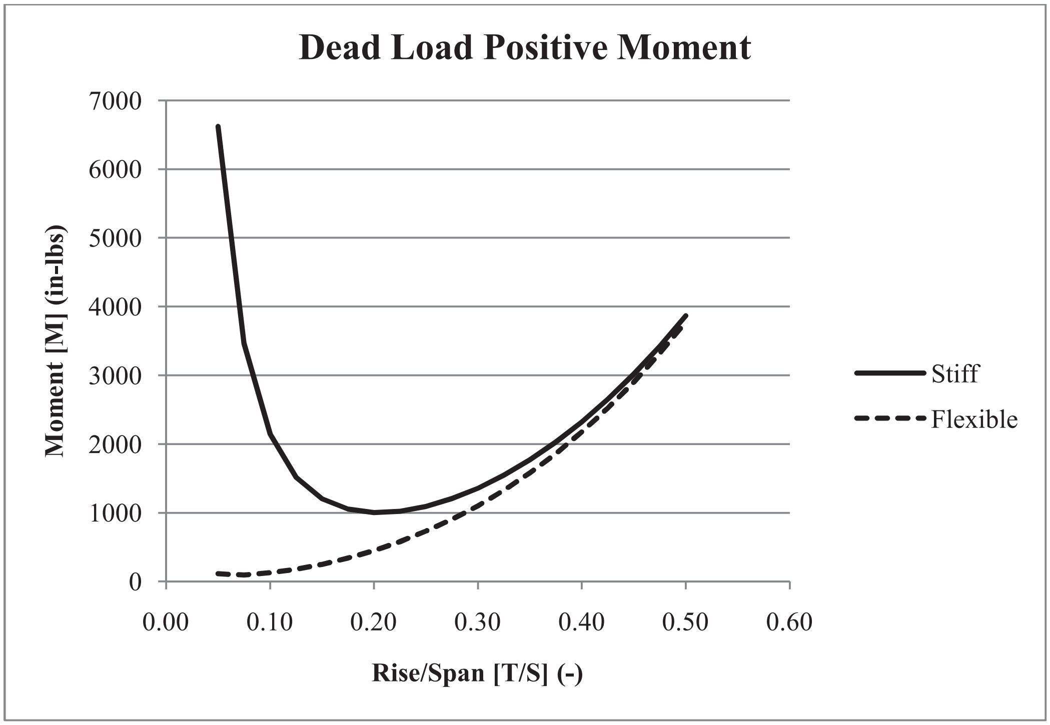

Figure 37 - Dead Load Positive Moment Graph.

The stiff arch curve gives greater values for design forces for all *r* values. Its greater stiffness gathers more moment than the flexible arch.

3.3.2 Construction Load

Since the construction load type is very similar to the dead load, the graphs are also similar. The same holds true here where the horizontal reaction, axial force, and negative moment graphs have the stiff and flexible curves very similar. The positive moment graph has the curves very different but the graph is similar to the dead load case, as seen in Figure 38.

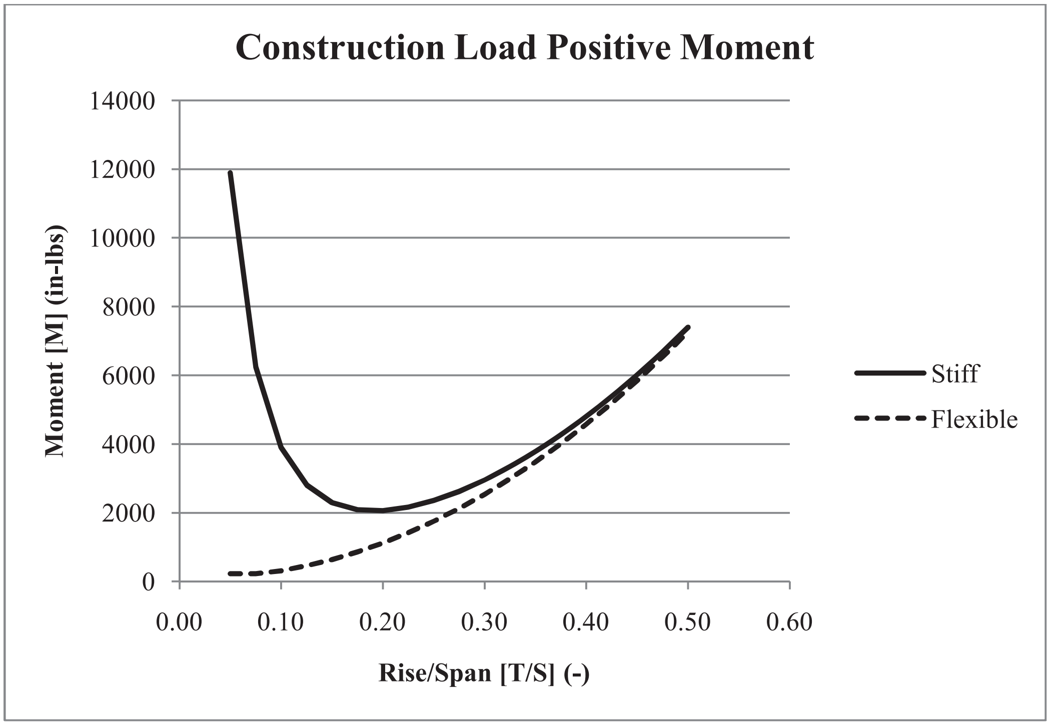

Figure 38 - Construction Load Positive Moment Graph.

Again, the same V-shaped curve appears for the stiff arch, showing that its stiffness allows it to accrue more moment than the flexible arch.

3.3.3 Wind Load

Since uplift plays a large role in the wind load, the graphs for the axial force, negative moment, and positive moment look a little different than for the other gravity loads. For starters, the axial force is in tension instead of compression, and looks like the reverse view of the dead load or construction load graphs for axial force. The horizontal reaction graph is similar to the previous two loading types. The two moment graphs are different, however, as shown in Figure 39 and Figure 40.

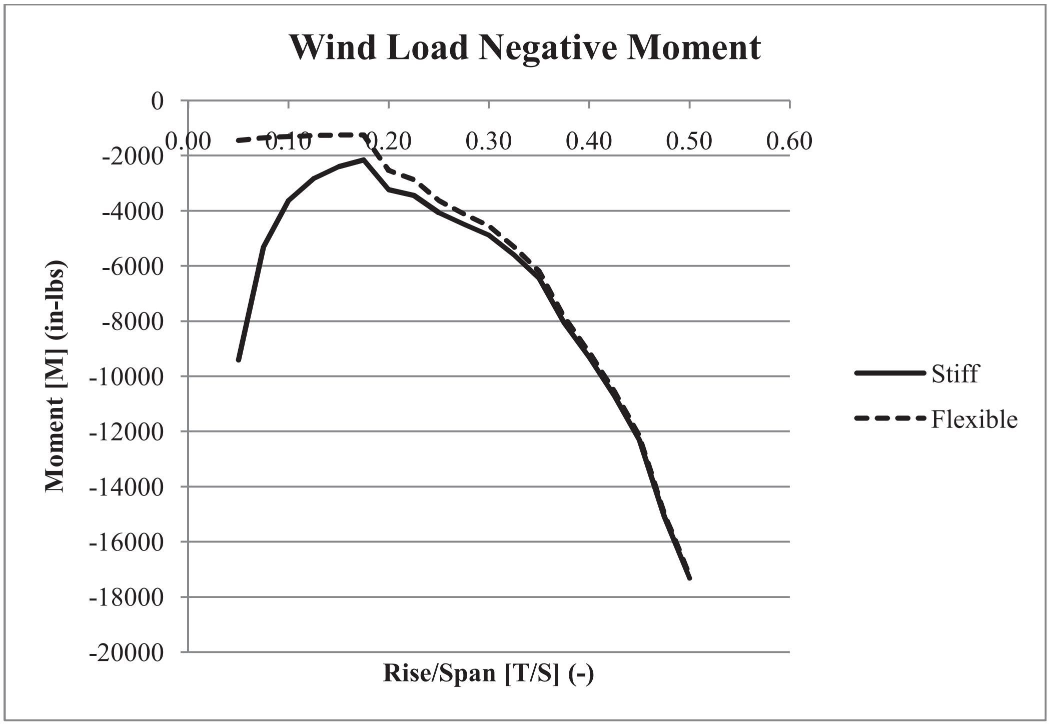

Figure 39 - Wind Load Negative Moment Graph.

The stiff arch has greater forces early on and then follows the flexible curve closely after the *r* ratio passes 0.17.

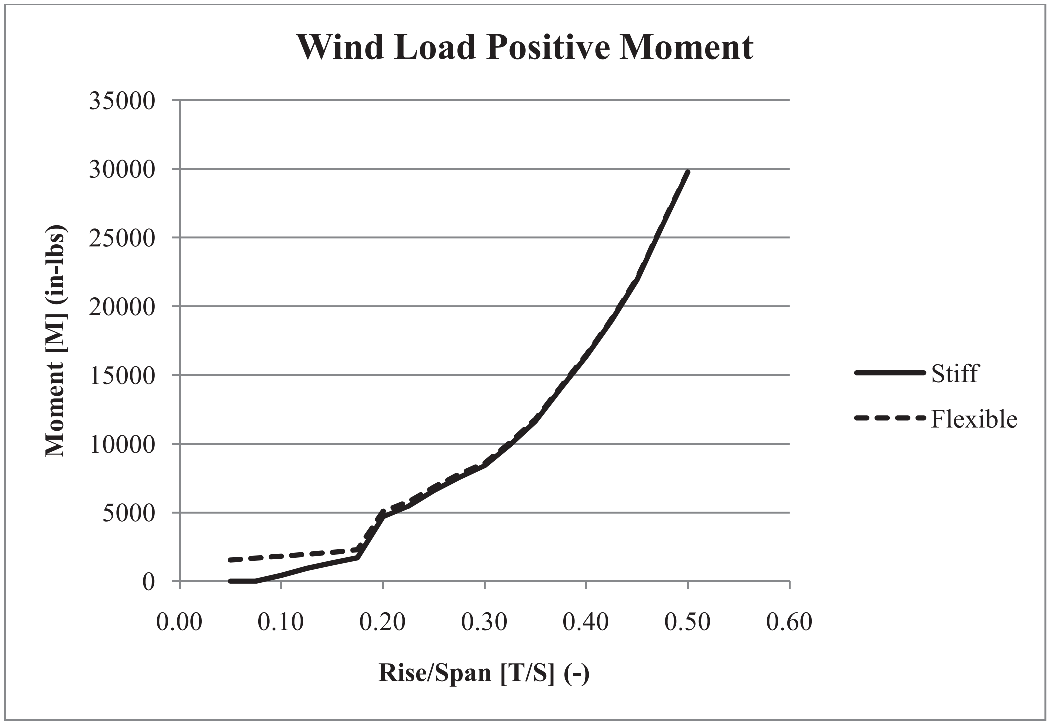

Figure 40 - Wind Load Positive Moment Graph.

In Figure 40 the curves follow closer to the dead load and construction load positive moment curve for a flexible arch. There is little difference between the stiff and flexible arch.

3.3.4 Snow Drift Load

The drift load horizontal reaction and axial force graphs are similar to the other gravity load types but have bumps due to the changing loadings as the curvature of the roof changes. The two moment graphs are nothing like the others, as seen in Figure 41 and Figure 42.

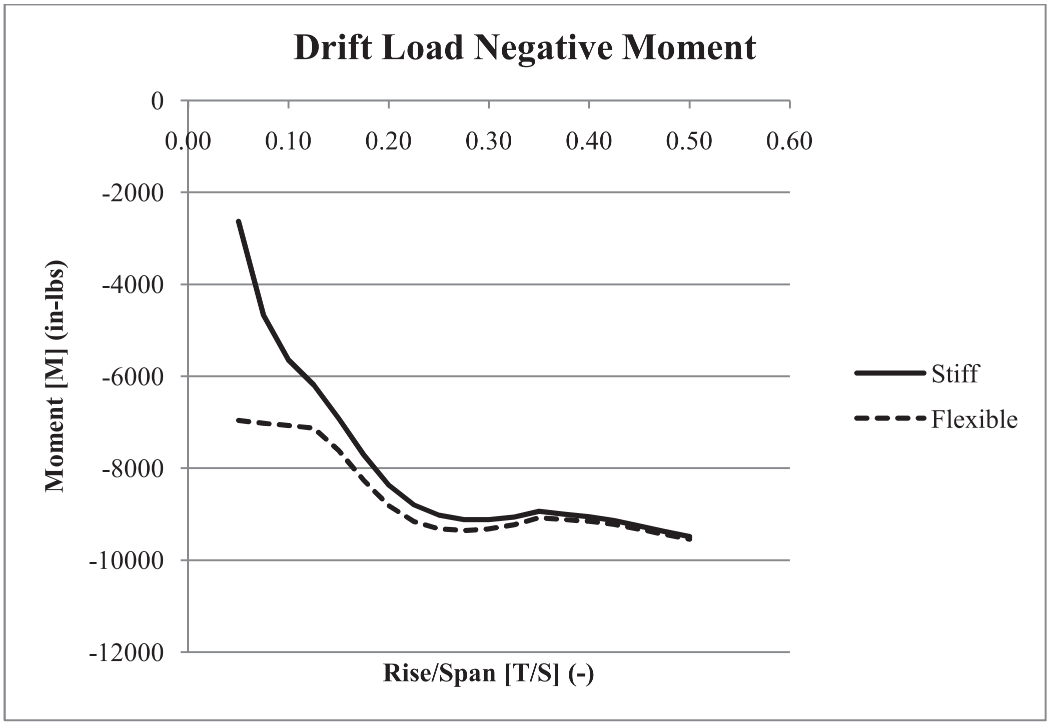

Figure 41 - Drift Load Negative Moment Graph.

Figure 41 shows that the flexible arch takes on a little more moment for lower rises but then the two curves follow each other when *r* is greater than 0.15. The bumps in Figure 41 are due to the changing curvature of the roof affecting the load pattern.

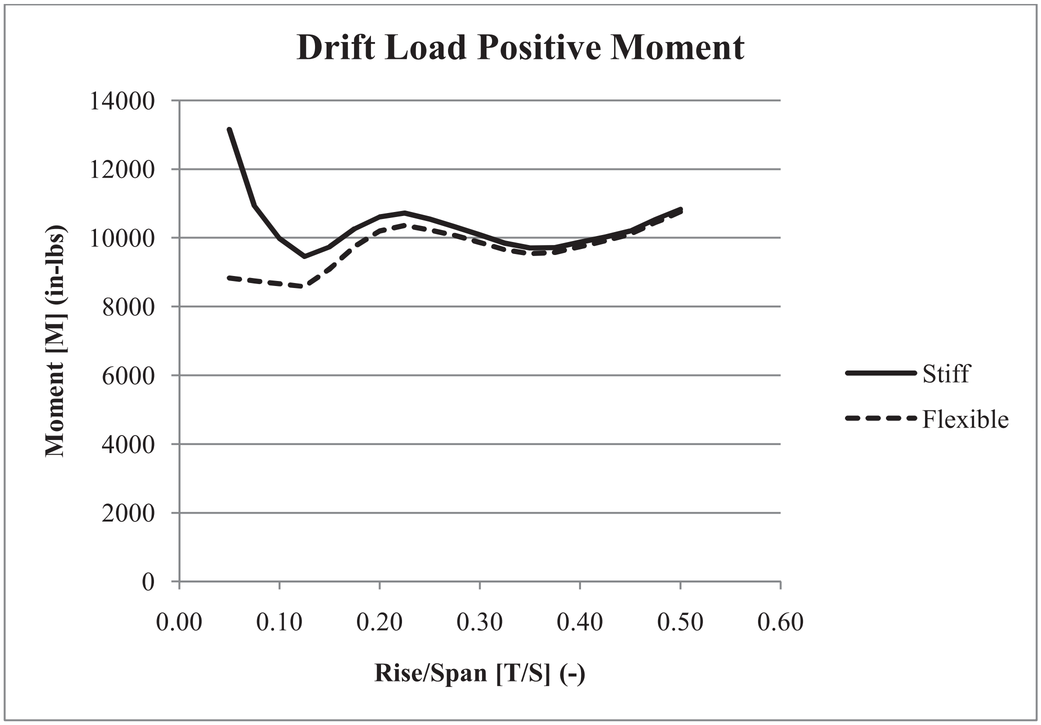

Figure 42 - Drift Load Positive Moment Graph.

The curves in Figure 42 are close, for the most part, with the stiff arch getting more moment in low rises. The bumps are again due to the changing loading patterns.

3.3.5 Balanced Snow Load

The balanced snow load is a similar loading to the construction load except where the load tapers off at the ends due to the roof slope. Because of this, the four graphs for each of the arch forces are very similar to the corresponding dead load and construction load graphs, including the V-shaped curve for the stiff arch positive moment. Figure 43 displays one of these graphs.

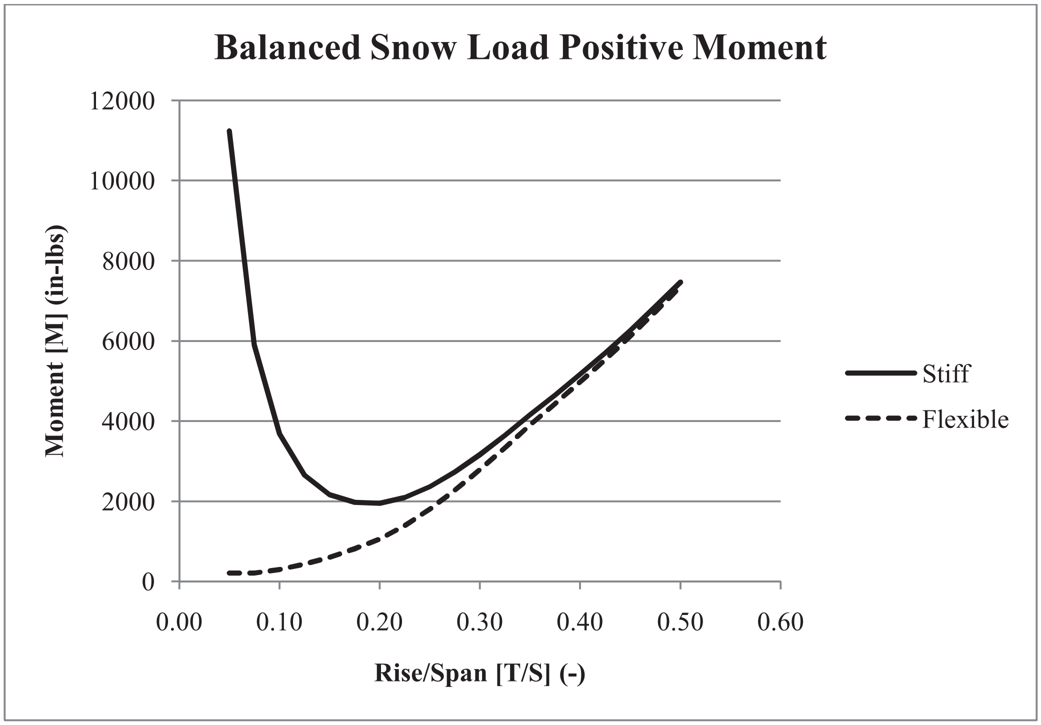

Figure 43 - Balanced Snow Load Positive Moment Graph.

Like the two other balanced gravity loads, the stiff arch takes on much higher positive moment in low rises.

3.3.6 Application for Load Tables

The load tables developed by the author will use the stiff arch curves instead of the flexible curves. There are two reasons for this choice. One is that the stiff arch gives higher moments (for the most part) and moment contributes more to the stress in the lamella than axial loads do. Second is that the roof will more likely act like a stiff arch because of the interplay in the rhomboid grid of the lamellas and the fact that the roof diaphragm over the lamellas will stiffen them as well.

It should also be noted that arched roofs are generally not designed to have *r* values close to 0 or 0.5, but fall somewhere in between. The most disparity between the stiff and flexible arch curves occurs in the low rise range in which few, if any, arched roofs are built.

3.3.7 Example Moment Diagrams

As the arch starts out with a low rise, under uniform vertical loading, the majority of the moment will be positive moment, which would be analogous to the bending of a simple beam. As the rise of the arch increases, the "sides" of the arch will incur negative moment from the arch resisting outward buckling. This is illustrated in Figure 44, Figure 45, and Figure 46.

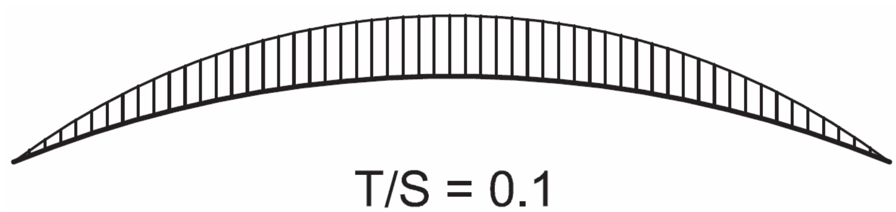

Figure 44 - Moment Diagram for Arch with Low Rise.

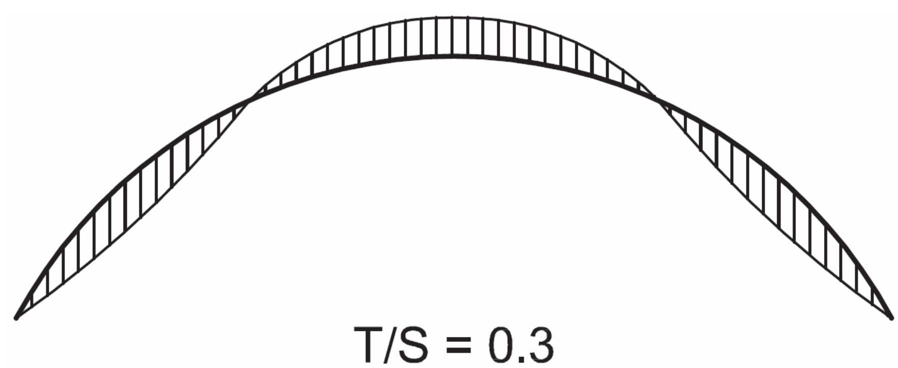

Figure 45 - Moment Diagram for Arch with Medium Rise.

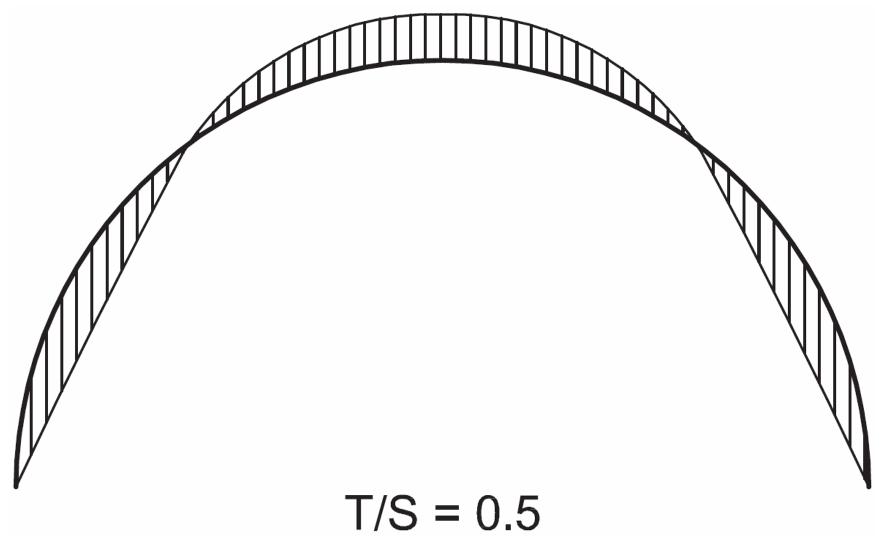

Figure 46 - Moment Diagram for Semi-Circular Arch.

The cut-off point for the beginning of negative moment depends on the stiffness of the arch. The stiffer the arch, the more moment capacity it has and the sooner it can take on negative moment as the rise increases. Generally, this point appears to be where the rise of the arch is around 10% of the span.

4 Development of Design Tables

To facilitate the design of a lamella roof, the author developed a set of design tables – one for the loads on the lamella roof (Section 4.1) and another for the connection between the lamellas (Section 4.2).

4.1 Load Tables

These tables display roof spans from 20 to 120 feet and show loads based on a changing rise. Two different sets were developed: one in the 115 mph wind zone with varying snow loads and one with zero snow loading but with varying wind speeds. The former is meant to be used in non-hurricane regions of the United States and the latter in hurricane regions, like Florida, which can expect zero annual snowfall.

The tables were created in Microsoft Excel using the finite element analysis approach discussed in Section 3.1.3 and using the ASD load combinations and loading patterns stipulated in ASCE 7-10. To aid in table generation, the author programmed a macro in which the user inputs the system parameters (span, rise, cross-sectional area, moment of inertia, and loadings) and the macro runs the various rise-to-span ratios through the FEA matrices, finds loads for each load case, and takes the worst loading from all cases for the design loads. This means that the maximum moment may come from one load case and the maximum axial force from another. The same can be said about the base reactions. Also, the point of maximum moment and maximum axial force most likely do not coincide, but designing a lumber beam-column (i.e., lamella) to resist those simultaneous maximum forces will give a conservative design.

Values in the tables are given in units per foot of arch.

Discussed earlier was the notion of the arch stiffness being a function of the moment of inertia over the cross-sectional area. In keeping with the conclusions drawn in Section 3.3.6, the author uses an I/A value of 100, representing a stiff arch, for the FEA calculations.

Additionally, when designing for ASD while using the NDS design specification, one must pay attention to the load duration factor C_D. Since wood has a load carrying capacity that increases when the load duration decreases, the NDS assigns different C_D values based on the load case. For example, NDS Table 2.3.2 specifies that an occupancy live load with a ten-year duration gets a C_D value of 1.0 while a wind load with a ten-minute duration gets a C_D value of 1.6. The load duration factor is used to increase (or decrease, if the dead load controls) the design values of the lumber used, essentially making the wood stronger.

Since the load duration factor changes depending on the loads used in the load combination, the various loads found through the FEA method must be normalized. Consider, for example, the load case $D + 0.75(0.6W) + 0.75S$. The NDS specification states that the C_D value for the shortest duration load be used for the combination, which means that the above load combination has a C_D value of 1.6. To normalize it, the loads found by the FEA spreadsheet are divided by that C_D value. Then, when designing the lamella to carry the load, the load duration factors can all be assumed to be 1.0.

The finished load tables are found in Appendix F.

4.2 Connection Tables

Connection design is based on the assumption that the lamella connection can be modeled as a double-shear connection, as shown in Figure 47.

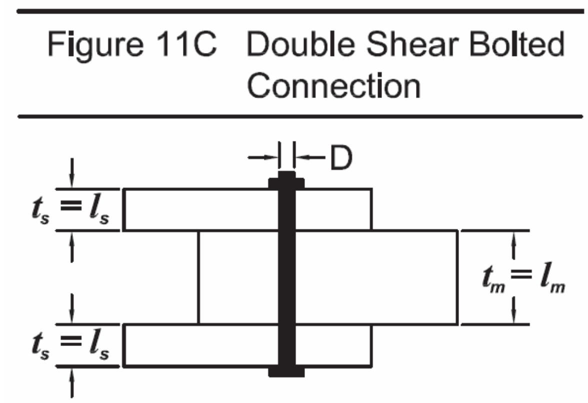

Figure 47 - Double Shear Bolted Connection [10].

As seen in Section 2.1.1, the actual geometry is a little more complicated (see Figure 17) but the approximation is close enough. Since the lamellas are all the same thickness, ℓ_s would be equal to t, the thickness of the member, and

$$\ell_m = \frac{t}{\cos 2\theta}. \tag{83}$$

These two values are used in determining the shear capacity of the connection.

The NDS stipulates finding several yield limit states for a double shear connection. These limit states are shown in Appendix A, Figure A-1. Since the connection is double shear, only modes $\mathrm{I_m}$, $\mathrm{I_s}$, $\mathrm{III_s}$, and IV apply, each with its own yield limit equation. They are

$$\mathrm{I_m}: \; Z = \frac{D\ell_m F_{em}}{R_d}, \tag{84}$$

$$\mathrm{I_s}: \ Z = \frac{D\ell_s F_{es}}{R_d}, \tag{85}$$

$$\mathrm{III_s}: \ Z = \frac{2k_3 D\ell_s F_{em}}{\left(2+R_e\right)R_d}, \tag{86}$$

and

$$\mathrm{IV}: \ Z = \frac{2D^2}{R_d}\sqrt{\frac{2F_{em}F_{yb}}{3\left(1+R_e\right)}}, \tag{87}$$

where

$D =$ dowel diameter, in,
$F_{yb} =$ dowel bending yield strength, psi,
$R_d =$ reduction term,
$R_e = F_{em}/F_{es}$,
$\ell_m =$ main member dowel bearing length, in,
$\ell_s =$ side member dowel bearing length, in,
$F_{em} =$ main member dowel bearing strength, psi,
$F_{es} =$ side member dowel bearing strength, psi,

and

$$k_3 = -1 + \sqrt{\frac{2\left(1+R_e\right)}{R_e} + \frac{2F_{yb}\left(2+R_e\right)D^2}{3F_{em}\ell_s^2}}. \tag{88}$$

At this point some simplifications and substitutions can be made. To start, F_{em} and F_{es} are dependent only on the wood specific gravity and the dowel diameter, making them the same value [10]:

$$F_{em} = F_{es} = F_{e\perp} = \frac{6{,}100G^{1.45}}{\sqrt{D}}.$$

The $F_{e\perp}$ equation is used since the shear load acts perpendicular to grain. Since F_{em} and F_{es} are the same value, R_e simplifies to one. Completing the substitutions yields:

$$k_3 = -1 + \sqrt{4 + \frac{F_{yb} D^{2.5}}{3{,}050 t^2 G^{1.45}}}, \tag{89}$$

$$\mathrm{I_m}:\ Z = \frac{6{,}100 G^{1.45} t \sqrt{D}}{R_d \cos 2\theta}, \tag{90}$$

$$\mathrm{I_s}:\ Z = \frac{12{,}200 G^{1.45} t \sqrt{D}}{R_d}, \tag{91}$$

$$\mathrm{III_m}:\ Z = \frac{12{,}200 k_3 G^{1.45} t \sqrt{D}}{3 R_d}, \tag{92}$$

and

$$\mathrm{IV}:\ Z = \frac{2D^2}{R_d} \sqrt{\frac{6{,}100 G^{1.45} F_{yb}}{9\sqrt{D}}}. \tag{93}$$

The R_d value changes depending on the yield mode. Figure 48 shows how it is determined. The footnote in the table notes that for threaded fasteners with a nomimal diameter greater than or equal to ¼″ and a root diameter, D_r, less than ¼″ (i.e., ¼″ and 5/16″ bolts),

$$R_d = K_D K_\theta,$$

where

$$K_D = 10 D_r + 0.5,$$

and K_θ is the same as shown in Figure 48. In all cases, since the shear is perpendicular to grain, θ is 90° and K_θ becomes 1.25.

Table 11.3.1B Reduction Term, R_d

Fastener Size	Yield Mode	Reduction Term, R_d
0.25″ ≤ D ≤ 1″	I_m, I_s	4 K_θ
	II	3.6 K_θ
	III_m, III_s, IV	3.2 K_θ
D < 0.25″	I_m, I_s, II, III_m, III_s, IV	K_D[1]

Notes:

$K_\theta = 1 + 0.25(\theta - 90)$

$\theta =$ maximum angle of load to grain $(0 \le \theta \le 90)$ for any member in a connection

$D =$ diameter, in. (see 11.3.6)

$K_D = 2.2$ for $D \le 0.17"$

$K_D = 10D + 0.5$ for $0.17" < D < 0.25"$

1. For threaded fasteners where nominal diameter (see Appendix L) is greater than or equal to 0.25″ and root diameter is less than 0.25″, $R_d = K_D K_\theta$.

Figure 48 - Reduction Term, R_d [10].

5 Lamella Strength and Connection Design

The following sections will display how one analyzes a lamella section for design adequacy and how one would design the connection to withstand the loads applied on it.

5.1 Lamella Strength Analysis

The lamella is designed based on the assumption that it acts like a beam-column with biaxial bending and compression. Testing done by the author (see Section 7.3.1) backs up this assumption. According to the NDS Section 3.9.2, the equation for bending and axial compression is

$$\left[\frac{f_c}{F_c'}\right]^2 + \frac{f_{b1}}{F_{b1}'\left[1-\left(f_c/F_{cE1}\right)\right]} + \frac{f_{b2}}{F_{b2}'\left[1-\left(f_c/F_{cE2}\right)-\left(f_{b1}/F_{bE}\right)^2\right]} \leq 1.0 \tag{94}$$

where

$$f_c < F_{cE1} = \frac{0.822E_{\min}'}{\left(\frac{\ell_{e1}}{d_1}\right)^2}, \tag{95}$$

$$f_c < F_{cE2} = \frac{0.822E_{\min}'}{\left(\frac{\ell_{e2}}{d_2}\right)^2}, \tag{96}$$

$$f_{b1} < F_{bE} = \frac{1.20E_{\min}'}{\left(R_B\right)^2}, \tag{97}$$

with

f_{b1} = actual edgewise bending stress (bending load applied to narrow face of member),
f_{b2} = actual flatwise bending stress (bending load applied to wide face of member),
f_c = actual compressive stress from axial load,
d_1 = wide face dimension (lamella depth),
d_2 = narrow face dimension (lamella thickness),
ℓ_e = effective column length (NDS Section 3.7.1.2),

and

$$F'_{b1} = F_b C_D C_M C_t C_L C_F C_{fu} C_i C_r, \tag{98}$$

$$F'_{b2} = F_b C_D C_M C_t C_L C_F C_{fu} C_i C_r, \tag{99}$$

$$F'_c = F_c C_D C_M C_t C_F C_i C_P \tag{100}$$

and

$$E'_{\min} = E_{\min} C_M C_t C_i C_T. \tag{101}$$

Since the lamella is continually braced in the weak direction by the roof diaphragm, Equation (96) essentially becomes infinite, which reduces Equation (94) to

$$\left[\frac{f_c}{F'_c}\right]^2 + \frac{f_{b1}}{F'_{b1}\left[1-\left(f_c/F_{cE1}\right)\right]} + \frac{f_{b2}}{F'_{b2}\left[1-\left(f_{b1}/F_{bE}\right)^2\right]} \leq 1.0. \tag{102}$$

As stated before, the C_D factor has already been normalized to 1.0. Also, for most of the adjustment factor C values, the values can be eliminated by setting them equal to 1.0, as well. Since the lamella roof is most likely going to be built indoors, the moisture, temperature, and incising factors - C_M, C_t, and C_i, respectively - will be equal to 1.0.

In strong-axis bending, the flat use factor C_{fu} drops to 1.0 since it is bending edge-wise. For the maximum positive moment, the compression edge of the lamella is continually braced by the sheathing on top, and the beam stability factor C_L becomes 1.0, as well. For the maximum negative moment, the compression edge is only braced at the lamella ends and at the halfway point by the adjacent lamellas. Assuming the lamella is loaded with a uniformly distributed load, the effective length ℓ_e can be one of two values. If the unsupported length ℓ_u divided by the lamella depth is less than seven ($\ell_u/d < 7$), then

$$\ell_e = 2.06\ell_u. \tag{103}$$

If the ratio is above seven, then the effective length becomes

$$\ell_e = 1.63\ell_u + 3d. \tag{104}$$

The beam stability factor is then found by

$$C_L = \frac{1+\left(F_{bE}/F_b^*\right)}{1.9} - \sqrt{\left[\frac{1+\left(F_{bE}/F_b^*\right)}{1.9}\right]^2 - \frac{F_{bE}/F_b^*}{0.95}}, \tag{105}$$

where

$$F_b^* = F_b C_D C_M C_t C_F C_i C_r,$$

$$F_{bE} = \frac{1.20E'_{\min}}{R_B^2}, \tag{106}$$

and

$$R_B = \sqrt{\frac{\ell_e d}{b^2}}, \tag{107}$$

where b is the thickness of the lamella and R_B shall not exceed 50. The two different C_L values must be used in conjunction with their respective moments when using Equation (102) to check the beam-column.

In weak-axis bending, the flat-use factor C_{fu} is given by Tables 4A, 4B, 4C, and 4F of the NDS 2005 Supplement. The beam stability factor C_L is 1.0 since its depth is less than its width.

The size factor C_F depends on the size of the member and the species and will change depending on the lamella size. Unless the lamellas are spaced at 24 inches or less, the repetitive member factor C_r will be equal to 1.0, as well (it will be 1.15 otherwise). Since the lamella roof does not meet any of the specifications of NDS Section 4.4.2, the buckling stability factor C_T is also equal to 1.0.

Finding the column stability factor C_P is a little more involved. For starters, the NDS limits the slenderness ratio ℓ_e/d to 50 (75 during construction), where

$$\ell_e = K_e \ell. \tag{108}$$

The connections between the lamellas are assumed to be pinned-pinned so the effective length factor K_e is equal to 1.0. The lamellas are braced continuously in the weak direction by the roof sheathing so the Y-Y axis slenderness ratio is zero. The side lamellas, though they brace the continuous lamella at the half-points, only brace in the weak direction; thus, the effective length in the X-X axis is

$$\ell_e = \ell. \tag{109}$$

In reality, the lamella would have to be very long and very shallow in order for the slenderness ratio to be greater than 50. For example, a 2x8 lamella with a depth of 7.25 inches would have to be over 30 feet long for this to happen.

Equation 3.7-1 of the NDS then gives the column stability factor as

$$C_P = \frac{1+\left(F_{cE}/F_c^*\right)}{2c} - \sqrt{\left[\frac{1+\left(F_{cE}/F_c^*\right)}{2c}\right]^2 - \frac{F_{cE}/F_c^*}{c}}, \tag{110}$$

where

$F_c^* = F_c C_D C_M C_t C_F C_i$,
$c = 0.8$ for sawn lumber,
$c = 0.85$ for round timber poles and piles,
$c = 0.9$ for structural glued laminated timber or structural composite lumber,

and F_{cE} is the same as in Equation (95).

The thrust and moments found in the Load Tables must be adjusted to take the skew of the lamella arches and the length of the lamellas into consideration. The moment in the strong direction must be multiplied by the spacing of the lamellas and divided by the cosine of the skew angle since the lamella follows the skewed arch [3]:

$$M_{x,lam} = \frac{(\text{Spacing})\left(M_{load\ table}\right)}{\cos\theta}. \tag{111}$$

The thrust is taken up by two lamellas, since the compressive force can go two ways in each connection node [3]:

$$F_{a,lam} = \frac{(\text{Spacing})\left(F_{a,load\ table}\right)}{2\cos\theta}. \tag{112}$$

In the weak direction, the moment is generated by the force couple created by the side lamellas abutting the middle lamella, which is simply the axial thrust multiplied by the shift of the connection:

$$M_{y,lam} = \left(F_{a,lam}\right)(s). \tag{113}$$

With a chosen trial section one can begin the process of checking the section for adequacy. First, one finds the bending and compressive stresses by

$$f_{b1} = \frac{M_{x,lam}}{S_{xx}}, \tag{114}$$

$$f_{b2} = \frac{M_{y,lam}}{S_{yy}}, \tag{115}$$

and

$$f_c = \frac{F_{a,lam}}{A}. \tag{116}$$

After these calculations, it is a simple matter of checking the calculated stresses for compliance in the interaction equation from Equation (102). It is important to note that this calculation must be done twice – once for the maximum positive moment and once for the maximum negative moment, each calculated with their respective C_L values.

5.2 Connection Design

Since the connections between lamellas are achieved using dowel-type fasteners, the equation for the reference design value is

$$Z' = ZC_D C_M C_t C_g C_\Delta C_{eg} C_{di} C_{tn}, \tag{117}$$

where

C_D = Load Duration Factor,
C_M = Wet Service Factor,
C_t = Temperature Factor,
C_g = Group Action Factor,
C_Δ = Geometry Factor,
C_{eg} = End Grain Factor,
C_{di} = Diaphragm Factor,
C_{tn} = Toe-Nail Factor.

Again, the C_D factor is normalized to 1.0 as in Section 4.1. Unless the building is exposed to the elements, the C_M and C_t factors will most likely be 1.0 as well.

The calculation for the group action factor is rather long. To begin,

$$C_g = \left[\frac{m\left(1-m^{2n}\right)}{n\left[\left(1+R_{EA}m^n\right)\left(1+m\right)-1+m^{2n}\right]} \right] \left[\frac{1+R_{EA}}{1-m} \right], \tag{118}$$

where

$n =$ number of fasteners in a row,

$R_{EA} = \min\left[\frac{E_s A_s}{E_m A_m}, \frac{E_m A_m}{E_s A_s}\right],$

$E_m =$ modulus of elasticity of main member, psi,

$E_S =$ modulus of elasticity of side member, psi,

$A_m =$ cross-sectional area of main member, in^2,

$A_s =$ cross-sectional area of side member, in^2,

$m = u - \sqrt{u^2 - 1},$

$u = 1 + \gamma \frac{s}{2}\left[\frac{1}{E_m A_m} + \frac{1}{E_s A_s}\right],$

$s =$ center-to-center spacing between adjacent fasteners in a row, in,

$\gamma = 180,000 D^{1.5}$ (for dowel-type fasteners in wood-to-wood connections).

However, since the side member and main members are the same material, and the side lamella area will always be less than the middle lamella due to the curvature cut,

$$E_m = E_s = E,$$
$$R_{EA} = \frac{A_s}{A_m},$$
$$u = 1 + \frac{180,000 D^{1.5} s}{2E}\left[\frac{1}{A_m} + \frac{1}{A_s}\right].$$

The geometry factor, if the designer follows the diagrams in Figure 15 and Figure 16, can be equal to the value shown for those figures. If it falls somewhere between, C_Δ can be found through one of two ways. To quote the NDS,

> When dowel-type fasteners are used and the actual end distance for parallel or perpendicular to grain loading is greater than or equal to the minimum end distance (see Figure 11) for $C_\Delta = 0.5$, but less than the minimum end distance for $C_\Delta = 1.0$, the geometry factor, C_Δ, shall be determined as follows:

$$C_\Delta = \frac{\text{actual end distance}}{\text{minimum end distance for } C_\Delta = 1.0},$$

and

> When the actual spacing between dowel-type fasteners in a row for parallel or perpendicular to grain loading is greater than or equal to the minimum spacing (see Figure 12), but less than the minimum spacing for C_{Δ} = 1.0, the geometry factor, C_{Δ}, shall be determined as follows:
>
> $$C_{\Delta} = \frac{\text{actual spacing}}{\text{minimum spacing for } C_{\Delta} = 1.0}. \quad [10]$$

The end grain factor, C_{eg}, only applies when a fastener is loaded in withdrawal from the end grain of a member and can be set to 1.0. Since the lamella connection is not part of a diaphragm, the C_{di} is also 1.0. And, since the connections are not toe-nailed, C_{tn} is equal to 1.0 as well.

The connection joint between the continuous and non-continuous lamellas must be designed to handle both vertical shear perpendicular to grain and thrust parallel to grain as a result of the eccentric connection. The vertical shear can be found by [16]:

$$V_{\perp} = \frac{4M_{x,lam}}{\ell}, \tag{119}$$

where $M_{x,lam}$ is the moment in the strong axis of the lamella resulting from the chosen loading combination.

The thrust parallel to grain results in tension in the bolts. According to Scofield [3], the magnitude of this tension is found by

$$T_{bolts} = \frac{2F_{a,lam}\cos\theta}{\tan 2\theta}, \tag{120}$$

where $F_{a,lam}$ is the thrust in each lamella and θ is the skew angle of the lamella arch. This tension would be split evenly between the bolts in the connection. Also, the tension in the bolt would need to be transferred to the lamella through a washer of appropriate surface area so as not to crush the surrounding wood, as discussed later in this section [16].

The tensile capacity of a bolt is found by multiplying the diameter of the bolt by its yielding stress [4]. However, since there is a reduction in area due to the threads at the end of the bolt, one must use the root diameter D_r for calculations:

$$T_{cap} = D_r F_{y,bolt}. \tag{121}$$

The yielding stress of the bolts is usually 36,000 psi. Using this information, Table 11 was created.

Table 11 - Strength Properties for Standard Hex Bolts.

Properties for Standard Hex Bolts			
Diameter [D]	Root Diameter [D_r] (in)	Root Area [A_r] (in^2)	Tensile Capacity [Z] (lbs)
1/4"	0.189	0.028	1005
5/16"	0.245	0.047	1695
3/8"	0.298	0.070	2510
1/2"	0.406	0.129	4660
5/8"	0.514	0.207	7465
3/4"	0.627	0.309	11115
7/8"	0.739	0.429	15440
1"	0.847	0.563	20280

Washers are used to transfer the tension load from the bolts to the lamellas and must be designed so as not to crush the surrounding wood. First, one must compute the compression strength of the wood perpendicular to grain [10]:

$$F'_{c\perp} = F_{c\perp} C_M C_t C_i C_b. \tag{122}$$

If the lamella roof is enclosed such that the lamellas are indoors, the C_M, C_t, and C_i, factors will all drop to 1.0. The NDS has the following to say about the bearing area factor C_b:

> Reference compression design values perpendicular to grain, $F_{c\perp}$,apply to bearings of any length at the ends of a member, and to all bearings 6″ or more in length at any other location. For bearings less than 6″ in length and not nearer than 3″ to the end of a member, the reference compression design value perpendicular to grain, $F_{c\perp}$, shall be permitted to be multiplied by the following bearing area factor, C_b:
>
> $$C_b = \frac{\ell_b + 0.375}{\ell_b} \tag{123}$$
>
> where
>
> ℓ_b = bearing length measured parallel to grain, in. [10]

Since the bolts, and therefore the washers, are closer than 3″ to the end of the lamella, the bearing area factor does not increase the design compression strength perpendicular to grain and can be set to 1.0, as well.

From there, the necessary washer area needed for the tension developed in the bolts is found by

$$A_{washer} \geq \frac{T_{bolts}}{F'_{c\perp}}. \tag{124}$$

This washer area is split between the bolts in the connection and applies for the entire connection. In other words, half of the washer area is for one side of the connection and the other half for the other side.

It should be noted that due to friction between the bolts and the surrounding wood, the forces in the connection will be slightly less than those computed, yielding slightly conservative design values [16].

6 Design Example

In this section, the tables developed by the author are used to design an example lamella roof. The example is designed following the NDS 2005 Specification using the Allowable Stress Design (ASD) process. It should be noted that Load & Resistance Factor Design (LRFD) is a perfectly acceptable design approach; however, the tables developed by the author use ASD load combinations.

In this example, the combination of snow drift and dead loads likely generates the largest loads on the structure; however, due to the nature of the load tables it is impossible to tell. The following design criteria apply:

- 40 ft span (S = 40 ft)
- 10 ft rise (T = 10 ft)
- Southern Pine No.1 lumber
- Structure dead load (D) = 10 psf
- Construction live load (L_r) = 20 psf
- Grounld snow load (p_g) = 30 psf
- Basic wind speed (V) = 120 mph
- 10 lamellas per arch (n = 10)
- Skew angle of 19° (θ = 19°)

6.1 Lamella Strength Check

First one must find the nominal length ℓ of the lamellas. Thus,

$$R = \frac{4T^2 + S^2}{8T} = \frac{4(10')^2 + (40')^2}{8(10')} = 25',$$

$$2\phi = \frac{\beta}{n} = \frac{2}{n}\arccos\left(\frac{R-T}{R}\right) = \frac{2}{10}\arccos\left(\frac{25'-10'}{25'}\right) = 10.62°,$$

$$\ell_{c-c} = 2R\sin\phi = 2(25')\sin\left(\frac{10.62°}{2}\right) = 4.63',$$

$$\ell = \frac{\ell_{c-c}}{\cos\theta} = \frac{6.604'}{\cos(19°)} = \boxed{4.90'}.$$

Looking at Table 1, this length of lamella at a skew of 19° gives a spacing of about 1.59 feet. From looking at the load tables in Appendix E, the following loads (per foot section of arch) are caused by the aforementioned design criteria:

- R_y = 545 lbs
- R_x = 520 lbs
- F_a = 755 lbs
- M^- = -8800 in-lbs
- M^+ = 10110 in-lbs

The axial thrust in each lamella is then found by

$$F_{a,lam} = \frac{\left(755 \ ^{\text{lbs}}\!/_{\text{ft}}\right)(1.59')}{2\cos(19°)} = \boxed{636 \text{ lbs}},$$

and the moments are

$$M^{-}_{x,lam} = \frac{(1.59')\left(-8800 \ \text{in-lbs}/\text{ft}\right)}{\cos(19°)} = \boxed{-14837 \text{ in-lbs}},$$

$$M^{+}_{x,lam} = \frac{(1.59')\left(10110 \ \text{in-lbs}/\text{ft}\right)}{\cos(19°)} = \boxed{17046 \text{ in-lbs}},$$

$$M_{y,lam} = (636 \text{ lbs})(3.79'') = \boxed{2865 \text{ in-lbs}}.$$

The lamella must now be designed as a biaxial beam-column to withstand the combined thrust and moment for both positive and negative moment. For the positive moment, the compression side of the member is assumed to be braced continuously by the sheathing on the rooftop. For the negative moment, the side lamellas abut the continuous lamella at the half-points providing lateral bracing, giving an unbraced length of half of the lamella length. The weak-axis bending is assumed to be braced at the endpoints only. A 2x10 trial section will be used for the strength checks – it has the following characteristics [10]:

- A = 13.88 in^2
- S_{xx} = 21.39 in^3
- S_{yy} = 3.469 in^3
- F_b = 1300 psi
- F_c = 1600 psi
- E_{min} = 620,000 psi

Since the size of the bolts is unknown, the shift of the connection cannot be immediately found. The author assumes ½″ bolts in design which, according to Table 2, gives a shift of 3.79″. The forces due to the thrust and moments are as follows:

$$f_c = \frac{F_{a,lam}}{A} = \frac{636 \text{ lbs}}{13.88 \text{ in}^2} = \boxed{45.9 \text{ psi}},$$

$$f_{b1}^{-} = \frac{M_{x,lam}^{-}}{S_{xx}} = \frac{14837 \text{ in-lbs}}{21.39 \text{ in}^3} = \boxed{693.6 \text{ psi}},$$

$$f_{b1}^{+} = \frac{M_{x,lam}^{+}}{S_{xx}} = \frac{17046 \text{ in-lbs}}{21.39 \text{ in}^3} = \boxed{796.9 \text{ psi}},$$

and

$$f_{b2} = \frac{M_{y,lam}}{S_{yy}} = \frac{2865 \text{ in-lbs}}{3.469 \text{ in}^3} = \boxed{825.8 \text{ psi}}.$$

Now the adjustment factors must be found. Since the lamellas are spaced at less than 24″ on-center, the repetitive member factor C_r can be set to 1.15, which increases the bending strength of the lumber. From here, the beam stability factor C_L for the negative moment is calculated:

$$\frac{\ell_u}{d_1} = \frac{\left(4.90'/2\right)\left(12 \text{ in}/\text{ft}\right)}{9.25''} = 3.18' < 7.0,$$

$$\ell_e = 2.06\ell_u = 2.06\left(4.90'/2\right)\left(12 \text{ in}/\text{ft}\right) = 60.52'',$$

$$R_B = \sqrt{\frac{\ell_e d}{b^2}} = \sqrt{\frac{(60.52'')(9.25'')}{(1.5'')^2}} = 15.77,$$

$$E'_{\min} = E_{\min} C_M C_t C_i C_T = (620{,}000 \text{ psi})(1.0)(1.0)(1.0)(1.0) = 620{,}000 \text{ psi},$$

$$F_{bE} = \frac{1.20 E'_{\min}}{R_B^2} = \frac{1.20(620{,}000 \text{ psi})}{(15.77)^2} = 2990 \text{ psi},$$

$$F_b^* = F_b C_D C_M C_t C_F C_i C_r = (1300 \text{ psi})(1.0)(1.0)(1.0)(1.0)(1.0)(1.15),$$

$$F_b^* = 1495 \text{ psi},$$

$$C_L = \frac{1+\left(F_{bE}/F_b^*\right)}{1.9} - \sqrt{\left[\frac{1+\left(F_{bE}/F_b^*\right)}{1.9}\right]^2 - \frac{F_{bE}/F_b^*}{0.95}},$$

$$C_L = \frac{1+\left(2990/1495\right)}{1.9} - \sqrt{\left[\frac{1+\left(2990/1495\right)}{1.9}\right]^2 - \frac{2990/1495}{0.95}},$$

$$C_L = \boxed{0.956}.$$

Now, the column stability factor C_P is determined:

$$F_{cE} = \frac{0.822E'_{\min}}{\left(\frac{\ell_e}{d}\right)^2} = \frac{0.822\left(620{,}000\text{ psi}\right)}{\left(\frac{\left(4.90'\right)\left(12\,\text{in/ft}\right)}{9.25''}\right)^2} = 12630\text{ psi},$$

$$F_c^* = F_c C_D C_M C_t C_F C_i = \left(1600\text{ psi}\right)\left(1.0\right)\left(1.0\right)\left(1.0\right)\left(1.0\right)\left(1.0\right) = 1600\text{ psi},$$

$$c = 0.8,$$

$$C_P = \frac{1+\left(F_{cE}/F_c^*\right)}{2c} - \sqrt{\left[\frac{1+\left(F_{cE}/F_c^*\right)}{2c}\right]^2 - \frac{F_{cE}/F_c^*}{c}},$$

$$C_P = \frac{1+\left(12630/1600\right)}{2\left(0.8\right)} - \sqrt{\left[\frac{1+\left(12630/1600\right)}{2\left(0.8\right)}\right]^2 - \frac{12630/1600}{0.8}},$$

$$C_P = \boxed{0.973}.$$

Now, the remaining three design stresses for the unity check equation follow:

$$F'_{b1} = F_b C_D C_M C_t C_L C_F C_{fu} C_i C_r = \left(1300\text{ psi}\right)\left(1.0\right)\left(1.0\right)\left(1.0\right)\left(0.956\right)\left(1.0\right)\left(1.0\right)\left(1.0\right)\left(1.15\right),$$

$$F'_{b1} = 1430\text{ psi}.$$

The above F'_{b1} applies to the negative moment since the C_L value is for an unbraced length of 2.45 feet. For the positive moment with the compression edge continually braced, C_L = 1.0 and

$$F'_{b1} = F_b C_D C_M C_t C_L C_F C_{fu} C_i C_r = (1300 \text{ psi})(1.0)(1.0)(1.0)(1.0)(1.0)(1.0)(1.0)(1.15),$$
$$F'_{b1} = 1495 \text{ psi}.$$

For the compressive strength parallel to grain,

$$F'_c = F_c C_D C_M C_t C_F C_i C_P = (1600 \text{ psi})(1.0)(1.0)(1.0)(1.0)(1.0)(0.973),$$
$$F'_c = 1556 \text{ psi}.$$

From here, it is a simple matter to plug the values into the modified unity equation. For the negative moment:

$$\left[\frac{f_c}{F'_c}\right]^2 + \frac{f_{b1}}{F'_{b1}\left[1-\left(f_c/F_{cE1}\right)\right]} + \frac{f_{b2}}{F'_{b2}\left[1-\left(f_{b1}/F_{bE}\right)^2\right]} \le 1.0,$$

$$\left[\frac{45.9 \text{ psi}}{1556 \text{ psi}}\right]^2 + \frac{693.6 \text{ psi}}{(1430 \text{ psi})\left[1-\left(\frac{45.9 \text{ psi}}{12630 \text{ psi}}\right)\right]} + \frac{825.8 \text{ psi}}{(1794 \text{ psi})\left[1-\left(\frac{693.6 \text{ psi}}{2990 \text{ psi}}\right)^2\right]} \le 1.0,$$
$$\boxed{0.974 < 1.0 \text{ O.K.}},$$

and the positive moment is

$$\left[\frac{45.9 \text{ psi}}{1556 \text{ psi}}\right]^2 + \frac{796.9 \text{ psi}}{(1495 \text{ psi})\left[1-\left(\frac{45.9 \text{ psi}}{12630 \text{ psi}}\right)\right]} + \frac{825.8 \text{ psi}}{(1794 \text{ psi})\left[1-\left(\frac{796.9 \text{ psi}}{2990 \text{ psi}}\right)^2\right]} \le 1.0,$$
$$\boxed{1.031 > 1.0}.$$

The unity equation checks out for the negative moment but is about 3% high for the positive moment. However, since the loads on the arch are generally overstated and the stiffness of the roof will increase with the addition of the roof diaphragm, this extra 3% is of small concern and can most likely be ignored. Thus, a 2x10 section is adequate for design.

It should also be noted that the end supports of the arch need to be designed to carry 520 lbs. of lateral force per foot and 545 lbs. of gravity load per foot.

6.2 Connection Design

As mentioned in Section 4, there are two load paths in the connection. First, the vertical shear through the connection is found by

$$V_{\perp} = \frac{4M^{+}_{x,lam}}{\ell} = \frac{4(17046 \text{ in-lbs})}{4.90'\left(12 \,{}^{\text{in}}\!/_{\text{ft}}\right)} = \boxed{1160 \text{ lbs}}.$$

The positive moment is used because its magnitude is greater than that of the negative moment.

The tension due to the eccentric connection is

$$T_{bolts} = \frac{2F_{a,lam}\cos\theta}{\tan 2\theta} = \frac{2(636 \text{ lbs})(\cos 19°)}{\tan 38°} = \boxed{1540 \text{ lbs}}.$$

From Equation (117), we know that the strength of a connection is determined by

$$Z' = ZC_D C_M C_t C_g C_\Delta C_{eg} C_{di} C_{tn}.$$

The duration, moisture, temperature, end grain, diaphragm action, and toe-nail factors can all be set to 1.0 as discussed in Section 5.2. For determining the group action factor, a couple properties of the lamella must be found first. From Equation (11), the total length of the lamella, assuming ½″ bolts, is

$$\ell_T = \frac{2R\sin\phi}{\cos\theta} + \frac{t + 2D\tan 2\theta}{2\sin\theta\cos\theta} + \frac{t}{\tan 2\theta},$$

$$\ell_T = \frac{2(25')\left(\frac{12''}{1'}\right)\sin(5.31°)}{\cos(19°)} + \frac{1.5'' + 2(0.5'')\tan(38°)}{2\sin(19°)\cos(19°)} + \frac{1.5''}{\tan(38°)},$$

$$\ell_T = 65.09'' \approx 5' - 5\tfrac{3}{32}''.$$

Then, the angle ϕ_T is

$$\phi_T = \arcsin\left(\frac{\ell_T}{2R}\right) = \arcsin\left(\frac{65.09''}{2(25')\left(\frac{12''}{1'}\right)}\right) = 6.228°,$$

which means that the rise of the individual lamella, according to Equation (16), is

$$T' = R - \frac{\ell_T}{2\tan\phi_T} = (25')\left(\frac{12''}{1'}\right) - \frac{65.09''}{2\tan(6.228°)} = 1.77'',$$

which must be subtracted from the depth of the lamella to find its depth at the connecting end. Since a 2x10 has a depth of 9.25″, the depth at the connecting ends would be 7.48″.

Looking at Table B-4, the maximum length of a lamella for ½″ bolts while still keeping the geometry factor C_Δ equal to 1.0 is 8.5′ for three bolts and a radius of 25′. Since the total length of lamella is under that maximum, the spacing for keeping C_Δ equal to 1.0 should be used. According to Figure 16, this spacing is 4*D*, which would be 2″ for ½″ bolts.

For the group action factor,

$$E_m = E_s = E = 620{,}000 \text{ psi},$$

$$R_{EA} = \frac{A_s}{A_m} = \frac{(7.48'')(1.5'')}{13.88 \text{ in}^2} = 0.808.$$

Then, with a spacing of 2″,

$$u = 1 + \frac{180,000 D^{1.5} s}{2E}\left[\frac{1}{A_m} + \frac{1}{A_s}\right],$$

$$u = 1 + \frac{180,000\left(0.5''\right)^{1.5}\left(2''\right)}{2\left(620,000 \text{ psi}\right)}\left[\frac{1}{13.88 \text{ in}^2} + \frac{1}{\left(7.48''\right)\left(1.5''\right)}\right],$$

$$u = 1.107,$$

$$m = u - \sqrt{u^2 - 1} = \left(1.107\right) - \sqrt{\left(1.107\right)^2 - 1} = 0.8339.$$

Plugging these values in to solve for the geometry factor yields

$$C_g = \left[\frac{m\left(1 - m^{2n}\right)}{n\left[\left(1 + R_{EA} m^n\right)\left(1 + m\right) - 1 + m^{2n}\right]}\right]\left[\frac{1 + R_{EA}}{1 - m}\right],$$

$$C_g = \left[\frac{\left(0.8339\right)\left(1 - \left(0.8339\right)^{2(3)}\right)}{\left(3\right)\left[\left(1 + \left(0.808\right)\left(0.8339\right)^3\right)\left(1 + 0.8339\right) - 1 + \left(0.8339\right)^{2(3)}\right]}\right]\left[\frac{1 + 0.808}{1 - 0.8339}\right],$$

$$\boxed{C_g = 0.990.}$$

Essentially, the design strength of the connection will only be reduced by 1% since the geometry factor is the only one not equal to 1.0.

Table F-1 shows that a ½″ bolt can withstand 530 lbs of shear for southern pine (G = 0.55), so three bolts would have a shear capacity of

$$Z' = Z C_D C_M C_t C_g C_\Delta C_{eg} C_{di} C_{tn},$$

$$Z' = \left(3\right)\left(530 \text{ lbs}\right)\left(1.0\right)\left(1.0\right)\left(1.0\right)\left(0.990\right)\left(1.0\right)\left(1.0\right)\left(1.0\right)\left(1.0\right) = 1570 \text{ lbs},$$

which is greater than the 1160 lbs required. Table 11 shows that a ½″ bolt has a tensile capacity of 4460 lbs so by observation, three of them are more than sufficient for the 1540 lbs required.

The compression strength perpendicular to grain of the lamella is

$$F'_{c\perp} = F_{c\perp} C_M C_t C_i C_b = (565 \text{ psi})(1.0)(1.0)(1.0)(1.0) = \boxed{565 \text{ psi}},$$

and the required area of washers is then

$$A_{washer} \geq \frac{T_{bolts}}{F'_{c\perp}} = \frac{1540 \text{ lbs}}{565 \text{ psi}} = \boxed{2.72 \text{ in}^2}.$$

Washer size should be specified by the engineer based on availability of materials. If regular stamped washers have insufficient area, oversized square washers may need to be used.

7 Prototype Models

In order to better visualize and demonstrate the concept of the lamella roof, two models were created. They gave the author a better understanding of how the lamella roof fits together and also demonstrated the ease of assembly of the system. Also, a steel model allowed the author to perform load testing with strain gauges.

7.2 Matboard Model

A proof-of-concept model was created using matboard connected with #3 solid brass fasteners. The lamella pieces were cut using a laser cutter and assembled by hand. While assembling the model (shown in Figure 49), the author noted that as more pieces were added to the lamella arch, the arch itself became more stiff, indicating an interaction having to do with the interesting connection style used by lamella construction.

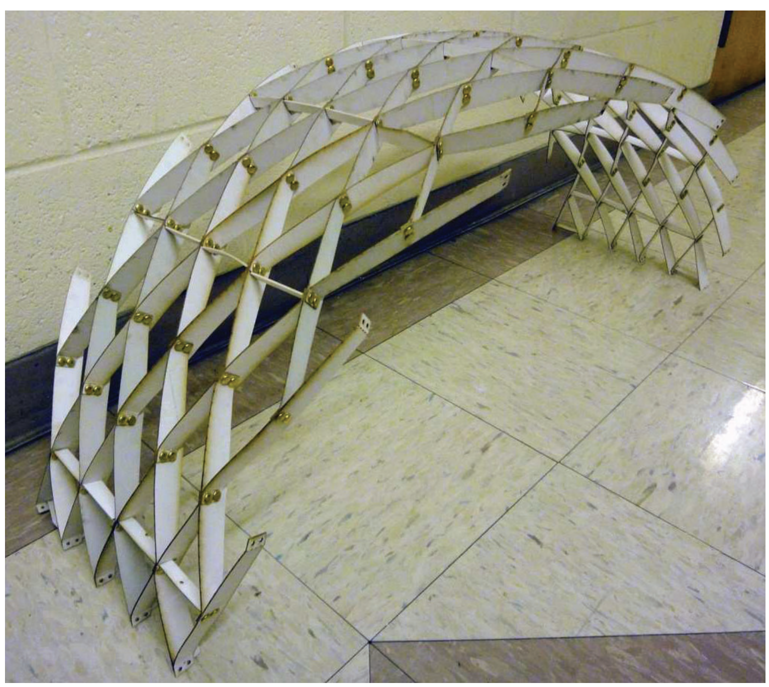

Figure 49 - Matboard Proof-of-Concept Model.

7.3 Steel Model

After the proof-of-concept model was made, a model made of sheet steel was fabricated and donated by H. Kubenik Metals of Milwaukee, WI. The model was precision-cut using a computer-controlled plasma cutter with the ends bent in a machine press (see Figure 50 and Figure 51). The steel model was approximately a two-times scale copy of the matboard model.

Figure 50 - Plasma Cutting of Steel Lamellas.

Figure 51 - Bending of Steel Lamellas.

After cutting and bending, the lamellas were assembled with machine screws, lock washers, and nuts to create a section of a lamella arch. The finished product is displayed in Figure 52.

Figure 52 - Assembled Steel Lamella Arch.

Though hard to see in Figure 52, the top of the arch had a distinct curvature in the short direction, resulting in “cupping” of the entire structure. This is most likely due to the fact that the drafting model used for fabrication was not as exact as required for a perfect fit.

The properties of the steel arch ended up being:

- Span [S] = 75″
- Rise [T] = 37″
- Arch width of 24″

- 12 ga. A36 steel (thickness [t] = 0.1084″)
- 10-32 x ½″ machine screws
- 8.5 lamellas per arch (n = 8.5)
- Spacing = 4.145″
- Nominal depth of lamella [d] = 2.05″

7.3.1 Load Testing

The steel model was tested to see if the resultant stresses on the model fit with those predicted by the load table program created by the author. Special bearing plates were fabricated out of 2x4 lumber to act like pinned connections at the springing ends of the arch as shown in Figure 53.

Figure 53 - Steel Model Bearing Plates.

To find the stresses in the lamellas during testing, several strain gauges were affixed to the model, as depicted in Figure 54.

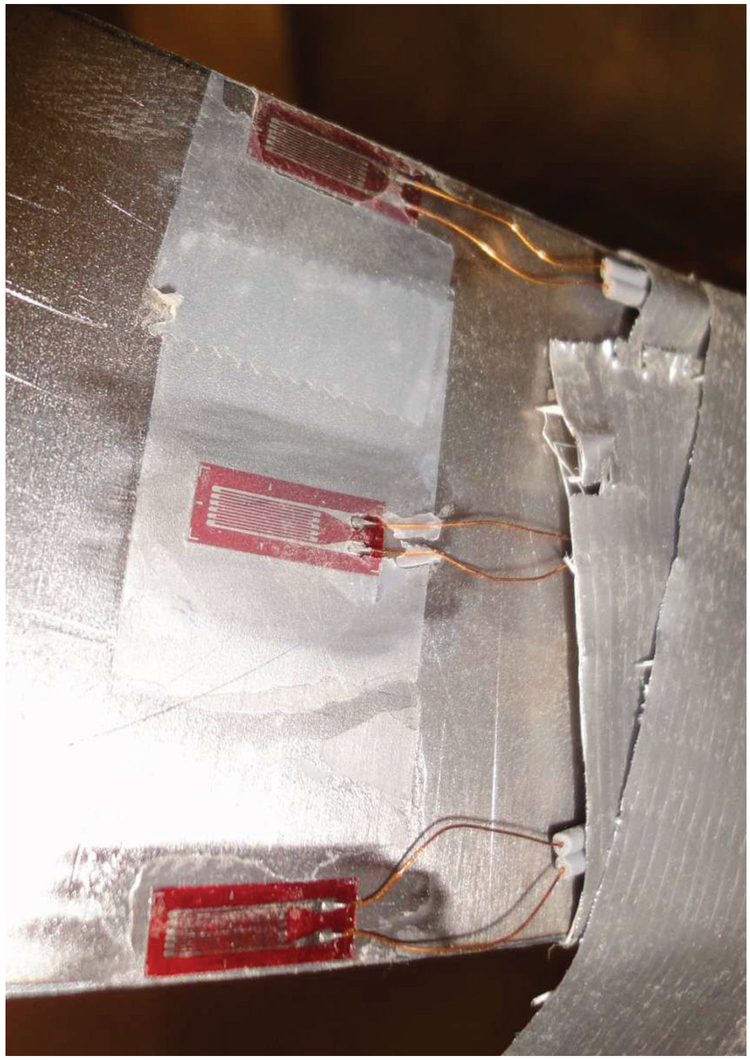

Figure 54 - Strain Gauge Close-up.

The strain gauges were placed in the middle of a lamella span to reduce any affects that stress concentrations might have had on the results. They were placed in three groups at different parts of the arch, as shown in Figure 55. The gauge groups are depicted with a black rectangle.

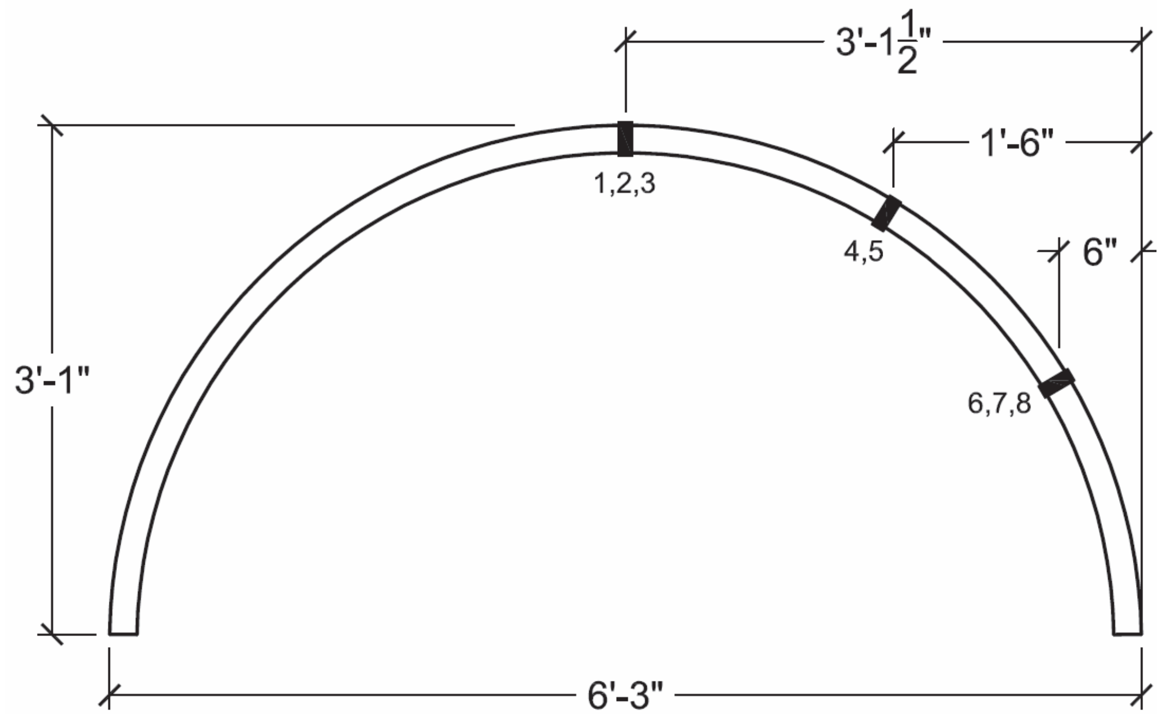

Figure 55 - Strain Gauge Locations.

The numbers next to the rectangles represent the locations of the numbered strain gauges. The gauge with the lower number is closer to the outside of the arch, i.e., SG1 is at the very top of the arch while SG3 is directly below it on the inside of the arch.

Three different loading patterns were used for testing, shown in Figure 56, Figure 57, and Figure 58, each to simulate a different real-world loading. Plastic bags, each filled with ten pounds of sand, were used to control the amount of load. The first series was to simulate a balanced snow load.

Figure 56 - Balanced Snow Load Simulation.

The second simulated a snow drift load by stacking sand bags on half of the structure. The sand bag loading does not exactly reflect the loading pattern depicted in the Simplified Figure 7-3 found in Appendix C since the loading is uniform. To counter this discrepancy, the loading pattern in the Simplified Figure 7-3 was averaged to 1.35p_f and the load put into the load table program was adjusted to match this value.

Figure 57 - Snow Drift Load Simulation.

The final loading stacked bags on the apex of the arch to simulate a point load. This point load would essentially be a lineal load along the length of the apex if the roof.

Figure 58 - Point Load Simulation.

Since the bags had a total bearing area of 10″ by 10″ (or 100 in^2), the corresponding area load would be 14.4 psf. Also, the point load simulation is modeled as a lineal load on the length of the apex, which would correlate to 12 plf per bag. These corresponding loads were inputted into the load table program developed by the author, then adjusted using the process outlined in the end of Section 5.1 to find the predicted stresses on the lamellas. Since the lamellas are in biaxial bending and compression, the stresses are summed to reflect correlate to the correct combination of compression and moment.

Table 12 displays a list of data found during the different loading tests. Perhaps most interesting are the data from Strain Gauges 6-8. It appears that weak axis bending was so large that on the face the strain gauges were attached, the effects of strong axis bending and compression were not enough to put compressive stress into the fibers.

Table 12 - Strain Gauge Testing Data.

Load			Actual Stress [σ] (psi)							
			SG1	SG2	SG3	SG4	SG5	SG6	SG7	SG8
Balanced Snow	1	12 bags	-348	580	319	-290	435	1769	1682	841
	2	24 bags	-696	1160	1073	-377	841	3712	3219	1682
	3	36 bags	-1015	1653	1798	0	1624	5887	4901	2813
	4	48 bags	-1305	2291	2610	812	2755	8671	7308	4611
	5	60 bags	-1537	3045	3451	1885	4408	11687	10092	6902
	6	72 bags	-1769	4205	5423	2465	5771	15573	13949	10527
Snow Drift	7	6 bags	29	522	464	-1160	203	522	551	464
	8	12 bags	58	870	870	2523	493	1131	1189	1044
	9	18 bags	58	1218	1218	-3770	870	1769	1827	1624
	10	24 bags	87	1566	1595	-4901	1305	2436	2581	2291
	11	30 bags	87	1914	1943	-5829	1885	3219	3364	2987
	12	36 bags	116	2291	2407	-6728	2494	4031	4176	3654
Point Load	13	4 bags	-435	261	493	261	290	609	464	174
	14	8 bags	-725	725	1073	203	493	1044	725	290
	15	12 bags	-957	1131	1682	348	841	1624	1160	464
	16	16 bags	-1218	1508	2204	464	1131	2175	1566	667
	17	20 bags	-1537	1827	2813	638	1479	2871	2059	957
	18	24 bags	-1682	2291	3480	783	1769	3509	2523	1218

The data showing the predicted stress values are shown in Table 13.

Table 13 - Predicted Fiber Stresses.

Load			Program Stress [σ] (psi)							
			SG1	SG2	SG3	SG4	SG5	SG6	SG7	SG8
Balanced Snow	1	12 bags	-1125	-355	414	521	516	1463	670	-122
	2	24 bags	-2249	-711	828	1042	1031	2926	1341	-244
	3	36 bags	-3374	-1066	1243	1564	1547	4389	2011	-367
	4	48 bags	-4499	-1421	1657	2085	2062	5852	2681	-489
	5	60 bags	-5624	-1776	2071	2606	2578	7315	3352	-612
	6	72 bags	-6748	-2131	2486	3127	3094	8778	4022	-734
Snow Drift	7	6 bags	-872	-346	179	-741	1861	1219	968	717
	8	12 bags	-1744	-692	359	-1482	3721	2437	1936	1435
	9	18 bags	-2615	-1038	538	-2223	5582	3655	2903	2151
	10	24 bags	-3487	-1385	718	-2964	7443	4873	3871	2869
	11	30 bags	-4359	-1731	897	-3705	9303	6092	4839	3586
	12	36 bags	-5231	-2077	1076	-4446	11164	7310	5807	4303
Point Load	13	4 bags	-1102	-172	759	83	406	711	264	-184
	14	8 bags	-2204	-343	1518	166	812	1424	527	-369
	15	12 bags	-3306	-515	2277	248	1218	2135	791	-553
	16	16 bags	-4408	-686	3036	331	1625	2846	1054	-737
	17	20 bags	-5510	-858	3795	414	2031	3558	1318	-922
	18	24 bags	-6612	-1029	4554	495	2439	4270	1582	-1106

One can compare the predicted stresses to the actual stresses, which results in Table 14.

Table 14 - Percent Difference in Predicted versus Observed Stress.

Load			Percent Difference in Predicted versus Observed Stress							
			SG1	SG2	SG3	SG4	SG5	SG6	SG7	SG8
Balanced Snow	1	12 bags	69%	263%	23%	156%	16%	-21%	-151%	788%
	2	24 bags	69%	263%	-30%	136%	18%	-27%	-140%	788%
	3	36 bags	70%	255%	-45%	100%	-5%	-34%	-144%	867%
	4	48 bags	71%	261%	-57%	61%	-34%	-48%	-173%	1042%
	5	60 bags	73%	271%	-67%	28%	-71%	-60%	-201%	1229%
	6	72 bags	74%	297%	-118%	21%	-87%	-77%	-247%	1534%
Snow Drift	7	6 bags	103%	251%	-159%	-57%	89%	57%	43%	35%
	8	12 bags	103%	226%	-143%	270%	87%	54%	39%	27%
	9	18 bags	102%	217%	-126%	-70%	84%	52%	37%	25%
	10	24 bags	102%	213%	-122%	-65%	82%	50%	33%	20%
	11	30 bags	102%	211%	-117%	-57%	80%	47%	30%	17%
	12	36 bags	102%	210%	-124%	-51%	78%	45%	28%	15%
Point Load	13	4 bags	61%	252%	35%	-216%	29%	14%	-76%	194%
	14	8 bags	67%	311%	29%	-23%	39%	27%	-37%	179%
	15	12 bags	71%	320%	26%	-40%	31%	24%	-47%	184%
	16	16 bags	72%	320%	27%	-40%	30%	24%	-49%	190%
	17	20 bags	72%	313%	26%	-54%	27%	19%	-56%	204%
	18	24 bags	75%	323%	24%	-58%	27%	18%	-60%	210%

Unfortunately, this comparison of values appears to be inconclusive. There are enough values within the 10-40% overestimate range to make one wonder if the matrix program is predicting values correctly. Yet there are also plenty of values so far out of range that the predictions seem wildly incorrect. More testing would help clarify these inconsistencies.

Another factor that may contribute to the discrepancy in values is the stiffness of the steel arch. The exact stiffness is difficult to determine due to the nature of the lattice structure, and, as mentioned before, a stiffer structure has a tendency to take on more moment. A more flexible arch would see more axial thrust, which could help bring some of the values closer to those predicted by the matrix program.

The author also tested to see if the horizontal reaction of the arch matched that predicted by the matrix program. For testing, two tension gauges were attached to either end of the steel lamella arch to measure the horizontal reaction. One end of the arch was placed atop rollers to facilitate the stretching of the tension gauges while the other end was held in place. This setup is show in Figure 59.

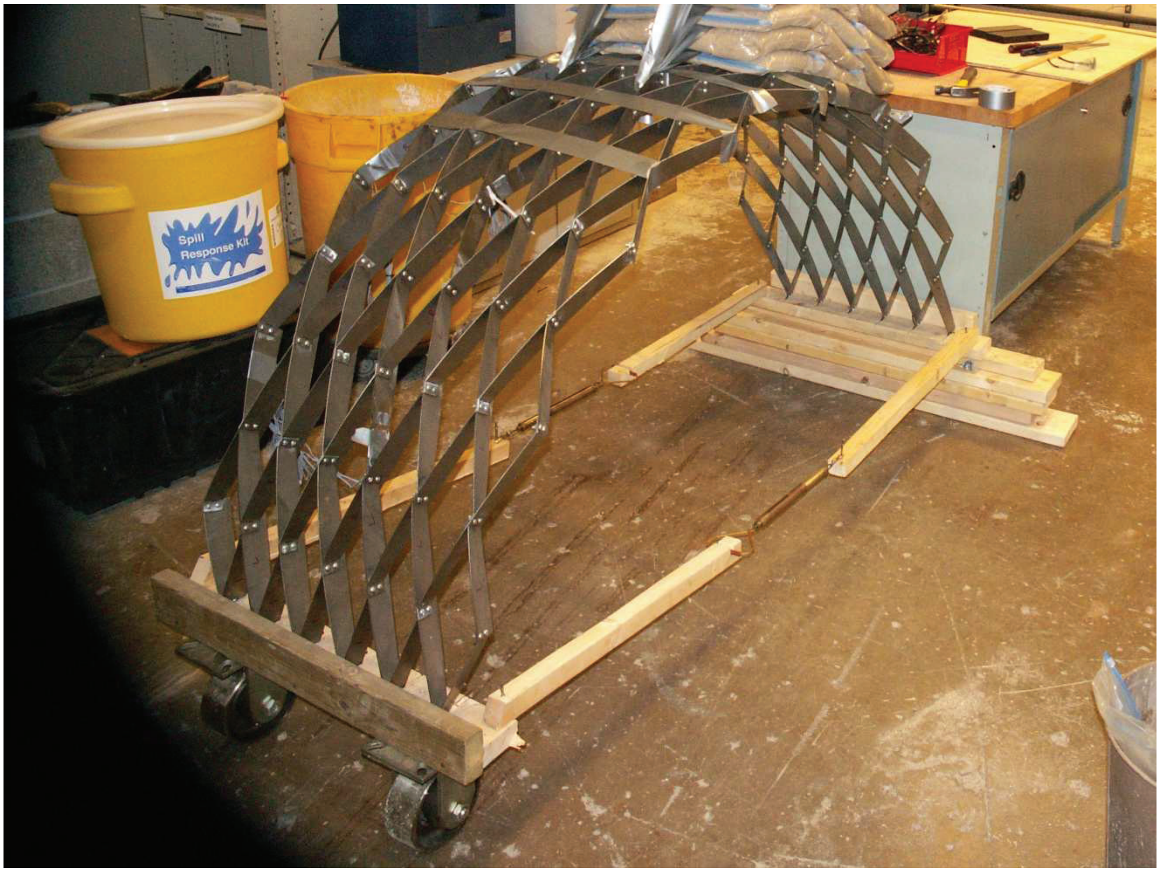

Figure 59 - Horizontal Reaction Test Setup.

The steel arch was subjected to the same loading conditions as the strain gauge tests. The measurements found on the tension gauges were averaged. Since the arch was two feet wide, the average of the two reactions is directly proportionate to the horizontal reaction per foot given by the matrix program developed by the author. The actual values are compared to the predicted values in Table 15.

Table 15 - Horizontal Reaction Comparison.

Horizontal Reaction					
Load			Actual (lbs)	Predicted (lbs)	% Diff
Balanced Snow	1	12 bags	6.25	17	63%
	2	24 bags	13.5	34.1	60%
	3	36 bags	19.75	51.1	61%
	4	48 bags	27.75	68.1	59%
	5	60 bags	37.5	85.1	56%
	6	72 bags	-	102.2	-
Snow Drift	7	6 bags	4.25	17.4	76%
	8	12 bags	8.25	34.8	76%
	9	18 bags	12.75	52.1	76%
	10	24 bags	16	69.5	77%
	11	30 bags	22.25	86.9	74%
	12	36 bags	27.25	104.3	74%
Point Load	13	4 bags	3.5	8.7	60%
	14	8 bags	6.5	17.3	62%
	15	12 bags	8.5	26	67%
	16	16 bags	14.5	34.6	58%
	17	20 bags	17.25	43.3	60%
	18	24 bags	20.75	51.9	60%

In all cases, the predicted values are gross overestimates of the actual horizontal reactions. Again, this could have to do with the stiffness of the steel arch being different than that used in the matrix program. Fortunately, none of the values are underestimates and the design horizontal reaction would be a conservative design value.

8 Conclusion

The lamella structure offers a unique and aesthetically pleasing architectural roof that has the added bonus of using less material than what a "traditional" roof spanning the same distance might. Its modular nature makes fabrication a cost-effective, repetitive task, and its use of widely-available dimensional lumber makes its construction an attainable goal for many smaller projects.

Previous efforts to engineer the structure relied on approximations due to the lack of computer analysis. Modern matrix systems can be used to accurately solve for the forces in a two-pinned arch with a given stiffness and updated building codes allow the engineer the peace of mind to know that he or she is designing for a real-life loading scenario.

The load tables developed by the author, coupled with a detailed explanation of the calculations necessary to check for member and connection adequacy, should allow one to perform an introductory strength check and come up with a preliminary design for a lamella roof. However, due to the fact that the loading patterns employed by the ASCE 7-10 are generally overestimates and due to the fact that the calculations assume absolutely worst case loads, a more in-depth analysis should be undertaken to more accurately find the forces in the arched roof.

Through testing, the author was unfortunately unable to find conclusive evidence that the values predicted by his matrix program matched those found from testing. Some values were close enough to be matches while others were clearly not. More testing and refining of the matrix program should be undertaken to determine how exactly the two relate.

References

[1] Allen, J. S. 1999. "A Short History of 'Lamella' Roof Construction." *Transactions of the Newcomen Society* Vol. 71 (1).

[2] "Design Forum IX Features Adjaye, Eizenberg, Freear, Cruz." 15 January 2010. [Internet, WWW]. *Available:* Available from ArchiThings website; *Address:* http://www.archithings.com/design-forum-ix-features-adjaye-eizenberg-freear-cruz/2010/01/15. [Accessed 30 January 2010]. A copy of this article is available from the author.

[3] Scofield, W. Fleming and W. H. O'Brien. 1963. *Modern Timber Engineering*, 5th ed. New Orleans: Southern Pine Association.

[4] Masani, N. J. 1982. "Theory & Practice of Timber and Lamella Frames." *Timber Engineering Manual Part III.* Delhi: F.R.I. Press

[5] Heise, Karen. 2004. "Ingenieurporträt: Friedrich Reinhardt Balthasar Zollinger." [Internet, WWW, PDF]. *Available:* Available in .PDF format from Deutsche Bauzeitung; *Address:* http://bauzeitung.de/files/db_essays/ingportrait_imp_0402.pdf. [Accessed 30 January, 2011].

[6] Otzen, Robert. 1926. *Handbibliothek für Bauingenieure.* Julius Springer: Berlin.

[7] "The Lamella Roof (Revised Edition)." 1931. *Volume IV: Construction Information Series*. Washington D.C.: National Lumber Manufacturers Association. Ch. 12.

[8] American Institute of Steel Construction (AISC). 2005. *Steel Construction Manual,* 13th ed. Chicago: American Institute of Steel Construction.

[9] "The Lamella Roof (Revised Edition)." 1931. *Volume IV: Construction Information Series*. Washington D.C.: National Lumber Manufacturers Association. Ch. 12.

[10] American Forest & Paper Association. 2006. *National Design Specification for Wood Construction*, 2005 Edition. Washington D.C.: American Forest & Paper Association.

[11] Warner, Tim. January 2011. "The Geometry of a Lamella Roof." Paper received in email from the author. Milwaukee, WI.

[12] von Kármán, Theodor. Late 1930's. "Analysis of the Lamella Roof." Paper borrowed from California Institute of Technology. Pasadena, CA.

[13] Frazee, Glenn. 28 September, 2009. "The Beam Element Stiffness." Class notes from AE-610: Finite Element Analysis. Professor H. P. Huttelmaier. Milwaukee School of Engineering, Milwaukee, Wisconsin. Available from the author.

[14] Chandrupatla, Tirupathi R. and Ashok D. Belegundu. 2002. *Introduction to Finite Elements in Engineering*, 3rd ed. Upper Saddle River, New Jersey: Prentice Hall.

[15] American Society of Civil Engineers (ASCE). 2010. *ASCE 7-10 Minimum Design Loads for Buildings and Other Structures.* New York: American Society of Civil Engineers.

[16] *Timber Design and Construction Handbook.* 1956. New York: McGraw-Hill Book Company, Inc.

Bibliography

Allen, J. S. 1999. "A Short History of 'Lamella' Roof Construction." *Transactions of the Newcomen Society* Vol. 71 (1).

American Forest & Paper Association. 2006. *National Design Specification for Wood Construction*, 2005 Edition. Washington D.C.: American Forest & Paper Association.

American Institute of Steel Construction (AISC). 2005. *Steel Construction Manual,* 13th ed. Chicago: American Institute of Steel Construction.

American Society of Civil Engineers (ASCE). 2010. *ASCE 7-10 Minimum Design Loads for Buildings and Other Structures.* New York: American Society of Civil Engineers.

Chandrupatla, Tirupathi R. and Ashok D. Belegundu. 2002. *Introduction to Finite Elements in Engineering*, 3rd ed. Upper Saddle River, New Jersey: Prentice Hall.

Cuoco, Daniel A. 1981. "State-of-the-Art of Space Frame Roof Structures." *Long Span Roof Structures.* New York: American Society of Civil Engineers.

Dean, Donald L. 1964. "Lamella Beams and Grids." *Journal of the Engineering Mechanics Division.* New York: American Society of Civil Engineers.

"Design Forum IX Features Adjaye, Eizenberg, Freear, Cruz." 15 January 2010. [Internet, WWW]. *Available:* Available from ArchiThings website; *Address:* http://www.archithings.com/design-forum-ix-features-adjaye-eizenberg-freear-cruz/2010/01/15. [Accessed 30 January 2010]. A copy of this article is available from the author.

Frazee, Glenn. 28 September, 2009. "The Beam Element Stiffness." Class notes from AE-610: Finite Element Analysis. Professor H. P. Huttelmaier. Milwaukee School of Engineering, Milwaukee, Wisconsin. Available from the author.

Heise, Karen. 2004. "Ingenieurporträt: Friedrich Reinhardt Balthasar Zollinger." [Internet, WWW, PDF]. *Available:* Available in .PDF format from Deutsche Bauzeitung; *Address:* http://bauzeitung.de/files/db_essays/ingportrait_imp_0402.pdf. [Accessed 30 January 2011].

Holzer, Siegfried M., Layne T. Watson, and Phap Vu. 1981. "Stability Analysis of Lamella Domes." *Long Span Roof Structures*. New York: American Society of Civil Engineers.

Masani, N. J. 1961. "Theory & Practice of a Three-Hinged Arch Nail-Jointed Timber Truss." *Timber Engineering Manual Part I.* Delhi: Government of India Press.

Masani, N. J. 1982. "Theory & Practice of Timber and Lamella Frames." *Timber Engineering Manual Part III.* Delhi: F.R.I. Press

Nathern, Mark S. and Jan J. Tuma. 1979. "Analysis of Spherical Lamella Domes." *Electronic Computation.* New York: American Society of Civil Engineers.

Otzen, Robert. 1926. *Handbibliothek für Bauingenieure.* Berlin: Julius Springer.

Scofield, W. Fleming and W. H. O'Brien. 1963. *Modern Timber Engineering*, 5th ed. New Orleans: Southern Pine Association.

Sherman, D. R. 1976. "Latticed Structures: State-of-the-Art Report." *Journal of the Structural Division,* Vol. 102 (11), pp. 2197-2230.

"The Lamella Roof (Revised Edition)." 1931. *Volume IV: Construction Information Series*. Washington D.C.: National Lumber Manufacturers Association. Ch. 12.

Timber Design and Construction Handbook. 1956. New York: McGraw-Hill Book Company, Inc.

Timoshenko, S. P. and D. H. Young. 1965. *Theory of Structures*, 2nd ed. New York: McGraw-Hill.

von Kármán, Theodor. Late 1930's. "Analysis of the Lamella Roof." Paper borrowed from California Institute of Technology. Pasadena, CA.

Warner, Tim. January 2011. "The Geometry of a Lamella Roof." Paper received in email from the author. Milwaukee, WI.

Appendix A: NDS 2005 Tables and Figures

This appendix features a copy of a relevant figure (Figure A-1) and copies of relevant tables (Tables A-1 through A-5) from the American Forest and Paper Association's National Design Specification for Wood Construction.[1]

Table A-1 – Edge Distance Requirements.

Table 11.5.1A Edge Distance Requirements [1,2]

Direction of Loading	Minimum Edge Distance
Parallel to Grain:	
when $\ell/D \leq 6$	1.5D
when $\ell/D > 6$	1.5D or ½ the spacing between rows, whichever is greater
Perpendicular to Grain:[2]	
loaded edge	4D
unloaded edge	1.5D

1. The ℓ/D ratio used to determine the minimum edge distance shall be the lesser of:
   (a) length of fastener in wood main member/D = ℓ_m/D
   (b) total length of fastener in wood side member(s)/D = ℓ_s/D
2. Heavy or medium concentrated loads shall not be suspended below the neutral axis of a single sawn lumber or structural glued laminated timber beam except where mechanical or equivalent reinforcement is provided to resist tension stresses perpendicular to grain (see 3.8.2 and 10.1.3).

Table A-2 – End Distance Requirements.

Table 11.5.1B End Distance Requirements

Direction of Loading	End Distances: Minimum end distance for $C_\Delta = 0.5$	End Distances: Minimum end distance for $C_\Delta = 1.0$
Perpendicular to Grain	2D	4D
Parallel to Grain, Compression: (fastener bearing away from member end)	2D	4D
Parallel to Grain, Tension: (fastener bearing towards member end)		
for softwoods	3.5D	7D
for hardwoods	2.5D	5D

[1] American Forest & Paper Association. 2006. *National Design Specification for Wood Construction*, 2005 Edition. Washington D.C.: American Forest & Paper Association.

Table A-3 – Spacing Requirements for Fasteners in a Row.

Table 11.5.1C Spacing Requirements for Fasteners in a Row

Direction of Loading	Spacing: Minimum spacing	Spacing: Minimum spacing for $C_\Delta = 1.0$
Parallel to Grain	3D	4D
Perpendicular to Grain	3D	Required spacing for attached members

Table A-4 – Spacing Requirements Between Rows.

Table 11.5.1D Spacing Requirements Between Rows [1,2]

Direction of Loading	Minimum Edge Distance
Parallel to Grain:	1.5D
Perpendicular to Grain:	
when $\ell/D \le 2$	2.5D
when $2 < \ell/D < 6$	$(5\ell + 10D) / 8$
when $\ell/D \ge 6$	5D

1. The ℓ/D ratio used to determine the minimum edge distance shall be the lesser of:
   (a) length of fastener in wood main member/D = ℓ_m/D
   (b) total length of fastener in wood side member(s)/D = ℓ_s/D
2. The spacing between outer rows of fasteners paralleling the member on a single splife plate shall not exceed 5" (see Figure 11H).

Table A-5 – Reduction Term, R_d.

Table 11.3.1B Reduction Term, R_d

Fastener Size	Yield Mode	Reduction Term, R_d
$0.25'' \le D \le 1''$	I_m, I_s	$4\,K_\theta$
	II	$3.6\,K_\theta$
	III_m, III_s, IV	$3.2\,K_\theta$
$D < 0.25''$	I_m, I_s, II, III_m, III_s, IV	K_D [1]

Notes:

$K_\theta = 1 + 0.25(\theta - 90)$

$\theta =$ maximum angle of load to grain $(0 \le \theta \le 90)$ for any member in a connection

$D =$ diameter, in. (see 11.3.6)

$K_D = 2.2$ for $D \le 0.17''$

$K_D = 10D + 0.5$ for $0.17'' < D < 0.25''$

1. For threaded fasteners where nominal diameter (see Appendix L) is greater than or equal to 0.25″ and root diameter is less than 0.25″, $R_d = K_D K_\theta$.

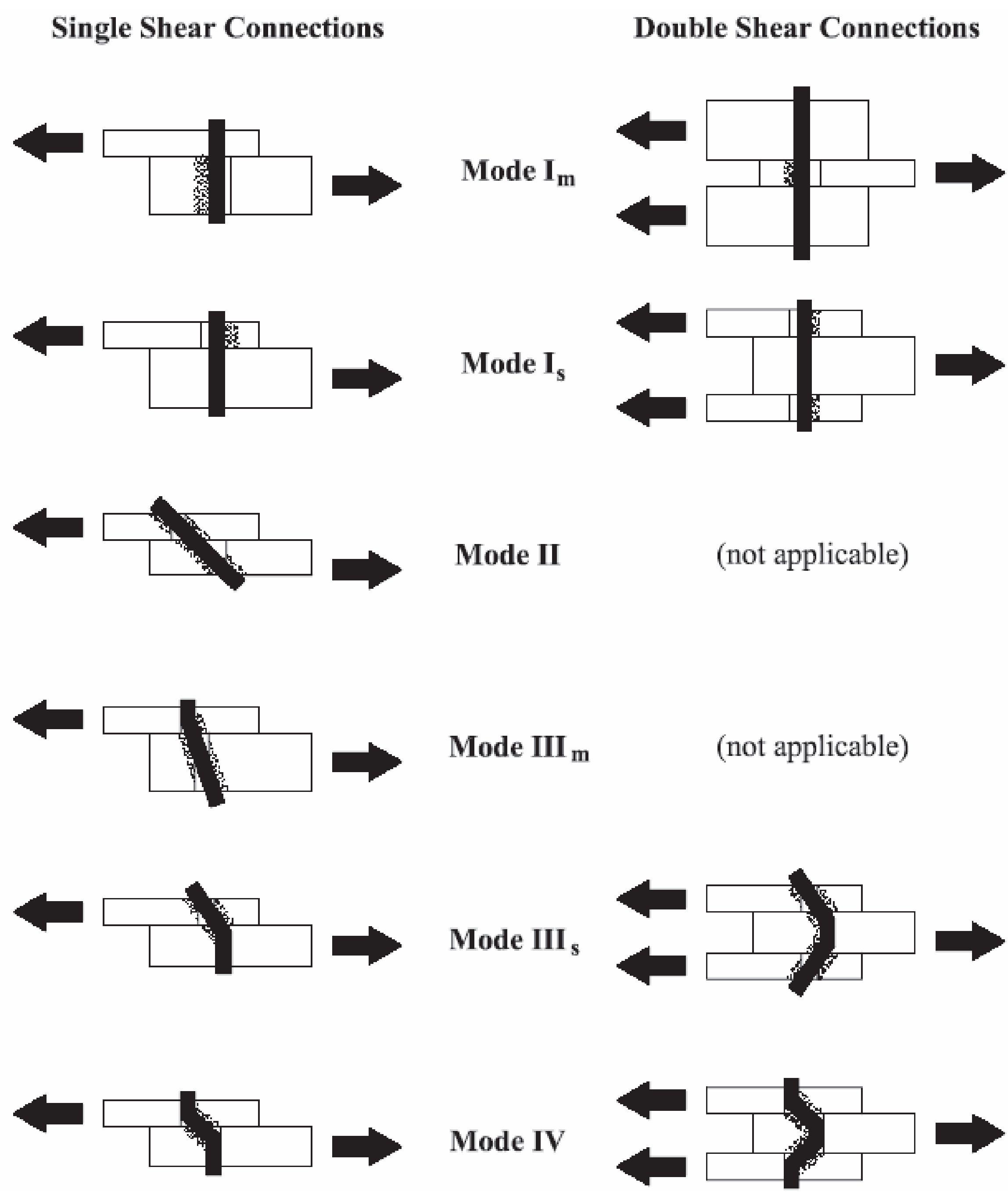

Figure A-1 – Connection Yield Modes.

Appendix B: Curvature versus Length Tables

Tables B-1 through B-10 feature curvature versus lamella length data for 1/4″, 5/16″, 3/8″, 1/2″, 3/4″, 7/8″, and 1″ bolts.

Table B-1 - 1/4" Bolts - Maximum Lamella Length [ℓ] (ft)

$C_\Delta = 1.0$

Radius [R] (ft)	(2) Bolts per Connection				(3) Bolts per Connection			(4) Bolts per Connection		
	2 x 4	2 x 6	2 x 8	2 x 10	2 x 6	2 x 8	2 x 10	2 x 6	2 x 8	2 x 10
1000	31.0	55.9	70.8	84.7	42.1	60.5	76.3	20.4	48.1	66.9
900	29.4	53.1	67.2	80.4	40.0	57.5	72.4	19.4	45.7	63.5
800	27.8	50.0	63.4	75.8	37.7	54.2	68.3	18.3	43.1	59.9
700	26.0	46.8	59.3	70.9	35.3	50.7	63.9	17.1	40.3	56.0
600	24.1	43.4	54.9	65.7	32.7	47.0	59.2	15.9	37.4	51.9
500	22.0	39.6	50.2	60.0	29.9	42.9	54.1	14.5	34.1	47.4
400	19.7	35.5	44.9	53.7	26.8	38.4	48.4	13.0	30.6	42.4
450	20.9	37.6	47.6	56.9	28.4	40.7	51.3	13.8	32.4	45.0
400	19.7	35.5	44.9	53.7	26.8	38.4	48.4	13.0	30.6	42.4
350	18.5	33.2	42.0	50.2	25.1	36.0	45.3	12.2	28.6	39.7
300	17.1	30.8	38.9	46.5	23.2	33.3	41.9	11.3	26.5	36.8
275	16.4	29.5	37.3	44.6	22.3	31.9	40.2	10.9	25.4	35.2
250	15.7	28.1	35.6	42.5	21.2	30.4	38.3	10.4	24.2	33.6
225	14.9	26.7	33.8	40.3	20.2	28.9	36.4	9.9	23.0	31.9
200	14.1	25.2	31.9	38.0	19.0	27.3	34.3	9.3	21.7	30.1
175	13.2	23.6	29.8	35.6	17.8	25.5	32.1	8.7	20.3	28.2
150	12.2	21.9	27.6	33.0	16.5	23.7	29.8	8.1	18.8	26.1
125	11.2	20.0	25.3	30.1	15.1	21.6	27.2	7.4	17.2	23.9
100	10.0	17.9	22.6	27.0	13.6	19.4	24.4	6.7	15.5	21.4
90	9.5	17.0	21.5	25.6	12.9	18.4	23.1	6.4	14.7	20.3
80	9.0	16.1	20.3	24.2	12.2	17.4	21.8	6.0	13.9	19.2
70	8.5	15.0	19.0	22.6	11.4	16.3	20.4	5.7	13.0	17.9
60	7.9	14.0	17.6	21.0	10.6	15.1	18.9	5.3	12.0	16.6
50	7.2	12.8	16.1	19.2	9.7	13.8	17.3	4.8	11.0	15.2
40	6.5	11.5	14.4	17.2	8.7	12.4	15.5	4.4	9.9	13.6
30	5.7	10.0	12.5	14.9	7.6	10.8	13.5	3.8	8.6	11.8
20	4.7	8.2	10.3	12.2	6.3	8.8	11.0	3.2	7.1	9.7
18	4.5	7.8	9.8	11.6	5.9	8.4	10.5	3.0	6.7	9.2
16	4.2	7.4	9.2	10.9	5.6	7.9	9.9	2.9	6.4	8.7
14	4.0	6.9	8.6	10.2	5.3	7.4	9.3	2.7	6.0	8.2
12	3.7	6.4	8.0	9.5	4.9	6.9	8.6	2.6	5.6	7.6
10	3.4	5.9	7.3	8.7	4.5	6.3	7.9	2.4	5.1	7.0

Table B-2 - 5/16" Bolts - Maximum Lamella Length [ℓ] (ft)

$C_\Delta = 1.0$

Radius [R] (ft)	(2) Bolts per Connection				(3) Bolts per Connection			(4) Bolts per Connection		
	2 x 4	2 x 6	2 x 8	2 x 10	2 x 6	2 x 8	2 x 10	2 x 8	2 x 10	2 x 12
1000	22.4	51.7	67.5	82.0	35.1	55.9	72.7	41.1	62.1	77.5
900	21.3	49.0	64.1	77.8	33.3	53.1	69.0	39.0	58.9	73.6
800	20.1	46.3	60.4	73.3	31.4	50.0	65.1	36.8	55.5	69.4
700	18.8	43.3	56.6	68.6	29.4	46.8	60.9	34.5	52.0	64.9
600	17.4	40.1	52.4	63.6	27.3	43.4	56.4	31.9	48.1	60.1
500	16.0	36.6	47.8	58.0	24.9	39.6	51.5	29.2	44.0	54.9
400	14.3	32.8	42.8	52.0	22.3	35.5	46.1	26.1	39.4	49.1
450	15.2	34.8	45.4	55.1	23.7	37.6	48.9	27.7	41.7	52.1
400	14.3	32.8	42.8	52.0	22.3	35.5	46.1	26.1	39.4	49.1
350	13.4	30.7	40.1	48.6	20.9	33.2	43.1	24.5	36.9	46.0
300	12.4	28.5	37.1	45.0	19.4	30.8	40.0	22.7	34.1	42.6
275	11.9	27.3	35.6	43.1	18.6	29.5	38.3	21.7	32.7	40.8
250	11.4	26.0	33.9	41.1	17.7	28.1	36.5	20.7	31.2	38.9
225	10.8	24.7	32.2	39.0	16.8	26.7	34.7	19.7	29.6	36.9
200	10.2	23.3	30.4	36.8	15.9	25.2	32.7	18.6	27.9	34.8
175	9.6	21.8	28.4	34.5	14.9	23.6	30.6	17.4	26.2	32.6
150	8.9	20.2	26.4	31.9	13.8	21.9	28.4	16.1	24.2	30.2
125	8.2	18.5	24.1	29.2	12.6	20.0	25.9	14.8	22.2	27.6
100	7.3	16.6	21.6	26.1	11.3	17.9	23.2	13.2	19.9	24.7
90	7.0	15.7	20.5	24.8	10.8	17.0	22.0	12.6	18.9	23.5
80	6.6	14.9	19.3	23.4	10.2	16.1	20.8	11.9	17.8	22.2
70	6.2	13.9	18.1	21.9	9.5	15.0	19.5	11.1	16.7	20.7
60	5.8	12.9	16.8	20.3	8.9	14.0	18.0	10.3	15.5	19.2
50	5.3	11.8	15.4	18.6	8.1	12.8	16.5	9.5	14.1	17.6
40	4.8	10.6	13.8	16.6	7.3	11.5	14.8	8.5	12.7	15.7
30	4.2	9.2	12.0	14.4	6.4	10.0	12.8	7.4	11.0	13.7
20	3.5	7.6	9.8	11.8	5.3	8.2	10.5	6.1	9.1	11.2
18	3.3	7.2	9.3	11.2	5.0	7.8	10.0	5.8	8.6	10.6
16	3.1	6.8	8.8	10.6	4.7	7.4	9.4	5.5	8.1	10.0
14	3.0	6.4	8.3	9.9	4.5	6.9	8.9	5.2	7.6	9.4
12	2.8	6.0	7.7	9.2	4.2	6.4	8.2	4.8	7.1	8.7
10	2.6	5.5	7.0	8.4	3.8	5.9	7.5	4.4	6.5	8.0

Table B-3 - 3/8" Bolts - Maximum Lamella Length [ℓ] (ft)

$C_\Delta = 1.0$

Radius [R] (ft)	(2) Bolts per Connection			(3) Bolts per Connection			(4) Bolts per Connection		
	2 x 6	2 x 8	2 x 10	2 x 6	2 x 8	2 x 10	2 x 8	2 x 10	2 x 12
1000	46.0	63.3	78.5	22.0	48.8	67.4	27.5	54.1	71.3
900	43.6	60.0	74.5	20.9	46.3	64.0	26.1	51.3	67.6
800	41.1	56.6	70.2	19.7	43.7	60.3	24.7	48.4	63.8
700	38.5	53.0	65.7	18.5	40.9	56.4	23.1	45.3	59.7
600	35.7	49.1	60.9	17.1	37.9	52.3	21.4	42.0	55.3
500	32.6	44.8	55.6	15.7	34.6	47.8	19.6	38.3	50.5
400	29.2	40.1	49.8	14.1	31.0	42.8	17.5	34.3	45.2
450	30.9	42.6	52.8	14.9	32.9	45.3	18.6	36.4	47.9
400	29.2	40.1	49.8	14.1	31.0	42.8	17.5	34.3	45.2
350	27.3	37.6	46.6	13.2	29.0	40.0	16.4	32.1	42.3
300	25.3	34.8	43.1	12.2	26.9	37.1	15.2	29.8	39.2
275	24.3	33.3	41.3	11.7	25.8	35.5	14.6	28.5	37.5
250	23.2	31.8	39.4	11.2	24.6	33.9	13.9	27.2	35.8
225	22.0	30.2	37.4	10.6	23.3	32.1	13.2	25.8	34.0
200	20.7	28.5	35.3	10.0	22.0	30.3	12.5	24.4	32.1
175	19.4	26.7	33.0	9.4	20.6	28.4	11.7	22.8	30.0
150	18.0	24.7	30.6	8.7	19.1	26.3	10.9	21.2	27.8
125	16.5	22.6	28.0	8.0	17.5	24.0	10.0	19.3	25.4
100	14.8	20.2	25.0	7.2	15.7	21.5	8.9	17.3	22.8
90	14.0	19.2	23.8	6.9	14.9	20.5	8.5	16.5	21.6
80	13.2	18.1	22.4	6.5	14.1	19.3	8.0	15.5	20.4
70	12.4	17.0	21.0	6.1	13.2	18.1	7.5	14.6	19.1
60	11.5	15.7	19.5	5.7	12.2	16.8	7.0	13.5	17.7
50	10.5	14.4	17.8	5.2	11.2	15.3	6.4	12.4	16.2
40	9.5	12.9	15.9	4.7	10.0	13.7	5.8	11.1	14.5
30	8.2	11.2	13.8	4.1	8.7	11.9	5.1	9.6	12.6
20	6.8	9.2	11.3	3.4	7.2	9.8	4.2	7.9	10.3
18	6.5	8.8	10.8	3.3	6.8	9.3	4.0	7.5	9.8
16	6.1	8.3	10.2	3.1	6.5	8.8	3.8	7.1	9.3
14	5.7	7.8	9.5	2.9	6.1	8.2	3.6	6.7	8.7
12	5.3	7.2	8.8	2.7	5.6	7.6	3.3	6.2	8.1
10	4.9	6.6	8.1	2.5	5.2	7.0	3.1	5.7	7.4

Table B-4 - 1/2" Bolts - Maximum Lamella Length [ℓ] (ft) $C_\Delta = 1.0$										
Radius [R] (ft)	(2) Bolts per Connection				(3) Bolts per Connection			(4) Bolts per Connection		
	2 x 6	2 x 8	2 x 10	2 x 12	2 x 8	2 x 10	2 x 12	2 x 10	2 x 12	2 x 14
1000	28.7	52.2	69.9	83.9	23.5	52.2	69.9	23.5	52.2	69.9
900	27.3	49.5	66.3	79.6	22.3	49.5	66.3	22.3	49.5	66.3
800	25.7	46.7	62.5	75.1	21.1	46.7	62.5	21.1	46.7	62.5
700	24.1	43.7	58.5	70.2	19.7	43.7	58.5	19.7	43.7	58.5
600	22.3	40.5	54.2	65.0	18.3	40.5	54.2	18.3	40.5	54.2
500	20.4	37.0	49.5	59.4	16.7	37.0	49.5	16.7	37.0	49.5
400	18.3	33.1	44.3	53.2	15.0	33.1	44.3	15.0	33.1	44.3
450	19.4	35.1	47.0	56.4	15.9	35.1	47.0	15.9	35.1	47.0
400	18.3	33.1	44.3	53.2	15.0	33.1	44.3	15.0	33.1	44.3
350	17.1	31.0	41.5	49.8	14.1	31.0	41.5	14.1	31.0	41.5
300	15.9	28.7	38.4	46.1	13.0	28.7	38.4	13.0	28.7	38.4
275	15.2	27.5	36.8	44.1	12.5	27.5	36.8	12.5	27.5	36.8
250	14.5	26.3	35.1	42.1	11.9	26.3	35.1	11.9	26.3	35.1
225	13.8	24.9	33.3	40.0	11.3	24.9	33.3	11.3	24.9	33.3
200	13.0	23.5	31.4	37.7	10.7	23.5	31.4	10.7	23.5	31.4
175	12.2	22.0	29.4	35.3	10.0	22.0	29.4	10.0	22.0	29.4
150	11.3	20.4	27.3	32.7	9.3	20.4	27.3	9.3	20.4	27.3
125	10.4	18.7	24.9	29.9	8.5	18.7	24.9	8.5	18.7	24.9
100	9.3	16.7	22.3	26.7	7.7	16.7	22.3	7.7	16.7	22.3
90	8.9	15.9	21.2	25.4	7.3	15.9	21.2	7.3	15.9	21.2
80	8.4	15.0	20.0	23.9	6.9	15.0	20.0	6.9	15.0	20.0
70	7.9	14.1	18.7	22.4	6.5	14.1	18.7	6.5	14.1	18.7
60	7.3	13.0	17.4	20.8	6.0	13.0	17.4	6.0	13.0	17.4
50	6.7	11.9	15.9	19.0	5.5	11.9	15.9	5.5	11.9	15.9
40	6.0	10.7	14.2	17.0	5.0	10.7	14.2	5.0	10.7	14.2
30	5.3	9.3	12.4	14.8	4.4	9.3	12.4	4.4	9.3	12.4
20	4.4	7.7	10.1	12.1	3.6	7.7	10.1	3.6	7.7	10.1
18	4.2	7.3	9.6	11.5	3.5	7.3	9.6	3.5	7.3	9.6
16	3.9	6.9	9.1	10.8	3.3	6.9	9.1	3.3	6.9	9.1
14	3.7	6.5	8.5	10.1	3.1	6.5	8.5	3.1	6.5	8.5
12	3.5	6.0	7.9	9.4	2.9	6.0	7.9	2.9	6.0	7.9
10	3.2	5.5	7.2	8.6	2.7	5.5	7.2	2.7	5.5	7.2

Table B-5 - 3/8" Bolts - Maximum Lamella Length [ℓ] (ft) $C_\Delta = 0.5$										
Radius [R] (ft)	(2) Bolts per Connection				(3) Bolts per Connection			(4) Bolts per Connection		
	2 x 4	2 x 6	2 x 8	2 x 10	2 x 6	2 x 8	2 x 10	2 x 8	2 x 10	2 x 12
1000	6.1	47.1	64.1	79.1	26.3	50.8	68.9	32.6	56.8	73.4
900	5.9	44.7	60.8	75.1	24.9	48.3	65.4	31.0	53.9	69.6
800	5.5	42.1	57.3	70.8	23.5	45.5	61.6	29.2	50.8	65.7
700	5.2	39.4	53.7	66.3	22.0	42.6	57.7	27.3	47.6	61.5
600	4.8	36.5	49.7	61.4	20.4	39.5	53.4	25.3	44.1	56.9
500	4.5	33.4	45.4	56.1	18.7	36.1	48.8	23.2	40.3	52.0
400	4.0	29.9	40.6	50.2	16.7	32.3	43.7	20.8	36.1	46.5
450	4.2	31.7	43.1	53.2	17.7	34.2	46.3	22.0	38.2	49.3
400	4.0	29.9	40.6	50.2	16.7	32.3	43.7	20.8	36.1	46.5
350	3.8	28.0	38.0	46.9	15.7	30.2	40.9	19.4	33.7	43.6
300	3.5	25.9	35.2	43.5	14.5	28.0	37.9	18.0	31.3	40.3
275	3.4	24.8	33.8	41.7	13.9	26.8	36.3	17.3	30.0	38.6
250	3.3	23.7	32.2	39.7	13.3	25.6	34.6	16.5	28.6	36.9
225	3.1	22.5	30.6	37.7	12.6	24.3	32.9	15.7	27.1	35.0
200	2.9	21.2	28.8	35.6	11.9	22.9	31.0	14.8	25.6	33.0
175	2.8	19.9	27.0	33.3	11.2	21.5	29.0	13.8	24.0	30.9
150	2.6	18.4	25.0	30.8	10.4	19.9	26.9	12.8	22.2	28.6
125	2.4	16.9	22.9	28.2	9.5	18.2	24.6	11.8	20.3	26.2
100	2.2	15.1	20.5	25.2	8.5	16.3	22.0	10.6	18.2	23.4
90	2.1	14.4	19.5	24.0	8.1	15.5	20.9	10.0	17.3	22.2
80	2.0	13.6	18.4	22.6	7.7	14.6	19.7	9.5	16.3	21.0
70	1.9	12.7	17.2	21.2	7.2	13.7	18.5	8.9	15.3	19.7
60	1.8	11.8	15.9	19.6	6.7	12.7	17.1	8.3	14.2	18.2
50	1.7	10.8	14.6	17.9	6.1	11.6	15.7	7.6	13.0	16.7
40	1.5	9.7	13.1	16.1	5.5	10.4	14.0	6.8	11.6	14.9
30	1.4	8.4	11.4	13.9	4.8	9.1	12.2	5.9	10.1	13.0
20	1.2	6.9	9.3	11.4	4.0	7.5	10.0	4.9	8.3	10.6
18	1.1	6.6	8.9	10.9	3.8	7.1	9.5	4.7	7.9	10.1
16	1.1	6.2	8.4	10.2	3.6	6.7	9.0	4.4	7.5	9.5
14	1.0	5.9	7.9	9.6	3.4	6.3	8.4	4.2	7.0	8.9
12	1.0	5.5	7.3	8.9	3.2	5.9	7.8	3.9	6.5	8.3
10	0.9	5.0	6.7	8.1	2.9	5.4	7.1	3.6	6.0	7.6

Table B-6 - 1/2" Bolts - Maximum Lamella Length [ℓ] (ft) $C_\Delta = 0.5$										
Radius [R] (ft)	(2) Bolts per Connection				(3) Bolts per Connection			(4) Bolts per Connection		
	2 x 6	2 x 8	2 x 10	2 x 12	2 x 8	2 x 10	2 x 12	2 x 10	2 x 12	2 x 14
1000	36.1	56.5	73.2	86.6	38.8	60.5	76.3	44.5	64.3	79.3
900	34.2	53.6	69.4	82.2	36.8	57.5	72.4	42.2	61.0	75.3
800	32.3	50.6	65.5	77.5	34.7	54.2	68.3	39.8	57.6	71.0
700	30.2	47.3	61.3	72.5	32.5	50.7	63.9	37.3	53.9	66.4
600	28.0	43.9	56.7	67.2	30.1	47.0	59.2	34.5	49.9	61.5
500	25.6	40.1	51.8	61.4	27.5	42.9	54.1	31.5	45.6	56.2
400	22.9	35.9	46.4	54.9	24.7	38.4	48.4	28.3	40.8	50.3
450	24.3	38.0	49.2	58.2	26.1	40.7	51.3	29.9	43.3	53.3
400	22.9	35.9	46.4	54.9	24.7	38.4	48.4	28.3	40.8	50.3
350	21.5	33.6	43.4	51.4	23.1	36.0	45.3	26.5	38.2	47.1
300	19.9	31.1	40.2	47.6	21.4	33.3	41.9	24.5	35.4	43.6
275	19.1	29.8	38.5	45.6	20.5	31.9	40.2	23.5	33.9	41.8
250	18.2	28.4	36.7	43.5	19.6	30.4	38.3	22.4	32.3	39.8
225	17.3	27.0	34.9	41.3	18.6	28.9	36.4	21.3	30.7	37.8
200	16.3	25.5	32.9	38.9	17.5	27.3	34.3	20.1	29.0	35.7
175	15.3	23.8	30.8	36.4	16.4	25.5	32.1	18.8	27.1	33.4
150	14.2	22.1	28.5	33.7	15.2	23.7	29.8	17.4	25.1	30.9
125	13.0	20.2	26.1	30.8	13.9	21.6	27.2	15.9	23.0	28.3
100	11.6	18.1	23.4	27.6	12.5	19.4	24.4	14.3	20.6	25.3
90	11.1	17.2	22.2	26.2	11.9	18.4	23.1	13.6	19.5	24.0
80	10.5	16.2	20.9	24.7	11.2	17.4	21.8	12.8	18.4	22.7
70	9.8	15.2	19.6	23.1	10.5	16.3	20.4	12.0	17.3	21.2
60	9.1	14.1	18.2	21.4	9.8	15.1	18.9	11.2	16.0	19.7
50	8.3	12.9	16.6	19.6	8.9	13.8	17.3	10.2	14.6	18.0
40	7.5	11.6	14.9	17.6	8.0	12.4	15.5	9.2	13.1	16.1
30	6.5	10.1	12.9	15.2	7.0	10.8	13.5	8.0	11.4	14.0
20	5.4	8.3	10.6	12.5	5.8	8.8	11.0	6.6	9.4	11.5
18	5.1	7.9	10.1	11.8	5.5	8.4	10.5	6.3	8.9	10.9
16	4.9	7.4	9.5	11.2	5.2	7.9	9.9	5.9	8.4	10.3
14	4.6	7.0	8.9	10.5	4.9	7.4	9.3	5.6	7.9	9.6
12	4.3	6.5	8.3	9.7	4.6	6.9	8.6	5.2	7.3	8.9
10	3.9	5.9	7.6	8.9	4.2	6.3	7.9	4.8	6.7	8.2

Table B-7 - 5/8" Bolts - Maximum Lamella Length [ℓ] (ft) $C_\Delta = 0.5$										
Radius [R] (ft)	(2) Bolts per Connection				(3) Bolts per Connection			(4) Bolts per Connection		
	2 x 6	2 x 8	2 x 10	2 x 12	2 x 8	2 x 10	2 x 12	2 x 10	2 x 12	2 x 14
1000	14.5	46.0	65.4	80.2	8.5	47.4	66.4	14.5	48.8	67.4
900	13.8	43.6	62.0	76.1	8.1	45.0	63.0	13.8	46.3	64.0
800	13.0	41.1	58.5	71.8	7.7	42.4	59.4	13.0	43.7	60.3
700	12.2	38.5	54.7	67.1	7.2	39.7	55.6	12.2	40.9	56.4
600	11.3	35.7	50.7	62.2	6.7	36.8	51.5	11.3	37.9	52.3
500	10.4	32.6	46.3	56.8	6.1	33.6	47.0	10.4	34.6	47.8
400	9.3	29.2	41.5	50.8	5.5	30.1	42.1	9.3	31.0	42.8
450	9.9	30.9	44.0	53.9	5.9	31.9	44.6	9.9	32.9	45.3
400	9.3	29.2	41.5	50.8	5.5	30.1	42.1	9.3	31.0	42.8
350	8.7	27.3	38.8	47.6	5.2	28.2	39.4	8.7	29.0	40.0
300	8.1	25.3	36.0	44.1	4.8	26.1	36.5	8.1	26.9	37.1
275	7.8	24.3	34.4	42.2	4.7	25.0	35.0	7.8	25.8	35.5
250	7.5	23.2	32.9	40.3	4.5	23.9	33.4	7.5	24.6	33.9
225	7.1	22.0	31.2	38.2	4.2	22.7	31.7	7.1	23.3	32.1
200	6.7	20.7	29.4	36.0	4.0	21.4	29.9	6.7	22.0	30.3
175	6.3	19.4	27.5	33.7	3.8	20.0	28.0	6.3	20.6	28.4
150	5.9	18.0	25.5	31.3	3.5	18.6	25.9	5.9	19.1	26.3
125	5.4	16.5	23.3	28.6	3.3	17.0	23.7	5.4	17.5	24.0
100	4.8	14.8	20.9	25.6	2.9	15.2	21.2	4.8	15.7	21.5
90	4.6	14.0	19.8	24.3	2.8	14.5	20.1	4.6	14.9	20.5
80	4.4	13.2	18.7	22.9	2.7	13.7	19.0	4.4	14.1	19.3
70	4.1	12.4	17.5	21.4	2.5	12.8	17.8	4.1	13.2	18.1
60	3.8	11.5	16.3	19.9	2.4	11.9	16.5	3.8	12.2	16.8
50	3.5	10.5	14.9	18.2	2.2	10.9	15.1	3.5	11.2	15.3
40	3.2	9.5	13.3	16.3	2.0	9.8	13.5	3.2	10.0	13.7
30	2.8	8.2	11.6	14.1	1.8	8.5	11.8	2.8	8.7	11.9
20	2.4	6.8	9.5	11.6	1.5	7.0	9.7	2.4	7.2	9.8
18	2.3	6.5	9.0	11.0	1.5	6.7	9.2	2.3	6.8	9.3
16	2.2	6.1	8.5	10.4	1.4	6.3	8.7	2.2	6.5	8.8
14	2.0	5.7	8.0	9.7	1.3	5.9	8.1	2.0	6.1	8.2
12	1.9	5.3	7.4	9.0	1.3	5.5	7.5	1.9	5.6	7.6
10	1.8	4.9	6.8	8.2	1.2	5.0	6.9	1.8	5.2	7.0

Table B-8 - 3/4" Bolts - Maximum Lamella Length [ℓ] (ft) $C_\Delta = 0.5$									
Radius [R] (ft)	(2) Bolts per Connection				(3) Bolts per Connection			(4) Bolts per Connection	
	2 x 8	2 x 10	2 x 12	2 x 14	2 x 10	2 x 12	2 x 14	2 x 12	2 x 14
1000	31.0	55.9	72.7	86.3	26.3	53.4	70.8	20.4	50.8
900	29.4	53.1	69.0	81.8	24.9	50.7	67.2	19.4	48.3
800	27.8	50.0	65.1	77.2	23.5	47.8	63.4	18.3	45.5
700	26.0	46.8	60.9	72.2	22.0	44.8	59.3	17.1	42.6
600	24.1	43.4	56.4	66.9	20.4	41.5	54.9	15.9	39.5
500	22.0	39.6	51.5	61.1	18.7	37.9	50.2	14.5	36.1
400	19.7	35.5	46.1	54.7	16.7	33.9	44.9	13.0	32.3
450	20.9	37.6	48.9	58.0	17.7	36.0	47.6	13.8	34.2
400	19.7	35.5	46.1	54.7	16.7	33.9	44.9	13.0	32.3
350	18.5	33.2	43.1	51.2	15.7	31.8	42.0	12.2	30.2
300	17.1	30.8	40.0	47.4	14.5	29.4	38.9	11.3	28.0
275	16.4	29.5	38.3	45.4	13.9	28.2	37.3	10.9	26.8
250	15.7	28.1	36.5	43.3	13.3	26.9	35.6	10.4	25.6
225	14.9	26.7	34.7	41.1	12.6	25.5	33.8	9.9	24.3
200	14.1	25.2	32.7	38.7	11.9	24.1	31.9	9.3	22.9
175	13.2	23.6	30.6	36.3	11.2	22.6	29.8	8.7	21.5
150	12.2	21.9	28.4	33.6	10.4	20.9	27.6	8.1	19.9
125	11.2	20.0	25.9	30.7	9.5	19.1	25.3	7.4	18.2
100	10.0	17.9	23.2	27.5	8.5	17.1	22.6	6.7	16.3
90	9.5	17.0	22.0	26.1	8.1	16.3	21.5	6.4	15.5
80	9.0	16.1	20.8	24.6	7.7	15.4	20.3	6.0	14.6
70	8.5	15.0	19.5	23.0	7.2	14.4	19.0	5.7	13.7
60	7.9	14.0	18.0	21.4	6.7	13.3	17.6	5.3	12.7
50	7.2	12.8	16.5	19.5	6.1	12.2	16.1	4.8	11.6
40	6.5	11.5	14.8	17.5	5.5	11.0	14.4	4.4	10.4
30	5.7	10.0	12.8	15.2	4.8	9.5	12.5	3.8	9.1
20	4.7	8.2	10.5	12.4	4.0	7.8	10.3	3.2	7.5
18	4.5	7.8	10.0	11.8	3.8	7.5	9.8	3.0	7.1
16	4.2	7.4	9.4	11.1	3.6	7.0	9.2	2.9	6.7
14	4.0	6.9	8.9	10.4	3.4	6.6	8.6	2.7	6.3
12	3.7	6.4	8.2	9.7	3.2	6.1	8.0	2.6	5.9
10	3.4	5.9	7.5	8.8	2.9	5.6	7.3	2.4	5.4

Table B-9 - 7/8" Bolts - Maximum Lamella Length [ℓ] (ft) $C_\Delta = 0.5$						
Radius [R] (ft)	(2) Bolts per Connection			(3) Bolts per Connection		(4) Bolts per Connection
	2 x 10	2 x 12	2 x 14	2 x 12	2 x 14	2 x 14
1000	44.5	64.3	79.3	36.1	58.9	24.9
900	42.2	61.0	75.3	34.2	55.8	23.7
800	39.8	57.6	71.0	32.3	52.7	22.3
700	37.3	53.9	66.4	30.2	49.3	20.9
600	34.5	49.9	61.5	28.0	45.7	19.4
500	31.5	45.6	56.2	25.6	41.7	17.7
400	28.3	40.8	50.3	22.9	37.3	15.9
450	29.9	43.3	53.3	24.3	39.6	16.8
400	28.3	40.8	50.3	22.9	37.3	15.9
350	26.5	38.2	47.1	21.5	35.0	14.9
300	24.5	35.4	43.6	19.9	32.4	13.8
275	23.5	33.9	41.8	19.1	31.0	13.2
250	22.4	32.3	39.8	18.2	29.6	12.6
225	21.3	30.7	37.8	17.3	28.1	12.0
200	20.1	29.0	35.7	16.3	26.5	11.3
175	18.8	27.1	33.4	15.3	24.8	10.6
150	17.4	25.1	30.9	14.2	23.0	9.9
125	15.9	23.0	28.3	13.0	21.0	9.0
100	14.3	20.6	25.3	11.6	18.8	8.1
90	13.6	19.5	24.0	11.1	17.9	7.7
80	12.8	18.4	22.7	10.5	16.9	7.3
70	12.0	17.3	21.2	9.8	15.8	6.9
60	11.2	16.0	19.7	9.1	14.7	6.4
50	10.2	14.6	18.0	8.3	13.4	5.8
40	9.2	13.1	16.1	7.5	12.0	5.3
30	8.0	11.4	14.0	6.5	10.5	4.6
20	6.6	9.4	11.5	5.4	8.6	3.8
18	6.3	8.9	10.9	5.1	8.2	3.7
16	5.9	8.4	10.3	4.9	7.7	3.5
14	5.6	7.9	9.6	4.6	7.2	3.3
12	5.2	7.3	8.9	4.3	6.7	3.0
10	4.8	6.7	8.2	3.9	6.2	2.8

Table B-10 - 1" Bolts - Maximum Lamella Length [ℓ] (ft)

$C_\Delta = 0.5$

Radius [R] (ft)	(2) Bolts per Connection			(3) Bolts per Connection
	2 x 10	2 x 12	2 x 14	2 x 14
1000	28.7	54.7	71.8	43.7
900	27.3	51.9	68.1	41.5
800	25.8	49.0	64.2	39.1
700	24.1	45.8	60.1	36.6
600	22.4	42.5	55.7	33.9
500	20.4	38.8	50.9	31.0
400	18.3	34.7	45.5	27.8
450	19.4	36.8	48.3	29.4
400	18.3	34.7	45.5	27.8
350	17.2	32.5	42.6	26.0
300	15.9	30.1	39.5	24.1
275	15.3	28.9	37.8	23.1
250	14.6	27.5	36.1	22.0
225	13.8	26.1	34.2	20.9
200	13.1	24.7	32.3	19.8
175	12.2	23.1	30.2	18.5
150	11.4	21.4	28.0	17.2
125	10.4	19.6	25.6	15.7
100	9.3	17.5	22.9	14.1
90	8.9	16.7	21.8	13.4
80	8.4	15.7	20.5	12.6
70	7.9	14.7	19.2	11.8
60	7.3	13.7	17.8	11.0
50	6.7	12.5	16.3	10.1
40	6.0	11.2	14.6	9.0
30	5.3	9.8	12.7	7.9
20	4.4	8.0	10.4	6.5
18	4.2	7.6	9.9	6.2
16	4.0	7.2	9.3	5.8
14	3.7	6.8	8.8	5.5
12	3.5	6.3	8.1	5.1
10	3.2	5.8	7.4	4.7

Appendix C: ASCE 7-10 Tables and Figures

Appendix C features copies of Table 7-2 and Figure 7-3 (complete and author-simplified versions) from the ASCE standard 7-10.

Table 7-2 Exposure Factor, C_e

Terrain Category	Exposure of Roof[a] Fully Exposed	Partially Exposed	Sheltered
B (see Section 26.7)	0.9	1.0	1.2
C (see Section 26.7)	0.9	1.0	1.1
D (see Section 26.7)	0.8	0.9	1.0
Above the treeline in windswept mountainous areas.	0.7	0.8	N/A
In Alaska, in areas where trees do not exist within a 2-mile (3-km) radius of the site.	0.7	0.8	N/A

The terrain category and roof exposure condition chosen shall be representative of the anticipated conditions during the life of the structure. An exposure factor shall be determined for each roof of a structure.

[a] Definitions: Partially Exposed: All roofs except as indicated in the following text. Fully Exposed: Roofs exposed on all sides with no shelter[b] afforded by terrain, higher structures, or trees. Roofs that contain several large pieces of mechanical equipment, parapets that extend above the height of the balanced snow load (h_b), or other obstructions are not in this category. Sheltered: Roofs located tight in among conifers that qualify as obstructions.

[b] Obstructions within a distance of $10h_o$ provide "shelter," where h_o is the height of the obstruction above the roof level. If the only obstructions are a few deciduous trees that are leafless in winter, the "fully exposed" category shall be used. Note that these are heights above the roof. Heights used to establish the Exposure Category in Section 26.7 are heights above the ground.

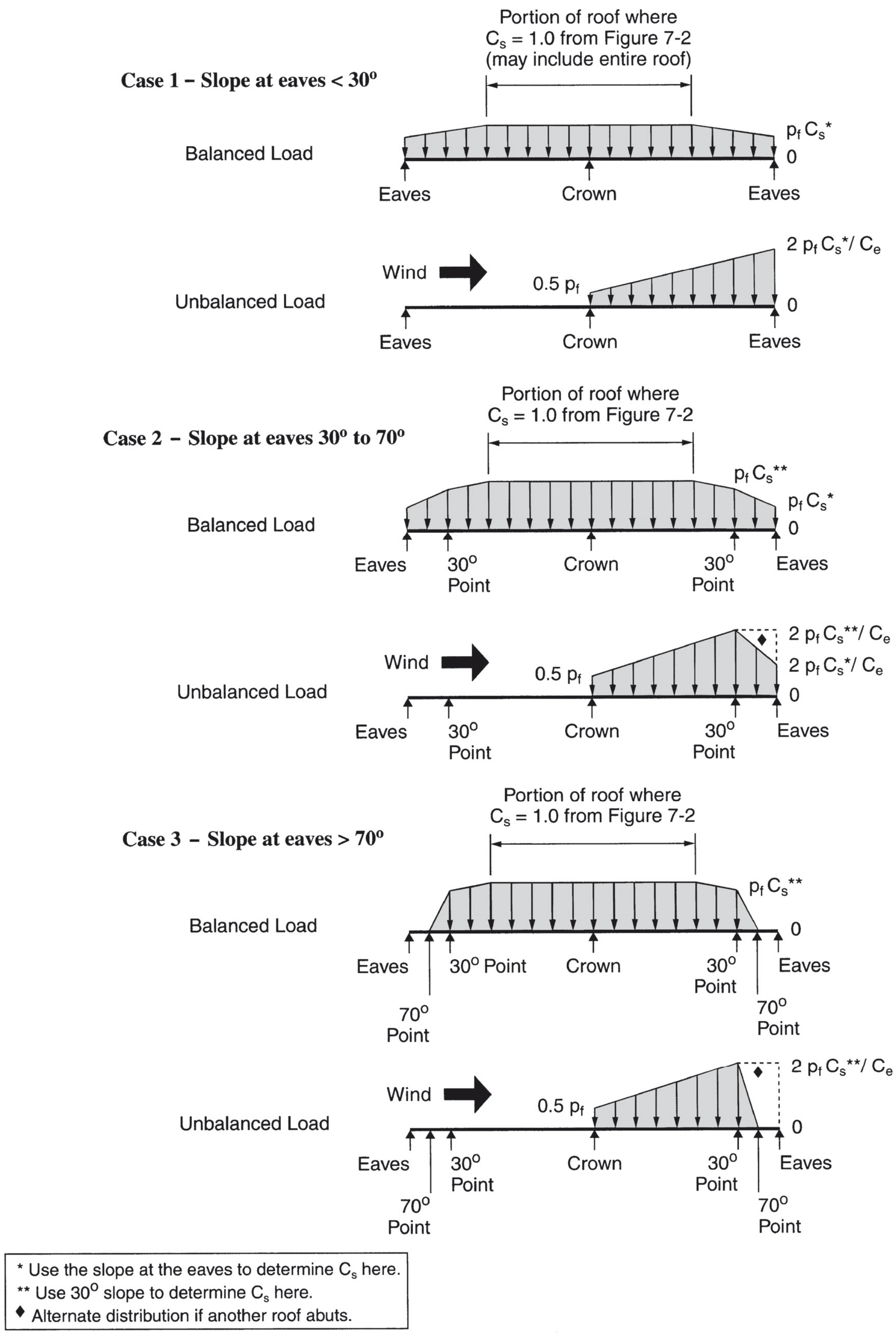

FIGURE 7-3 Balanced and Unbalanced Loads for Curved Roofs

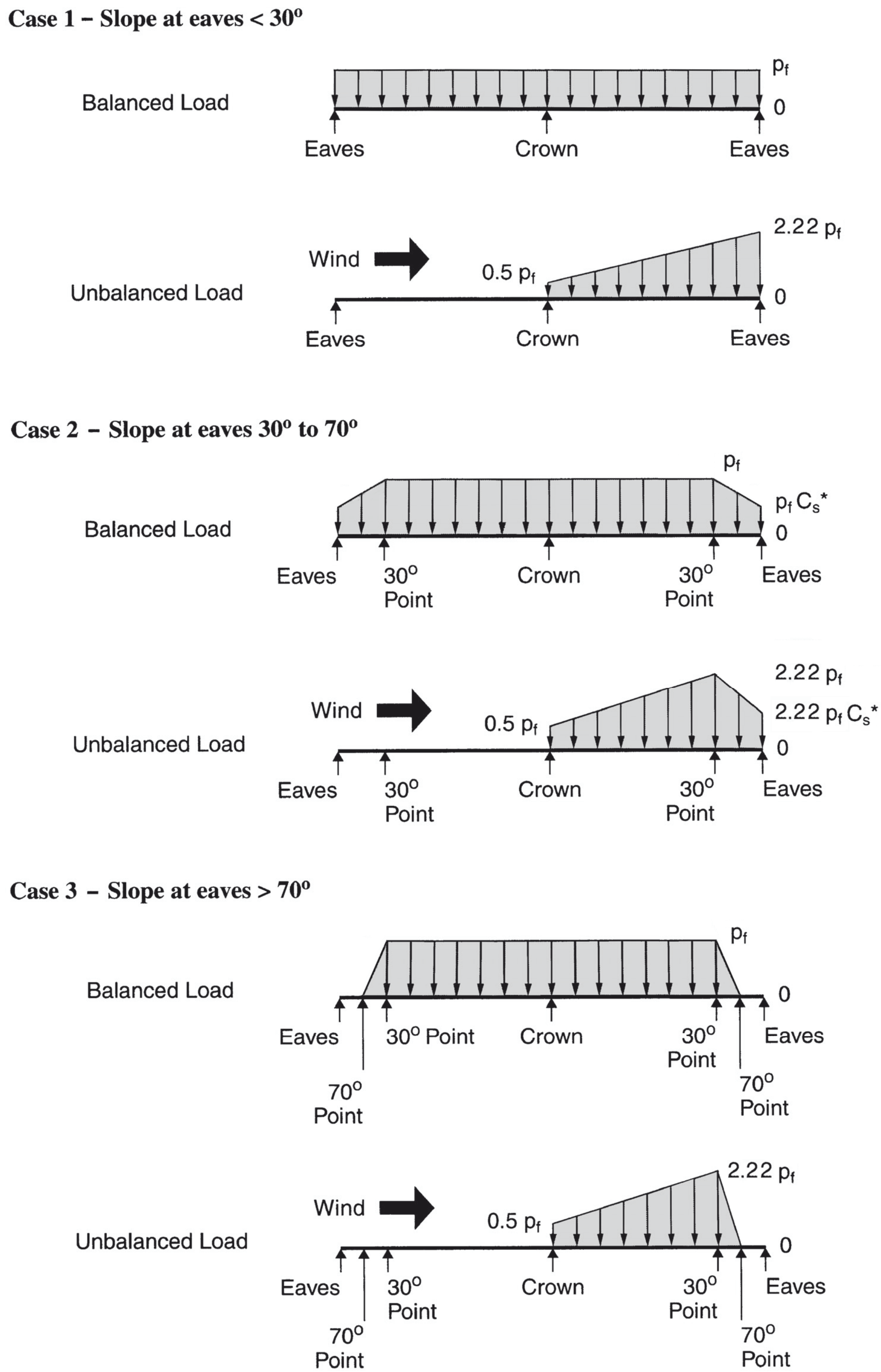

SIMPLIFIED FIGURE 7-3 Balanced and Unbalanced Loads for Curved Roofs

Appendix D: Load versus Curvature Graphs

Appendix D displays graphs showing the theoretical behavior of a lamella arch with two different stiffness characteristics. Results are based on a finite element analysis conducted by the author.

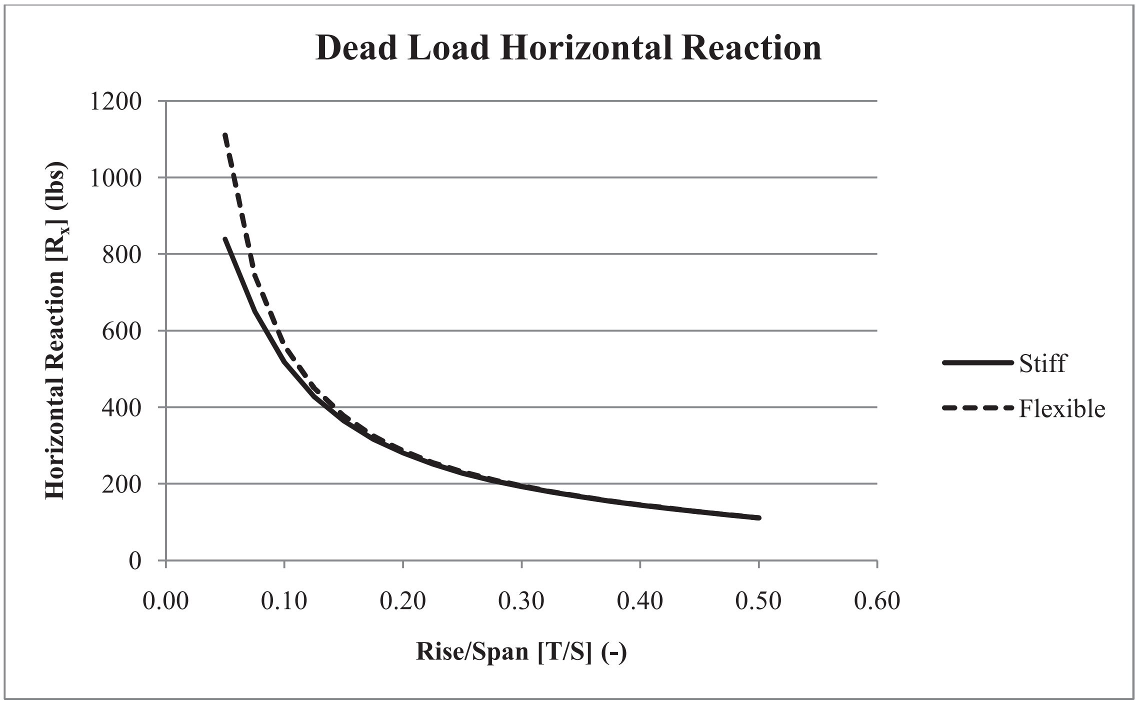

Figure D-1 – Dead Load Horizontal Reaction.

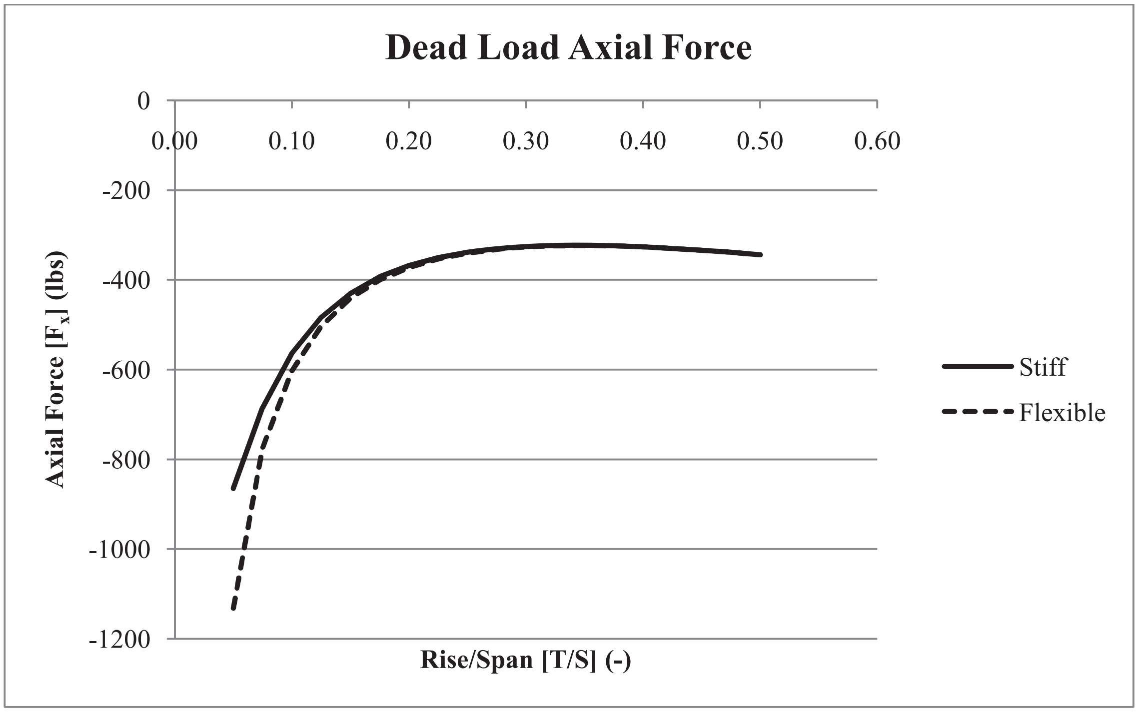

Figure D-2 – Dead Load Axial Force.

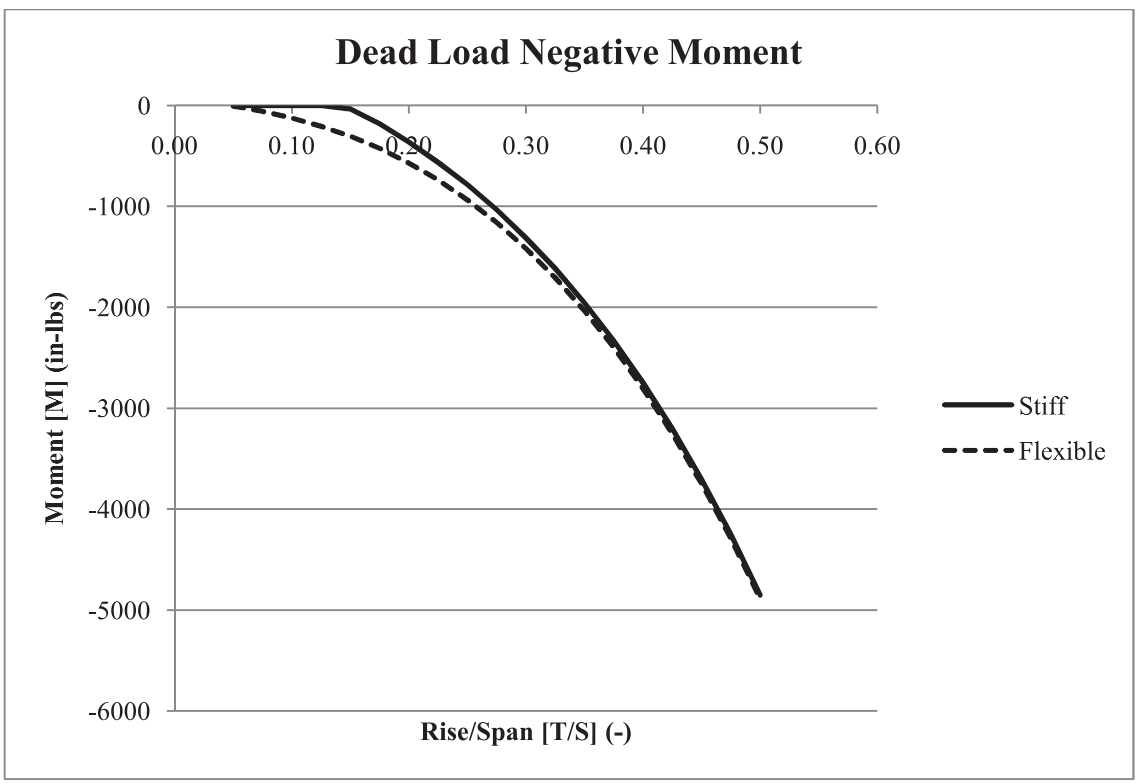

Figure D-3 – Dead Load Negative Moment.

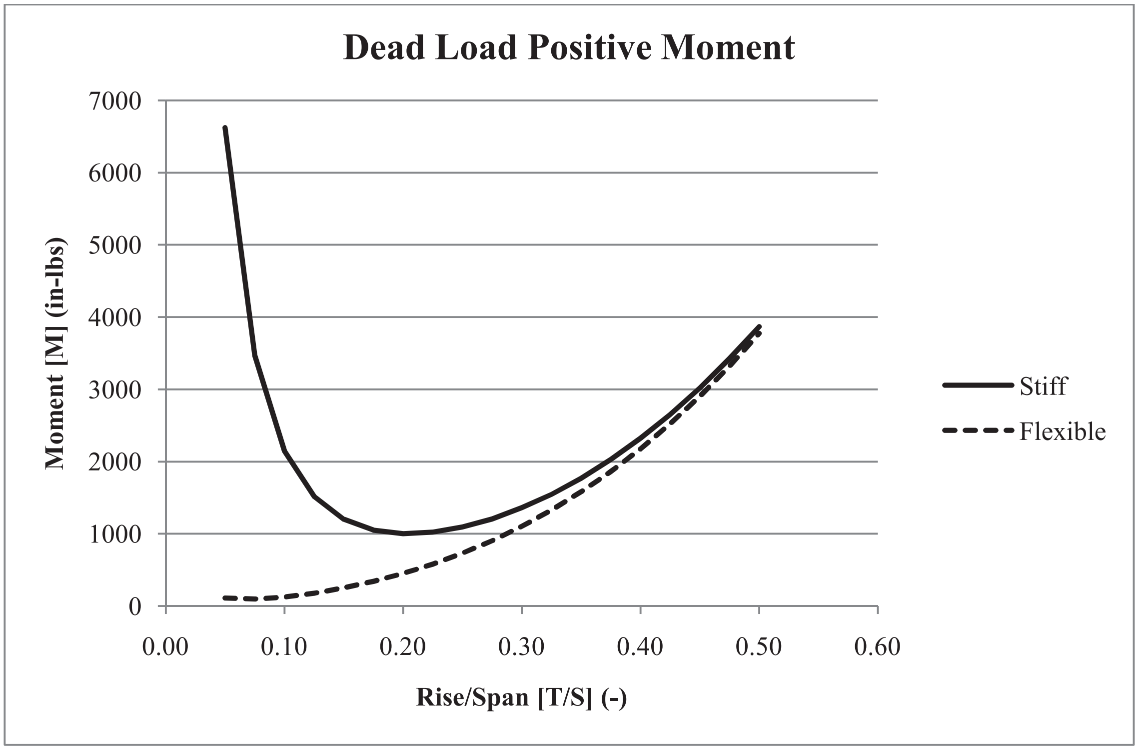

Figure D-4 – Dead Load Negative Moment.

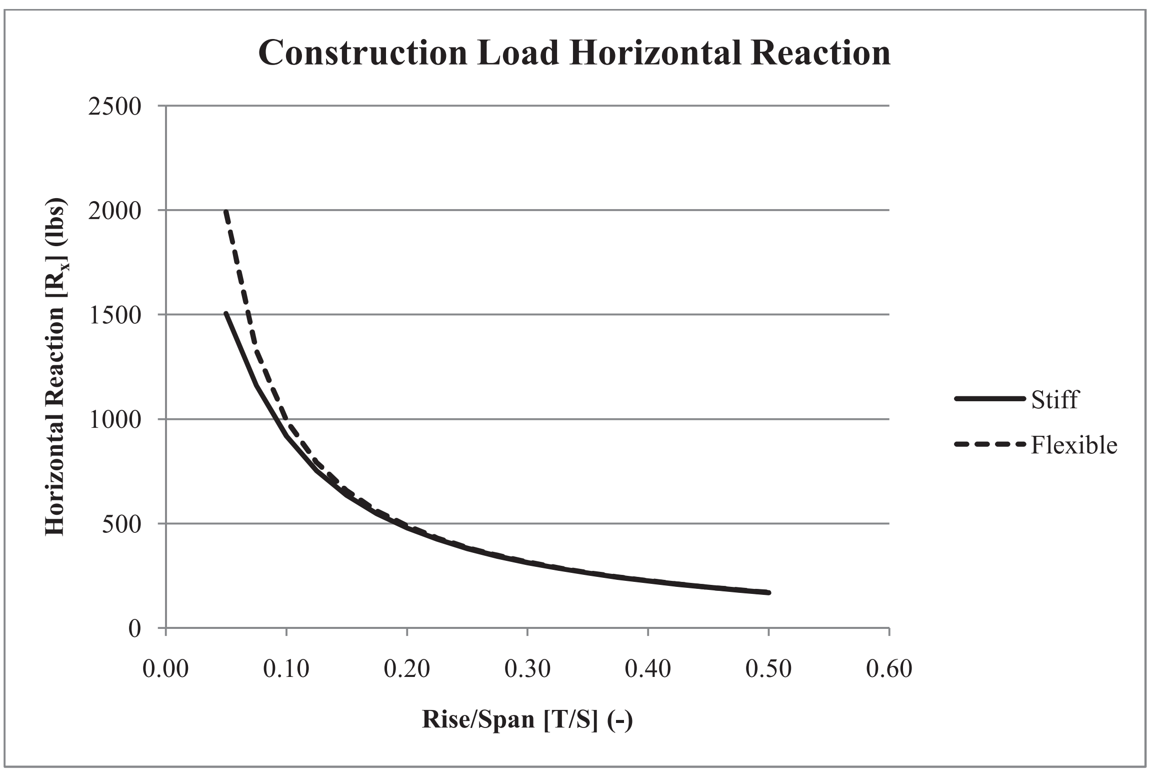

Figure D-5 – Dead Load Negative Moment.

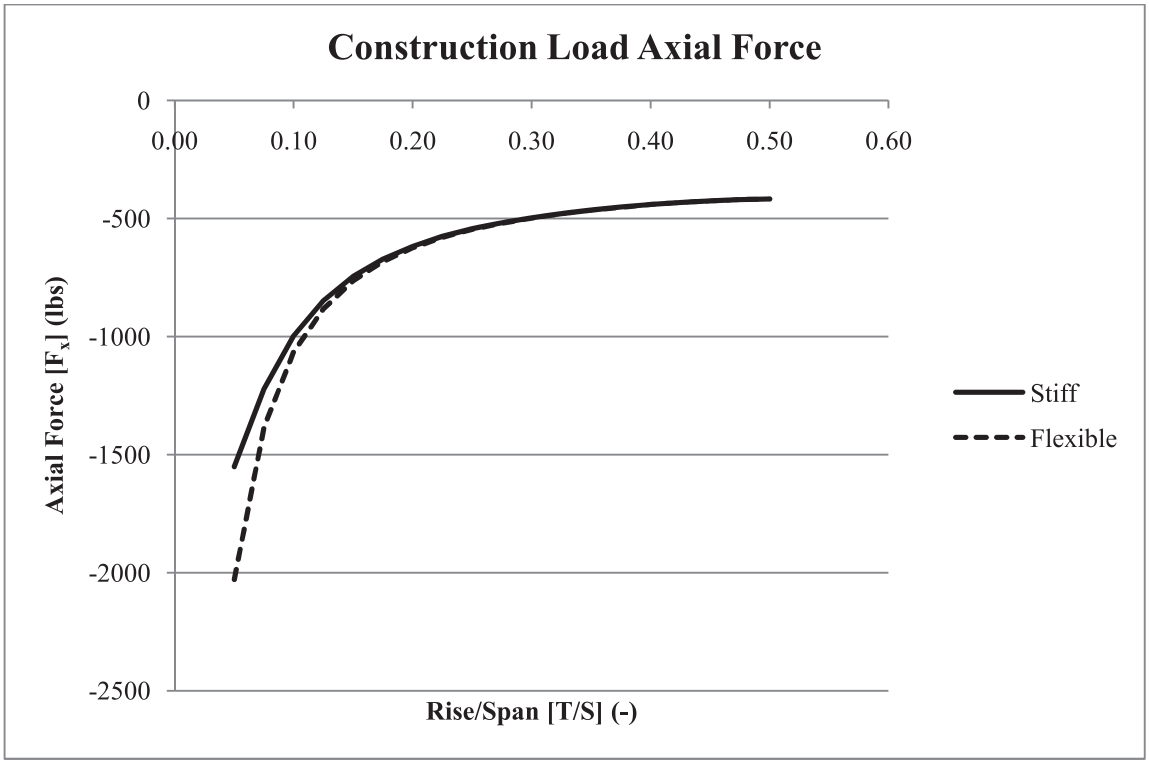

Figure D-6 – Dead Load Negative Moment.

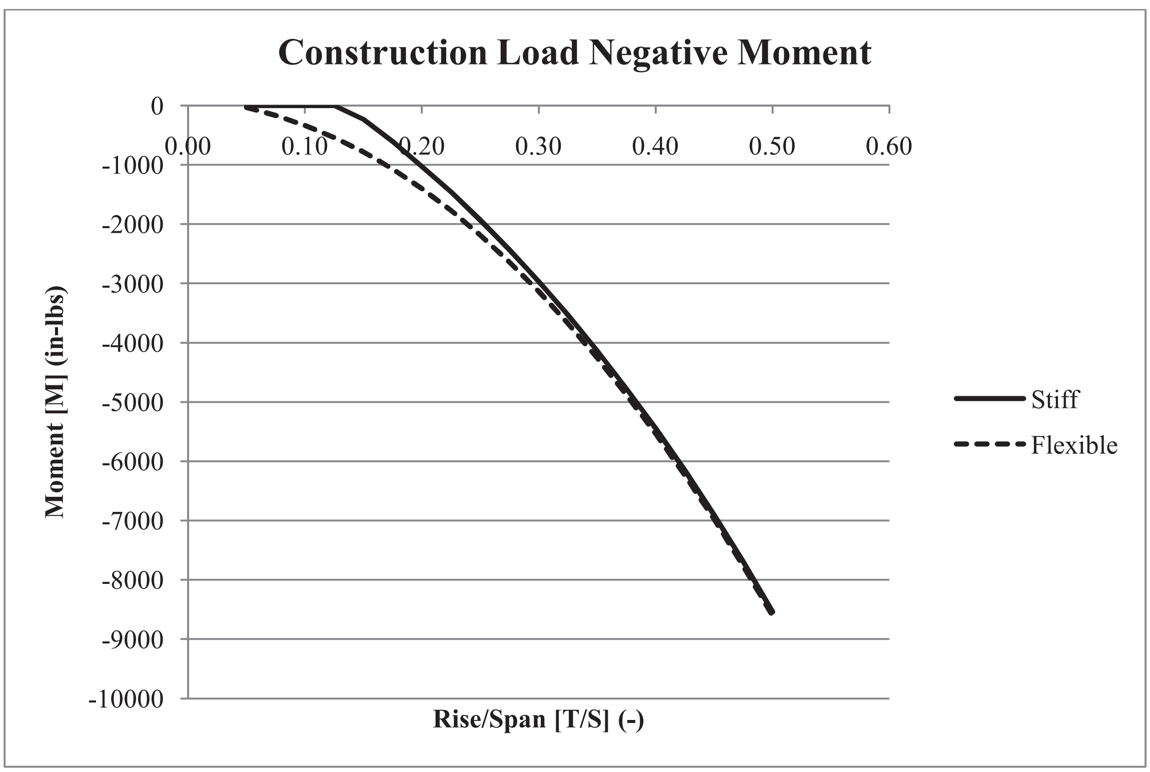

Figure D-7 – Dead Load Negative Moment.

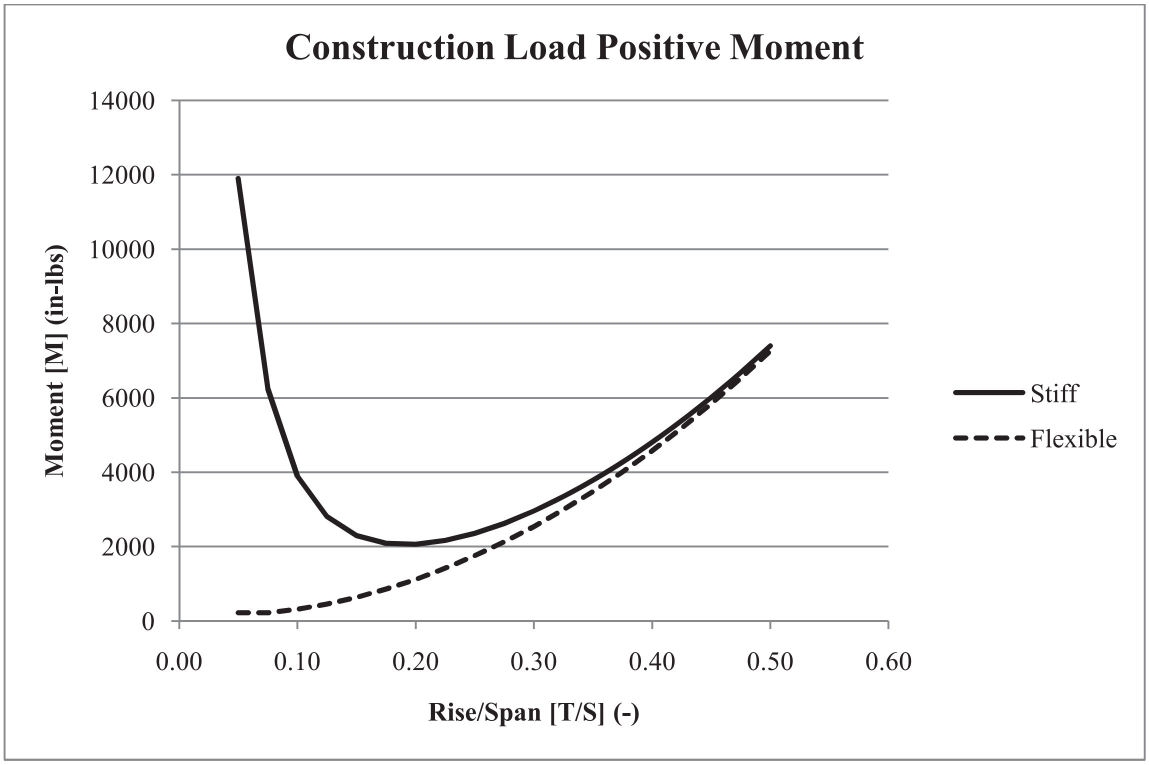

Figure D-8 – Dead Load Negative Moment.

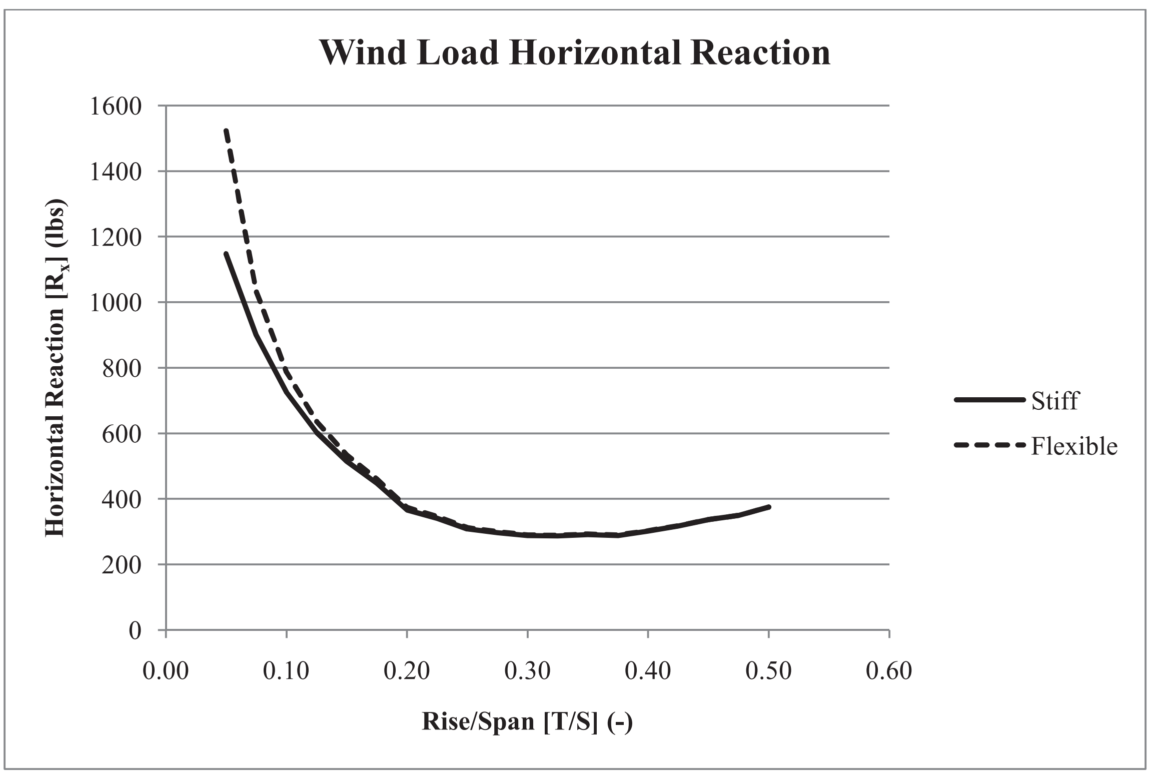

Figure D-9 – Dead Load Negative Moment.

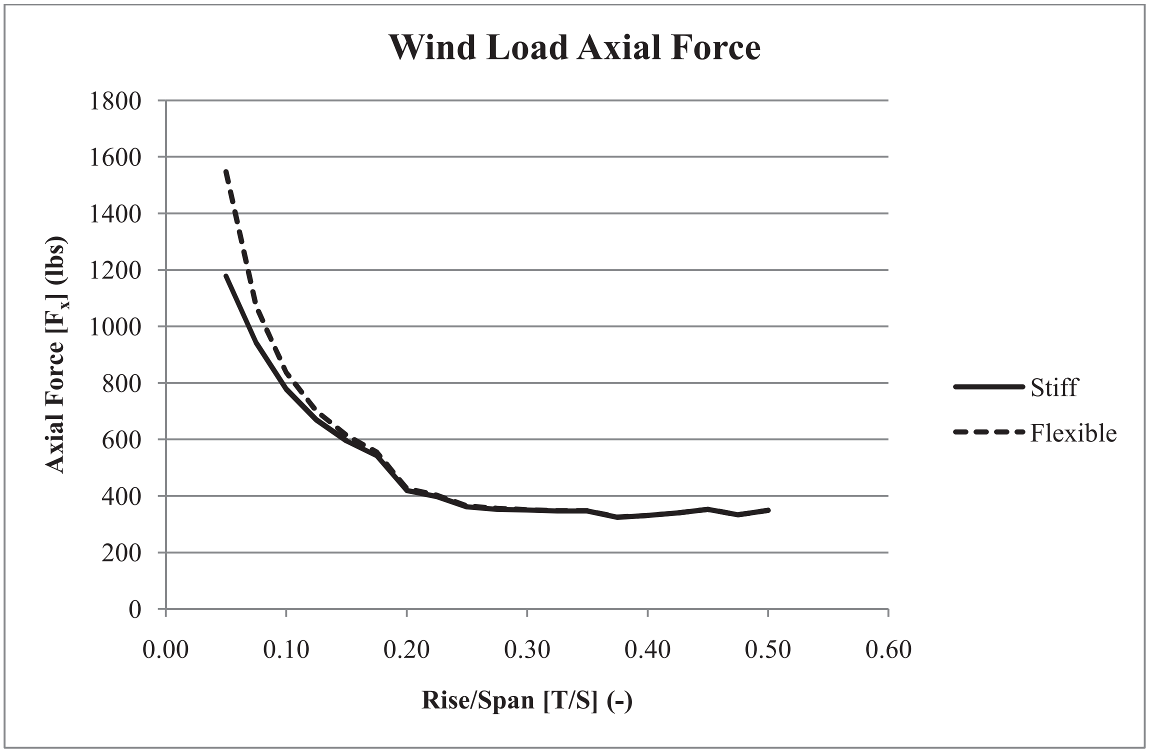

Figure D-10 – Dead Load Negative Moment.

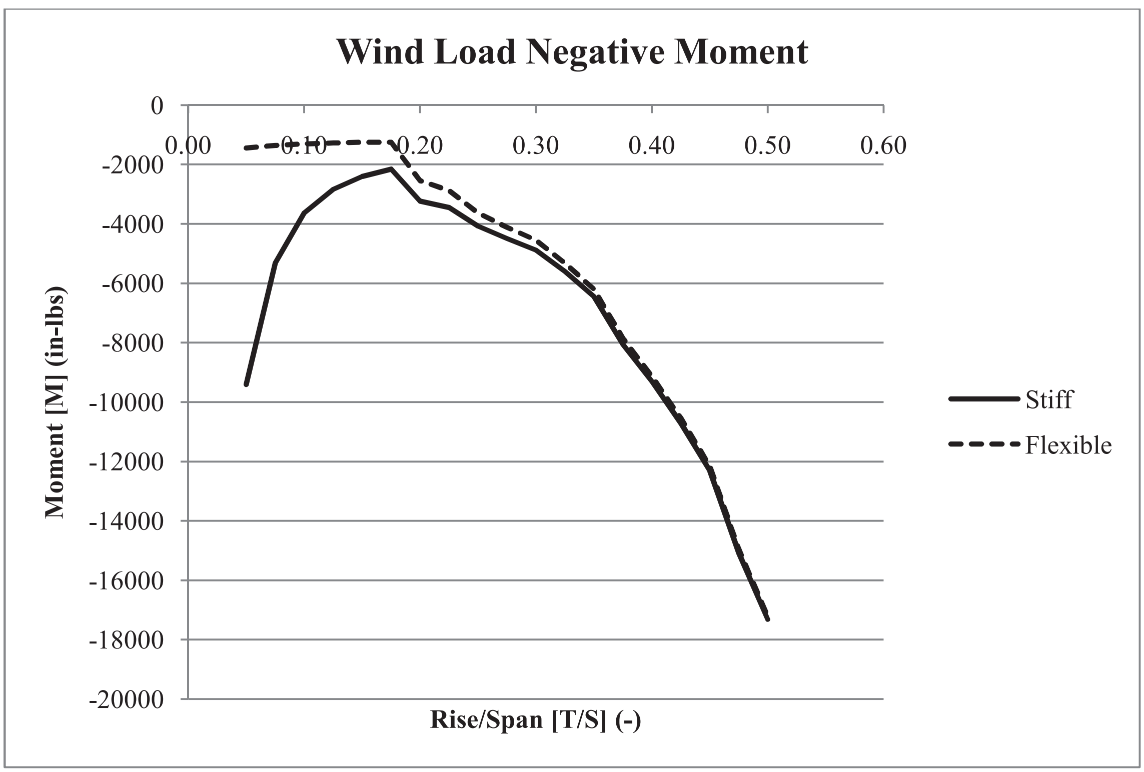

Figure D-11 – Dead Load Negative Moment.

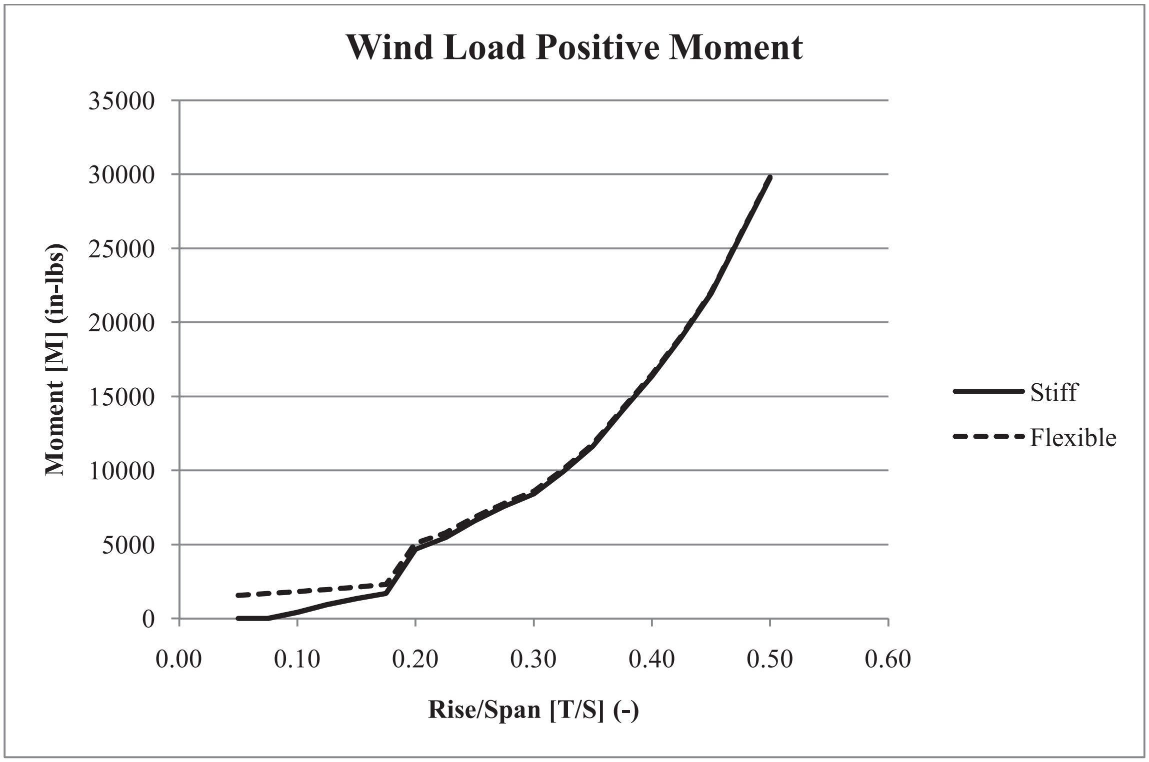

Figure D-12 – Dead Load Negative Moment.

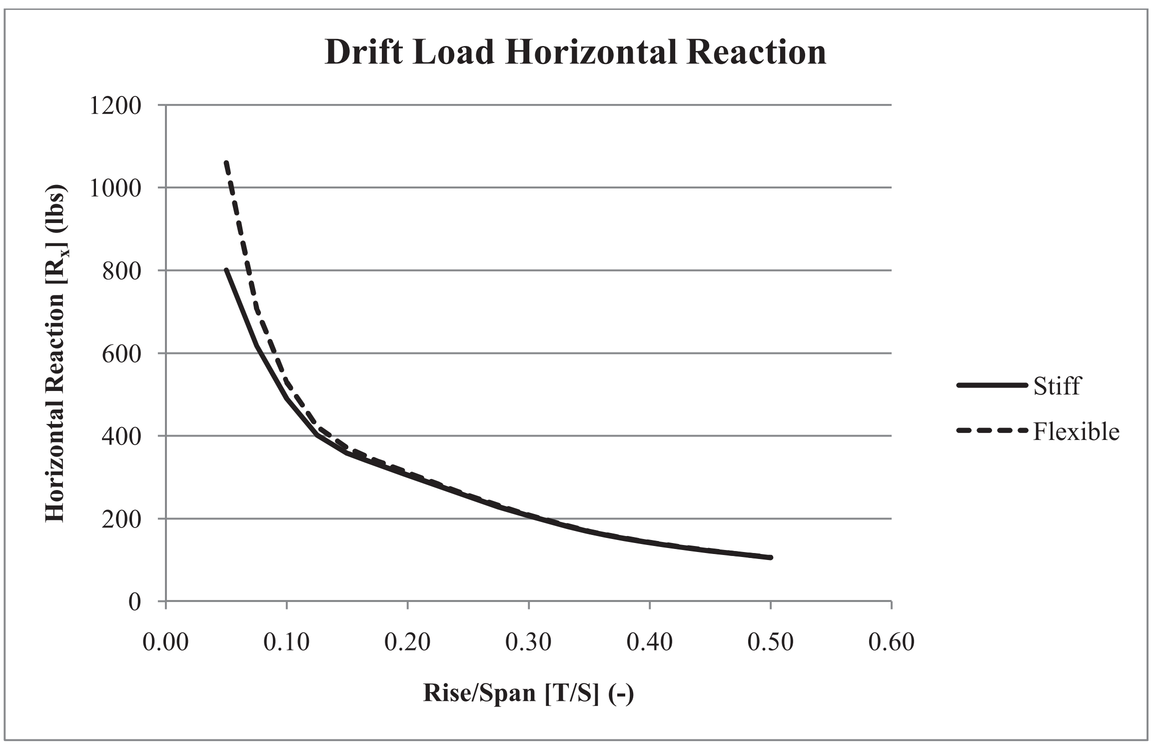

Figure D-13 – Dead Load Negative Moment.

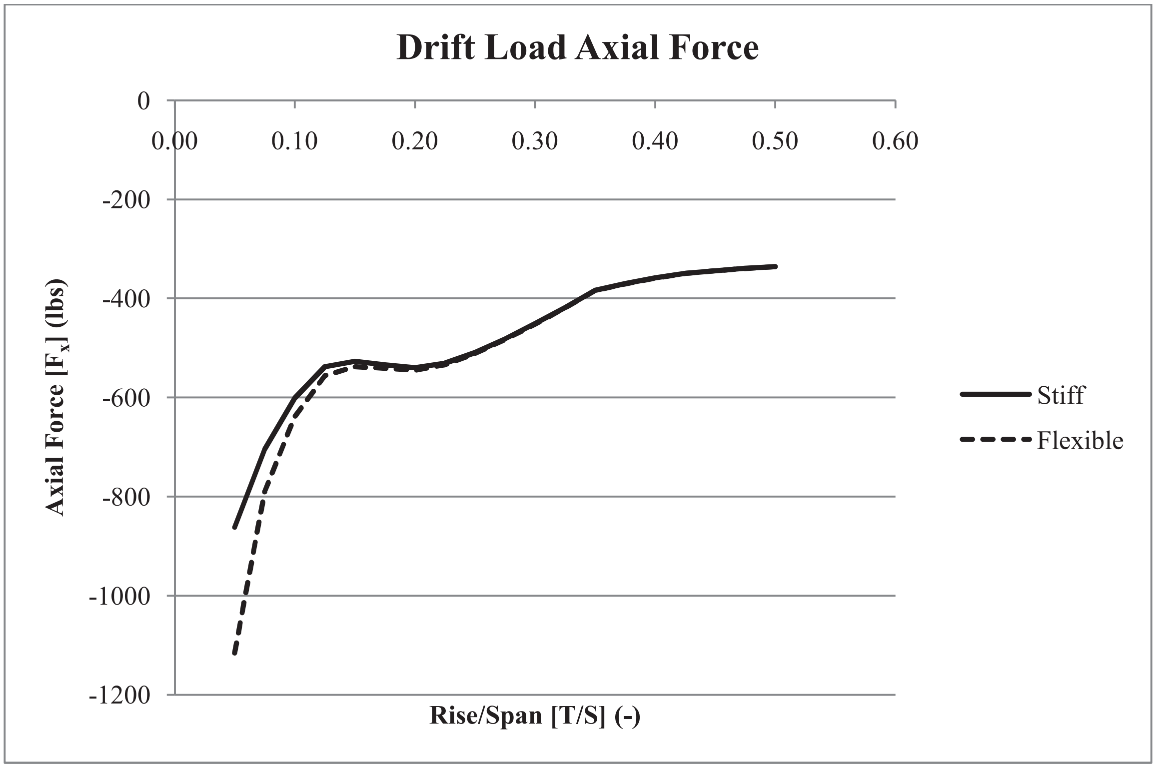

Figure D-14 – Dead Load Negative Moment.

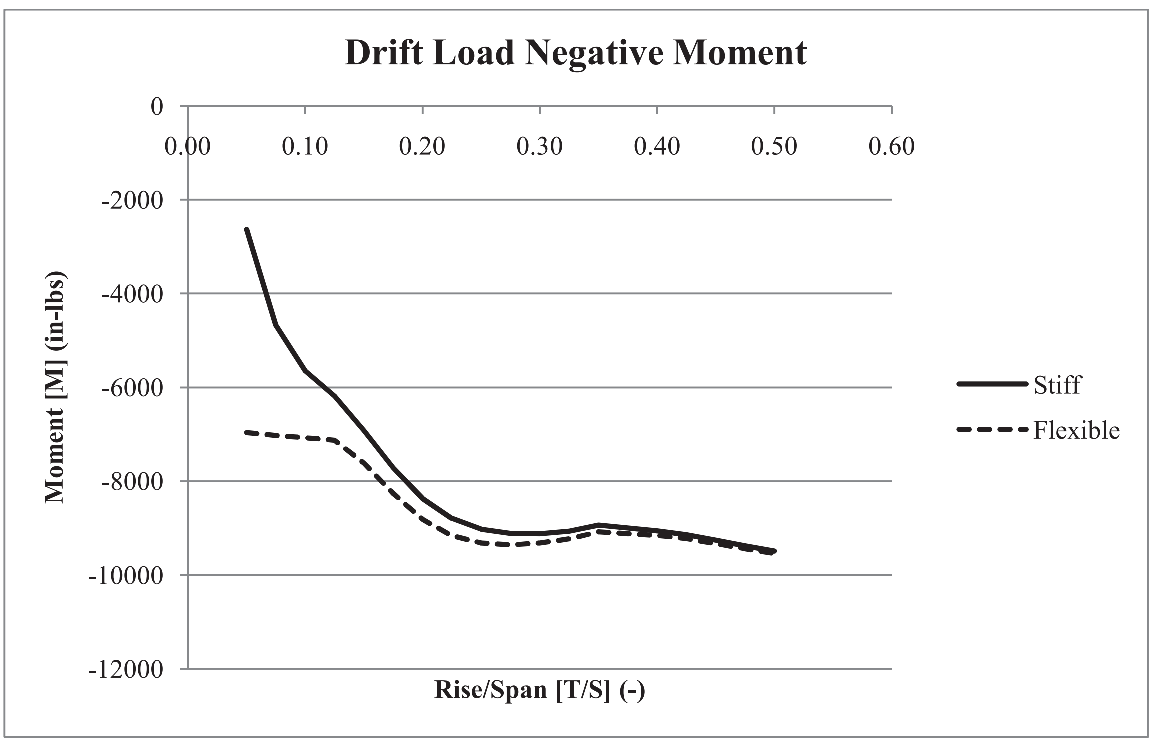

Figure D-15 – Dead Load Negative Moment.

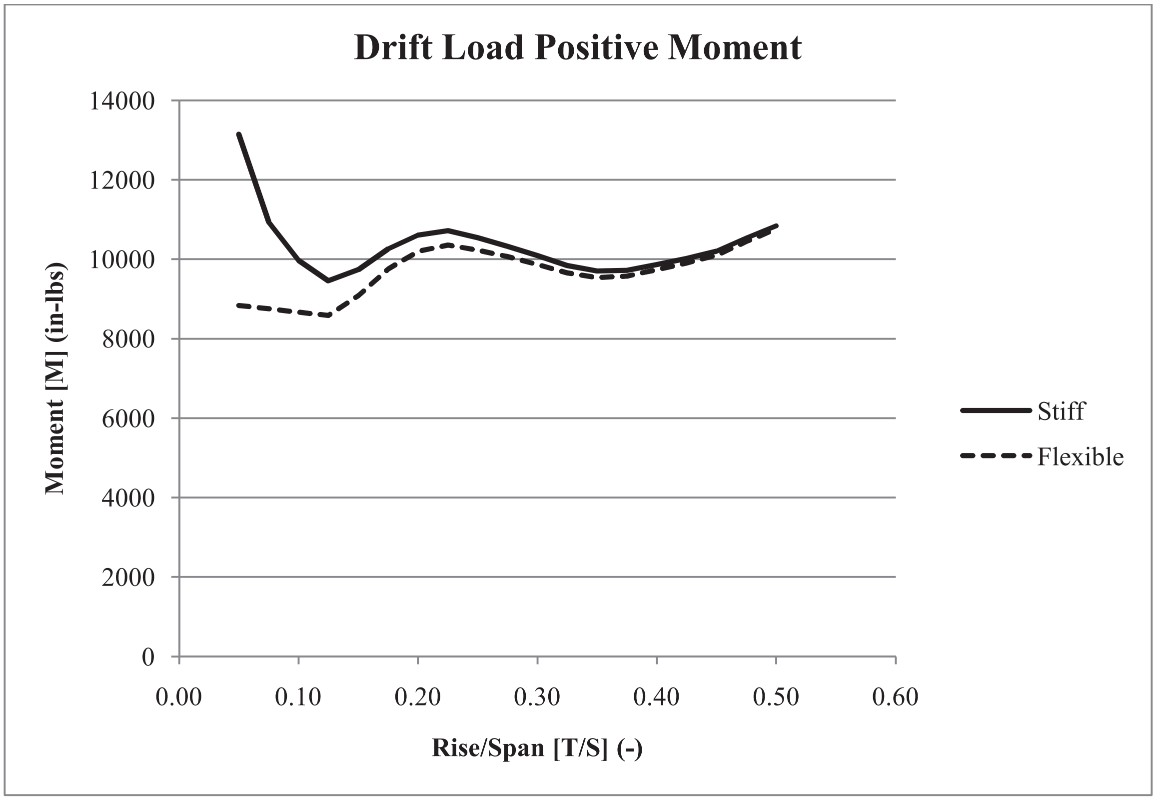

Figure D-16 – Dead Load Negative Moment.

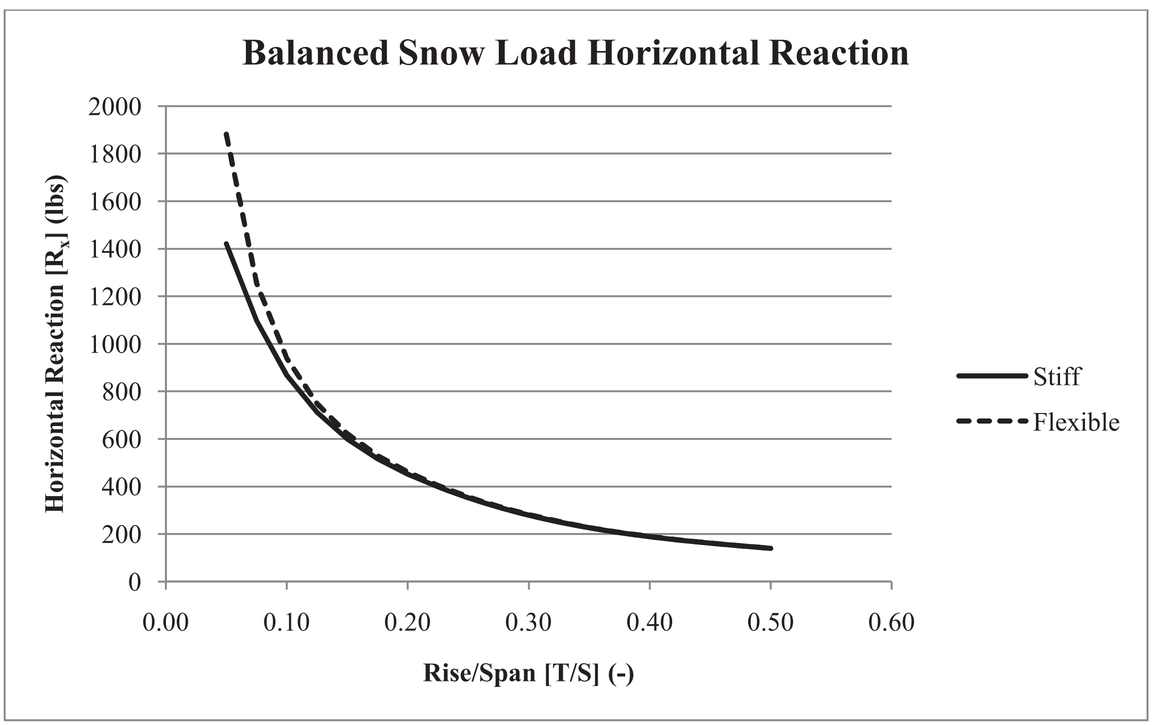

Figure D-17 – Dead Load Negative Moment.

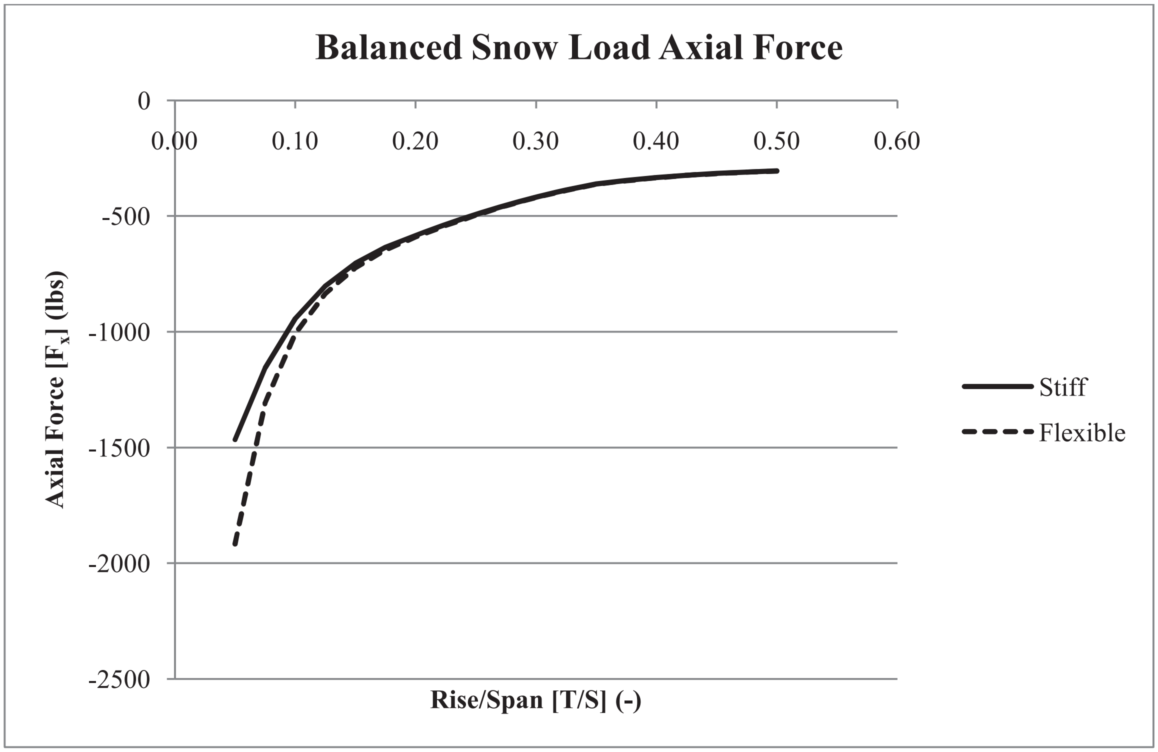

Figure D-18 – Dead Load Negative Moment.

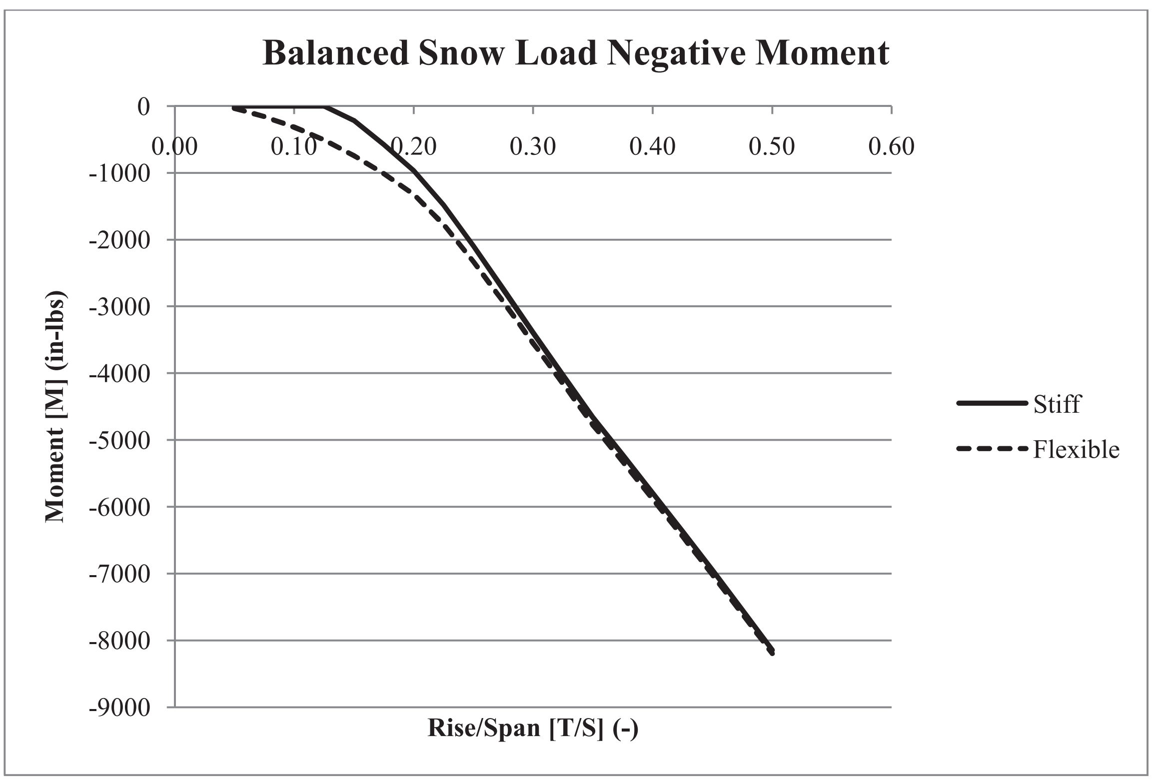

Figure D-19 – Dead Load Negative Moment.

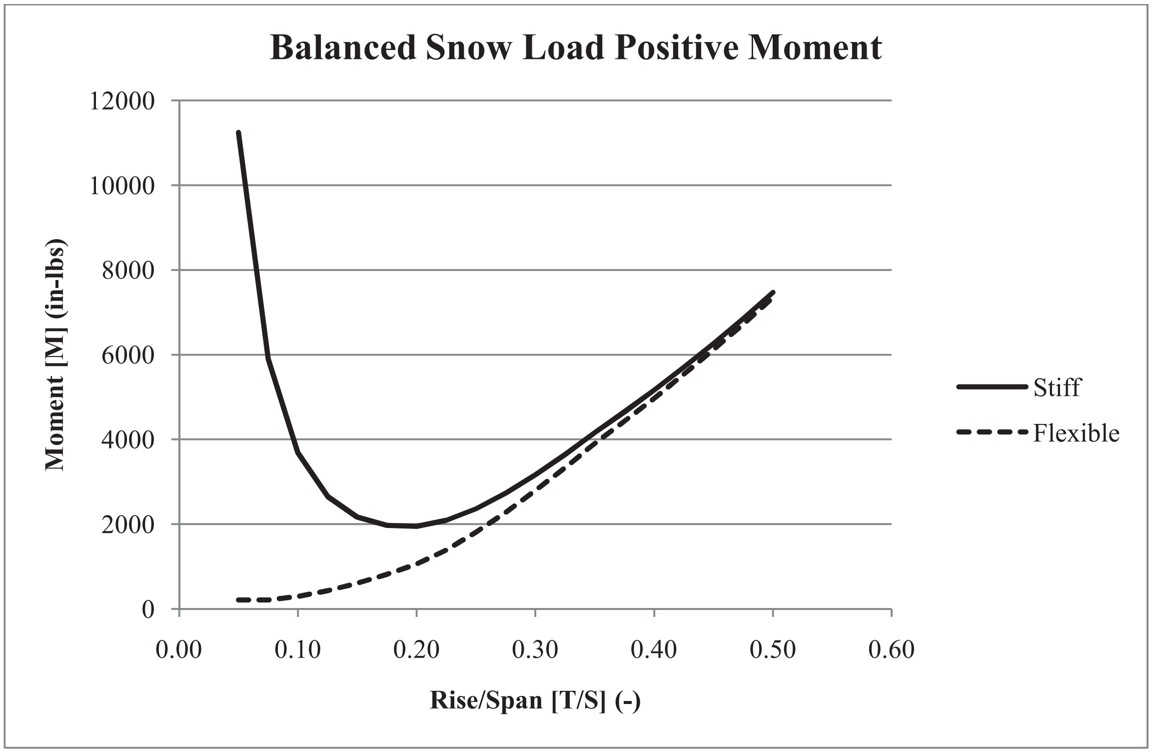

Figure D-20 – Dead Load Negative Moment.

Appendix E: Arched Roof Load Tables

Appendix E contains load tables developed by the author for use in the preliminary design of a lamella roof.

Table E-1 - 20 ft Span, Variable Snow Load.

10 psf Dead Load
20 psf Construction Load
120 mph Wind Zone

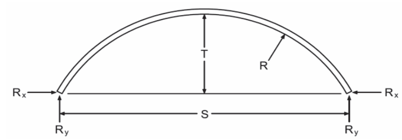

Notes:

All values normalized to C_D = 1.0.
Use ASD design procedure only.

Snow Load

C_e = 0.9
C_t = 1.2
I_s = 1.10

Wind Load

K_{zt} = 1.0
K_d = 0.85

Rise [T] (ft)	Radius [R] (ft)	Ground Snow Load [p_g]														
		15 psf					20 psf					25 psf				
		R_y lbs	R_x lbs	F_a lbs	M^- in-lb	M^+ in-lb	R_y lbs	R_x lbs	F_a lbs	M^- in-lb	M^+ in-lb	R_y lbs	R_x lbs	F_a lbs	M^- in-lb	M^+ in-lb
2	26.00	245	450	510	-485	3665	245	450	510	-485	3665	245	450	510	-485	3665
3	18.17	245	350	425	-400	2025	245	350	425	-510	2330	245	350	425	-630	2780
4	14.50	250	280	370	-655	1700	250	280	370	-930	2165	250	280	370	-1205	2630
5	12.50	255	230	335	-915	1560	255	230	335	-1235	2010	255	230	335	-1550	2455
6	11.33	260	190	315	-1085	1460	260	190	315	-1415	1880	260	190	315	-1745	2305
7	10.64	265	165	305	-1230	1430	265	165	305	-1550	1830	265	165	305	-1885	2230
8	10.25	275	145	295	-1500	1595	275	145	295	-1745	1910	275	145	295	-2080	2305
9	10.06	280	150	290	-1985	1975	280	150	290	-1985	2055	280	150	290	-2315	2460
10	10.00	290	160	290	-2525	2700	290	160	290	-2525	2700	290	160	290	-2595	2705

Rise [T] (ft)	Radius [R] (ft)	Ground Snow Load [p_g]														
		30 psf					35 psf					40 psf				
		R_y lbs	R_x lbs	F_a lbs	M^- in-lb	M^+ in-lb	R_y lbs	R_x lbs	F_a lbs	M^- in-lb	M^+ in-lb	R_y lbs	R_x lbs	F_a lbs	M^- in-lb	M^+ in-lb
2	26.00	275	505	565	-485	4160	305	560	630	-485	4680	335	615	695	-485	5200
3	18.17	275	390	475	-825	3235	305	435	525	-1020	3690	335	475	575	-1220	4150
4	14.50	280	310	410	-1485	3100	310	345	455	-1765	3570	340	375	500	-2050	4045
5	12.50	275	250	375	-1870	2910	300	280	415	-2195	3370	330	305	455	-2520	3825
6	11.33	265	205	345	-2080	2725	290	230	380	-2415	3145	315	250	415	-2755	3570
7	10.64	265	170	310	-2215	2630	275	190	340	-2550	3030	300	205	370	-2880	3430
8	10.25	275	145	300	-2420	2700	280	160	330	-2765	3100	300	175	355	-3110	3505
9	10.06	280	150	295	-2655	2880	285	150	320	-3010	3300	305	155	345	-3365	3720
10	10.00	290	160	290	-2945	3135	290	160	315	-3295	3565	310	160	345	-3655	3995

Table E-1 - 20 ft Span, Variable Snow Load.

10 psf Dead Load
20 psf Construction Load
120 mph Wind Zone

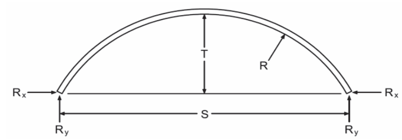

Notes:

All values normalized to C_D = 1.0.
Use ASD design procedure only.

Snow Load

C_e = 0.9
C_t = 1.2
I_s = 1.10

Wind Load

K_{zt} = 1.0
K_d = 0.85

Rise [T] (ft)	Radius [R] (ft)	Ground Snow Load [p_g] 50 psf					60 psf					70 psf				
		R_y lbs	R_x lbs	F_a lbs	M^- in-lb	M^+ in-lb	R_y lbs	R_x lbs	F_a lbs	M^- in-lb	M^+ in-lb	R_y lbs	R_x lbs	F_a lbs	M^- in-lb	M^+ in-lb
2	26.00	395	730	820	-575	6240	455	840	945	-690	7280	515	955	1070	-815	8320
3	18.17	395	565	680	-1625	5065	455	650	785	-2025	5980	515	735	890	-2430	6895
4	14.50	400	445	590	-2615	4990	460	515	680	-3180	5940	520	580	770	-3745	6885
5	12.50	385	360	535	-3165	4740	445	415	615	-3815	5655	500	465	695	-4460	6565
6	11.33	365	295	485	-3430	4425	415	335	560	-4110	5285	470	380	630	-4785	6140
7	10.64	345	240	435	-3555	4230	390	275	495	-4235	5035	440	315	555	-4915	5850
8	10.25	345	205	410	-3795	4320	390	235	470	-4480	5140	435	265	525	-5175	5955
9	10.06	350	180	400	-4075	4555	390	205	455	-4780	5395	435	230	510	-5490	6230
10	10.00	355	160	395	-4385	4850	400	180	445	-5120	5730	440	200	500	-5850	6615

Rise [T] (ft)	Radius [R] (ft)	Ground Snow Load [p_g] 80 psf					90 psf					100 psf				
		R_y lbs	R_x lbs	F_a lbs	M^- in-lb	M^+ in-lb	R_y lbs	R_x lbs	F_a lbs	M^- in-lb	M^+ in-lb	R_y lbs	R_x lbs	F_a lbs	M^- in-lb	M^+ in-lb
2	26.00	575	1065	1200	-1020	9360	635	1180	1325	-1225	10410	695	1290	1450	-1435	11455
3	18.17	575	820	995	-2830	7810	635	910	1100	-3230	8730	695	995	1205	-3640	9645
4	14.50	580	650	860	-4310	7830	640	715	950	-4875	8780	700	785	1040	-5440	9725
5	12.50	555	520	775	-5110	7480	610	575	855	-5760	8395	670	630	935	-6405	9310
6	11.33	520	425	700	-5465	7000	570	465	770	-6140	7855	625	510	845	-6820	8715
7	10.64	485	350	615	-5595	6660	530	385	675	-6275	7475	575	420	740	-6955	8290
8	10.25	480	295	580	-5875	6775	525	325	640	-6575	7590	565	355	695	-7270	8410
9	10.06	480	255	560	-6200	7070	525	280	615	-6905	7910	565	305	670	-7625	8745
10	10.00	485	220	555	-6585	7495	530	245	605	-7315	8380	570	265	660	-8050	9265

Table E-2 - 30 ft Span, Variable Snow Load.

10 psf Dead Load
20 psf Construction Load
120 mph Wind Zone

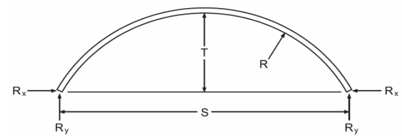

Notes:

All values normalized to C_D = 1.0.
Use ASD design procedure only.

Snow Load

C_e = 0.9
C_t = 1.2
I_s = 1.10

Wind Load

K_{zt} = 1.0
K_d = 0.85

Rise [T] (ft)	Radius [R] (ft)	Ground Snow Load [p_g] 15 psf					20 psf					25 psf				
		R_y lbs	R_x lbs	F_a lbs	M^- in-lb	M^+ in-lb	R_y lbs	R_x lbs	F_a lbs	M^- in-lb	M^+ in-lb	R_y lbs	R_x lbs	F_a lbs	M^- in-lb	M^+ in-lb
3	39.00	365	785	865	-785	4305	365	785	865	-1010	4995	365	785	865	-1230	5965
4	30.13	370	625	720	-1010	3275	370	625	720	-1500	4155	370	625	720	-2000	5035
5	25.00	370	515	630	-1570	3190	370	515	630	-2190	4125	370	515	630	-2815	5065
6	21.75	375	435	565	-2000	3155	375	435	565	-2715	4135	375	435	565	-3425	5115
7	19.57	380	375	525	-2305	3085	380	375	525	-3070	4060	380	375	525	-3835	5035
8	18.06	385	330	495	-2520	2990	385	330	495	-3295	3930	385	330	495	-4085	4870
9	17.00	390	290	475	-2690	2930	390	290	475	-3470	3830	390	290	475	-4250	4735
10	16.25	395	260	460	-2850	2935	395	260	460	-3625	3800	395	260	460	-4400	4665
11	15.73	400	235	450	-3045	3010	400	235	450	-3810	3865	400	235	450	-4585	4740
12	15.38	410	215	445	-3515	3345	410	215	445	-4065	4050	410	215	445	-4850	4915
13	15.15	415	220	440	-4205	4055	415	220	440	-4375	4280	415	220	440	-5140	5180
14	15.04	425	235	435	-4955	5060	425	235	435	-4955	5060	425	235	435	-5525	5505
15	15.00	430	240	430	-5765	6085	430	240	430	-5765	6085	430	240	430	-5925	6085

Rise [T] (ft)	Radius [R] (ft)	Ground Snow Load [p_g] 30 psf					35 psf					40 psf				
		R_y lbs	R_x lbs	F_a lbs	M^- in-lb	M^+ in-lb	R_y lbs	R_x lbs	F_a lbs	M^- in-lb	M^+ in-lb	R_y lbs	R_x lbs	F_a lbs	M^- in-lb	M^+ in-lb
3	39.00	410	875	960	-1590	6935	455	975	1070	-2000	7910	500	1075	1175	-2415	8880
4	30.13	410	695	805	-2505	5915	455	775	890	-3015	6795	500	850	980	-3525	7675
5	25.00	415	575	700	-3435	6005	460	635	775	-4060	6940	505	700	855	-4685	7880
6	21.75	420	485	630	-4140	6100	465	535	700	-4850	7080	510	590	770	-5565	8065
7	19.57	415	415	580	-4600	6010	455	460	640	-5370	6985	500	505	705	-6135	7960
8	18.06	405	360	550	-4875	5810	445	400	610	-5665	6755	485	435	665	-6460	7695
9	17.00	395	315	515	-5050	5635	430	345	570	-5850	6550	470	380	625	-6650	7470
10	16.25	395	275	485	-5175	5560	420	305	530	-5970	6450	455	335	580	-6765	7345
11	15.73	400	245	460	-5365	5615	415	270	505	-6140	6495	450	295	550	-6915	7370
12	15.38	410	220	450	-5635	5785	415	245	490	-6425	6655	450	265	535	-7210	7545
13	15.15	415	220	440	-5945	6085	420	220	480	-6745	6985	455	240	520	-7545	7890
14	15.04	425	235	440	-6310	6425	425	235	480	-7130	7370	460	235	515	-7945	8310
15	15.00	430	240	435	-6725	6870	435	240	475	-7525	7815	465	240	515	-8355	8765

Table E-2 - 30 ft Span, Variable Snow Load.

10 psf Dead Load
20 psf Construction Load
120 mph Wind Zone

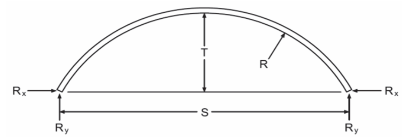

Notes:

All values normalized to $C_D = 1.0$.
Use ASD design procedure only.

Snow Load

$C_e = 0.9$
$C_t = 1.2$
$I_s = 1.10$

Wind Load

$K_{zt} = 1.0$
$K_d = 0.85$

Rise [T] (ft)	Radius [R] (ft)	Ground Snow Load [p_g] 50 psf R_y lbs	R_x lbs	F_a lbs	M^- in-lb	M^+ in-lb	60 psf R_y lbs	R_x lbs	F_a lbs	M^- in-lb	M^+ in-lb	70 psf R_y lbs	R_x lbs	F_a lbs	M^- in-lb	M^+ in-lb
3	39.00	590	1270	1390	-3250	10825	680	1465	1605	-4080	12765	770	1660	1820	-4915	14710
4	30.13	590	1005	1160	-4545	9440	680	1160	1340	-5570	11210	770	1315	1515	-6590	12980
5	25.00	595	825	1010	-5935	9755	685	955	1165	-7185	11635	775	1080	1320	-8440	13520
6	21.75	600	695	910	-6995	10025	690	805	1045	-8435	11990	780	910	1185	-9875	13955
7	19.57	585	595	830	-7670	9910	675	685	955	-9215	11860	760	775	1080	-10765	13825
8	18.06	570	515	785	-8040	9600	650	590	900	-9625	11505	735	670	1020	-11205	13415
9	17.00	550	445	730	-8245	9310	625	515	840	-9840	11155	700	580	945	-11440	12995
10	16.25	530	390	680	-8355	9130	600	450	775	-9950	10915	670	505	875	-11540	12700
11	15.73	515	345	640	-8500	9120	585	400	725	-10090	10870	655	450	815	-11680	12625
12	15.38	515	310	620	-8790	9335	585	355	705	-10385	11125	650	400	785	-12000	12910
13	15.15	520	280	605	-9150	9690	585	325	685	-10750	11495	650	365	765	-12355	13300
14	15.04	525	255	595	-9585	10195	590	295	675	-11225	12080	655	330	755	-12865	13965
15	15.00	530	240	590	-10025	10660	595	270	670	-11690	12615	660	300	750	-13360	14570

Rise [T] (ft)	Radius [R] (ft)	Ground Snow Load [p_g] 80 psf R_y lbs	R_x lbs	F_a lbs	M^- in-lb	M^+ in-lb	90 psf R_y lbs	R_x lbs	F_a lbs	M^- in-lb	M^+ in-lb	100 psf R_y lbs	R_x lbs	F_a lbs	M^- in-lb	M^+ in-lb
3	39.00	860	1855	2035	-5750	16655	950	2055	2250	-6590	18595	1040	2250	2465	-7435	20545
4	30.13	860	1470	1695	-7610	14755	955	1625	1875	-8635	16530	1045	1780	2050	-9655	18305
5	25.00	865	1205	1470	-9700	15410	955	1335	1625	-10960	17295	1045	1460	1780	-12220	19185
6	21.75	870	1015	1325	-11315	15920	960	1120	1460	-12755	17880	1050	1230	1600	-14195	19845
7	19.57	850	865	1205	-12315	15790	935	955	1330	-13860	17755	1025	1045	1455	-15410	19715
8	18.06	815	745	1135	-12800	15320	900	820	1250	-14395	17230	980	900	1370	-15995	19135
9	17.00	780	645	1055	-13035	14835	855	710	1160	-14635	16675	935	780	1270	-16230	18520
10	16.25	745	565	970	-13130	14490	815	620	1065	-14720	16275	885	680	1165	-16315	18060
11	15.73	720	500	905	-13270	14375	790	550	995	-14860	16125	855	600	1085	-16450	17880
12	15.38	715	445	870	-13610	14700	785	490	955	-15220	16485	850	535	1040	-16830	18275
13	15.15	715	405	850	-13985	15105	780	445	930	-15620	16910	845	485	1015	-17255	18710
14	15.04	720	365	835	-14500	15850	785	405	920	-16140	17740	850	440	1000	-17800	19625
15	15.00	725	335	830	-15025	16525	790	370	910	-16695	18480	855	400	985	-18365	20435

Table E-3 - 40 ft Span, Variable Snow Load.

10 psf Dead Load
20 psf Construction Load
120 mph Wind Zone

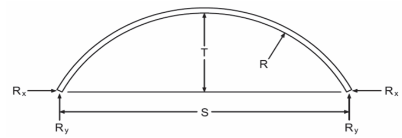

Notes:

All values normalized to C_D = 1.0.
Use ASD design procedure only.

Snow Load

C_e = 0.9
C_t = 1.2
I_s = 1.10

Wind Load

K_{zt} = 1.0
K_d = 0.85

Rise [T] (ft)	Radius [R] (ft)	Ground Snow Load [p_g]														
		15 psf					20 psf					25 psf				
		R_y lbs	R_x lbs	F_a lbs	M^- in-lb	M^+ in-lb	R_y lbs	R_x lbs	F_a lbs	M^- in-lb	M^+ in-lb	R_y lbs	R_x lbs	F_a lbs	M^- in-lb	M^+ in-lb
4	52.00	485	1110	1205	-1725	5860	485	1110	1205	-2565	7430	485	1110	1205	-3440	9000
5	42.50	490	915	1030	-2305	5180	490	915	1030	-3285	6670	490	915	1030	-4265	8170
6	36.33	490	770	910	-2905	5055	490	770	910	-3995	6590	490	770	910	-5085	8130
7	32.07	495	670	825	-3465	5140	495	670	825	-4680	6765	495	670	825	-5895	8390
8	29.00	500	585	760	-3930	5200	500	585	760	-5250	6890	500	585	760	-6565	8580
9	26.72	505	525	715	-4280	5175	505	525	715	-5665	6860	505	525	715	-7050	8545
10	25.00	510	470	680	-4535	5085	510	470	680	-5955	6750	510	470	680	-7380	8430
11	23.68	515	430	655	-4745	5010	515	430	655	-6170	6645	515	430	655	-7610	8275
12	22.67	520	390	635	-4945	4985	520	390	635	-6345	6560	520	390	635	-7780	8130
13	21.88	525	360	620	-5130	5000	525	360	620	-6530	6525	525	360	620	-7930	8095
14	21.29	530	330	605	-5310	5070	530	330	605	-6695	6590	530	330	605	-8080	8105
15	20.83	535	310	595	-5620	5280	535	310	595	-6995	6755	535	310	595	-8395	8305
16	20.50	545	285	590	-6340	6045	545	285	590	-7310	7050	545	285	590	-8725	8575
17	20.26	550	285	585	-7235	7090	550	285	585	-7705	7370	550	285	585	-9095	8940
18	20.11	560	290	580	-8195	8280	560	290	580	-8195	8280	560	290	580	-9540	9345
19	20.03	565	310	575	-9215	9955	565	310	575	-9215	9955	565	310	575	-10050	9955
20	20.00	575	315	575	-10300	11560	575	315	575	-10300	11560	575	315	575	-10590	11560

Rise [T] (ft)	Radius [R] (ft)	Ground Snow Load [p_g]														
		30 psf					35 psf					40 psf				
		R_y lbs	R_x lbs	F_a lbs	M^- in-lb	M^+ in-lb	R_y lbs	R_x lbs	F_a lbs	M^- in-lb	M^+ in-lb	R_y lbs	R_x lbs	F_a lbs	M^- in-lb	M^+ in-lb
4	52.00	545	1240	1345	-4340	10585	605	1375	1495	-5235	12175	665	1515	1645	-6130	13765
5	42.50	545	1020	1150	-5240	9675	605	1130	1275	-6220	11185	665	1245	1405	-7200	12690
6	36.33	550	860	1015	-6180	9685	610	955	1125	-7270	11235	670	1050	1240	-8375	12785
7	32.07	550	745	920	-7115	10010	610	825	1020	-8345	11635	670	910	1120	-9575	13270
8	29.00	555	655	850	-7885	10270	615	725	940	-9220	11965	675	800	1035	-10555	13655
9	26.72	550	580	790	-8435	10250	610	645	875	-9825	11960	670	710	960	-11225	13665
10	25.00	545	520	755	-8800	10110	600	575	835	-10225	11795	655	630	915	-11645	13475
11	23.68	535	465	720	-9050	9910	590	515	800	-10490	11545	640	565	875	-11925	13175
12	22.67	525	420	690	-9220	9710	575	465	760	-10665	11315	625	510	835	-12105	12925
13	21.88	525	380	655	-9355	9665	565	420	725	-10790	11235	610	460	790	-12230	12805
14	21.29	530	350	620	-9465	9625	550	385	685	-10860	11140	600	420	745	-12280	12660
15	20.83	535	320	610	-9790	9855	550	355	665	-11190	11405	595	385	725	-12590	12950
16	20.50	545	295	595	-10135	10095	555	325	655	-11550	11630	600	355	710	-12960	13205
17	20.26	550	285	590	-10520	10510	560	305	645	-11945	12085	600	330	700	-13375	13655
18	20.11	560	290	585	-10970	10970	565	290	640	-12420	12600	610	310	690	-13865	14225
19	20.03	565	310	580	-11460	11450	570	310	635	-12920	13110	615	310	685	-14390	14790
20	20.00	575	315	580	-12020	12090	580	315	630	-13445	13765	620	315	685	-14935	15445

Table E-3 - 40 ft Span, Variable Snow Load.

10 psf Dead Load
20 psf Construction Load
120 mph Wind Zone

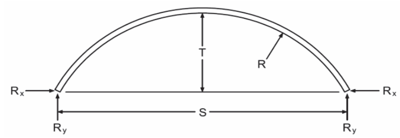

Notes:

All values normalized to C_D = 1.0.
Use ASD design procedure only.

Snow Load

C_e = 0.9
C_t = 1.2
I_s = 1.10

Wind Load

K_{zt} = 1.0
K_d = 0.85

Rise [T] (ft)	Radius [R] (ft)	Ground Snow Load [p_g] 50 psf R_y lbs	50 psf R_x lbs	50 psf F_a lbs	50 psf M^- in-lb	50 psf M^+ in-lb	60 psf R_y lbs	60 psf R_x lbs	60 psf F_a lbs	60 psf M^- in-lb	60 psf M^+ in-lb	70 psf R_y lbs	70 psf R_x lbs	70 psf F_a lbs	70 psf M^- in-lb	70 psf M^+ in-lb
4	52.00	785	1790	1945	-7925	16945	905	2070	2250	-9720	20125	1025	2345	2550	-11515	23305
5	42.50	785	1470	1660	-9155	15705	905	1700	1915	-11130	18720	1025	1925	2170	-13100	21730
6	36.33	790	1245	1460	-10580	15890	910	1435	1685	-12785	18995	1030	1625	1910	-14990	22095
7	32.07	795	1075	1325	-12030	16545	915	1240	1525	-14490	19815	1035	1405	1730	-16950	23090
8	29.00	795	945	1220	-13220	17035	920	1085	1405	-15890	20420	1040	1230	1595	-18555	23805
9	26.72	790	835	1135	-14030	17085	905	960	1305	-16835	20500	1025	1090	1475	-19640	23920
10	25.00	770	745	1080	-14510	16835	885	855	1240	-17385	20200	995	970	1405	-20265	23560
11	23.68	750	665	1030	-14805	16445	860	765	1185	-17685	19710	965	865	1335	-20590	22975
12	22.67	730	600	975	-14990	16140	830	690	1120	-17875	19360	935	775	1265	-20760	22575
13	21.88	710	540	925	-15105	15945	805	620	1055	-17975	19080	905	700	1190	-20850	22220
14	21.29	690	490	865	-15120	15715	780	565	990	-17960	18805	875	635	1110	-20800	21900
15	20.83	685	450	845	-15445	16050	780	520	960	-18315	19145	870	585	1080	-21180	22240
16	20.50	685	415	825	-15785	16355	775	475	935	-18665	19500	865	540	1050	-21555	22645
17	20.26	690	385	810	-16230	16800	780	440	920	-19080	19945	865	495	1030	-21980	23090
18	20.11	695	360	800	-16765	17480	780	410	905	-19660	20730	870	460	1015	-22555	23985
19	20.03	700	335	790	-17330	18150	790	385	900	-20270	21510	875	430	1005	-23210	24865
20	20.00	710	315	790	-17915	18795	795	355	895	-20890	22250	880	400	1000	-23870	25705

Rise [T] (ft)	Radius [R] (ft)	Ground Snow Load [p_g] 80 psf R_y lbs	80 psf R_x lbs	80 psf F_a lbs	80 psf M^- in-lb	80 psf M^+ in-lb	90 psf R_y lbs	90 psf R_x lbs	90 psf F_a lbs	90 psf M^- in-lb	90 psf M^+ in-lb	100 psf R_y lbs	100 psf R_x lbs	100 psf F_a lbs	100 psf M^- in-lb	100 psf M^+ in-lb
4	52.00	1145	2625	2850	-13310	26485	1265	2900	3150	-15100	29665	1385	3175	3450	-16895	32845
5	42.50	1150	2155	2425	-15075	24745	1270	2380	2680	-17050	27760	1390	2605	2940	-19020	30775
6	36.33	1150	1815	2135	-17200	25200	1270	2010	2360	-19405	28305	1390	2200	2585	-21610	31405
7	32.07	1155	1570	1930	-19410	26360	1275	1735	2135	-21870	29630	1395	1895	2335	-24330	32905
8	29.00	1160	1375	1780	-21225	27185	1280	1520	1965	-23895	30570	1400	1665	2150	-26560	33950
9	26.72	1140	1215	1645	-22445	27335	1260	1345	1820	-25245	30750	1375	1470	1990	-28050	34170
10	25.00	1110	1080	1565	-23140	26925	1220	1195	1730	-26015	30290	1335	1305	1890	-28890	33650
11	23.68	1075	965	1490	-23495	26265	1180	1065	1645	-26405	29560	1290	1165	1800	-29310	32850
12	22.67	1040	865	1410	-23645	25795	1140	955	1550	-26530	29010	1245	1045	1695	-29440	32230
13	21.88	1000	780	1325	-23725	25360	1100	860	1455	-26600	28500	1195	940	1590	-29470	31635
14	21.29	965	705	1235	-23640	24995	1060	780	1355	-26480	28090	1150	850	1480	-29325	31185
15	20.83	960	650	1195	-24045	25340	1050	715	1310	-26910	28435	1140	780	1430	-29775	31535
16	20.50	955	600	1165	-24440	25795	1045	660	1275	-27330	28940	1130	720	1390	-30215	32085
17	20.26	955	555	1140	-24895	26245	1040	610	1250	-27805	29440	1130	665	1360	-30720	32635
18	20.11	955	515	1125	-25470	27235	1045	565	1230	-28420	30490	1130	615	1340	-31370	33745
19	20.03	960	480	1110	-26145	28225	1050	525	1220	-29085	31585	1135	575	1325	-32050	34940
20	20.00	970	445	1105	-26850	29160	1055	490	1210	-29825	32615	1140	535	1315	-32805	36070

Table E-4 - 50 ft Span, Variable Snow Load.

10 psf Dead Load
20 psf Construction Load
120 mph Wind Zone

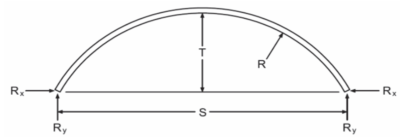

Notes:

All values normalized to C_D = 1.0.
Use ASD design procedure only.

Snow Load

C_e = 0.9
C_t = 1.2
I_s = 1.10

Wind Load

K_{zt} = 1.0
K_d = 0.85

Rise [T] (ft)	Radius [R] (ft)	Ground Snow Load [p_g] 15 psf R_y lbs	15 psf R_x lbs	15 psf F_a lbs	15 psf M^- in-lb	15 psf M^+ in-lb	20 psf R_y lbs	20 psf R_x lbs	20 psf F_a lbs	20 psf M^- in-lb	20 psf M^+ in-lb	25 psf R_y lbs	25 psf R_x lbs	25 psf F_a lbs	25 psf M^- in-lb	25 psf M^+ in-lb
5	65.00	610	1425	1545	-3510	8150	610	1425	1545	-5025	10520	610	1425	1545	-6545	12890
6	55.08	610	1205	1345	-4115	7545	610	1205	1345	-5705	9835	610	1205	1345	-7295	12130
8	43.06	615	920	1095	-5320	7510	615	920	1095	-7160	9920	615	920	1095	-9015	12350
10	36.25	625	740	955	-6420	7820	625	740	955	-8515	10425	625	740	955	-10615	13025
12	32.04	630	615	870	-7135	7775	630	615	870	-9365	10380	630	615	870	-11595	12985
14	29.32	640	525	815	-7615	7620	640	525	815	-9860	10140	640	525	815	-12135	12665
16	27.53	655	460	775	-8055	7635	655	460	775	-10255	10045	655	460	775	-12465	12480
18	26.36	665	405	755	-8545	7890	665	405	755	-10725	10260	665	405	755	-12905	12635
20	25.63	680	360	735	-9965	9965	680	360	735	-11495	10910	680	360	735	-13710	13275
22	25.20	695	355	725	-12245	12830	695	355	725	-12500	12830	695	355	725	-14660	14240
24	25.02	710	385	720	-14770	16880	710	385	720	-14770	16880	710	385	720	-15910	16880
25	25.00	715	390	720	-16135	19020	715	390	720	-16135	19020	715	390	720	-16590	19020

Rise [T] (ft)	Radius [R] (ft)	Ground Snow Load [p_g] 30 psf R_y lbs	30 psf R_x lbs	30 psf F_a lbs	30 psf M^- in-lb	30 psf M^+ in-lb	35 psf R_y lbs	35 psf R_x lbs	35 psf F_a lbs	35 psf M^- in-lb	35 psf M^+ in-lb	40 psf R_y lbs	40 psf R_x lbs	40 psf F_a lbs	40 psf M^- in-lb	40 psf M^+ in-lb
5	65.00	680	1590	1720	-8060	15260	755	1770	1915	-9575	17630	830	1945	2105	-11090	20000
6	55.08	680	1345	1500	-8895	14420	755	1495	1665	-10505	16715	830	1645	1835	-12110	19010
8	43.06	685	1025	1225	-10875	14780	760	1140	1360	-12740	17210	835	1250	1495	-14605	19645
10	36.25	695	825	1065	-12740	15630	770	915	1180	-14865	18230	845	1005	1300	-16985	20835
12	32.04	685	680	960	-13825	15590	755	755	1065	-16055	18195	825	830	1165	-18315	20800
14	29.32	665	570	895	-14405	15190	730	635	990	-16680	17715	800	695	1085	-18950	20240
16	27.53	655	485	830	-14725	14915	705	540	910	-16985	17350	770	590	995	-19250	19785
18	26.36	665	420	770	-15085	15010	690	465	845	-17265	17385	745	510	920	-19500	19760
20	25.63	680	370	745	-15920	15645	690	410	815	-18135	18035	745	445	885	-20350	20480
22	25.20	695	355	730	-16915	16735	700	360	800	-19170	19235	755	395	865	-21425	21730
24	25.02	710	385	725	-18120	17990	715	385	790	-20405	20540	770	385	855	-22710	23170
25	25.00	715	390	725	-18825	19020	725	390	790	-21065	21420	775	390	855	-23395	24030

Table E-4 - 50 ft Span, Variable Snow Load.

10 psf Dead Load
20 psf Construction Load
120 mph Wind Zone

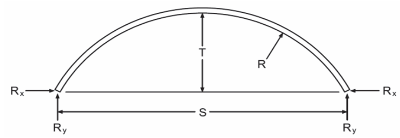

Notes:

All values normalized to $C_D = 1.0$.
Use ASD design procedure only.

Snow Load

$C_e = 0.9$
$C_t = 1.2$
$I_s = 1.10$

Wind Load

$K_{zt} = 1.0$
$K_d = 0.85$

Rise [T] (ft)	Radius [R] (ft)	Ground Snow Load [p_g]														
		50 psf					60 psf					70 psf				
		R_y lbs	R_x lbs	F_a lbs	M^- in-lb	M^+ in-lb	R_y lbs	R_x lbs	F_a lbs	M^- in-lb	M^+ in-lb	R_y lbs	R_x lbs	F_a lbs	M^- in-lb	M^+ in-lb
5	65.00	980	2305	2490	-14145	24735	1130	2660	2875	-17205	29475	1280	3015	3260	-20265	34215
6	55.08	980	1945	2170	-15330	23595	1130	2245	2505	-18545	28180	1285	2545	2840	-21765	32765
8	43.06	990	1480	1765	-18330	24505	1140	1705	2035	-22060	29365	1290	1935	2305	-25785	34225
10	36.25	995	1185	1530	-21235	26040	1145	1370	1765	-25485	31245	1295	1550	2000	-29735	36450
12	32.04	970	975	1375	-22830	26010	1115	1125	1580	-27345	31220	1260	1275	1790	-31860	36430
14	29.32	930	815	1275	-23495	25285	1065	940	1465	-28045	30335	1200	1060	1655	-32630	35380
16	27.53	890	690	1165	-23770	24655	1015	795	1335	-28295	29525	1135	895	1505	-32815	34400
18	26.36	860	595	1070	-23970	24510	975	680	1220	-28445	29260	1090	770	1370	-32920	34010
20	25.63	860	520	1030	-24780	25375	970	595	1170	-29310	30270	1080	675	1310	-33840	35165
22	25.20	865	460	1000	-25935	26725	975	530	1135	-30445	31720	1085	595	1275	-34955	36710
24	25.02	880	415	990	-27325	28430	985	470	1120	-31940	33690	1095	530	1255	-36555	38950
25	25.00	885	390	985	-28060	29255	995	445	1115	-32720	34640	1100	500	1245	-37385	40020

Rise [T] (ft)	Radius [R] (ft)	Ground Snow Load [p_g]														
		80 psf					90 psf					100 psf				
		R_y lbs	R_x lbs	F_a lbs	M^- in-lb	M^+ in-lb	R_y lbs	R_x lbs	F_a lbs	M^- in-lb	M^+ in-lb	R_y lbs	R_x lbs	F_a lbs	M^- in-lb	M^+ in-lb
5	65.00	1430	3370	3645	-23325	38955	1580	3725	4030	-26385	43690	1730	4080	4415	-29440	48430
6	55.08	1435	2845	3170	-24985	37355	1585	3150	3505	-28200	41940	1735	3450	3840	-31420	46525
8	43.06	1440	2160	2575	-29510	39085	1590	2390	2845	-33240	43945	1740	2615	3120	-36965	48805
10	36.25	1450	1730	2235	-33980	41655	1600	1915	2465	-38230	46865	1750	2095	2700	-42480	52070
12	32.04	1400	1420	1995	-36380	41640	1545	1570	2200	-40895	46870	1690	1720	2410	-45410	52105
14	29.32	1335	1185	1845	-37220	40430	1465	1305	2035	-41810	45480	1600	1430	2225	-46395	50525
16	27.53	1260	1000	1675	-37340	39270	1385	1100	1845	-41860	44140	1505	1205	2015	-46385	49010
18	26.36	1205	855	1520	-37390	38760	1315	940	1670	-41865	43570	1430	1030	1820	-46335	48375
20	25.63	1190	750	1455	-38370	40055	1305	825	1595	-42895	44950	1415	900	1735	-47425	49845
22	25.20	1190	660	1410	-39555	41705	1300	730	1545	-44155	46700	1410	795	1685	-48755	51695
24	25.02	1205	590	1385	-41165	44210	1310	650	1520	-45780	49470	1420	710	1655	-50410	54735
25	25.00	1210	560	1380	-42050	45405	1320	615	1510	-46710	50790	1425	670	1645	-51375	56175

Table E-5 - 60 ft Span, Variable Snow Load.

10 psf Dead Load
20 psf Construction Load
120 mph Wind Zone

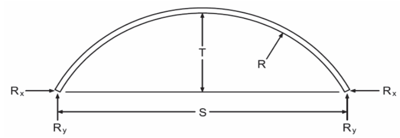

Notes:

All values normalized to $C_D = 1.0$.
Use ASD design procedure only.

Snow Load

$C_e = 0.9$
$C_t = 1.2$
$I_s = 1.10$

Wind Load

$K_{zt} = 1.0$
$K_d = 0.85$

Rise [T] (ft)	Radius [R] (ft)	Ground Snow Load [p_g] 15 psf					20 psf					25 psf				
		R_y lbs	R_x lbs	F_a lbs	M^- in-lb	M^+ in-lb	R_y lbs	R_x lbs	F_a lbs	M^- in-lb	M^+ in-lb	R_y lbs	R_x lbs	F_a lbs	M^- in-lb	M^+ in-lb
6	78.00	730	1740	1875	-5820	10970	730	1740	1875	-8095	14290	730	1740	1875	-10380	17610
8	60.25	735	1325	1505	-6790	9985	735	1325	1505	-9195	13180	735	1325	1505	-11625	16375
10	50.00	740	1065	1285	-8260	10580	740	1065	1285	-11025	14075	740	1065	1285	-13825	17590
12	43.50	745	890	1150	-9465	11025	745	890	1150	-12510	14740	745	890	1150	-15585	18455
14	39.14	755	760	1060	-10305	11055	755	760	1060	-13520	14785	755	760	1060	-16740	18515
16	36.13	765	665	995	-10860	10900	765	665	995	-14140	14530	765	665	995	-17420	18155
18	34.00	775	590	950	-11375	10850	775	590	950	-14570	14345	775	590	950	-17855	17840
20	32.50	790	525	920	-11885	11010	790	525	920	-15050	14370	790	525	920	-18215	17785
22	31.45	800	475	900	-12540	12040	800	475	900	-15685	14785	800	475	900	-18840	18215
24	30.75	815	430	885	-14400	14985	815	430	885	-16605	15620	815	430	885	-19800	19020
26	30.31	830	420	875	-17100	18505	830	420	875	-17775	18505	830	420	875	-20910	20180
28	30.07	845	450	865	-20050	23385	845	450	865	-20050	23385	845	450	865	-22350	23385
30	30.00	860	465	860	-23265	28560	860	465	860	-23265	28560	860	465	860	-23920	28560

Rise [T] (ft)	Radius [R] (ft)	Ground Snow Load [p_g] 30 psf					35 psf					40 psf				
		R_y lbs	R_x lbs	F_a lbs	M^- in-lb	M^+ in-lb	R_y lbs	R_x lbs	F_a lbs	M^- in-lb	M^+ in-lb	R_y lbs	R_x lbs	F_a lbs	M^- in-lb	M^+ in-lb
6	78.00	815	1940	2095	-12680	20925	905	2155	2325	-14985	24245	995	2370	2560	-17290	27565
8	60.25	820	1475	1675	-14055	19565	910	1640	1865	-16485	22760	1000	1805	2050	-18915	25955
10	50.00	825	1190	1435	-16620	21105	915	1320	1590	-19415	24620	1005	1450	1750	-22210	28135
12	43.50	835	990	1280	-18675	22175	925	1100	1420	-21765	25890	1015	1210	1560	-24855	29605
14	39.14	825	845	1165	-19955	22245	910	935	1290	-23210	25975	1000	1030	1415	-26470	29730
16	36.13	805	725	1100	-20695	21780	885	805	1220	-23975	25440	970	885	1335	-27255	29120
18	34.00	785	635	1035	-21135	21360	860	700	1140	-24420	24930	940	765	1250	-27700	28505
20	32.50	790	555	965	-21435	21265	840	615	1065	-24690	24745	910	670	1160	-27940	28230
22	31.45	800	495	920	-21995	21640	825	545	1005	-25150	25070	895	595	1095	-28360	28500
24	30.75	815	445	895	-22995	22420	830	490	980	-26190	25860	895	535	1065	-29380	29375
26	30.31	830	420	880	-24150	23735	840	445	960	-27390	27290	905	485	1045	-30625	30840
28	30.07	845	450	875	-25550	25190	850	450	955	-28860	28915	915	450	1030	-32165	32640
30	30.00	860	465	870	-27140	28560	865	465	945	-30375	30770	930	465	1025	-33735	34525

Table E-5 - 60 ft Span, Variable Snow Load.

10 psf Dead Load
20 psf Construction Load
120 mph Wind Zone

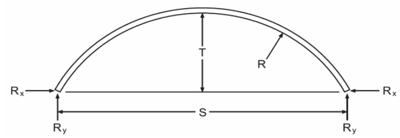

Notes:

All values normalized to $C_D = 1.0$.
Use ASD design procedure only.

Snow Load

$C_e = 0.9$
$C_t = 1.2$
$I_s = 1.10$

Wind Load

$K_{zt} = 1.0$
$K_d = 0.85$

Rise [T] (ft)	Radius [R] (ft)	Ground Snow Load [p_g] 50 psf R_y lbs	R_x lbs	F_a lbs	M^- in-lb	M^+ in-lb	60 psf R_y lbs	R_x lbs	F_a lbs	M^- in-lb	M^+ in-lb	70 psf R_y lbs	R_x lbs	F_a lbs	M^- in-lb	M^+ in-lb
6	78.00	1175	2805	3030	-21895	34200	1355	3240	3500	-26500	40840	1535	3675	3965	-31105	47475
8	60.25	1180	2135	2425	-23775	32340	1360	2460	2795	-28635	38725	1540	2790	3170	-33495	45115
10	50.00	1185	1715	2070	-27805	35165	1365	1980	2385	-33395	42195	1550	2240	2700	-38985	49225
12	43.50	1195	1430	1840	-31035	37040	1375	1650	2125	-37215	44475	1555	1865	2405	-43395	51905
14	39.14	1170	1215	1670	-32985	37265	1345	1395	1920	-39500	44795	1520	1580	2170	-46015	52330
16	36.13	1135	1040	1570	-33840	36485	1300	1195	1805	-40470	43845	1465	1355	2045	-47100	51210
18	34.00	1095	900	1465	-34270	35655	1245	1035	1680	-40835	42800	1400	1170	1895	-47400	49950
20	32.50	1055	790	1355	-34445	35190	1195	905	1550	-40950	42155	1340	1020	1745	-47455	49120
22	31.45	1030	700	1275	-34830	35355	1165	800	1455	-41305	42210	1305	900	1630	-47775	49065
24	30.75	1030	625	1235	-35785	36400	1165	715	1405	-42320	43430	1295	810	1575	-48855	50460
26	30.31	1035	565	1205	-37105	37950	1165	645	1370	-43585	45060	1300	730	1530	-50130	52170
28	30.07	1045	515	1190	-38775	40090	1180	590	1350	-45390	47540	1310	660	1510	-52000	54990
30	30.00	1060	470	1180	-40460	42035	1190	535	1340	-47180	49780	1320	600	1495	-53905	57520

Rise [T] (ft)	Radius [R] (ft)	Ground Snow Load [p_g] 80 psf R_y lbs	R_x lbs	F_a lbs	M^- in-lb	M^+ in-lb	90 psf R_y lbs	R_x lbs	F_a lbs	M^- in-lb	M^+ in-lb	100 psf R_y lbs	R_x lbs	F_a lbs	M^- in-lb	M^+ in-lb
6	78.00	1715	4105	4435	-35715	54110	1895	4540	4900	-40320	60750	2080	4975	5370	-44925	67385
8	60.25	1720	3120	3545	-38355	51500	1905	3450	3915	-43215	57890	2085	3775	4290	-48075	64275
10	50.00	1730	2505	3020	-44580	56260	1910	2770	3335	-50170	63290	2090	3030	3655	-55765	70320
12	43.50	1735	2085	2685	-49580	59340	1915	2305	2965	-55760	66770	2100	2525	3245	-61940	74205
14	39.14	1695	1765	2425	-52535	59860	1870	1950	2675	-59050	67390	2045	2135	2925	-65565	74925
16	36.13	1630	1510	2280	-53730	58575	1795	1670	2515	-60360	65935	1955	1825	2750	-66990	73300
18	34.00	1555	1305	2115	-53980	57100	1710	1440	2330	-60600	64245	1865	1575	2545	-67225	71395
20	32.50	1485	1135	1940	-53965	56080	1630	1255	2135	-60470	63045	1770	1370	2330	-66975	70010
22	31.45	1440	1005	1810	-54245	55920	1575	1105	1990	-60720	62780	1710	1205	2165	-67190	69635
24	30.75	1430	900	1745	-55390	57490	1565	990	1915	-61925	64515	1695	1080	2085	-68460	71545
26	30.31	1430	810	1695	-56745	59275	1560	890	1860	-63355	66385	1690	975	2025	-69970	73495
28	30.07	1440	735	1675	-58615	62440	1570	810	1835	-65275	69890	1700	885	1995	-72010	77340
30	30.00	1450	670	1655	-60625	65265	1580	735	1815	-67350	73005	1710	805	1975	-74070	80750

Table E-6 - 70 ft Span, Variable Snow Load.

15 psf Dead Load
20 psf Construction Load
120 mph Wind Zone

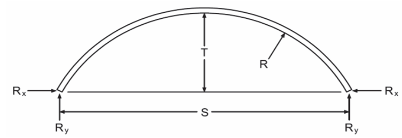

Notes:

All values normalized to C_D = 1.0.
Use ASD design procedure only.

Snow Load

C_e = 0.9
C_t = 1.2
I_s = 1.10

Wind Load

K_{zt} = 1.0
K_d = 0.85

Rise [T]	Radius [R]	Ground Snow Load [p_g]														
		15 psf					20 psf					25 psf				
(ft)	(ft)	R_y lbs	R_x lbs	F_a lbs	M^- in-lb	M^+ in-lb	R_y lbs	R_x lbs	F_a lbs	M^- in-lb	M^+ in-lb	R_y lbs	R_x lbs	F_a lbs	M^- in-lb	M^+ in-lb
6	105.08	990	2760	2925	-7125	15735	990	2760	2925	-10210	20265	995	2775	2940	-13295	24795
8	80.56	995	2105	2320	-8765	14080	995	2105	2320	-12010	18455	1000	2115	2330	-15270	22825
10	66.25	1005	1695	1960	-10085	13585	1005	1695	1960	-13535	18005	1010	1705	1970	-17000	22440
12	57.04	1015	1420	1730	-11835	14255	1015	1420	1730	-15680	19005	1020	1425	1740	-19525	23755
14	50.75	1025	1220	1575	-13335	14665	1025	1220	1575	-17505	19695	1035	1225	1585	-21675	24730
16	46.28	1040	1065	1470	-14485	14780	1040	1065	1470	-18855	19825	1040	1070	1470	-23230	24865
18	43.03	1055	950	1390	-15490	14755	1055	950	1390	-19830	19675	1055	950	1395	-24300	24595
20	40.63	1070	850	1340	-16385	14845	1070	850	1340	-20740	19580	1070	850	1340	-25095	24320
22	38.84	1085	770	1300	-17270	15160	1085	770	1300	-21595	19670	1085	770	1300	-25930	24375
24	37.52	1105	705	1270	-18370	15740	1105	705	1270	-22480	20205	1105	705	1270	-26775	24785
26	36.56	1125	645	1250	-19790	16795	1125	645	1250	-23895	21230	1125	645	1250	-28055	25670
28	35.88	1145	625	1235	-22715	20055	1145	625	1235	-25615	22550	1145	625	1235	-29765	27170
30	35.42	1165	640	1230	-26410	24065	1165	640	1230	-27555	24230	1165	640	1230	-31760	28740
32	35.14	1185	655	1225	-30425	28735	1185	655	1225	-30425	28735	1185	655	1225	-34075	31035
34	35.01	1210	695	1220	-34765	35465	1210	695	1220	-34765	35465	1210	695	1220	-36560	35465
35	35.00	1220	710	1220	-37060	38615	1220	710	1220	-37060	38615	1220	710	1220	-37900	38615

Rise [T]	Radius [R]	Ground Snow Load [p_g]														
		30 psf					35 psf					40 psf				
(ft)	(ft)	R_y lbs	R_x lbs	F_a lbs	M^- in-lb	M^+ in-lb	R_y lbs	R_x lbs	F_a lbs	M^- in-lb	M^+ in-lb	R_y lbs	R_x lbs	F_a lbs	M^- in-lb	M^+ in-lb
6	105.08	1100	3070	3250	-16385	29325	1205	3365	3565	-19490	33855	1310	3660	3875	-22615	38385
8	80.56	1105	2340	2575	-18555	27195	1215	2565	2820	-21845	31565	1320	2785	3070	-25130	35940
10	66.25	1115	1885	2175	-20495	26875	1220	2065	2385	-23995	31310	1325	2245	2590	-27490	35745
12	57.04	1125	1575	1920	-23420	28540	1230	1725	2105	-27320	33345	1340	1875	2285	-31225	38150
14	50.75	1140	1355	1750	-25850	29760	1245	1480	1915	-30065	34795	1350	1610	2080	-34300	39825
16	46.28	1135	1180	1615	-27600	29910	1240	1290	1765	-31975	34955	1340	1400	1915	-36345	40020
18	43.03	1120	1040	1540	-28765	29530	1220	1135	1680	-33235	34565	1320	1230	1820	-37700	39600
20	40.63	1110	920	1465	-29580	29220	1200	1005	1595	-34070	34120	1295	1090	1730	-38560	39020
22	38.84	1095	825	1395	-30265	29115	1180	900	1515	-34645	33855	1270	970	1635	-39110	38600
24	37.52	1105	740	1325	-31065	29365	1165	810	1435	-35360	33945	1245	875	1545	-39655	38525
26	36.56	1125	675	1290	-32365	30240	1165	735	1390	-36675	34915	1245	790	1495	-40985	39595
28	35.88	1145	625	1265	-33970	31790	1180	670	1365	-38320	36405	1255	725	1465	-42675	41025
30	35.42	1165	640	1255	-35960	33540	1195	640	1350	-40195	38340	1270	665	1445	-44600	43140
32	35.14	1185	655	1250	-38355	35765	1215	655	1345	-42640	40495	1290	655	1435	-46925	45480
34	35.01	1210	695	1250	-40910	38395	1240	695	1340	-45265	43370	1315	695	1430	-49615	48350
35	35.00	1220	710	1250	-42290	39765	1250	710	1340	-46680	44870	1325	710	1430	-51070	49970

Table E-6 - 70 ft Span, Variable Snow Load.

15 psf Dead Load
20 psf Construction Load
120 mph Wind Zone

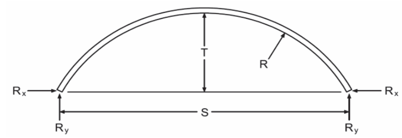

Notes:

All values normalized to C_D = 1.0.
Use ASD design procedure only.

Snow Load

C_e = 0.9
C_t = 1.2
I_s = 1.10

Wind Load

K_{zt} = 1.0
K_d = 0.85

Rise [T] (ft)	Radius [R] (ft)	Ground Snow Load [p_g] 50 psf					60 psf					70 psf				
		R_y lbs	R_x lbs	F_a lbs	M^- in-lb	M^+ in-lb	R_y lbs	R_x lbs	F_a lbs	M^- in-lb	M^+ in-lb	R_y lbs	R_x lbs	F_a lbs	M^- in-lb	M^+ in-lb
6	105.08	1520	4250	4505	-28860	47445	1735	4840	5130	-35105	56505	1945	5435	5755	-41355	65565
8	80.56	1530	3235	3565	-31705	44680	1740	3685	4055	-38285	53425	1950	4135	4550	-44860	62165
10	66.25	1540	2605	3005	-34490	44620	1750	2965	3420	-41485	53490	1960	3325	3835	-48480	62360
12	57.04	1550	2175	2650	-39030	47760	1760	2475	3010	-46835	57375	1970	2775	3375	-54640	66985
14	50.75	1560	1865	2405	-42765	49890	1770	2120	2735	-51230	59955	1985	2375	3060	-59695	70020
16	46.28	1545	1620	2210	-45195	50240	1750	1840	2510	-54060	60460	1955	2065	2805	-62920	70685
18	43.03	1515	1420	2100	-46635	49670	1710	1615	2380	-55585	59740	1905	1805	2660	-64625	69810
20	40.63	1480	1260	1990	-47540	48815	1665	1425	2250	-56520	58615	1850	1595	2515	-65500	68415
22	38.84	1445	1120	1875	-48035	48080	1620	1265	2120	-56960	57565	1795	1415	2360	-65885	67050
24	37.52	1410	1005	1765	-48380	47720	1575	1135	1985	-57205	57125	1740	1265	2205	-66025	66530
26	36.56	1405	910	1700	-49605	48950	1565	1025	1910	-58290	58300	1720	1145	2115	-67130	67655
28	35.88	1410	830	1665	-51380	50270	1565	935	1860	-60085	59820	1720	1040	2060	-68790	69375
30	35.42	1425	760	1635	-53405	52740	1580	860	1825	-62210	62335	1730	955	2020	-71015	71935
32	35.14	1445	700	1625	-55860	55480	1595	790	1810	-64815	65480	1750	880	1995	-73770	75475
34	35.01	1465	695	1610	-58405	58305	1615	730	1795	-67490	68425	1770	810	1975	-76575	78775
35	35.00	1480	710	1610	-59845	60180	1630	710	1790	-68935	70385	1780	780	1970	-78090	80595

Rise [T] (ft)	Radius [R] (ft)	Ground Snow Load [p_g] 80 psf					90 psf					100 psf				
		R_y lbs	R_x lbs	F_a lbs	M^- in-lb	M^+ in-lb	R_y lbs	R_x lbs	F_a lbs	M^- in-lb	M^+ in-lb	R_y lbs	R_x lbs	F_a lbs	M^- in-lb	M^+ in-lb
6	105.08	2155	6025	6380	-47600	74625	2365	6615	7005	-53850	83685	2575	7205	7630	-60095	92745
8	80.56	2160	4580	5045	-51435	70910	2375	5030	5540	-58010	79650	2585	5480	6030	-64585	88395
10	66.25	2170	3685	4250	-55480	71230	2380	4045	4665	-62475	80105	2595	4405	5080	-69470	88975
12	57.04	2180	3075	3740	-62445	76595	2390	3375	4100	-70250	86205	2605	3675	4465	-78055	95815
14	50.75	2195	2635	3390	-68160	80085	2405	2890	3720	-76625	90150	2615	3145	4045	-85090	100215
16	46.28	2160	2285	3105	-71785	80905	2365	2505	3400	-80650	91130	2570	2725	3700	-89515	101350
18	43.03	2100	1995	2940	-73665	79880	2295	2190	3225	-82705	89950	2490	2380	3505	-91745	100020
20	40.63	2035	1760	2775	-74480	78215	2220	1930	3040	-83475	88015	2405	2095	3300	-92540	97815
22	38.84	1965	1560	2600	-74815	76535	2140	1710	2845	-83740	86015	2315	1855	3085	-92665	95500
24	37.52	1905	1395	2425	-74845	75935	2065	1525	2645	-83665	85340	2230	1655	2865	-92490	94745
26	36.56	1880	1260	2320	-75965	77010	2040	1375	2530	-84805	86365	2195	1495	2735	-93640	95720
28	35.88	1880	1145	2255	-77635	78925	2035	1255	2455	-86545	88480	2190	1360	2655	-95450	98030
30	35.42	1885	1050	2210	-79820	81535	2040	1145	2400	-88625	91135	2190	1245	2590	-97560	100735
32	35.14	1900	965	2180	-82725	85475	2055	1055	2370	-91680	95470	2205	1145	2560	-100640	105470
34	35.01	1920	890	2160	-85660	89130	2070	975	2345	-94750	99480	2225	1055	2530	-103835	109830
35	35.00	1930	855	2155	-87245	90980	2085	935	2340	-96405	101510	2235	1015	2525	-105560	112040

Table E-7 - 80 ft Span, Variable Snow Load.

15 psf Dead Load
20 psf Construction Load
120 mph Wind Zone

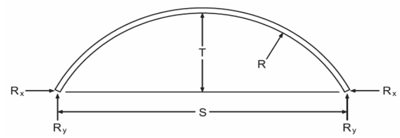

Notes:

All values normalized to $C_D = 1.0$.
Use ASD design procedure only.

Snow Load

$C_e = 0.9$
$C_t = 1.2$
$I_s = 1.10$

Wind Load

$K_{zt} = 1.0$
$K_d = 0.85$

Rise [T] (ft)	Radius [R] (ft)	Ground Snow Load [p_g]														
		15 psf					20 psf					25 psf				
		R_y lbs	R_x lbs	F_a lbs	M^- in-lb	M^+ in-lb	R_y lbs	R_x lbs	F_a lbs	M^- in-lb	M^+ in-lb	R_y lbs	R_x lbs	F_a lbs	M^- in-lb	M^+ in-lb
8	104.00	1135	2750	2960	-11280	18570	1135	2750	2960	-15495	24300	1140	2760	2975	-19775	30030
12	72.67	1150	1855	2165	-14120	17620	1150	1855	2165	-18795	23495	1160	1865	2175	-23520	29395
16	58.00	1170	1395	1800	-17615	18935	1170	1395	1800	-23085	25485	1180	1405	1815	-28555	32035
20	50.00	1200	1115	1610	-20025	19115	1200	1115	1610	-25740	25505	1200	1115	1615	-31565	31985
24	45.33	1230	925	1505	-22045	19345	1230	925	1505	-27730	25500	1230	925	1505	-33415	31680
28	42.57	1265	785	1445	-24415	20760	1265	785	1445	-29735	26435	1265	785	1445	-35315	32420
32	41.00	1305	710	1415	-29710	27045	1305	710	1415	-33495	29375	1305	710	1415	-38920	35405
36	40.22	1350	740	1400	-38420	37090	1350	740	1400	-38420	37090	1350	740	1400	-43745	39680
40	40.00	1395	805	1395	-48430	52060	1395	805	1395	-48430	52060	1395	805	1395	-49530	52060

Rise [T] (ft)	Radius [R] (ft)	Ground Snow Load [p_g]														
		30 psf					35 psf					40 psf				
		R_y lbs	R_x lbs	F_a lbs	M^- in-lb	M^+ in-lb	R_y lbs	R_x lbs	F_a lbs	M^- in-lb	M^+ in-lb	R_y lbs	R_x lbs	F_a lbs	M^- in-lb	M^+ in-lb
8	104.00	1260	3055	3290	-24050	35760	1380	3345	3610	-28330	41485	1500	3640	3925	-32605	47215
12	72.67	1280	2060	2405	-28265	35290	1400	2255	2635	-33010	41185	1520	2450	2865	-37755	47085
16	58.00	1300	1550	2000	-34025	38590	1420	1695	2190	-39575	45140	1540	1840	2375	-45125	51690
20	50.00	1285	1225	1780	-37390	38560	1400	1340	1940	-43210	45135	1510	1450	2105	-49035	51705
24	45.33	1260	995	1635	-39150	37865	1360	1085	1775	-45010	44045	1465	1175	1920	-50870	50225
28	42.57	1265	825	1495	-40905	38410	1325	900	1620	-46500	44395	1420	970	1740	-52095	50385
32	41.00	1305	710	1450	-44425	41430	1345	765	1560	-50115	47455	1435	825	1675	-55805	53480
36	40.22	1350	740	1430	-49315	45765	1380	740	1535	-54880	52075	1470	740	1645	-60515	58535
40	40.00	1395	805	1430	-55265	52060	1430	805	1530	-61000	58540	1515	805	1635	-66735	65205

Table E-7 - 80 ft Span, Variable Snow Load.

15 psf Dead Load
20 psf Construction Load
120 mph Wind Zone

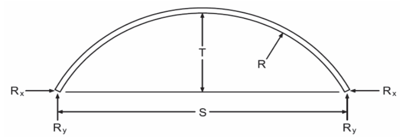

Notes:

All values normalized to C_D = 1.0.
Use ASD design procedure only.

Snow Load

C_e = 0.9
C_t = 1.2
I_s = 1.10

Wind Load

K_{zt} = 1.0
K_d = 0.85

Rise [T] (ft)	Radius [R] (ft)	Ground Snow Load [p_g] 50 psf					60 psf					70 psf				
		R_y lbs	R_x lbs	F_a lbs	M^- in-lb	M^+ in-lb	R_y lbs	R_x lbs	F_a lbs	M^- in-lb	M^+ in-lb	R_y lbs	R_x lbs	F_a lbs	M^- in-lb	M^+ in-lb
8	104.00	1745	4230	4555	-41160	58675	1985	4815	5190	-49715	70135	2225	5400	5820	-58270	81595
12	72.67	1760	2845	3320	-47245	58880	2000	3240	3780	-56735	70670	2240	3630	4240	-66225	82465
16	58.00	1785	2135	2750	-56225	64795	2025	2430	3125	-67325	77895	2265	2720	3500	-78425	90995
20	50.00	1740	1680	2430	-60680	64855	1965	1905	2755	-72440	78000	2190	2135	3080	-84230	91145
24	45.33	1670	1355	2210	-62590	62825	1875	1535	2495	-74305	75475	2080	1715	2785	-86025	88125
28	42.57	1605	1115	1985	-63375	62360	1790	1260	2230	-74860	74335	1970	1405	2475	-86345	86375
32	41.00	1610	950	1900	-67180	65550	1790	1070	2125	-78560	78010	1970	1190	2355	-89935	90475
36	40.22	1645	820	1855	-72165	71445	1820	920	2070	-83810	84360	1990	1025	2285	-95460	97275
40	40.00	1690	805	1840	-78205	78530	1860	805	2045	-90090	91855	2035	890	2255	-102050	105175

Rise [T] (ft)	Radius [R] (ft)	Ground Snow Load [p_g] 80 psf					90 psf					100 psf				
		R_y lbs	R_x lbs	F_a lbs	M^- in-lb	M^+ in-lb	R_y lbs	R_x lbs	F_a lbs	M^- in-lb	M^+ in-lb	R_y lbs	R_x lbs	F_a lbs	M^- in-lb	M^+ in-lb
8	104.00	2465	5990	6455	-66825	93055	2705	6575	7085	-75380	104515	2950	7165	7720	-83935	115975
12	72.67	2485	4025	4695	-75720	94260	2725	4415	5155	-85210	106055	2965	4810	5615	-94700	117850
16	58.00	2505	3015	3880	-89530	104100	2750	3305	4255	-100630	117200	2990	3600	4630	-111730	130305
20	50.00	2420	2360	3405	-96020	104295	2645	2585	3730	-107810	117440	2870	2815	4055	-119600	130590
24	45.33	2285	1895	3075	-97745	100775	2490	2075	3360	-109465	113425	2695	2255	3650	-121185	126080
28	42.57	2155	1550	2720	-97835	98590	2340	1695	2965	-109320	110805	2525	1840	3210	-120805	123025
32	41.00	2145	1310	2580	-101515	102935	2325	1435	2805	-113155	115400	2500	1555	3030	-124795	127865
36	40.22	2165	1130	2500	-107110	110190	2340	1230	2715	-118760	123100	2515	1335	2930	-130410	136015
40	40.00	2210	980	2465	-114015	118735	2380	1070	2675	-125980	132480	2555	1160	2885	-137940	146225

Table E-8 - 90 ft Span, Variable Snow Load.

15 psf Dead Load
20 psf Construction Load
120 mph Wind Zone

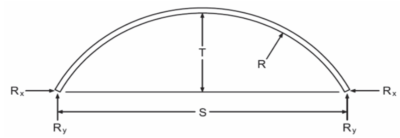

Notes:

All values normalized to C_D = 1.0.
Use ASD design procedure only.

Snow Load

C_e = 0.9
C_t = 1.2
I_s = 1.10

Wind Load

K_{zt} = 1.0
K_d = 0.85

Rise [T] (ft)	Radius [R] (ft)	Ground Snow Load [p_g]														
		15 psf					20 psf					25 psf				
		R_y lbs	R_x lbs	F_a lbs	M^- in-lb	M^+ in-lb	R_y lbs	R_x lbs	F_a lbs	M^- in-lb	M^+ in-lb	R_y lbs	R_x lbs	F_a lbs	M^- in-lb	M^+ in-lb
8	130.56	1275	3475	3690	-14125	23650	1275	3475	3690	-19480	30920	1280	3490	3710	-24880	38190
12	90.38	1290	2345	2660	-16530	21210	1290	2345	2660	-22105	28240	1295	2355	2675	-27740	35270
16	71.28	1305	1765	2175	-20670	23180	1305	1765	2175	-27210	31095	1315	1775	2190	-33765	39010
20	60.63	1330	1415	1915	-23920	24055	1330	1415	1915	-31130	32325	1330	1420	1920	-38340	40590
24	54.19	1360	1175	1765	-26310	23990	1360	1175	1765	-33500	32080	1360	1175	1770	-40900	40180
28	50.16	1390	1000	1675	-28520	24725	1390	1000	1675	-35710	32195	1390	1000	1675	-42895	40010
32	47.64	1430	870	1620	-31410	26545	1430	870	1620	-38155	33685	1430	870	1620	-45180	41215
36	46.13	1470	795	1590	-37635	35205	1470	795	1590	-42435	37115	1470	795	1590	-49300	44735
40	45.31	1515	825	1575	-47345	46650	1515	825	1575	-47615	46650	1515	825	1575	-54640	49395
42	45.11	1535	870	1570	-52685	55450	1535	870	1570	-52685	55450	1535	870	1570	-57760	55450
45	45.00	1570	900	1570	-61315	67755	1570	900	1570	-61315	67755	1570	900	1570	-62710	67755

Rise [T] (ft)	Radius [R] (ft)	Ground Snow Load [p_g]														
		30 psf					35 psf					40 psf				
		R_y lbs	R_x lbs	F_a lbs	M^- in-lb	M^+ in-lb	R_y lbs	R_x lbs	F_a lbs	M^- in-lb	M^+ in-lb	R_y lbs	R_x lbs	F_a lbs	M^- in-lb	M^+ in-lb
8	130.56	1415	3865	4105	-30280	45455	1550	4235	4495	-35680	52725	1685	4610	4890	-41080	59995
12	90.38	1430	2605	2955	-33375	42295	1565	2855	3240	-39015	49325	1700	3105	3520	-44650	56355
16	71.28	1450	1960	2420	-40405	46930	1585	2150	2645	-47045	54925	1720	2335	2875	-53680	62920
20	60.63	1460	1565	2115	-45550	48940	1595	1710	2310	-52760	57350	1730	1860	2505	-60040	65765
24	54.19	1435	1285	1945	-48325	48280	1560	1400	2120	-55750	56375	1685	1520	2300	-63180	64475
28	50.16	1410	1075	1800	-50080	47825	1520	1170	1960	-57415	55640	1635	1265	2115	-64815	63455
32	47.64	1430	915	1675	-52275	48825	1495	995	1810	-59370	56430	1595	1075	1950	-66465	64035
36	46.13	1470	795	1630	-56275	52355	1515	860	1755	-63480	59975	1615	930	1885	-70685	67600
40	45.31	1515	825	1610	-61660	57040	1550	825	1730	-68685	65140	1645	825	1850	-75875	73240
42	45.11	1535	870	1605	-64890	60450	1570	870	1725	-72020	68405	1670	870	1845	-79150	76355
45	45.00	1570	900	1605	-69970	67755	1605	900	1720	-77230	74040	1705	900	1840	-84490	82465

Table E-8 - 90 ft Span, Variable Snow Load.

15 psf Dead Load
20 psf Construction Load
120 mph Wind Zone

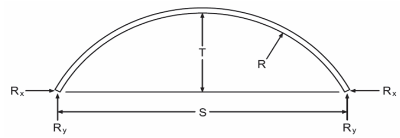

Notes:

All values normalized to C_D = 1.0.
Use ASD design procedure only.

Snow Load

C_e = 0.9
C_t = 1.2
I_s = 1.10

Wind Load

K_{zt} = 1.0
K_d = 0.85

Rise [T] (ft)	Radius [R] (ft)	Ground Snow Load [p_g]														
		50 psf					60 psf					70 psf				
		R_y lbs	R_x lbs	F_a lbs	M^- in-lb	M^+ in-lb	R_y lbs	R_x lbs	F_a lbs	M^- in-lb	M^+ in-lb	R_y lbs	R_x lbs	F_a lbs	M^- in-lb	M^+ in-lb
8	130.56	1960	5350	5680	-51875	74530	2230	6095	6470	-62675	89070	2500	6840	7260	-73470	103605
12	90.38	1975	3605	4085	-55925	70410	2245	4100	4650	-67195	84465	2515	4600	5215	-78470	98520
16	71.28	1995	2705	3330	-66960	78915	2265	3080	3790	-80240	94910	2535	3450	4245	-93520	110900
20	60.63	1995	2155	2895	-74665	82590	2260	2445	3290	-89290	99415	2525	2740	3680	-103910	116245
24	54.19	1930	1755	2650	-78030	80775	2175	1990	3005	-92880	97230	2425	2225	3360	-107830	113685
28	50.16	1860	1460	2430	-79615	79090	2085	1650	2745	-94420	94720	2310	1845	3055	-109225	110350
32	47.64	1805	1230	2220	-80685	79245	2010	1390	2495	-95250	94455	2215	1550	2765	-109815	109670
36	46.13	1815	1065	2140	-85090	82860	2015	1205	2390	-99500	98625	2215	1340	2645	-113905	114385
40	45.31	1845	935	2090	-90575	89445	2040	1055	2335	-105270	105650	2235	1170	2575	-119970	121855
42	45.11	1865	875	2080	-93885	93055	2060	990	2320	-108790	109780	2255	1100	2555	-123690	126500
45	45.00	1900	900	2070	-99015	99325	2095	900	2300	-114060	116180	2290	1000	2535	-129205	133035

Rise [T] (ft)	Radius [R] (ft)	Ground Snow Load [p_g]														
		80 psf					90 psf					100 psf				
		R_y lbs	R_x lbs	F_a lbs	M^- in-lb	M^+ in-lb	R_y lbs	R_x lbs	F_a lbs	M^- in-lb	M^+ in-lb	R_y lbs	R_x lbs	F_a lbs	M^- in-lb	M^+ in-lb
8	130.56	2770	7585	8050	-84270	118145	3040	8330	8840	-95070	132680	3315	9070	9630	-105865	147220
12	90.38	2785	5100	5780	-89745	112580	3055	5600	6345	-101015	126635	3330	6095	6910	-112290	140690
16	71.28	2805	3825	4700	-106795	126895	3080	4195	5160	-120075	142890	3350	4570	5615	-133355	158880
20	60.63	2790	3035	4070	-118535	133070	3060	3330	4465	-133160	149895	3325	3620	4855	-147785	166720
24	54.19	2670	2465	3715	-122850	130145	2920	2700	4065	-137870	146600	3165	2935	4420	-152895	163055
28	50.16	2540	2035	3370	-124025	126005	2765	2230	3685	-138830	141845	2990	2420	3995	-153630	157685
32	47.64	2420	1710	3040	-124380	124880	2630	1870	3310	-138940	140135	2835	2030	3585	-153505	155590
36	46.13	2415	1475	2900	-128575	130150	2615	1610	3155	-143315	145910	2815	1750	3410	-158060	161675
40	45.31	2430	1290	2815	-134670	138060	2630	1405	3060	-149370	154265	2825	1525	3305	-164065	170470
42	45.11	2450	1210	2795	-138595	143225	2645	1320	3035	-153495	159950	2845	1430	3280	-168400	176675
45	45.00	2485	1100	2770	-144350	150195	2680	1200	3005	-159495	167580	2875	1305	3245	-174645	184970

Table E-9 - 100 ft Span, Variable Snow Load.

15 psf Dead Load
20 psf Construction Load
120 mph Wind Zone

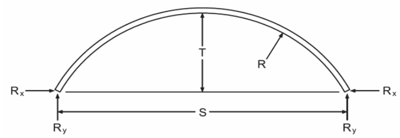

Notes:

All values normalized to C_D = 1.0.
Use ASD design procedure only.

Snow Load

C_e = 0.9
C_t = 1.2
I_s = 1.10

Wind Load

K_{zt} = 1.0
K_d = 0.85

Rise [T] (ft)	Radius [R] (ft)	Ground Snow Load [p_g] 15 psf					20 psf					25 psf				
		R_y lbs	R_x lbs	F_a lbs	M^- in-lb	M^+ in-lb	R_y lbs	R_x lbs	F_a lbs	M^- in-lb	M^+ in-lb	R_y lbs	R_x lbs	F_a lbs	M^- in-lb	M^+ in-lb
10	130.00	1420	3460	3725	-18985	27655	1420	3460	3725	-25805	36485	1425	3475	3740	-32625	45310
14	96.29	1435	2490	2855	-21500	26240	1435	2490	2855	-28610	35085	1440	2500	2865	-35790	43925
18	78.44	1455	1940	2400	-25940	28510	1455	1940	2400	-34085	38315	1465	1950	2415	-42255	48115
22	67.82	1475	1585	2140	-29505	29550	1475	1585	2140	-38395	39725	1475	1595	2145	-47285	49920
26	61.08	1505	1340	1980	-32165	29575	1505	1340	1980	-41085	39570	1505	1340	1985	-50255	49560
30	56.67	1535	1155	1880	-34595	30005	1535	1155	1880	-43490	39605	1535	1155	1880	-52390	49245
34	53.76	1575	1015	1820	-37450	31610	1575	1015	1820	-45935	40790	1575	1015	1820	-54730	50100
38	51.89	1610	895	1780	-41610	39160	1610	895	1780	-49980	43880	1610	895	1780	-58425	53035
42	50.76	1655	890	1755	-51695	50665	1655	890	1755	-55110	50665	1655	890	1755	-63665	57400
46	50.17	1700	920	1745	-63045	64980	1700	920	1745	-63045	64980	1700	920	1745	-70165	64980
50	50.00	1745	995	1745	-75720	85750	1745	995	1745	-75720	85750	1745	995	1745	-77440	85750

Rise [T] (ft)	Radius [R] (ft)	Ground Snow Load [p_g] 30 psf					35 psf					40 psf				
		R_y lbs	R_x lbs	F_a lbs	M^- in-lb	M^+ in-lb	R_y lbs	R_x lbs	F_a lbs	M^- in-lb	M^+ in-lb	R_y lbs	R_x lbs	F_a lbs	M^- in-lb	M^+ in-lb
10	130.00	1575	3845	4140	-39440	54140	1725	4215	4535	-46260	62965	1875	4585	4935	-53080	71790
14	96.29	1590	2765	3170	-42970	52770	1745	3030	3470	-50150	61610	1895	3290	3775	-57330	70455
18	78.44	1615	2155	2665	-50530	57920	1765	2360	2920	-58800	67795	1915	2565	3170	-67070	77695
22	67.82	1625	1760	2365	-56175	60290	1775	1925	2585	-65065	70660	1920	2090	2805	-74080	81030
26	61.08	1600	1465	2185	-59420	59550	1740	1605	2385	-68585	69655	1880	1740	2585	-77755	79860
30	56.67	1570	1245	2040	-61385	58880	1700	1360	2220	-70560	68520	1830	1470	2400	-79730	78155
34	53.76	1575	1070	1905	-63530	59405	1665	1165	2060	-72325	68715	1785	1260	2220	-81120	78020
38	51.89	1610	940	1830	-67275	62195	1670	1020	1975	-76125	71645	1780	1100	2120	-84975	81245
42	50.76	1655	890	1795	-72215	67060	1695	900	1935	-80995	76720	1805	975	2070	-89955	86380
46	50.17	1700	920	1785	-78930	73310	1740	920	1915	-87700	83000	1845	920	2050	-96470	93060
50	50.00	1745	995	1785	-86410	85750	1785	995	1915	-95375	91360	1895	995	2040	-104340	101760

Table E-9 - 100 ft Span, Variable Snow Load.

15 psf Dead Load
20 psf Construction Load
120 mph Wind Zone

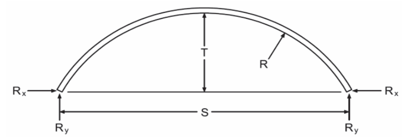

Notes:

All values normalized to C_D = 1.0.
Use ASD design procedure only.

Snow Load

C_e = 0.9
C_t = 1.2
I_s = 1.10

Wind Load

K_{zt} = 1.0
K_d = 0.85

Rise [T] (ft)	Radius [R] (ft)	Ground Snow Load [p_g]														
		50 psf					60 psf					70 psf				
		R_y lbs	R_x lbs	F_a lbs	M^- in-lb	M^+ in-lb	R_y lbs	R_x lbs	F_a lbs	M^- in-lb	M^+ in-lb	R_y lbs	R_x lbs	F_a lbs	M^- in-lb	M^+ in-lb
10	130.00	2180	5325	5730	-66715	89445	2480	6060	6525	-80355	107100	2780	6800	7320	-93990	124755
14	96.29	2195	3820	4380	-71690	88140	2495	4350	4985	-86050	105820	2795	4880	5590	-100410	123505
18	78.44	2215	2975	3675	-83615	97495	2515	3380	4175	-100155	117290	2820	3790	4680	-116700	137090
22	67.82	2220	2420	3240	-92120	101770	2515	2750	3680	-110155	122510	2810	3080	4120	-128190	143250
26	61.08	2155	2010	2985	-96085	100270	2435	2280	3385	-114465	120680	2710	2550	3785	-133020	141090
30	56.67	2085	1695	2760	-98075	97815	2345	1920	3120	-116420	117540	2600	2145	3480	-134765	137265
34	53.76	2020	1450	2540	-99100	97025	2255	1640	2855	-117180	116190	2490	1825	3175	-135260	135355
38	51.89	2010	1265	2415	-102670	100445	2235	1425	2705	-120370	119640	2460	1590	2995	-138485	138840
42	50.76	2025	1115	2345	-107880	105700	2245	1255	2620	-125805	125020	2465	1400	2900	-143725	144340
46	50.17	2065	995	2315	-114730	113520	2280	1120	2580	-133060	133975	2500	1245	2845	-151395	154435
50	50.00	2110	995	2300	-122270	122565	2325	1000	2555	-140855	143370	2545	1110	2815	-159555	164175

Rise [T] (ft)	Radius [R] (ft)	Ground Snow Load [p_g]														
		80 psf					90 psf					100 psf				
		R_y lbs	R_x lbs	F_a lbs	M^- in-lb	M^+ in-lb	R_y lbs	R_x lbs	F_a lbs	M^- in-lb	M^+ in-lb	R_y lbs	R_x lbs	F_a lbs	M^- in-lb	M^+ in-lb
10	130.00	3080	7540	8120	-107630	142410	3385	8280	8915	-121265	160060	3685	9020	9710	-134905	177715
14	96.29	3100	5405	6195	-114770	141190	3400	5935	6800	-129130	158875	3700	6465	7405	-143490	176560
18	78.44	3120	4200	5185	-133240	156890	3420	4610	5690	-149785	176690	3725	5020	6190	-166330	196490
22	67.82	3105	3410	4560	-146225	163990	3405	3740	4995	-164265	184730	3700	4070	5435	-182300	205470
26	61.08	2990	2820	4180	-151575	161505	3270	3090	4580	-170125	181915	3545	3360	4980	-188680	202325
30	56.67	2855	2370	3840	-153110	156990	3115	2595	4200	-171455	176715	3370	2820	4560	-189800	196440
34	53.76	2725	2015	3490	-153340	154520	2965	2205	3810	-171420	173685	3200	2390	4125	-189500	192850
38	51.89	2685	1750	3290	-156620	158035	2910	1910	3580	-174755	177235	3135	2075	3870	-192890	196430
42	50.76	2685	1540	3175	-161650	163660	2905	1680	3450	-179740	182980	3125	1825	3725	-198055	202600
46	50.17	2715	1370	3110	-169730	174890	2935	1495	3380	-188065	195345	3150	1620	3650	-206395	215805
50	50.00	2760	1225	3080	-178255	185350	2975	1335	3340	-196960	206810	3195	1450	3605	-215660	228270

Table E-10 - 110 ft Span, Variable Snow Load.

20 psf Dead Load
20 psf Construction Load
120 mph Wind Zone

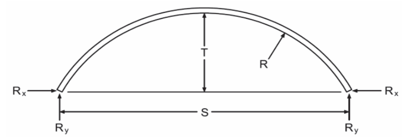

Notes:

All values normalized to $C_D = 1.0$.
Use ASD design procedure only.

Snow Load

$C_e = 0.9$
$C_t = 1.2$
$I_s = 1.10$

Wind Load

$K_{zt} = 1.0$
$K_d = 0.85$

Rise [T] (ft)	Radius [R] (ft)	Ground Snow Load [p_g] 15 psf					20 psf					25 psf				
		R_y lbs	R_x lbs	F_a lbs	M^- in-lb	M^+ in-lb	R_y lbs	R_x lbs	F_a lbs	M^- in-lb	M^+ in-lb	R_y lbs	R_x lbs	F_a lbs	M^- in-lb	M^+ in-lb
10	156.25	1780	4785	5090	-22260	34170	1780	4785	5090	-30435	44870	1810	4855	5165	-38670	55570
14	115.04	1800	3445	3865	-25100	31290	1800	3445	3865	-33425	41760	1830	3495	3925	-41860	52230
18	93.03	1825	2690	3225	-29955	33045	1825	2690	3225	-39335	44390	1855	2730	3275	-48715	55745
22	79.75	1855	2205	2850	-34785	34785	1855	2205	2850	-45185	46890	1885	2240	2895	-55585	59210
26	71.17	1890	1865	2615	-38895	35440	1890	1865	2615	-49485	47395	1890	1885	2645	-60420	59795
30	65.42	1930	1615	2465	-42450	36115	1930	1615	2465	-53220	47655	1930	1620	2500	-63990	59405
34	61.49	1970	1420	2370	-46470	37835	1970	1420	2370	-56770	48870	1970	1420	2370	-67520	59965
38	58.80	2020	1265	2310	-51070	40980	2020	1265	2310	-61160	51490	2020	1265	2310	-71250	62250
42	57.01	2070	1175	2275	-57700	46955	2070	1175	2275	-67435	56210	2070	1175	2275	-77645	67315
46	55.88	2130	1215	2260	-70485	59420	2130	1215	2260	-74745	62605	2130	1215	2260	-85085	73390
50	55.25	2185	1260	2250	-84795	74595	2185	1260	2250	-84795	74595	2185	1260	2250	-94060	81705
55	55.00	2265	1360	2260	-104925	102015	2265	1360	2260	-104925	102015	2265	1360	2260	-107170	102015

Rise [T] (ft)	Radius [R] (ft)	Ground Snow Load [p_g] 30 psf					35 psf					40 psf				
		R_y lbs	R_x lbs	F_a lbs	M^- in-lb	M^+ in-lb	R_y lbs	R_x lbs	F_a lbs	M^- in-lb	M^+ in-lb	R_y lbs	R_x lbs	F_a lbs	M^- in-lb	M^+ in-lb
10	156.25	1975	5305	5645	-46900	66275	2140	5750	6120	-55135	76975	2305	6200	6595	-63365	87675
14	115.04	1995	3815	4285	-50320	62700	2160	4140	4640	-58780	73165	2325	4460	5000	-67235	83635
18	93.03	2020	2980	3570	-58180	67255	2185	3230	3865	-67705	78770	2350	3475	4165	-77235	90280
22	79.75	2050	2440	3155	-65980	71530	2220	2645	3415	-76380	83850	2385	2845	3670	-86865	96175
26	71.17	2050	2055	2875	-71370	72190	2210	2220	3105	-82325	84590	2370	2390	3335	-93280	96985
30	65.42	2035	1760	2710	-74850	71470	2185	1900	2925	-85970	83535	2330	2040	3135	-97095	95600
34	61.49	2020	1525	2560	-78275	71620	2155	1645	2755	-89025	83280	2295	1765	2945	-99780	94935
38	58.80	2020	1340	2420	-81785	73530	2135	1440	2590	-92400	84805	2265	1540	2765	-103020	96085
42	57.01	2070	1190	2360	-87855	78420	2160	1280	2520	-98230	89525	2285	1370	2680	-108950	100630
46	55.88	2130	1215	2330	-95430	84425	2205	1215	2480	-105770	96085	2325	1225	2635	-116110	107740
50	55.25	2185	1260	2325	-104630	93300	2260	1260	2470	-115200	104895	2380	1260	2615	-125770	116495
55	55.00	2265	1360	2335	-117730	105390	2340	1360	2475	-128580	117975	2460	1360	2615	-139430	130555

Table E-10 - 110 ft Span, Variable Snow Load.

20 psf Dead Load
20 psf Construction Load
120 mph Wind Zone

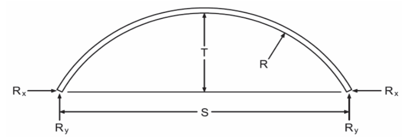

Notes:

All values normalized to C_D = 1.0.
Use ASD design procedure only.

Snow Load

C_e = 0.9
C_t = 1.2
I_s = 1.10

Wind Load

K_{zt} = 1.0
K_d = 0.85

Rise [T] (ft)	Radius [R] (ft)	Ground Snow Load [p_g]														
		50 psf					60 psf					70 psf				
		R_y lbs	R_x lbs	F_a lbs	M^- in-lb	M^+ in-lb	R_y lbs	R_x lbs	F_a lbs	M^- in-lb	M^+ in-lb	R_y lbs	R_x lbs	F_a lbs	M^- in-lb	M^+ in-lb
10	156.25	2635	7095	7545	-79830	109080	2970	7990	8500	-96295	130485	3300	8885	9450	-112760	151885
14	115.04	2655	5100	5720	-84155	104575	2990	5740	6435	-101070	125510	3320	6380	7155	-117990	146450
18	93.03	2685	3975	4755	-96295	113300	3015	4470	5350	-115355	136320	3345	4965	5940	-134415	159340
22	79.75	2715	3250	4190	-107980	120815	3045	3655	4705	-129100	145455	3380	4055	5220	-150215	170100
26	71.17	2685	2725	3790	-115185	121780	3005	3060	4250	-137205	146575	3325	3395	4710	-159410	171370
30	65.42	2630	2320	3560	-119335	119735	2930	2600	3990	-141575	143870	3230	2880	4415	-163820	168000
34	61.49	2575	2000	3330	-121865	118250	2850	2240	3715	-144015	141565	3130	2475	4100	-166170	164880
38	58.80	2520	1745	3105	-124255	118640	2775	1945	3450	-145535	141190	3035	2150	3790	-167350	163745
42	57.01	2530	1545	3000	-130390	123515	2780	1725	3320	-151830	146775	3025	1900	3640	-173275	170035
46	55.88	2565	1380	2935	-137545	131050	2810	1540	3240	-159220	154360	3050	1695	3545	-180895	177670
50	55.25	2620	1260	2910	-146910	140335	2860	1385	3205	-168740	164880	3095	1525	3495	-190850	189430
55	55.00	2695	1360	2900	-161130	155725	2935	1360	3180	-182830	180890	3170	1360	3465	-204655	206060

Rise [T] (ft)	Radius [R] (ft)	Ground Snow Load [p_g]														
		80 psf					90 psf					100 psf				
		R_y lbs	R_x lbs	F_a lbs	M^- in-lb	M^+ in-lb	R_y lbs	R_x lbs	F_a lbs	M^- in-lb	M^+ in-lb	R_y lbs	R_x lbs	F_a lbs	M^- in-lb	M^+ in-lb
10	156.25	3630	9780	10405	-129225	173290	3965	10675	11355	-145690	194695	4295	11575	12305	-162160	216095
14	115.04	3650	7020	7870	-134905	167385	3985	7660	8590	-151820	188325	4315	8300	9310	-168740	209260
18	93.03	3675	5460	6535	-153475	182365	4010	5960	7125	-172530	205385	4340	6455	7720	-191590	228405
22	79.75	3710	4460	5740	-171330	194740	4040	4865	6255	-192445	219380	4370	5265	6775	-213565	244025
26	71.17	3640	3725	5170	-181615	196165	3960	4060	5630	-203820	221100	4280	4395	6090	-226025	246105
30	65.42	3525	3160	4840	-186060	192135	3825	3440	5265	-208300	216265	4125	3720	5690	-230735	240595
34	61.49	3405	2710	4490	-188320	188200	3680	2950	4875	-210475	211515	3960	3185	5260	-232625	235160
38	58.80	3290	2350	4135	-189160	186770	3545	2555	4475	-210975	209880	3800	2755	4820	-232790	232985
42	57.01	3275	2080	3960	-194715	193300	3520	2255	4280	-216590	216560	3770	2435	4600	-238560	239820
46	55.88	3295	1855	3850	-202570	200980	3535	2010	4150	-224245	224295	3775	2165	4455	-245925	247605
50	55.25	3335	1665	3790	-212955	213980	3575	1805	4085	-235065	238525	3815	1945	4375	-257170	263075
55	55.00	3410	1465	3745	-227285	231225	3650	1590	4035	-249920	256395	3885	1710	4320	-272555	281640

Table E-11 - 120 ft Span, Variable Snow Load.

20 psf Dead Load
20 psf Construction Load
120 mph Wind Zone

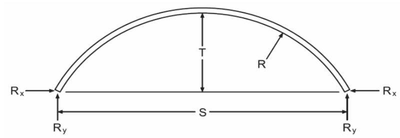

Notes:

All values normalized to $C_D = 1.0$.
Use ASD design procedure only.

Snow Load

$C_e = 0.9$
$C_t = 1.2$
$I_s = 1.10$

Wind Load

$K_{zt} = 1.0$
$K_d = 0.85$

Rise [T] (ft)	Radius [R] (ft)	Ground Snow Load [p_g] 15 psf					20 psf					25 psf				
		R_y lbs	R_x lbs	F_a lbs	M^- in-lb	M^+ in-lb	R_y lbs	R_x lbs	F_a lbs	M^- in-lb	M^+ in-lb	R_y lbs	R_x lbs	F_a lbs	M^- in-lb	M^+ in-lb
12	156.00	1950	4765	5130	-28090	39060	1950	4765	5130	-37985	51670	1975	4840	5205	-47910	64285
16	120.50	1965	3595	4075	-30650	36445	1965	3595	4075	-40615	48840	2000	3650	4135	-50705	61235
20	100.00	1990	2885	3475	-36370	39310	1990	2885	3475	-47665	52910	2025	2930	3530	-58955	66515
24	87.00	2020	2405	3105	-41550	41220	2020	2405	3105	-53940	55620	2060	2445	3160	-66325	70270
28	78.29	2055	2060	2870	-46040	42005	2055	2060	2870	-58655	56360	2065	2085	2900	-71670	71105
32	72.25	2095	1800	2715	-49910	42685	2095	1800	2715	-62720	56370	2095	1810	2750	-75530	70730
36	68.00	2140	1600	2610	-54100	44340	2140	1600	2610	-66575	57375	2140	1600	2615	-79400	71175
40	65.00	2185	1430	2540	-58970	47345	2185	1430	2540	-71050	59875	2185	1430	2540	-83350	73235
44	62.91	2235	1290	2495	-64855	51715	2235	1290	2495	-76915	64350	2235	1290	2495	-88970	77245
48	61.50	2290	1295	2470	-76085	64290	2290	1295	2470	-84435	70365	2290	1295	2470	-96655	83200
52	60.62	2345	1340	2460	-90775	79500	2345	1340	2460	-93105	79500	2345	1340	2460	-105510	91275
56	60.14	2405	1425	2455	-107025	101435	2405	1425	2455	-107025	101435	2405	1425	2455	-115885	101435
60	60.00	2470	1475	2465	-124890	124010	2470	1475	2465	-124890	124010	2470	1475	2465	-127560	124010

Rise [T] (ft)	Radius [R] (ft)	Ground Snow Load [p_g] 30 psf					35 psf					40 psf				
		R_y lbs	R_x lbs	F_a lbs	M^- in-lb	M^+ in-lb	R_y lbs	R_x lbs	F_a lbs	M^- in-lb	M^+ in-lb	R_y lbs	R_x lbs	F_a lbs	M^- in-lb	M^+ in-lb
12	156.00	2160	5285	5685	-57840	76895	2340	5730	6165	-67765	89505	2520	6175	6645	-77690	102120
16	120.50	2180	3980	4515	-60830	73630	2360	4315	4890	-70960	86025	2540	4650	5270	-81085	98420
20	100.00	2205	3195	3850	-70350	80265	2385	3460	4170	-81825	94055	2570	3725	4490	-93300	107850
24	87.00	2240	2665	3440	-78715	84920	2420	2885	3725	-91105	99570	2600	3105	4005	-103610	114220
28	78.29	2240	2275	3150	-84690	85845	2415	2460	3400	-97705	100585	2585	2645	3655	-110725	115325
32	72.25	2220	1965	2985	-88595	85090	2385	2125	3220	-101825	99450	2550	2280	3455	-115060	113810
36	68.00	2205	1725	2835	-92230	85035	2360	1860	3050	-105055	98900	2515	1995	3265	-118090	112760
40	65.00	2195	1525	2690	-96070	86595	2335	1640	2885	-108795	99955	2480	1755	3080	-121515	113310
44	62.91	2235	1360	2595	-101030	90140	2340	1465	2770	-113695	103290	2480	1565	2950	-126370	116930
48	61.50	2290	1295	2555	-108870	96735	2380	1320	2725	-121090	110265	2510	1410	2895	-133585	123800
52	60.62	2345	1340	2535	-117920	104495	2425	1340	2700	-130330	117840	2560	1340	2860	-142735	132000
56	60.14	2405	1425	2535	-128565	114810	2485	1425	2695	-141250	128935	2615	1425	2855	-153930	143065
60	60.00	2470	1475	2545	-140135	125380	2550	1475	2700	-153045	140355	2680	1475	2855	-165960	155325

Table E-11 - 120 ft Span, Variable Snow Load.

20 psf Dead Load
20 psf Construction Load
120 mph Wind Zone

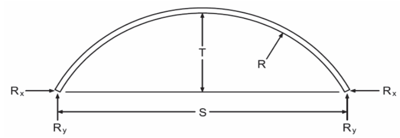

Notes:

All values normalized to C_D = 1.0.
Use ASD design procedure only.

Snow Load

C_e = 0.9
C_t = 1.2
I_s = 1.10

Wind Load

K_{zt} = 1.0
K_d = 0.85

Rise [T] (ft)	Radius [R] (ft)	Ground Snow Load [p_g] 50 psf R_y lbs	50 psf R_x lbs	50 psf F_a lbs	50 psf M^- in-lb	50 psf M^+ in-lb	60 psf R_y lbs	60 psf R_x lbs	60 psf F_a lbs	60 psf M^- in-lb	60 psf M^+ in-lb	70 psf R_y lbs	70 psf R_x lbs	70 psf F_a lbs	70 psf M^- in-lb	70 psf M^+ in-lb
12	156.00	2880	7065	7600	-97540	127340	3245	7955	8560	-117395	152565	3605	8845	9520	-137245	177785
16	120.50	2905	5315	6025	-101340	123215	3265	5985	6780	-121595	148005	3625	6650	7535	-141850	172795
20	100.00	2930	4255	5125	-116250	135430	3290	4790	5765	-139195	163015	3655	5320	6400	-162145	190595
24	87.00	2960	3545	4570	-128770	143515	3325	3985	5135	-153925	172815	3685	4425	5700	-179085	202115
28	78.29	2935	3015	4160	-136755	144805	3285	3385	4665	-163020	174285	3635	3755	5165	-189415	203950
32	72.25	2880	2595	3930	-141520	142530	3210	2910	4400	-167985	171250	3540	3225	4870	-194450	200420
36	68.00	2820	2260	3695	-144530	140485	3130	2530	4130	-170975	168520	3440	2800	4560	-197415	196895
40	65.00	2770	1990	3470	-146960	140480	3055	2225	3860	-172970	168155	3345	2455	4250	-199135	195830
44	62.91	2750	1770	3310	-151715	144200	3025	1975	3665	-177065	171475	3295	2180	4020	-202415	198745
48	61.50	2780	1595	3235	-159220	150865	3045	1775	3570	-184855	177930	3310	1955	3910	-210490	205360
52	60.62	2820	1440	3185	-167950	160330	3085	1605	3515	-193940	188655	3345	1770	3840	-219925	216985
56	60.14	2875	1425	3170	-179295	171315	3140	1460	3485	-205050	200485	3400	1610	3805	-231555	230190
60	60.00	2940	1475	3160	-191785	185275	3200	1475	3470	-217610	215220	3460	1475	3780	-243590	245165

Rise [T] (ft)	Radius [R] (ft)	Ground Snow Load [p_g] 80 psf R_y lbs	80 psf R_x lbs	80 psf F_a lbs	80 psf M^- in-lb	80 psf M^+ in-lb	90 psf R_y lbs	90 psf R_x lbs	90 psf F_a lbs	90 psf M^- in-lb	90 psf M^+ in-lb	100 psf R_y lbs	100 psf R_x lbs	100 psf F_a lbs	100 psf M^- in-lb	100 psf M^+ in-lb
12	156.00	3965	9735	10475	-157095	203010	4330	10625	11435	-176950	228235	4690	11515	12390	-196800	253455
16	120.50	3985	7320	8290	-162105	197585	4350	7985	9045	-182360	222375	4710	8655	9800	-202615	247165
20	100.00	4015	5855	7040	-185095	218180	4375	6385	7680	-208045	245760	4735	6915	8315	-230990	273345
24	87.00	4045	4865	6260	-204240	231410	4410	5310	6825	-229400	260710	4770	5750	7390	-254560	290010
28	78.29	3985	4125	5670	-215805	233750	4330	4495	6175	-242200	263550	4680	4870	6680	-268595	293350
32	72.25	3870	3540	5345	-220910	229605	4200	3855	5815	-247565	258790	4525	4170	6285	-274335	287975
36	68.00	3745	3070	4995	-223860	225265	4055	3340	5425	-250300	253640	4365	3610	5860	-276745	282010
40	65.00	3630	2690	4640	-225300	223500	3915	2920	5030	-251460	251175	4205	3155	5420	-277625	278845
44	62.91	3570	2380	4380	-228305	226020	3840	2585	4735	-254305	253290	4115	2790	5090	-280305	280565
48	61.50	3580	2140	4250	-236125	233350	3845	2320	4590	-261760	261340	4110	2500	4930	-287645	289335
52	60.62	3610	1930	4165	-245910	245310	3870	2095	4490	-271895	273640	4135	2260	4815	-297880	301965
56	60.14	3660	1755	4120	-258065	259900	3920	1905	4440	-284575	289605	4180	2050	4755	-311085	319315
60	60.00	3720	1600	4090	-270530	275110	3980	1735	4400	-297470	305060	4240	1865	4715	-324410	335100

Table E-12 - 130 ft Span, Variable Snow Load.

20 psf Dead Load
20 psf Construction Load
120 mph Wind Zone

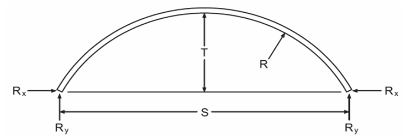

Notes:

All values normalized to $C_D = 1.0$.
Use ASD design procedure only.

Snow Load

$C_e = 0.9$
$C_t = 1.2$
$I_s = 1.10$

Wind Load

$K_{zt} = 1.0$
$K_d = 0.85$

Rise [T] (ft)	Radius [R] (ft)	Ground Snow Load [p_g]														
		15 psf					20 psf					25 psf				
		R_y lbs	R_x lbs	F_a lbs	M^- in-lb	M^+ in-lb	R_y lbs	R_x lbs	F_a lbs	M^- in-lb	M^+ in-lb	R_y lbs	R_x lbs	F_a lbs	M^- in-lb	M^+ in-lb
12	182.04	2105	5595	5960	-32720	46115	2105	5595	5960	-44350	60940	2140	5675	6045	-55975	75770
16	140.03	2125	4215	4695	-35475	43290	2125	4215	4695	-47200	57885	2155	4280	4770	-59050	72480
20	115.63	2145	3380	3975	-40390	44680	2145	3380	3975	-53085	60050	2180	3435	4040	-65820	75640
24	100.02	2175	2825	3530	-46195	47230	2175	2825	3530	-60190	63905	2210	2870	3585	-74185	80585
28	89.45	2205	2420	3235	-51460	48835	2205	2420	3235	-66285	65925	2235	2460	3280	-81265	83015
32	82.02	2245	2120	3035	-55880	49335	2245	2120	3035	-70785	66090	2245	2135	3075	-85990	82845
36	76.68	2285	1880	2900	-60015	50365	2285	1880	2900	-75080	66510	2285	1880	2935	-90150	82650
40	72.81	2330	1685	2805	-64785	52550	2330	1685	2805	-79230	67935	2330	1685	2805	-94260	83530
44	70.01	2375	1525	2745	-70145	56160	2375	1525	2745	-84290	70710	2375	1525	2745	-98550	86250
48	68.01	2425	1390	2700	-76775	62860	2425	1390	2700	-90950	75940	2425	1390	2700	-105120	91130
52	66.63	2480	1400	2675	-89320	76950	2480	1400	2675	-99125	82530	2480	1400	2675	-113465	97590
56	65.72	2540	1440	2665	-105170	93635	2540	1440	2665	-108450	93635	2540	1440	2665	-122990	106260
60	65.21	2600	1530	2660	-122570	117630	2600	1530	2660	-122570	117630	2600	1530	2660	-134090	117630

Rise [T] (ft)	Radius [R] (ft)	Ground Snow Load [p_g]														
		30 psf					35 psf					40 psf				
		R_y lbs	R_x lbs	F_a lbs	M^- in-lb	M^+ in-lb	R_y lbs	R_x lbs	F_a lbs	M^- in-lb	M^+ in-lb	R_y lbs	R_x lbs	F_a lbs	M^- in-lb	M^+ in-lb
12	182.04	2335	6200	6605	-67605	90595	2530	6720	7160	-79235	105420	2725	7245	7715	-90860	120245
16	140.03	2355	4670	5205	-70900	87075	2550	5065	5640	-82745	101670	2745	5455	6075	-94595	116265
20	115.63	2380	3745	4405	-78720	91225	2575	4060	4770	-91625	106815	2770	4375	5140	-104525	122400
24	100.02	2410	3125	3910	-88185	97260	2605	3385	4230	-102330	113940	2800	3645	4550	-116550	130620
28	89.45	2430	2680	3570	-96240	100335	2625	2900	3865	-111215	117800	2820	3120	4155	-126195	135265
32	82.02	2420	2325	3340	-101405	100025	2605	2515	3610	-116820	117310	2790	2700	3875	-132230	134595
36	76.68	2400	2045	3180	-105245	99405	2575	2205	3430	-120800	116230	2750	2370	3680	-136350	133055
40	72.81	2385	1815	3030	-109295	99800	2550	1955	3260	-124325	116065	2715	2095	3490	-139360	132335
44	70.01	2375	1620	2890	-113440	101955	2530	1745	3100	-128330	117655	2680	1865	3305	-143225	133355
48	68.01	2425	1465	2805	-119290	106320	2540	1575	3000	-134100	121555	2685	1680	3190	-148990	137595
52	66.63	2480	1400	2765	-127805	113470	2575	1430	2950	-142150	129345	2720	1530	3135	-156820	145225
56	65.72	2540	1440	2745	-137535	121695	2625	1440	2925	-152080	137520	2765	1440	3100	-166620	154080
60	65.21	2600	1530	2745	-148930	132825	2685	1530	2920	-163770	149245	2825	1530	3090	-178615	165665

Table E-12 - 130 ft Span, Variable Snow Load.

20 psf Dead Load
20 psf Construction Load
120 mph Wind Zone

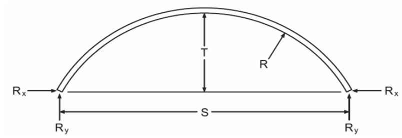

Notes:

All values normalized to C_D = 1.0.
Use ASD design procedure only.

Snow Load

C_e = 0.9
C_t = 1.2
I_s = 1.10

Wind Load

K_{zt} = 1.0
K_d = 0.85

Rise [T] (ft)	Radius [R] (ft)	Ground Snow Load [p_g] 50 psf R_y lbs	50 psf R_x lbs	50 psf F_a lbs	50 psf M^- in-lb	50 psf M^+ in-lb	60 psf R_y lbs	60 psf R_x lbs	60 psf F_a lbs	60 psf M^- in-lb	60 psf M^+ in-lb	70 psf R_y lbs	70 psf R_x lbs	70 psf F_a lbs	70 psf M^- in-lb	70 psf M^+ in-lb
12	182.04	3115	8290	8830	-114115	149900	3510	9335	9945	-137370	179550	3900	10385	11060	-160625	209205
16	140.03	3135	6240	6950	-118290	145455	3530	7025	7825	-141990	174645	3920	7810	8695	-165685	203835
20	115.63	3160	5000	5870	-130325	153575	3555	5625	6605	-156130	184750	3945	6250	7340	-181930	215925
24	100.02	3190	4165	5195	-144985	164030	3585	4685	5840	-173420	197675	3975	5200	6485	-201855	231325
28	89.45	3205	3560	4735	-156460	170200	3595	4000	5315	-186860	205130	3980	4440	5895	-217255	240065
32	82.02	3160	3080	4410	-163060	169160	3530	3455	4945	-193890	203730	3900	3835	5475	-225000	238300
36	76.68	3100	2695	4180	-167460	166705	3450	3020	4675	-198570	200360	3800	3345	5175	-229680	234010
40	72.81	3045	2375	3945	-170310	164865	3370	2660	4405	-201285	197400	3700	2940	4860	-232260	229935
44	70.01	2990	2115	3720	-173010	164755	3295	2360	4135	-203220	196750	3605	2610	4550	-233835	229130
48	68.01	2980	1900	3575	-178775	169670	3275	2120	3960	-208565	201745	3570	2340	4345	-238350	233820
52	66.63	3010	1725	3500	-186910	176980	3300	1920	3870	-217000	208735	3585	2120	4240	-247090	240930
56	65.72	3050	1575	3455	-196280	187200	3335	1750	3810	-226740	220315	3620	1930	4165	-257205	253435
60	65.21	3105	1530	3435	-208295	198545	3390	1605	3780	-238660	233175	3675	1765	4125	-269690	267805

Rise [T] (ft)	Radius [R] (ft)	Ground Snow Load [p_g] 80 psf R_y lbs	80 psf R_x lbs	80 psf F_a lbs	80 psf M^- in-lb	80 psf M^+ in-lb	90 psf R_y lbs	90 psf R_x lbs	90 psf F_a lbs	90 psf M^- in-lb	90 psf M^+ in-lb	100 psf R_y lbs	100 psf R_x lbs	100 psf F_a lbs	100 psf M^- in-lb	100 psf M^+ in-lb
12	182.04	4290	11430	12170	-183880	238885	4685	12475	13285	-207135	268605	5075	13520	14400	-230390	298325
16	140.03	4310	8595	9570	-189385	233020	4705	9380	10440	-213080	262210	5095	10165	11315	-236775	291400
20	115.63	4335	6875	8070	-207735	247100	4730	7500	8805	-233535	278275	5120	8125	9540	-259340	309450
24	100.02	4365	5720	7130	-230290	264970	4760	6240	7775	-258720	298615	5150	6760	8420	-287155	332260
28	89.45	4370	4880	6475	-247655	274995	4760	5320	7055	-278055	309930	5145	5760	7635	-308450	344860
32	82.02	4270	4210	6010	-256230	272865	4640	4585	6545	-287465	307435	5010	4965	7075	-318695	342005
36	76.68	4150	3670	5675	-260785	267660	4500	3995	6170	-291895	301310	4850	4320	6670	-323100	334960
40	72.81	4030	3225	5320	-263235	262470	4360	3505	5780	-294210	295405	4685	3790	6235	-325185	328480
44	70.01	3915	2855	4965	-264450	261505	4220	3100	5380	-295065	293885	4530	3350	5795	-325680	326260
48	68.01	3865	2560	4730	-268650	265895	4160	2780	5115	-299195	297975	4455	2995	5500	-329740	330050
52	66.63	3875	2315	4605	-277185	273770	4165	2515	4975	-307275	306615	4455	2710	5340	-337665	339455
56	65.72	3905	2110	4515	-287665	286555	4190	2285	4870	-318125	319670	4475	2465	5225	-348585	352790
60	65.21	3955	1930	4470	-300725	302435	4240	2090	4815	-331755	337065	4520	2255	5160	-362785	371690

Table E-13 - 140 ft Span, Variable Snow Load.

20 psf Dead Load
20 psf Construction Load
120 mph Wind Zone

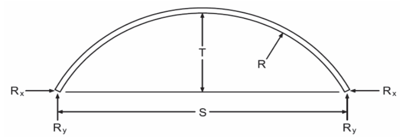

Notes:

All values normalized to C_D = 1.0.
Use ASD design procedure only.

Snow Load

C_e = 0.9
C_t = 1.2
I_s = 1.10

Wind Load

K_{zt} = 1.0
K_d = 0.85

Rise [T] (ft)	Radius [R] (ft)	Ground Snow Load [p_g]														
		15 psf					20 psf					25 psf				
		R_y lbs	R_x lbs	F_a lbs	M^- in-lb	M^+ in-lb	R_y lbs	R_x lbs	F_a lbs	M^- in-lb	M^+ in-lb	R_y lbs	R_x lbs	F_a lbs	M^- in-lb	M^+ in-lb
12	210.17	2265	6485	6850	-37760	53735	2265	6485	6850	-51225	70955	2300	6580	6950	-64690	88170
16	161.13	2280	4890	5370	-40695	50675	2280	4890	5370	-54355	67645	2315	4960	5450	-68065	84615
20	132.50	2300	3920	4515	-44510	50130	2300	3920	4515	-58645	67490	2340	3980	4585	-72930	84890
24	114.08	2330	3275	3980	-50950	53535	2330	3275	3980	-66585	72255	2370	3325	4045	-82225	90980
28	101.50	2360	2810	3625	-56845	55765	2360	2810	3625	-73730	75365	2400	2855	3685	-90620	95275
32	92.56	2390	2455	3380	-62045	56705	2390	2455	3380	-79270	76470	2410	2490	3415	-96920	96460
36	86.06	2430	2180	3210	-66660	57440	2430	2180	3210	-84070	76715	2430	2195	3255	-101550	96245
40	81.25	2470	1960	3090	-71175	58845	2470	1960	3090	-88580	77490	2470	1960	3120	-106085	96300
44	77.68	2515	1775	3005	-76460	61475	2515	1775	3005	-93010	79410	2515	1775	3005	-110425	97340
48	75.04	2565	1620	2945	-82310	65745	2565	1620	2945	-98685	82700	2565	1620	2945	-115060	100345
52	73.12	2615	1485	2905	-89705	75340	2615	1485	2905	-106160	88500	2615	1485	2905	-122615	106175
56	71.75	2670	1500	2880	-103615	90885	2670	1500	2880	-114990	95665	2670	1500	2880	-131625	113130
60	70.83	2730	1540	2870	-120620	109070	2730	1540	2870	-124970	109070	2730	1540	2870	-141815	122395

Rise [T] (ft)	Radius [R] (ft)	Ground Snow Load [p_g]														
		30 psf					35 psf					40 psf				
		R_y lbs	R_x lbs	F_a lbs	M^- in-lb	M^+ in-lb	R_y lbs	R_x lbs	F_a lbs	M^- in-lb	M^+ in-lb	R_y lbs	R_x lbs	F_a lbs	M^- in-lb	M^+ in-lb
12	210.17	2510	7185	7590	-78155	105385	2720	7795	8235	-91620	122605	2930	8400	8875	-105085	139820
16	161.13	2525	5415	5950	-81770	101585	2740	5870	6450	-95480	118550	2950	6325	6950	-109185	135520
20	132.50	2550	4345	5005	-87290	102290	2760	4710	5425	-101650	119690	2970	5070	5840	-116015	137090
24	114.08	2580	3625	4410	-97980	109755	2790	3930	4775	-113870	128715	3000	4230	5140	-129760	147680
28	101.50	2610	3110	4015	-107505	115190	2820	3365	4345	-124390	135105	3035	3625	4675	-141470	155015
32	92.56	2615	2710	3715	-114570	116455	2820	2930	4015	-132215	136450	3025	3155	4310	-149865	156440
36	86.06	2600	2390	3540	-119540	115775	2795	2580	3820	-137535	135300	2990	2775	4100	-155530	155050
40	81.25	2580	2125	3380	-123585	115105	2765	2295	3645	-141395	134255	2950	2460	3905	-159455	153735
44	77.68	2565	1905	3230	-127840	115745	2740	2050	3475	-145255	134610	2915	2200	3715	-162665	153475
48	75.04	2565	1720	3095	-132265	118580	2720	1850	3315	-149500	136810	2885	1980	3535	-166735	155045
52	73.12	2615	1565	3020	-139070	123850	2735	1680	3225	-156190	141525	2895	1800	3430	-173480	159955
56	71.75	2670	1500	2980	-148255	131540	2775	1540	3175	-164890	149955	2930	1645	3375	-181915	168365
60	70.83	2730	1540	2960	-158665	140215	2820	1540	3150	-175515	158725	2975	1540	3340	-192360	177870

Table E-13 - 140 ft Span, Variable Snow Load.

20 psf Dead Load
20 psf Construction Load
120 mph Wind Zone

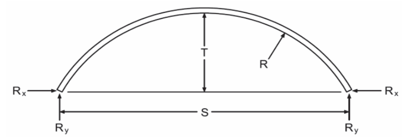

Notes:

All values normalized to $C_D = 1.0$.
Use ASD design procedure only.

Snow Load

$C_e = 0.9$
$C_t = 1.2$
$I_s = 1.10$

Wind Load

$K_{zt} = 1.0$
$K_d = 0.85$

Rise [T] (ft)	Radius [R] (ft)	Ground Snow Load [p_g] 50 psf					60 psf					70 psf				
		R_y lbs	R_x lbs	F_a lbs	M^- in-lb	M^+ in-lb	R_y lbs	R_x lbs	F_a lbs	M^- in-lb	M^+ in-lb	R_y lbs	R_x lbs	F_a lbs	M^- in-lb	M^+ in-lb
12	210.17	3355	9615	10155	-132015	174260	3775	10830	11440	-158945	208805	4195	12045	12720	-185880	243350
16	161.13	3370	7240	7950	-136600	169460	3795	8150	8950	-164015	203400	4215	9060	9950	-191425	237335
20	132.50	3395	5800	6675	-144735	171890	3815	6525	7510	-173460	206690	4240	7255	8345	-202185	241490
24	114.08	3420	4835	5870	-161540	185605	3845	5435	6600	-193320	223535	4265	6040	7330	-225100	261460
28	101.50	3455	4140	5335	-175765	194840	3875	4655	5990	-210060	234665	4300	5165	6650	-244355	274495
32	92.56	3435	3595	4905	-185165	196565	3845	4040	5505	-220955	237110	4255	4485	6100	-256755	277655
36	86.06	3380	3160	4665	-191515	195040	3770	3545	5225	-227500	235030	4160	3930	5790	-263485	275020
40	81.25	3320	2795	4430	-195575	192685	3690	3135	4955	-231700	231640	4065	3470	5480	-267820	270590
44	77.68	3265	2495	4200	-198225	191200	3615	2790	4680	-234095	228930	3960	3085	5165	-269960	266655
48	75.04	3210	2240	3975	-201205	191510	3540	2500	4415	-235925	227975	3870	2760	4855	-271340	265045
52	73.12	3210	2035	3845	-208060	197225	3530	2265	4260	-242645	234495	3845	2500	4670	-277225	271765
56	71.75	3240	1860	3770	-216815	205185	3550	2070	4165	-251720	242010	3865	2280	4565	-286620	279340
60	70.83	3280	1705	3725	-226825	216155	3590	1900	4105	-262120	254440	3895	2090	4485	-297410	292725

Rise [T] (ft)	Radius [R] (ft)	Ground Snow Load [p_g] 80 psf					90 psf					100 psf				
		R_y lbs	R_x lbs	F_a lbs	M^- in-lb	M^+ in-lb	R_y lbs	R_x lbs	F_a lbs	M^- in-lb	M^+ in-lb	R_y lbs	R_x lbs	F_a lbs	M^- in-lb	M^+ in-lb
12	210.17	4620	13260	14000	-212810	277895	5040	14470	15285	-239740	312445	5460	15685	16565	-266670	346990
16	161.13	4635	9970	10950	-218840	271275	5060	10885	11950	-246255	305215	5480	11795	12950	-273670	339150
20	132.50	4660	7980	9185	-230905	276290	5080	8705	10020	-259630	311090	5505	9435	10855	-288355	345890
24	114.08	4690	6645	8060	-256875	299385	5110	7245	8795	-288655	337315	5530	7850	9525	-320435	375240
28	101.50	4720	5680	7310	-278655	314320	5140	6195	7965	-312950	354145	5565	6710	8625	-347245	393970
32	92.56	4665	4925	6695	-292555	318205	5075	5370	7295	-328350	358750	5485	5815	7890	-364150	399295
36	86.06	4555	4310	6350	-299805	315005	4945	4695	6915	-336240	354995	5335	5080	7475	-372670	394985
40	81.25	4435	3805	6005	-303940	309545	4805	4140	6530	-340060	348495	5175	4480	7055	-376185	387450
44	77.68	4310	3380	5650	-305825	304385	4660	3675	6130	-341690	342110	5010	3970	6615	-377555	379835
48	75.04	4195	3025	5290	-306755	302495	4525	3285	5730	-342170	339945	4850	3545	6170	-377590	377395
52	73.12	4165	2735	5085	-312285	309035	4480	2970	5500	-347745	346305	4795	3205	5910	-383205	383575
56	71.75	4175	2495	4960	-321525	317420	4485	2705	5355	-356430	355505	4795	2920	5750	-391685	393590
60	70.83	4205	2285	4870	-332705	331010	4510	2480	5250	-367995	369295	4815	2670	5635	-403290	407580

Table E-14 - 150 ft Span, Variable Snow Load.

20 psf Dead Load
20 psf Construction Load
120 mph Wind Zone

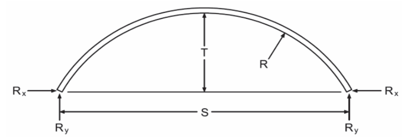

Notes:

All values normalized to C_D = 1.0.
Use ASD design procedure only.

Snow Load

C_e = 0.9
C_t = 1.2
I_s = 1.10

Wind Load

K_{zt} = 1.0
K_d = 0.85

Rise [T] (ft)	Radius [R] (ft)	Ground Snow Load [p_g]														
		15 psf					20 psf					25 psf				
		R_y lbs	R_x lbs	F_a lbs	M^- in-lb	M^+ in-lb	R_y lbs	R_x lbs	F_a lbs	M^- in-lb	M^+ in-lb	R_y lbs	R_x lbs	F_a lbs	M^- in-lb	M^+ in-lb
14	207.89	2430	6400	6820	-44955	60090	2430	6400	6820	-60540	79730	2465	6490	6925	-76125	99370
18	165.25	2450	4995	5535	-47610	57265	2450	4995	5535	-63335	76670	2485	5070	5620	-79140	96075
22	138.84	2470	4095	4750	-52335	57920	2470	4095	4750	-68820	78050	2510	4155	4825	-85470	98280
26	121.17	2495	3470	4235	-59105	61480	2495	3470	4235	-77175	83065	2540	3525	4305	-95240	104650
30	108.75	2525	3010	3885	-65375	63880	2525	3010	3885	-84770	86375	2570	3060	3950	-104165	109225
34	99.72	2560	2655	3640	-70940	64880	2560	2655	3640	-90730	87660	2580	2690	3680	-110955	110580
38	93.01	2600	2375	3460	-75880	65545	2600	2375	3460	-95825	87905	2600	2390	3510	-115975	110275
42	87.96	2640	2145	3335	-80590	67020	2640	2145	3335	-100670	88535	2640	2145	3370	-120750	110045
46	84.14	2685	1950	3240	-86120	69700	2685	1950	3240	-105410	90155	2685	1950	3240	-125435	111020
50	81.25	2730	1790	3175	-92270	73745	2730	1790	3175	-111155	93320	2730	1790	3175	-130410	114175
54	79.08	2780	1645	3130	-99320	81470	2780	1645	3130	-118120	98695	2780	1645	3130	-136920	118620
58	77.49	2835	1585	3100	-110450	97280	2835	1585	3100	-127260	105435	2835	1585	3100	-146285	126205
60	76.88	2860	1605	3090	-118970	106105	2860	1605	3090	-132025	109775	2860	1605	3090	-151125	129820

Rise [T] (ft)	Radius [R] (ft)	Ground Snow Load [p_g]														
		30 psf					35 psf					40 psf				
		R_y lbs	R_x lbs	F_a lbs	M^- in-lb	M^+ in-lb	R_y lbs	R_x lbs	F_a lbs	M^- in-lb	M^+ in-lb	R_y lbs	R_x lbs	F_a lbs	M^- in-lb	M^+ in-lb
14	207.89	2695	7090	7560	-91710	119010	2920	7690	8200	-107295	138655	3145	8285	8835	-122880	158295
18	165.25	2710	5535	6130	-94945	115485	2940	6000	6645	-110755	134890	3165	6465	7160	-126560	154295
22	138.84	2735	4535	5260	-102225	118510	2960	4915	5700	-118980	138740	3190	5295	6140	-135735	158975
26	121.17	2765	3845	4695	-113430	126235	2990	4165	5080	-131790	148060	3215	4485	5470	-150150	169910
30	108.75	2800	3335	4305	-123560	132070	3025	3610	4655	-142955	154920	3250	3885	5010	-162585	177770
34	99.72	2800	2930	4000	-131180	133495	3020	3170	4320	-151410	156415	3240	3410	4645	-171635	179330
38	93.01	2785	2600	3815	-136595	132650	2995	2810	4115	-157215	155295	3205	3020	4420	-177835	178260
42	87.96	2770	2330	3655	-140830	131975	2970	2515	3940	-161490	154350	3170	2700	4225	-182220	176725
46	84.14	2755	2100	3505	-145460	132665	2945	2265	3770	-165490	154310	3135	2425	4035	-185545	175955
50	81.25	2740	1905	3365	-150300	135030	2920	2050	3610	-170190	155885	3100	2195	3850	-190080	176740
54	79.08	2780	1740	3255	-155980	138615	2920	1870	3480	-175750	159780	3090	2000	3705	-195515	180940
58	77.49	2835	1600	3210	-165315	146975	2955	1720	3425	-184465	167750	3120	1835	3645	-204440	188520
60	76.88	2860	1605	3190	-170225	150955	2970	1650	3405	-189320	172085	3140	1765	3615	-208865	193215

Table E-14 - 150 ft Span, Variable Snow Load.

20 psf Dead Load
20 psf Construction Load
120 mph Wind Zone

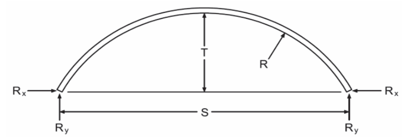

Notes:

All values normalized to C_D = 1.0.
Use ASD design procedure only.

Snow Load

C_e = 0.9
C_t = 1.2
I_s = 1.10

Wind Load

K_{zt} = 1.0
K_d = 0.85

Rise [T]	Radius [R]	Ground Snow Load [p_g]														
		50 psf					60 psf					70 psf				
(ft)	(ft)	R_y lbs	R_x lbs	F_a lbs	M^- in-lb	M^+ in-lb	R_y lbs	R_x lbs	F_a lbs	M^- in-lb	M^+ in-lb	R_y lbs	R_x lbs	F_a lbs	M^- in-lb	M^+ in-lb
14	207.89	3595	9485	10110	-154055	197575	4050	10680	11385	-185225	236855	4500	11875	12660	-216395	276225
18	165.25	3615	7395	8190	-158170	193110	4070	8325	9220	-189780	231920	4520	9255	10250	-221395	270735
22	138.84	3640	6055	7015	-169245	199435	4090	6815	7895	-202755	239895	4545	7570	8775	-236265	280355
26	121.17	3670	5120	6245	-186865	213615	4120	5760	7025	-223580	257315	4575	6400	7800	-260300	301020
30	108.75	3700	4435	5715	-201980	223465	4155	4985	6420	-241370	269160	4605	5535	7125	-280760	314860
34	99.72	3680	3890	5285	-212160	225655	4120	4370	5930	-253195	272190	4560	4850	6575	-294225	318720
38	93.01	3630	3440	5030	-219075	224195	4050	3860	5635	-260315	270125	4475	4280	6240	-301620	316060
42	87.96	3570	3070	4795	-223670	221475	3970	3440	5365	-265125	266230	4375	3810	5935	-306580	310980
46	84.14	3515	2755	4565	-226815	219245	3895	3080	5095	-268085	262530	4275	3410	5620	-309355	305820
50	81.25	3460	2485	4340	-229860	219170	3820	2780	4825	-270550	262375	4180	3070	5315	-311455	305580
54	79.08	3430	2260	4155	-235050	223265	3775	2520	4610	-274585	265590	4120	2785	5060	-314385	307915
58	77.49	3455	2075	4075	-244390	230410	3795	2315	4510	-284345	273775	4130	2550	4945	-324300	317140
60	76.88	3470	1990	4040	-248935	235480	3805	2220	4465	-289010	277745	4140	2445	4890	-329080	320595

Rise [T]	Radius [R]	Ground Snow Load [p_g]														
		80 psf					90 psf					100 psf				
(ft)	(ft)	R_y lbs	R_x lbs	F_a lbs	M^- in-lb	M^+ in-lb	R_y lbs	R_x lbs	F_a lbs	M^- in-lb	M^+ in-lb	R_y lbs	R_x lbs	F_a lbs	M^- in-lb	M^+ in-lb
14	207.89	4955	13075	13935	-247565	315605	5405	14270	15210	-278740	354985	5855	15465	16485	-309910	394370
18	165.25	4970	10185	11280	-253005	309550	5425	11115	12310	-284615	348360	5875	12045	13340	-316230	387175
22	138.84	4995	8330	9650	-269775	320815	5450	9090	10530	-303285	361275	5900	9850	11405	-336795	401735
26	121.17	5025	7040	8575	-297015	344720	5475	7680	9350	-333730	388420	5930	8320	10130	-370450	432125
30	108.75	5055	6090	7830	-320150	360555	5510	6640	8535	-359540	406250	5960	7190	9240	-398930	451950
34	99.72	5000	5330	7215	-335255	365255	5445	5810	7860	-376285	411785	5885	6290	8505	-417315	458315
38	93.01	4895	4700	6850	-343385	361990	5315	5120	7455	-385145	407925	5740	5540	8065	-426905	453855
42	87.96	4775	4180	6505	-348030	355730	5175	4550	7080	-389485	400480	5580	4915	7650	-430940	445230
46	84.14	4655	3735	6150	-350625	349310	5035	4065	6680	-391895	393355	5415	4390	7210	-433165	437405
50	81.25	4535	3360	5800	-352365	348785	4895	3655	6290	-393270	391990	5255	3945	6775	-434175	435195
54	79.08	4460	3045	5510	-354955	350240	4805	3305	5960	-395525	392565	5145	3570	6415	-436090	434890
58	77.49	4465	2790	5375	-364250	360510	4800	3025	5810	-404695	403875	5140	3265	6245	-445620	447240
60	76.88	4470	2670	5315	-369150	364305	4805	2900	5740	-409220	408020	5140	3125	6160	-449705	451730

Table E-15 - 20 ft Span, Variable Wind Load.

10 psf Dead Load
20 psf Construction Load
No Ground Snow Load

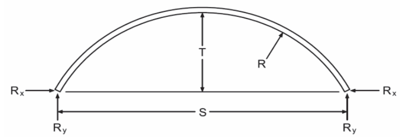

Notes:

All values normalized to C_D = 1.0.
Use ASD design procedure only.

Wind Load

K_{zt} = 1.0
K_d = 0.85

Rise [T] (ft)	Radius [R] (ft)	Basic Wind Speed [V] 105 mph					110 mph					115 mph				
		R_y lbs	R_x lbs	F_a lbs	M^- in-lb	M^+ in-lb	R_y lbs	R_x lbs	F_a lbs	M^- in-lb	M^+ in-lb	R_y lbs	R_x lbs	F_a lbs	M^- in-lb	M^+ in-lb
2	26.00	245	450	510	-255	3665	245	450	510	-325	3665	245	450	510	-405	3665
3	18.17	245	350	425	-200	2025	245	350	425	-245	2025	245	350	425	-285	2025
4	14.50	250	280	370	-215	1410	250	280	370	-255	1410	250	280	370	-295	1410
5	12.50	255	230	335	-335	1210	255	230	335	-335	1210	255	230	335	-355	1210
6	11.33	260	190	315	-680	1220	260	190	315	-680	1220	260	190	315	-680	1220
7	10.64	265	165	305	-1070	1360	265	165	305	-1070	1360	265	165	305	-1070	1360
8	10.25	275	150	295	-1500	1595	275	150	295	-1500	1595	275	145	295	-1500	1595
9	10.06	280	160	290	-1985	1915	280	155	290	-1985	1915	280	150	290	-1985	1915
10	10.00	290	170	290	-2525	2310	290	165	290	-2525	2310	290	165	290	-2525	2460

Rise [T] (ft)	Radius [R] (ft)	Basic Wind Speed [V] 120 mph					130 mph					140 mph				
		R_y lbs	R_x lbs	F_a lbs	M^- in-lb	M^+ in-lb	R_y lbs	R_x lbs	F_a lbs	M^- in-lb	M^+ in-lb	R_y lbs	R_x lbs	F_a lbs	M^- in-lb	M^+ in-lb
2	26.00	245	450	510	-485	3665	245	450	510	-660	3665	245	450	510	-855	3665
3	18.17	245	350	425	-335	2025	245	350	425	-435	2025	245	350	425	-550	2025
4	14.50	250	280	370	-335	1410	250	280	370	-425	1410	250	280	370	-525	1410
5	12.50	255	230	335	-400	1210	255	230	335	-495	1210	255	230	335	-595	1210
6	11.33	260	190	315	-680	1220	260	190	315	-680	1220	260	190	315	-680	1220
7	10.64	265	165	305	-1070	1360	265	165	305	-1070	1360	265	165	305	-1070	1445
8	10.25	275	145	295	-1500	1595	275	140	295	-1500	1760	275	140	295	-1500	2065
9	10.06	280	150	290	-1985	1975	280	140	290	-1985	2355	280	135	290	-1985	2770
10	10.00	290	160	290	-2525	2700	290	155	290	-2525	3210	290	150	290	-2570	3765

Table E-15 - 20 ft Span, Variable Wind Load.

10 psf Dead Load
20 psf Construction Load
No Ground Snow Load

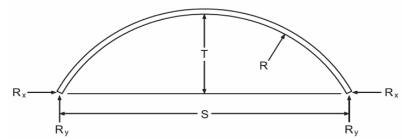

Notes:

All values normalized to C_D = 1.0.
Use ASD design procedure only.

Wind Load

K_{zt} = 1.0
K_d = 0.85

Rise [T] (ft)	Radius [R] (ft)	Basic Wind Speed [V]														
		150 mph					160 mph					170 mph				
		R_y	R_x	F_a	M^-	M^+	R_y	R_x	F_a	M^-	M^+	R_y	R_x	F_a	M^-	M^+
		lbs	lbs	lbs	in-lb	in-lb	lbs	lbs	lbs	in-lb	in-lb	lbs	lbs	lbs	in-lb	in-lb
2	26.00	245	450	510	-1060	3665	245	450	510	-1285	3665	245	450	510	-1520	3665
3	18.17	245	350	425	-670	2025	245	350	425	-800	2025	245	350	425	-940	2025
4	14.50	250	280	370	-635	1410	250	280	370	-750	1410	250	280	370	-870	1410
5	12.50	255	230	335	-705	1210	255	230	335	-820	1210	255	230	335	-945	1210
6	11.33	260	190	315	-800	1220	260	190	315	-925	1365	260	190	315	-1060	1550
7	10.64	265	165	305	-1070	1675	265	165	305	-1180	1915	265	165	305	-1350	2175
8	10.25	275	140	295	-1500	2395	275	140	295	-1650	2745	275	140	295	-1880	3120
9	10.06	280	125	290	-1985	3210	280	125	290	-2180	3685	280	125	290	-2475	4190
10	10.00	290	145	290	-2725	4355	290	135	290	-3055	4995	290	135	290	-3465	5675

Rise [T] (ft)	Radius [R] (ft)	Basic Wind Speed [V]														
		180 mph					190 mph					200 mph				
		R_y	R_x	F_a	M^-	M^+	R_y	R_x	F_a	M^-	M^+	R_y	R_x	F_a	M^-	M^+
		lbs	lbs	lbs	in-lb	in-lb	lbs	lbs	lbs	in-lb	in-lb	lbs	lbs	lbs	in-lb	in-lb
2	26.00	245	450	510	-1770	3665	245	450	510	-2035	3665	245	450	510	-2315	3665
3	18.17	245	350	425	-1090	2025	245	350	425	-1245	2025	245	350	425	-1410	2025
4	14.50	250	280	370	-1000	1410	250	280	370	-1135	1410	250	280	370	-1280	1410
5	12.50	255	230	335	-1080	1340	255	230	335	-1220	1495	255	230	335	-1370	1655
6	11.33	260	190	315	-1205	1745	260	190	315	-1360	1950	260	190	315	-1520	2165
7	10.64	265	165	305	-1525	2455	265	165	305	-1715	2750	265	165	305	-1915	3060
8	10.25	275	140	295	-2125	3515	275	140	295	-2385	3935	275	145	295	-2655	4380
9	10.06	280	135	290	-2790	4725	280	150	290	-3120	5290	280	170	290	-3465	5885
10	10.00	290	155	290	-3900	6400	290	175	290	-4355	7170	290	195	290	-4840	7975

Table E-16 - 30 ft Span, Variable Wind Load.

10 psf Dead Load
20 psf Construction Load
No Ground Snow Load

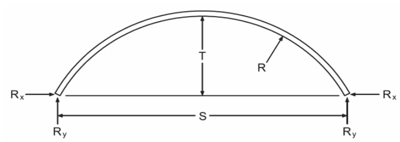

Notes:

All values normalized to $C_D = 1.0$.
Use ASD design procedure only.

Wind Load

$K_{zt} = 1.0$
$K_d = 0.85$

Rise [T] (ft)	Radius [R] (ft)	Basic Wind Speed [V] 105 mph					110 mph					115 mph				
		R_y lbs	R_x lbs	F_a lbs	M^- in-lb	M^+ in-lb	R_y lbs	R_x lbs	F_a lbs	M^- in-lb	M^+ in-lb	R_y lbs	R_x lbs	F_a lbs	M^- in-lb	M^+ in-lb
3	39.00	365	785	865	-405	4305	365	785	865	-490	4305	365	785	865	-580	4305
4	30.13	370	625	720	-355	2765	370	625	720	-415	2765	370	625	720	-480	2765
5	25.00	370	515	630	-340	2095	370	515	630	-390	2095	370	515	630	-440	2095
6	21.75	375	435	565	-440	1830	375	435	565	-500	1830	375	435	565	-565	1830
7	19.57	380	375	525	-850	1790	380	375	525	-850	1790	380	375	525	-850	1790
8	18.06	385	330	495	-1285	1895	385	330	495	-1285	1895	385	330	495	-1285	1895
9	17.00	390	290	475	-1775	2110	390	290	475	-1775	2110	390	290	475	-1775	2110
10	16.25	395	260	460	-2305	2410	395	260	460	-2305	2410	395	260	460	-2305	2410
11	15.73	400	235	450	-2885	2785	400	235	450	-2885	2785	400	235	450	-2885	2785
12	15.38	410	225	445	-3515	3230	410	225	445	-3515	3230	410	220	445	-3515	3230
13	15.15	415	235	440	-4205	3745	415	230	440	-4205	3745	415	225	440	-4205	3745
14	15.04	425	245	435	-4955	4330	425	240	435	-4955	4330	425	235	435	-4955	4605
15	15.00	430	250	430	-5765	4975	430	250	430	-5765	5015	430	245	430	-5765	5540

Rise [T] (ft)	Radius [R] (ft)	Basic Wind Speed [V] 120 mph					130 mph					140 mph				
		R_y lbs	R_x lbs	F_a lbs	M^- in-lb	M^+ in-lb	R_y lbs	R_x lbs	F_a lbs	M^- in-lb	M^+ in-lb	R_y lbs	R_x lbs	F_a lbs	M^- in-lb	M^+ in-lb
3	39.00	365	785	865	-680	4305	365	785	865	-890	4305	365	785	865	-1120	4305
4	30.13	370	625	720	-545	2765	370	625	720	-695	2765	370	625	720	-850	2765
5	25.00	370	515	630	-490	2095	370	515	630	-605	2095	370	515	630	-730	2095
6	21.75	375	435	565	-635	1830	375	435	565	-785	1830	375	435	565	-945	1830
7	19.57	380	375	525	-850	1790	380	375	525	-860	1790	380	375	525	-1030	1790
8	18.06	385	330	495	-1285	1895	385	330	495	-1285	1895	385	330	495	-1285	2085
9	17.00	390	290	475	-1775	2110	390	290	475	-1775	2110	390	290	475	-1775	2395
10	16.25	395	260	460	-2305	2410	395	260	460	-2305	2540	395	260	460	-2305	2980
11	15.73	400	235	450	-2885	2785	400	235	450	-2885	3265	400	235	450	-2885	3835
12	15.38	410	215	445	-3515	3345	410	215	445	-3515	3990	410	215	445	-3515	4690
13	15.15	415	220	440	-4205	4055	415	210	440	-4205	4845	415	200	440	-4205	5695
14	15.04	425	235	435	-4955	5060	425	225	435	-4955	6020	425	215	435	-4955	7060
15	15.00	430	240	430	-5765	6085	430	230	430	-5765	7240	430	225	430	-5825	8490

Table E-16 - 30 ft Span, Variable Wind Load.

10 psf Dead Load
20 psf Construction Load
No Ground Snow Load

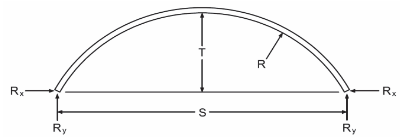

Notes:

All values normalized to C_D = 1.0.
Use ASD design procedure only.

Wind Load

K_{zt} = 1.0
K_d = 0.85

Rise [T] (ft)	Radius [R] (ft)	Basic Wind Speed [V] 150 mph					160 mph					170 mph				
		R_y lbs	R_x lbs	F_a lbs	M^- in-lb	M^+ in-lb	R_y lbs	R_x lbs	F_a lbs	M^- in-lb	M^+ in-lb	R_y lbs	R_x lbs	F_a lbs	M^- in-lb	M^+ in-lb
3	39.00	365	785	865	-1370	4305	365	785	865	-1640	4305	365	785	865	-1925	4305
4	30.13	370	625	720	-1025	2765	370	625	720	-1210	2765	370	625	720	-1405	2765
5	25.00	370	515	630	-865	2095	370	515	630	-1010	2095	370	515	630	-1165	2095
6	21.75	375	435	565	-1115	1830	375	435	565	-1305	1830	375	435	565	-1500	2030
7	19.57	380	375	525	-1210	1910	380	375	525	-1400	2180	380	375	525	-1605	2470
8	18.06	385	330	495	-1475	2410	385	330	495	-1700	2755	385	330	495	-1945	3130
9	17.00	390	290	475	-1775	2775	390	290	475	-1895	3180	390	290	475	-2160	3615
10	16.25	395	260	460	-2305	3455	395	260	460	-2305	3965	395	260	460	-2600	4505
11	15.73	400	235	450	-2885	4450	400	235	450	-2980	5100	400	235	450	-3395	5800
12	15.38	410	215	445	-3515	5440	410	215	445	-3610	6245	410	215	445	-4105	7100
13	15.15	415	195	440	-4205	6610	415	195	440	-4380	7585	415	195	440	-4970	8630
14	15.04	425	205	435	-5120	8175	425	195	435	-5650	9375	425	180	435	-6405	10660
15	15.00	430	215	430	-6170	9835	430	200	430	-6815	11270	430	200	430	-7725	12815

Rise [T] (ft)	Radius [R] (ft)	Basic Wind Speed [V] 180 mph					190 mph					200 mph				
		R_y lbs	R_x lbs	F_a lbs	M^- in-lb	M^+ in-lb	R_y lbs	R_x lbs	F_a lbs	M^- in-lb	M^+ in-lb	R_y lbs	R_x lbs	F_a lbs	M^- in-lb	M^+ in-lb
3	39.00	365	785	865	-2235	4305	365	785	865	-2555	4305	365	785	865	-2900	4305
4	30.13	370	625	720	-1620	2765	370	625	720	-1845	2765	370	625	720	-2080	2765
5	25.00	370	515	630	-1330	2095	370	515	630	-1510	2095	370	515	630	-1695	2095
6	21.75	375	435	565	-1710	2275	375	435	565	-1935	2535	375	435	565	-2165	2805
7	19.57	380	375	525	-1825	2775	380	375	525	-2060	3095	380	375	525	-2305	3440
8	18.06	385	330	495	-2200	3520	385	330	495	-2470	3935	385	330	495	-2760	4375
9	17.00	390	290	475	-2445	4075	390	290	475	-2745	4565	390	290	475	-3065	5075
10	16.25	395	260	460	-2940	5080	395	260	460	-3295	5690	395	260	460	-3675	6330
11	15.73	400	235	450	-3830	6535	400	235	450	-4295	7320	400	235	450	-4780	8140
12	15.38	410	215	445	-4630	8005	410	215	445	-5190	8965	410	220	445	-5775	9975
13	15.15	415	195	440	-5595	9730	415	215	440	-6255	10900	415	240	440	-6960	12130
14	15.04	425	205	435	-7210	12025	425	230	435	-8055	13465	425	260	435	-8945	14985
15	15.00	430	230	430	-8685	14455	430	260	430	-9705	16190	430	290	430	-10780	18015

Table E-17 - 40 ft Span, Variable Wind Load.

10 psf Dead Load
20 psf Construction Load
No Ground Snow Load

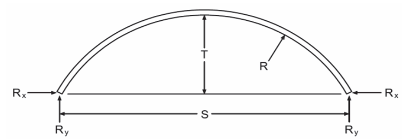

Notes:

All values normalized to C_D = 1.0.
Use ASD design procedure only.

Wind Load

K_{zt} = 1.0
K_d = 0.85

Rise [T] (ft)	Radius [R] (ft)	Basic Wind Speed [V] 105 mph R_y lbs	105 mph R_x lbs	105 mph F_a lbs	105 mph M^- in-lb	105 mph M^+ in-lb	110 mph R_y lbs	110 mph R_x lbs	110 mph F_a lbs	110 mph M^- in-lb	110 mph M^+ in-lb	115 mph R_y lbs	115 mph R_x lbs	115 mph F_a lbs	115 mph M^- in-lb	115 mph M^+ in-lb
4	52.00	485	1110	1205	-595	4665	485	1110	1205	-700	4665	485	1110	1205	-810	4665
5	42.50	490	915	1030	-560	3340	490	915	1030	-640	3340	490	915	1030	-725	3340
6	36.33	490	770	910	-545	2705	490	770	910	-615	2705	490	770	910	-685	2705
7	32.07	495	670	825	-655	2430	495	670	825	-685	2430	495	670	825	-720	2430
8	29.00	500	585	760	-1085	2375	500	585	760	-1085	2375	500	585	760	-1085	2375
9	26.72	505	525	715	-1570	2470	505	525	715	-1570	2470	505	525	715	-1570	2470
10	25.00	510	470	680	-2115	2675	510	470	680	-2115	2675	510	470	680	-2115	2675
11	23.68	515	430	655	-2695	2970	515	430	655	-2695	2970	515	430	655	-2695	2970
12	22.67	520	390	635	-3320	3345	520	390	635	-3320	3345	520	390	635	-3320	3345
13	21.88	525	360	620	-3995	3790	525	360	620	-3995	3790	525	360	620	-3995	3790
14	21.29	530	330	605	-4720	4305	530	330	605	-4720	4305	530	330	605	-4720	4305
15	20.83	535	310	595	-5500	4880	535	310	595	-5500	4880	535	310	595	-5500	4880
16	20.50	545	300	590	-6340	5520	545	295	590	-6340	5520	545	290	590	-6340	5520
17	20.26	550	305	585	-7235	6220	550	300	585	-7235	6220	550	295	585	-7235	6445
18	20.11	560	310	580	-8195	6985	560	305	580	-8195	6985	560	300	580	-8195	7525
19	20.03	565	325	575	-9215	7815	565	320	575	-9215	8220	565	315	575	-9215	9070
20	20.00	575	330	575	-10300	8705	575	325	575	-10300	9545	575	320	575	-10300	10530

Rise [T] (ft)	Radius [R] (ft)	Basic Wind Speed [V] 120 mph R_y lbs	120 mph R_x lbs	120 mph F_a lbs	120 mph M^- in-lb	120 mph M^+ in-lb	130 mph R_y lbs	130 mph R_x lbs	130 mph F_a lbs	130 mph M^- in-lb	130 mph M^+ in-lb	140 mph R_y lbs	140 mph R_x lbs	140 mph F_a lbs	140 mph M^- in-lb	140 mph M^+ in-lb
4	52.00	485	1110	1205	-925	4665	485	1110	1205	-1175	4665	485	1110	1205	-1445	4665
5	42.50	490	915	1030	-815	3340	490	915	1030	-1010	3340	490	915	1030	-1220	3340
6	36.33	490	770	910	-765	2705	490	770	910	-925	2705	490	770	910	-1105	2705
7	32.07	495	670	825	-755	2430	495	670	825	-885	2430	495	670	825	-1045	2430
8	29.00	500	585	760	-1085	2375	500	585	760	-1275	2375	500	585	760	-1520	2540
9	26.72	505	525	715	-1570	2470	505	525	715	-1570	2475	505	525	715	-1655	2890
10	25.00	510	470	680	-2115	2675	510	470	680	-2115	2955	510	470	680	-2115	3455
11	23.68	515	430	655	-2695	2970	515	430	655	-2695	3345	515	430	655	-2695	3920
12	22.67	520	390	635	-3320	3345	520	390	635	-3320	3670	520	390	635	-3320	4310
13	21.88	525	360	620	-3995	3790	525	360	620	-3995	4315	525	360	620	-3995	5070
14	21.29	530	330	605	-4720	4305	530	330	605	-4720	5045	530	330	605	-4720	5925
15	20.83	535	310	595	-5500	5135	535	310	595	-5500	6130	535	310	595	-5500	7205
16	20.50	545	285	590	-6340	6045	545	285	590	-6340	7220	545	285	590	-6340	8485
17	20.26	550	285	585	-7235	7090	550	275	585	-7235	8465	550	265	585	-7235	9955
18	20.11	560	290	580	-8195	8280	560	280	580	-8195	9890	560	265	580	-8195	11625
19	20.03	565	310	575	-9215	9955	565	295	575	-9215	11845	565	285	575	-9235	13885
20	20.00	575	315	575	-10300	11560	575	305	575	-10300	13755	575	290	575	-10640	16120

Table E-17 - 40 ft Span, Variable Wind Load.

10 psf Dead Load
20 psf Construction Load
No Ground Snow Load

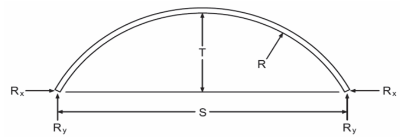

Notes:

All values normalized to C_D = 1.0.
Use ASD design procedure only.

Wind Load

K_{zt} = 1.0
K_d = 0.85

Rise [T] (ft)	Radius [R] (ft)	Basic Wind Speed [V] 150 mph R_y lbs	R_x lbs	F_a lbs	M^- in-lb	M^+ in-lb	160 mph R_y lbs	R_x lbs	F_a lbs	M^- in-lb	M^+ in-lb	170 mph R_y lbs	R_x lbs	F_a lbs	M^- in-lb	M^+ in-lb
4	52.00	485	1110	1205	-1740	4665	485	1110	1205	-2050	4665	485	1110	1205	-2385	4665
5	42.50	490	915	1030	-1450	3340	490	915	1030	-1695	3340	490	915	1030	-1960	3340
6	36.33	490	770	910	-1295	2705	490	770	910	-1505	2705	490	770	910	-1725	2705
7	32.07	495	670	825	-1215	2430	495	670	825	-1395	2430	495	670	825	-1595	2430
8	29.00	500	585	760	-1785	2925	500	585	760	-2065	3335	500	585	760	-2370	3775
9	26.72	505	525	715	-1935	3340	505	525	715	-2235	3820	505	525	715	-2555	4325
10	25.00	510	470	680	-2335	3995	510	470	680	-2690	4575	510	470	680	-3065	5195
11	23.68	515	430	655	-2695	4535	515	430	655	-2985	5200	515	430	655	-3405	5905
12	22.67	520	390	635	-3320	4995	520	390	635	-3320	5725	520	390	635	-3700	6510
13	21.88	525	360	620	-3995	5875	525	360	620	-3995	6740	525	360	620	-4285	7665
14	21.29	530	330	605	-4720	6880	530	330	605	-4720	7895	530	330	605	-4960	8975
15	20.83	535	310	595	-5500	8360	535	310	595	-5500	9595	535	310	595	-6240	10905
16	20.50	545	285	590	-6340	9850	545	285	590	-6445	11305	545	285	590	-7320	12855
17	20.26	550	265	585	-7235	11550	550	265	585	-7570	13260	550	265	585	-8580	15075
18	20.11	560	250	580	-8195	13490	560	250	580	-8860	15485	560	250	580	-10040	17610
19	20.03	565	270	575	-9775	16075	565	255	575	-11045	18435	565	260	575	-12515	20960
20	20.00	575	275	575	-11285	18660	575	260	575	-12855	21390	575	285	575	-14565	24315

Rise [T] (ft)	Radius [R] (ft)	Basic Wind Speed [V] 180 mph R_y lbs	R_x lbs	F_a lbs	M^- in-lb	M^+ in-lb	190 mph R_y lbs	R_x lbs	F_a lbs	M^- in-lb	M^+ in-lb	200 mph R_y lbs	R_x lbs	F_a lbs	M^- in-lb	M^+ in-lb
4	52.00	485	1110	1205	-2745	4665	485	1110	1205	-3120	4665	485	1110	1205	-3520	4665
5	42.50	490	915	1030	-2235	3340	490	915	1030	-2530	3340	490	915	1030	-2840	3340
6	36.33	490	770	910	-1960	2705	490	770	910	-2210	2705	490	770	910	-2475	2705
7	32.07	495	670	825	-1805	2430	495	670	825	-2030	2430	495	670	825	-2265	2430
8	29.00	500	585	760	-2690	4240	500	585	760	-3030	4730	500	585	760	-3390	5250
9	26.72	505	525	715	-2895	4870	505	525	715	-3255	5440	505	525	715	-3635	6040
10	25.00	510	470	680	-3465	5850	510	470	680	-3890	6540	510	470	680	-4340	7270
11	23.68	515	430	655	-3845	6655	515	430	655	-4310	7450	515	430	655	-4805	8285
12	22.67	520	390	635	-4180	7345	520	390	635	-4685	8225	520	390	635	-5220	9155
13	21.88	525	360	620	-4835	8640	525	360	620	-5425	9680	525	360	620	-6040	10775
14	21.29	530	330	605	-5600	10120	530	330	605	-6275	11335	530	330	605	-6990	12615
15	20.83	535	310	595	-7040	12300	535	310	595	-7885	13775	535	310	595	-8775	15325
16	20.50	545	285	590	-8255	14495	545	285	590	-9245	16235	545	300	590	-10290	18065
17	20.26	550	265	585	-9655	17005	550	290	585	-10810	19040	550	325	585	-12025	21190
18	20.11	560	280	580	-11295	19860	560	315	580	-12625	22240	560	355	580	-14020	24750
19	20.03	565	295	575	-14075	23635	565	335	575	-15725	26465	565	375	575	-17460	29445
20	20.00	575	325	575	-16375	27415	575	365	575	-18290	30695	575	410	575	-20310	34155

Table E-18 - 50 ft Span, Variable Wind Load.

10 psf Dead Load
20 psf Construction Load
No Ground Snow Load

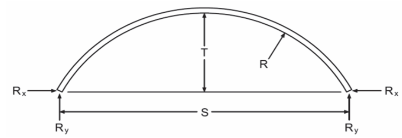

Notes:

All values normalized to C_D = 1.0.
Use ASD design procedure only.

Wind Load

K_{zt} = 1.0
K_d = 0.85

Rise [T] (ft)	Radius [R] (ft)	Basic Wind Speed [V] 105 mph					110 mph					115 mph				
		R_y lbs	R_x lbs	F_a lbs	M^- in-lb	M^+ in-lb	R_y lbs	R_x lbs	F_a lbs	M^- in-lb	M^+ in-lb	R_y lbs	R_x lbs	F_a lbs	M^- in-lb	M^+ in-lb
5	65.00	610	1425	1545	-845	4945	610	1425	1545	-970	4945	610	1425	1545	-1100	4945
6	55.08	610	1205	1345	-815	3835	610	1205	1345	-920	3835	610	1205	1345	-1030	3835
8	43.06	615	920	1095	-945	3010	615	920	1095	-990	3010	615	920	1095	-1040	3010
10	36.25	625	740	955	-1915	3060	625	740	955	-1915	3060	625	740	955	-1915	3060
12	32.04	630	615	870	-3145	3575	630	615	870	-3145	3575	630	615	870	-3145	3575
14	29.32	640	525	815	-4540	4415	640	525	815	-4540	4415	640	525	815	-4540	4415
16	27.53	655	460	775	-6130	5515	655	460	775	-6130	5515	655	460	775	-6130	5515
18	26.36	665	405	755	-7930	6870	665	405	755	-7930	6870	665	405	755	-7930	6960
20	25.63	680	370	735	-9965	8460	680	365	735	-9965	8460	680	360	735	-9965	9060
22	25.20	695	380	725	-12245	10295	695	375	725	-12245	10550	695	365	725	-12245	11665
24	25.02	710	405	720	-14770	12575	710	400	720	-14770	13945	710	390	720	-14770	15380
25	25.00	715	410	720	-16135	14170	715	405	720	-16135	15715	715	400	720	-16135	17330

Rise [T] (ft)	Radius [R] (ft)	Basic Wind Speed [V] 120 mph					130 mph					140 mph				
		R_y lbs	R_x lbs	F_a lbs	M^- in-lb	M^+ in-lb	R_y lbs	R_x lbs	F_a lbs	M^- in-lb	M^+ in-lb	R_y lbs	R_x lbs	F_a lbs	M^- in-lb	M^+ in-lb
5	65.00	610	1425	1545	-1240	4945	610	1425	1545	-1540	4945	610	1425	1545	-1865	4945
6	55.08	610	1205	1345	-1150	3835	610	1205	1345	-1400	3835	610	1205	1345	-1675	3835
8	43.06	615	920	1095	-1090	3010	615	920	1095	-1280	3010	615	920	1095	-1495	3010
10	36.25	625	740	955	-1915	3060	625	740	955	-1915	3455	625	740	955	-2265	4035
12	32.04	630	615	870	-3145	3735	630	615	870	-3145	4430	630	615	870	-3145	5180
14	29.32	640	525	815	-4540	4530	640	525	815	-4540	5390	640	525	815	-4540	6320
16	27.53	655	460	775	-6130	5575	655	460	775	-6130	6650	655	460	775	-6130	7815
18	26.36	665	405	755	-7930	7655	665	405	755	-7930	9135	665	405	755	-7930	10735
20	25.63	680	360	735	-9965	9965	680	360	735	-9965	11890	680	360	735	-9965	13975
22	25.20	695	355	725	-12245	12830	695	340	725	-12245	15310	695	320	725	-12245	17990
24	25.02	710	385	720	-14770	16880	710	365	720	-14770	20075	710	350	720	-15155	23520
25	25.00	715	390	720	-16135	19020	715	375	720	-16135	22610	715	355	720	-16970	26490

Table E-18 - 50 ft Span, Variable Wind Load.

10 psf Dead Load
20 psf Construction Load
No Ground Snow Load

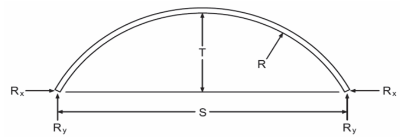

Notes:

All values normalized to C_D = 1.0.
Use ASD design procedure only.

Wind Load

K_{zt} = 1.0
K_d = 0.85

Rise [T] (ft)	Radius [R] (ft)	Basic Wind Speed [V] 150 mph					160 mph					170 mph				
		R_y lbs	R_x lbs	F_a lbs	M^- in-lb	M^+ in-lb	R_y lbs	R_x lbs	F_a lbs	M^- in-lb	M^+ in-lb	R_y lbs	R_x lbs	F_a lbs	M^- in-lb	M^+ in-lb
5	65.00	610	1425	1545	-2215	4945	610	1425	1545	-2585	4945	610	1425	1545	-2985	4945
6	55.08	610	1205	1345	-1970	3835	610	1205	1345	-2285	3835	610	1205	1345	-2620	3835
8	43.06	615	920	1095	-1740	3010	615	920	1095	-1995	3010	615	920	1095	-2270	3010
10	36.25	625	740	955	-2640	4655	625	740	955	-3045	5320	625	740	955	-3485	6025
12	32.04	630	615	870	-3400	5995	630	615	870	-3910	6865	630	615	870	-4455	7790
14	29.32	640	525	815	-4540	7320	640	525	815	-4670	8385	640	525	815	-5315	9535
16	27.53	655	460	775	-6130	9065	655	460	775	-6130	10400	655	460	775	-6495	11820
18	26.36	665	405	755	-7930	12450	665	405	755	-8110	14280	665	405	755	-9220	16235
20	25.63	680	360	735	-9965	16210	680	360	735	-10520	18600	680	360	735	-11955	21140
22	25.20	695	320	725	-12245	20865	695	320	725	-13605	23945	695	320	725	-15420	27220
24	25.02	710	330	720	-16320	27220	710	310	720	-18645	31220	710	350	720	-21120	35480
25	25.00	715	340	720	-18430	30660	715	330	720	-21055	35145	715	380	720	-23845	39940

Rise [T] (ft)	Radius [R] (ft)	Basic Wind Speed [V] 180 mph					190 mph					200 mph				
		R_y lbs	R_x lbs	F_a lbs	M^- in-lb	M^+ in-lb	R_y lbs	R_x lbs	F_a lbs	M^- in-lb	M^+ in-lb	R_y lbs	R_x lbs	F_a lbs	M^- in-lb	M^+ in-lb
5	65.00	610	1425	1545	-3410	4945	610	1425	1545	-3860	4945	610	1425	1545	-4335	4945
6	55.08	610	1205	1345	-2980	3835	610	1205	1345	-3355	3835	610	1205	1345	-3755	3835
8	43.06	615	920	1095	-2560	3010	615	920	1095	-2865	3010	615	920	1095	-3190	3030
10	36.25	625	740	955	-3945	6775	625	740	955	-4435	7565	625	740	955	-4955	8400
12	32.04	630	615	870	-5030	8770	630	615	870	-5645	9810	630	615	870	-6290	10905
14	29.32	640	525	815	-6005	10750	640	525	815	-6730	12035	640	525	815	-7490	13390
16	27.53	655	460	775	-7335	13330	655	460	775	-8220	14935	655	460	775	-9150	16625
18	26.36	665	405	755	-10400	18305	665	405	755	-11645	20490	665	405	755	-12955	22800
20	25.63	680	360	735	-13475	23840	680	360	735	-15085	26690	680	395	735	-16785	29700
22	25.20	695	355	725	-17340	30690	695	400	725	-19375	34360	695	450	725	-21545	38230
24	25.02	710	395	720	-23745	40000	710	450	720	-26520	44780	710	500	720	-29445	49815
25	25.00	715	430	720	-26805	45025	715	485	720	-29935	50400	715	540	720	-33230	56065

Table E-19 - 60 ft Span, Variable Wind Load.

10 psf Dead Load
20 psf Construction Load
No Ground Snow Load

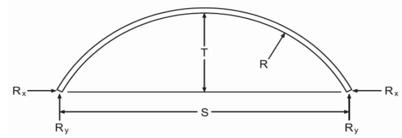

Notes:

All values normalized to C_D = 1.0.
Use ASD design procedure only.

Wind Load

K_{zt} = 1.0
K_d = 0.85

Rise [T] (ft)	Radius [R] (ft)	Basic Wind Speed [V] 105 mph					110 mph					115 mph				
		R_y lbs	R_x lbs	F_a lbs	M^- in-lb	M^+ in-lb	R_y lbs	R_x lbs	F_a lbs	M^- in-lb	M^+ in-lb	R_y lbs	R_x lbs	F_a lbs	M^- in-lb	M^+ in-lb
6	78.00	730	1740	1875	-1140	5215	730	1740	1875	-1295	5215	730	1740	1875	-1455	5215
8	60.25	735	1325	1505	-1110	3795	735	1325	1505	-1235	3795	735	1325	1505	-1365	3795
10	50.00	740	1065	1285	-1725	3555	740	1065	1285	-1725	3555	740	1065	1285	-1785	3555
12	43.50	745	890	1150	-2960	3900	745	890	1150	-2960	3900	745	890	1150	-2960	3900
14	39.14	755	760	1060	-4375	4615	755	760	1060	-4375	4615	755	760	1060	-4375	4615
16	36.13	765	665	995	-5960	5620	765	665	995	-5960	5620	765	665	995	-5960	5670
18	34.00	775	590	950	-7735	6875	775	590	950	-7735	6875	775	590	950	-7735	6875
20	32.50	790	525	920	-9730	8370	790	525	920	-9730	8370	790	525	920	-9730	8375
22	31.45	800	475	900	-11950	10095	800	475	900	-11950	10095	800	475	900	-11950	10950
24	30.75	815	440	885	-14400	12055	815	430	885	-14400	12330	815	430	885	-14400	13625
26	30.31	830	450	875	-17100	14250	830	440	875	-17100	15225	830	430	875	-17100	16830
28	30.07	845	475	865	-20050	17435	845	470	865	-20050	19330	845	460	865	-20050	21315
30	30.00	860	490	860	-23265	21300	860	480	860	-23265	23610	860	475	860	-23265	26030

Rise [T] (ft)	Radius [R] (ft)	Basic Wind Speed [V] 120 mph					130 mph					140 mph				
		R_y lbs	R_x lbs	F_a lbs	M^- in-lb	M^+ in-lb	R_y lbs	R_x lbs	F_a lbs	M^- in-lb	M^+ in-lb	R_y lbs	R_x lbs	F_a lbs	M^- in-lb	M^+ in-lb
6	78.00	730	1740	1875	-1625	5215	730	1740	1875	-1980	5215	730	1740	1875	-2370	5215
8	60.25	735	1325	1505	-1500	3795	735	1325	1505	-1790	3795	735	1325	1505	-2105	3795
10	50.00	740	1065	1285	-1850	3555	740	1065	1285	-1990	3555	740	1065	1285	-2160	3555
12	43.50	745	890	1150	-2960	4235	745	890	1150	-2960	5015	745	890	1150	-3170	5865
14	39.14	755	760	1060	-4375	4950	755	760	1060	-4375	5890	755	760	1060	-4375	6905
16	36.13	765	665	995	-5960	6225	765	665	995	-5960	7400	765	665	995	-5960	8675
18	34.00	775	590	950	-7735	7275	775	590	950	-7735	8675	775	590	950	-7735	10185
20	32.50	790	525	920	-9730	9210	790	525	920	-9730	10985	790	525	920	-9730	12905
22	31.45	800	475	900	-11950	12040	800	475	900	-11950	14360	800	475	900	-11950	16865
24	30.75	815	430	885	-14400	14985	815	430	885	-14400	17870	815	430	885	-14400	20990
26	30.31	830	420	875	-17100	18505	830	400	875	-17100	22070	830	390	875	-17100	25920
28	30.07	845	450	865	-20050	23385	845	430	865	-20050	27795	845	405	865	-20535	32555
30	30.00	860	465	860	-23265	28560	860	445	860	-23385	33940	860	420	860	-24850	39745

Table E-19 - 60 ft Span, Variable Wind Load.

10 psf Dead Load
20 psf Construction Load
No Ground Snow Load

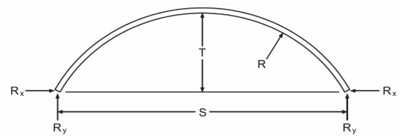

Notes:

All values normalized to C_D = 1.0.
Use ASD design procedure only.

Wind Load

K_{zt} = 1.0
K_d = 0.85

Rise [T] (ft)	Radius [R] (ft)	Basic Wind Speed [V]														
		150 mph					160 mph					170 mph				
		R_y lbs	R_x lbs	F_a lbs	M^- in-lb	M^+ in-lb	R_y lbs	R_x lbs	F_a lbs	M^- in-lb	M^+ in-lb	R_y lbs	R_x lbs	F_a lbs	M^- in-lb	M^+ in-lb
6	78.00	730	1740	1875	-2795	5215	730	1740	1875	-3245	5215	730	1740	1875	-3730	5215
8	60.25	735	1325	1505	-2440	3795	735	1325	1505	-2810	3795	735	1325	1505	-3200	3795
10	50.00	740	1065	1285	-2340	3555	740	1065	1285	-2635	3555	740	1065	1285	-2980	3555
12	43.50	745	890	1150	-3690	6770	745	890	1150	-4245	7740	745	890	1150	-4845	8775
14	39.14	755	760	1060	-4375	7995	755	760	1060	-4865	9155	755	760	1060	-5540	10395
16	36.13	765	665	995	-5960	10040	765	665	995	-6340	11510	765	665	995	-7215	13080
18	34.00	775	590	950	-7735	11810	775	590	950	-7735	13545	775	590	950	-8420	15395
20	32.50	790	525	920	-9730	14970	790	525	920	-9730	17170	790	525	920	-10580	19520
22	31.45	800	475	900	-11950	19555	800	475	900	-12660	22435	800	475	900	-14390	25495
24	30.75	815	430	885	-14400	24340	815	430	885	-15730	27920	815	430	885	-17870	31735
26	30.31	830	390	875	-17100	30060	830	390	875	-19505	34480	830	390	875	-22100	39185
28	30.07	845	385	865	-22500	37695	845	360	865	-25700	43230	845	415	865	-29110	49115
30	30.00	860	400	860	-27590	45985	860	415	860	-31510	52720	860	475	860	-35680	59900

Rise [T] (ft)	Radius [R] (ft)	Basic Wind Speed [V]														
		180 mph					190 mph					200 mph				
		R_y lbs	R_x lbs	F_a lbs	M^- in-lb	M^+ in-lb	R_y lbs	R_x lbs	F_a lbs	M^- in-lb	M^+ in-lb	R_y lbs	R_x lbs	F_a lbs	M^- in-lb	M^+ in-lb
6	78.00	730	1740	1875	-4240	5215	730	1740	1875	-4780	5215	730	1740	1875	-5350	5215
8	60.25	735	1325	1505	-3615	3795	735	1325	1505	-4050	3795	735	1325	1505	-4515	4080
10	50.00	740	1065	1285	-3350	3875	740	1065	1285	-3740	4330	740	1065	1285	-4150	4810
12	43.50	745	890	1150	-5480	9870	745	890	1150	-6155	11030	745	890	1150	-6860	12250
14	39.14	755	760	1060	-6255	11710	755	760	1060	-7010	13100	755	760	1060	-7810	14565
16	36.13	765	665	995	-8140	14745	765	665	995	-9120	16505	765	665	995	-10150	18360
18	34.00	775	590	950	-9500	17370	775	590	950	-10645	19455	775	590	950	-11850	21655
20	32.50	790	525	920	-11935	22005	790	525	920	-13365	24635	790	525	920	-14875	27425
22	31.45	800	475	900	-16220	28740	800	475	900	-18155	32175	800	475	900	-20195	35790
24	30.75	815	430	885	-20140	35775	815	440	885	-22540	40050	815	495	885	-25065	44555
26	30.31	830	435	875	-24850	44175	830	490	875	-27800	49450	830	550	875	-30915	55015
28	30.07	845	475	865	-32720	55365	845	535	865	-36545	61965	845	595	865	-40570	68925
30	30.00	860	535	860	-40105	67510	860	605	860	-44780	75555	860	675	860	-49710	84035

Table E-20 - 70 ft Span, Variable Wind Load.

15 psf Dead Load
20 psf Construction Load
No Ground Snow Load

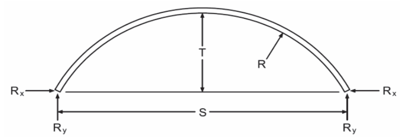

Notes:

All values normalized to C_D = 1.0.
Use ASD design procedure only.

Wind Load

K_{zt} = 1.0
K_d = 0.85

Rise [T] (ft)	Radius [R] (ft)	Basic Wind Speed [V] 105 mph R_y lbs	105 mph R_x lbs	105 mph F_a lbs	105 mph M^- in-lb	105 mph M^+ in-lb	110 mph R_y lbs	110 mph R_x lbs	110 mph F_a lbs	110 mph M^- in-lb	110 mph M^+ in-lb	115 mph R_y lbs	115 mph R_x lbs	115 mph F_a lbs	115 mph M^- in-lb	115 mph M^+ in-lb
6	105.08	990	2760	2925	-1255	7970	990	2760	2925	-1460	7970	990	2760	2925	-1670	7970
8	80.56	995	2105	2320	-1365	5470	995	2105	2320	-1530	5470	995	2105	2320	-1700	5470
10	66.25	1005	1695	1960	-1845	4775	1005	1695	1960	-1930	4775	1005	1695	1960	-2015	4775
12	57.04	1015	1420	1730	-3120	4920	1015	1420	1730	-3120	4920	1015	1420	1730	-3120	4920
14	50.75	1025	1220	1575	-4750	5575	1025	1220	1575	-4750	5575	1025	1220	1575	-4750	5575
16	46.28	1040	1065	1470	-6580	6605	1040	1065	1470	-6580	6605	1040	1065	1470	-6580	6605
18	43.03	1055	950	1390	-8620	7940	1055	950	1390	-8620	7940	1055	950	1390	-8620	7940
20	40.63	1070	850	1340	-10900	9560	1070	850	1340	-10900	9560	1070	850	1340	-10900	9560
22	38.84	1085	770	1300	-13430	11455	1085	770	1300	-13430	11455	1085	770	1300	-13430	11455
24	37.52	1105	705	1270	-16240	13615	1105	705	1270	-16240	13615	1105	705	1270	-16240	13615
26	36.56	1125	650	1250	-19330	16045	1125	645	1250	-19330	16045	1125	645	1250	-19330	16045
28	35.88	1145	665	1235	-22715	18750	1145	650	1235	-22715	18750	1145	640	1235	-22715	18750
30	35.42	1165	680	1230	-26410	21740	1165	665	1230	-26410	21740	1165	655	1230	-26410	21835
32	35.14	1185	695	1225	-30425	25015	1185	685	1225	-30425	25015	1185	670	1225	-30425	26075
34	35.01	1210	730	1220	-34765	28580	1210	720	1220	-34765	29065	1210	710	1220	-34765	32195
35	35.00	1220	740	1220	-37060	30480	1220	730	1220	-37060	31660	1220	720	1220	-37060	35060

Rise [T] (ft)	Radius [R] (ft)	Basic Wind Speed [V] 120 mph R_y lbs	120 mph R_x lbs	120 mph F_a lbs	120 mph M^- in-lb	120 mph M^+ in-lb	130 mph R_y lbs	130 mph R_x lbs	130 mph F_a lbs	130 mph M^- in-lb	130 mph M^+ in-lb	140 mph R_y lbs	140 mph R_x lbs	140 mph F_a lbs	140 mph M^- in-lb	140 mph M^+ in-lb
6	105.08	990	2760	2925	-1890	7970	990	2760	2925	-2370	7970	990	2760	2925	-2895	7970
8	80.56	995	2105	2320	-1880	5470	995	2105	2320	-2265	5470	995	2105	2320	-2690	5470
10	66.25	1005	1695	1960	-2110	4775	1005	1695	1960	-2305	4775	1005	1695	1960	-2640	4775
12	57.04	1015	1420	1730	-3120	4920	1015	1420	1730	-3200	4920	1015	1420	1730	-3405	4920
14	50.75	1025	1220	1575	-4750	5575	1025	1220	1575	-4750	6650	1025	1220	1575	-4750	7815
16	46.28	1040	1065	1470	-6580	6605	1040	1065	1470	-6580	7665	1040	1065	1470	-6580	9040
18	43.03	1055	950	1390	-8620	7965	1055	950	1390	-8620	9540	1055	950	1390	-8620	11235
20	40.63	1070	850	1340	-10900	9560	1070	850	1340	-10900	11175	1070	850	1340	-10900	13190
22	38.84	1085	770	1300	-13430	11455	1085	770	1300	-13430	12965	1085	770	1300	-13430	15330
24	37.52	1105	705	1270	-16240	13615	1105	705	1270	-16240	15795	1105	705	1270	-16240	18685
26	36.56	1125	645	1250	-19330	16625	1125	645	1250	-19330	19985	1125	645	1250	-19330	23625
28	35.88	1145	625	1235	-22715	20055	1145	600	1235	-22715	24085	1145	590	1235	-22715	28475
30	35.42	1165	640	1230	-26410	24065	1165	615	1230	-26410	28875	1165	585	1230	-26410	34135
32	35.14	1185	655	1225	-30425	28735	1185	630	1225	-30425	34450	1185	600	1225	-30425	40720
34	35.01	1210	695	1220	-34765	35465	1210	675	1220	-34765	42415	1210	645	1220	-35190	49925
35	35.00	1220	710	1220	-37060	38615	1220	685	1220	-37060	46180	1220	660	1220	-38130	54350

Table E-20 - 70 ft Span, Variable Wind Load.

15 psf Dead Load
20 psf Construction Load
No Ground Snow Load

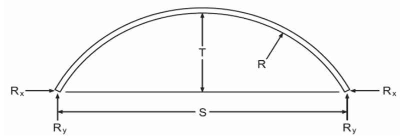

Notes:

All values normalized to C_D = 1.0.
Use ASD design procedure only.

Wind Load

K_{zt} = 1.0
K_d = 0.85

Rise [T] (ft)	Radius [R] (ft)	Basic Wind Speed [V] 150 mph R_y lbs	R_x lbs	F_a lbs	M^- in-lb	M^+ in-lb	160 mph R_y lbs	R_x lbs	F_a lbs	M^- in-lb	M^+ in-lb	170 mph R_y lbs	R_x lbs	F_a lbs	M^- in-lb	M^+ in-lb
6	105.08	990	2760	2925	-3460	7970	990	2760	2925	-4065	7970	990	2760	2925	-4710	7970
8	80.56	995	2105	2320	-3150	5470	995	2105	2320	-3645	5470	995	2105	2320	-4165	5470
10	66.25	1005	1695	1960	-3045	4775	1005	1695	1960	-3480	4775	1005	1695	1960	-3945	4775
12	57.04	1015	1420	1730	-3635	4920	1015	1420	1730	-3880	4920	1015	1420	1730	-4145	4920
14	50.75	1025	1220	1575	-4750	9065	1025	1220	1575	-5455	10400	1025	1220	1575	-6240	11820
16	46.28	1040	1065	1470	-6580	10515	1040	1065	1470	-6580	12090	1040	1065	1470	-7155	13770
18	43.03	1055	950	1390	-8620	13055	1055	950	1390	-8620	15005	1055	950	1390	-9300	17080
20	40.63	1070	850	1340	-10900	15350	1070	850	1340	-10900	17665	1070	850	1340	-10900	20125
22	38.84	1085	770	1300	-13430	17865	1085	770	1300	-13430	20580	1085	770	1300	-13430	23470
24	37.52	1105	705	1270	-16240	21790	1105	705	1270	-16240	25105	1105	705	1270	-16240	28635
26	36.56	1125	645	1250	-19330	27535	1125	645	1250	-19330	31710	1125	645	1250	-20375	36160
28	35.88	1145	590	1235	-22715	33185	1145	590	1235	-22715	38225	1145	590	1235	-24675	43590
30	35.42	1165	550	1230	-26410	39785	1165	545	1230	-26410	45820	1165	545	1230	-29715	52250
32	35.14	1185	565	1225	-30425	47450	1185	530	1225	-31375	54645	1185	505	1225	-35605	62305
34	35.01	1210	620	1220	-37195	57990	1210	590	1220	-40100	66615	1210	555	1220	-45480	75790
35	35.00	1220	630	1220	-40345	63125	1220	600	1220	-43745	72505	1220	570	1220	-49605	82490

Rise [T] (ft)	Radius [R] (ft)	Basic Wind Speed [V] 180 mph R_y lbs	R_x lbs	F_a lbs	M^- in-lb	M^+ in-lb	190 mph R_y lbs	R_x lbs	F_a lbs	M^- in-lb	M^+ in-lb	200 mph R_y lbs	R_x lbs	F_a lbs	M^- in-lb	M^+ in-lb
6	105.08	990	2760	2925	-5395	7970	990	2760	2925	-6130	7970	990	2760	2925	-6900	7970
8	80.56	995	2105	2320	-4720	5470	995	2105	2320	-5305	5470	995	2105	2320	-5925	5470
10	66.25	1005	1695	1960	-4435	4915	1005	1695	1960	-4950	5485	1005	1695	1960	-5500	6085
12	57.04	1015	1420	1730	-4430	5440	1015	1420	1730	-4895	6100	1015	1420	1730	-5400	6795
14	50.75	1025	1220	1575	-7070	13325	1025	1220	1575	-7945	14920	1025	1220	1575	-8875	16600
16	46.28	1040	1065	1470	-8105	15550	1040	1065	1470	-9105	17430	1040	1065	1470	-10165	19415
18	43.03	1055	950	1390	-10520	19280	1055	950	1390	-11810	21615	1055	950	1390	-13170	24090
20	40.63	1070	850	1340	-12325	22735	1070	850	1340	-13835	25495	1070	850	1340	-15430	28405
22	38.84	1085	770	1300	-14325	26535	1085	770	1300	-16085	29770	1085	770	1300	-17935	33185
24	37.52	1105	705	1270	-17415	32380	1105	705	1270	-19550	36340	1105	705	1270	-21795	40510
26	36.56	1125	645	1250	-23005	40880	1125	645	1250	-25805	45870	1125	645	1250	-28750	51125
28	35.88	1145	590	1235	-27790	49280	1145	590	1235	-31090	55290	1145	590	1235	-34630	61630
30	35.42	1165	545	1230	-33465	59065	1165	545	1230	-37430	66275	1165	615	1230	-41605	73870
32	35.14	1185	535	1225	-40085	70430	1185	605	1225	-44825	79020	1185	685	1225	-49825	88070
34	35.01	1210	580	1220	-51185	85530	1210	660	1220	-57215	95935	1210	740	1220	-63570	106905
35	35.00	1220	615	1220	-55820	93080	1220	695	1220	-62390	104375	1220	785	1220	-69315	116300

Table E-21 - 80 ft Span, Variable Wind Load.

15 psf Dead Load
20 psf Construction Load
No Ground Snow Load

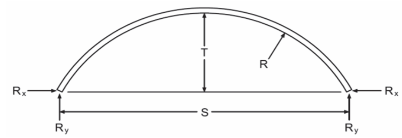

Notes:

All values normalized to C_D = 1.0.
Use ASD design procedure only.

Wind Load

K_{zt} = 1.0
K_d = 0.85

Rise [T] (ft)	Radius [R] (ft)	Basic Wind Speed [V] 105 mph R_y lbs	R_x lbs	F_a lbs	M^- in-lb	M^+ in-lb	110 mph R_y lbs	R_x lbs	F_a lbs	M^- in-lb	M^+ in-lb	115 mph R_y lbs	R_x lbs	F_a lbs	M^- in-lb	M^+ in-lb
8	104.00	1135	2750	2960	-1735	6725	1135	2750	2960	-1950	6725	1135	2750	2960	-2180	6725
12	72.67	1150	1855	2165	-2900	5470	1150	1855	2165	-2980	5470	1150	1855	2165	-3085	5470
16	58.00	1170	1395	1800	-6385	6865	1170	1395	1800	-6385	6865	1170	1395	1800	-6385	6865
20	50.00	1200	1115	1610	-10680	9630	1200	1115	1610	-10680	9630	1200	1115	1610	-10680	9630
24	45.33	1230	925	1505	-15925	13490	1230	925	1505	-15925	13490	1230	925	1505	-15925	13490
28	42.57	1265	785	1445	-22235	18400	1265	785	1445	-22235	18400	1265	785	1445	-22235	18400
32	41.00	1305	755	1415	-29710	24385	1305	740	1415	-29710	24385	1305	725	1415	-29710	24545
36	40.22	1350	785	1400	-38420	31480	1350	770	1400	-38420	31480	1350	755	1400	-38420	33660
40	40.00	1395	840	1395	-48430	39745	1395	830	1395	-48430	42710	1395	815	1395	-48430	47285

Rise [T] (ft)	Radius [R] (ft)	Basic Wind Speed [V] 120 mph R_y lbs	R_x lbs	F_a lbs	M^- in-lb	M^+ in-lb	130 mph R_y lbs	R_x lbs	F_a lbs	M^- in-lb	M^+ in-lb	140 mph R_y lbs	R_x lbs	F_a lbs	M^- in-lb	M^+ in-lb
8	104.00	1135	2750	2960	-2415	6725	1135	2750	2960	-2920	6725	1135	2750	2960	-3480	6725
12	72.67	1150	1855	2165	-3200	5470	1150	1855	2165	-3435	5470	1150	1855	2165	-3725	5470
16	58.00	1170	1395	1800	-6385	7395	1170	1395	1800	-6385	8830	1170	1395	1800	-6385	10380
20	50.00	1200	1115	1610	-10680	10335	1200	1115	1610	-10680	12360	1200	1115	1610	-10680	14550
24	45.33	1230	925	1505	-15925	13490	1230	925	1505	-15925	15805	1230	925	1505	-15925	18670
28	42.57	1265	785	1445	-22235	18590	1265	785	1445	-22235	22370	1265	785	1445	-22235	26450
32	41.00	1305	710	1415	-29710	27045	1305	675	1415	-29710	32485	1305	675	1415	-29710	38385
36	40.22	1350	740	1400	-38420	37090	1350	710	1400	-38420	44480	1350	670	1400	-38420	52545
40	40.00	1395	805	1395	-48430	52060	1395	775	1395	-48430	62225	1395	745	1395	-50375	73200

Table E-21 - 80 ft Span, Variable Wind Load.

15 psf Dead Load
20 psf Construction Load
No Ground Snow Load

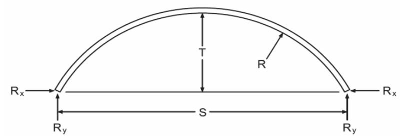

Notes:

All values normalized to C_D = 1.0.
Use ASD design procedure only.

Wind Load

K_{zt} = 1.0
K_d = 0.85

Rise [T] (ft)	Radius [R] (ft)	Basic Wind Speed [V]														
		150 mph					160 mph					170 mph				
		R_y lbs	R_x lbs	F_a lbs	M^- in-lb	M^+ in-lb	R_y lbs	R_x lbs	F_a lbs	M^- in-lb	M^+ in-lb	R_y lbs	R_x lbs	F_a lbs	M^- in-lb	M^+ in-lb
8	104.00	1135	2750	2960	-4085	6725	1135	2750	2960	-4725	6725	1135	2750	2960	-5410	6725
12	72.67	1150	1855	2165	-4035	5470	1150	1855	2165	-4475	5470	1150	1855	2165	-5020	5990
16	58.00	1170	1395	1800	-6385	12045	1170	1395	1800	-7160	13820	1170	1395	1800	-8175	15715
20	50.00	1200	1115	1610	-10680	16900	1200	1115	1610	-10680	19415	1200	1115	1610	-11970	22090
24	45.33	1230	925	1505	-15925	21750	1230	925	1505	-15925	25045	1230	925	1505	-15925	28550
28	42.57	1265	785	1445	-22235	30830	1265	785	1445	-22235	35515	1265	785	1445	-22235	40500
32	41.00	1305	675	1415	-29710	44720	1305	675	1415	-29710	51495	1305	675	1415	-33155	58705
36	40.22	1350	635	1400	-38420	61205	1350	595	1400	-40330	70465	1350	590	1400	-45760	80320
40	40.00	1395	710	1395	-53345	84990	1395	675	1395	-58810	97595	1395	640	1395	-66680	111010

Rise [T] (ft)	Radius [R] (ft)	Basic Wind Speed [V]														
		180 mph					190 mph					200 mph				
		R_y lbs	R_x lbs	F_a lbs	M^- in-lb	M^+ in-lb	R_y lbs	R_x lbs	F_a lbs	M^- in-lb	M^+ in-lb	R_y lbs	R_x lbs	F_a lbs	M^- in-lb	M^+ in-lb
8	104.00	1135	2750	2960	-6140	6725	1135	2750	2960	-6910	6725	1135	2750	2960	-7720	6925
12	72.67	1150	1855	2165	-5595	6745	1150	1855	2165	-6210	7545	1150	1855	2165	-6875	8390
16	58.00	1170	1395	1800	-9255	17725	1170	1395	1800	-10395	19845	1170	1395	1800	-11600	22080
20	50.00	1200	1115	1610	-13535	24930	1200	1115	1610	-15185	27960	1200	1115	1610	-16925	31150
24	45.33	1230	925	1505	-17385	32265	1230	925	1505	-19515	36195	1230	925	1505	-21760	40340
28	42.57	1265	785	1445	-24540	45785	1265	785	1445	-27535	51380	1265	785	1445	-30695	57270
32	41.00	1305	675	1415	-37335	66350	1305	675	1415	-41775	74430	1305	675	1415	-46530	82955
36	40.22	1350	610	1400	-51515	90775	1350	695	1400	-57605	101825	1350	785	1400	-64020	113475
40	40.00	1395	725	1395	-75025	125250	1395	820	1395	-83850	140455	1395	925	1395	-93150	156480

Table E-22 - 90 ft Span, Variable Wind Load.

15 psf Dead Load
20 psf Construction Load
No Ground Snow Load

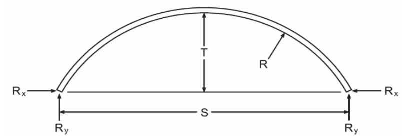

Notes:

All values normalized to C_D = 1.0.
Use ASD design procedure only.

Wind Load

K_{zt} = 1.0
K_d = 0.85

Rise [T] (ft)	Radius [R] (ft)	Basic Wind Speed [V]														
		105 mph					110 mph					115 mph				
		R_y lbs	R_x lbs	F_a lbs	M^- in-lb	M^+ in-lb	R_y lbs	R_x lbs	F_a lbs	M^- in-lb	M^+ in-lb	R_y lbs	R_x lbs	F_a lbs	M^- in-lb	M^+ in-lb
8	130.56	1275	3475	3690	-2160	8150	1275	3475	3690	-2435	8150	1275	3475	3690	-2725	8150
12	90.38	1290	2345	2660	-2990	6095	1290	2345	2660	-3125	6095	1290	2345	2660	-3260	6095
16	71.28	1305	1765	2175	-6185	7185	1305	1765	2175	-6185	7185	1305	1765	2175	-6185	7185
20	60.63	1330	1415	1915	-10485	9760	1330	1415	1915	-10485	9760	1330	1415	1915	-10485	9850
24	54.19	1360	1175	1765	-15670	13460	1360	1175	1765	-15670	13460	1360	1175	1765	-15670	13460
28	50.16	1390	1000	1675	-21870	18185	1390	1000	1675	-21870	18185	1390	1000	1675	-21870	18185
32	47.64	1430	870	1620	-29165	23945	1430	870	1620	-29165	23945	1430	870	1620	-29165	23945
36	46.13	1470	845	1590	-37635	30770	1470	825	1590	-37635	30770	1470	810	1590	-37635	31960
40	45.31	1515	875	1575	-47345	38700	1515	860	1575	-47345	38700	1515	840	1575	-47345	42350
42	45.11	1535	915	1570	-52685	43095	1535	900	1570	-52685	45500	1535	885	1570	-52685	50370
45	45.00	1570	945	1570	-61315	50245	1570	930	1570	-61315	55620	1570	915	1570	-61315	61555

Rise [T] (ft)	Radius [R] (ft)	Basic Wind Speed [V]														
		120 mph					130 mph					140 mph				
		R_y lbs	R_x lbs	F_a lbs	M^- in-lb	M^+ in-lb	R_y lbs	R_x lbs	F_a lbs	M^- in-lb	M^+ in-lb	R_y lbs	R_x lbs	F_a lbs	M^- in-lb	M^+ in-lb
8	130.56	1275	3475	3690	-3030	8150	1275	3475	3690	-3670	8150	1275	3475	3690	-4380	8150
12	90.38	1290	2345	2660	-3405	6095	1290	2345	2660	-3735	6095	1290	2345	2660	-4245	6095
16	71.28	1305	1765	2175	-6185	7185	1305	1765	2175	-6185	7185	1305	1765	2175	-6225	7185
20	60.63	1330	1415	1915	-10485	10860	1330	1415	1915	-10485	13010	1330	1415	1915	-10485	15325
24	54.19	1360	1175	1765	-15670	14740	1360	1175	1765	-15670	17655	1360	1175	1765	-15670	20805
28	50.16	1390	1000	1675	-21870	18535	1390	1000	1675	-21870	22275	1390	1000	1675	-21870	26315
32	47.64	1430	870	1620	-29165	26270	1430	870	1620	-29165	31560	1430	870	1620	-29165	37270
36	46.13	1470	795	1590	-37635	35205	1470	760	1590	-37635	42295	1470	760	1590	-37635	49950
40	45.31	1515	825	1575	-47345	46650	1515	785	1575	-47345	55960	1515	745	1575	-47345	66075
42	45.11	1535	870	1570	-52685	55450	1535	835	1570	-52685	66265	1535	800	1570	-53230	77945
45	45.00	1570	900	1570	-61315	67755	1570	865	1570	-61315	80940	1570	830	1570	-64405	95185

Table E-22 - 90 ft Span, Variable Wind Load.

15 psf Dead Load
20 psf Construction Load
No Ground Snow Load

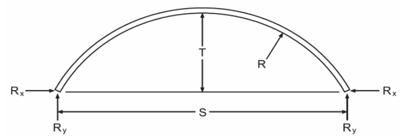

Notes:

All values normalized to C_D = 1.0.
Use ASD design procedure only.

Wind Load

K_{zt} = 1.0
K_d = 0.85

Rise [T] (ft)	Radius [R] (ft)	Basic Wind Speed [V]														
		150 mph					160 mph					170 mph				
		R_y lbs	R_x lbs	F_a lbs	M^- in-lb	M^+ in-lb	R_y lbs	R_x lbs	F_a lbs	M^- in-lb	M^+ in-lb	R_y lbs	R_x lbs	F_a lbs	M^- in-lb	M^+ in-lb
8	130.56	1275	3475	3690	-5145	8150	1275	3475	3690	-5965	8150	1275	3475	3690	-6835	8150
12	90.38	1290	2345	2660	-4855	6095	1290	2345	2660	-5505	6455	1290	2345	2660	-6205	7310
16	71.28	1305	1765	2175	-6585	7185	1305	1765	2175	-6965	7385	1305	1765	2175	-7370	8440
20	60.63	1330	1415	1915	-10485	17815	1330	1415	1915	-10485	20480	1330	1415	1915	-11925	23315
24	54.19	1360	1175	1765	-15670	24185	1360	1175	1765	-15670	27795	1360	1175	1765	-17025	31645
28	50.16	1390	1000	1675	-21870	30650	1390	1000	1675	-21870	35285	1390	1000	1675	-21870	40220
32	47.64	1430	870	1620	-29165	43400	1430	870	1620	-29165	49960	1430	870	1620	-31955	56935
36	46.13	1470	760	1590	-37635	58175	1470	760	1590	-37915	66965	1470	760	1590	-43030	76320
40	45.31	1515	700	1575	-47345	76940	1515	670	1575	-50555	88555	1515	670	1575	-57355	100920
42	45.11	1535	760	1570	-56265	90490	1535	720	1570	-62225	103900	1535	675	1570	-70560	118175
45	45.00	1570	795	1570	-68255	110480	1570	755	1570	-76360	126835	1570	735	1570	-86565	144245

Rise [T] (ft)	Radius [R] (ft)	Basic Wind Speed [V]														
		180 mph					190 mph					200 mph				
		R_y lbs	R_x lbs	F_a lbs	M^- in-lb	M^+ in-lb	R_y lbs	R_x lbs	F_a lbs	M^- in-lb	M^+ in-lb	R_y lbs	R_x lbs	F_a lbs	M^- in-lb	M^+ in-lb
8	130.56	1275	3475	3690	-7760	8150	1275	3475	3690	-8735	8150	1275	3475	3690	-9765	8600
12	90.38	1290	2345	2660	-6960	8215	1290	2345	2660	-7760	9175	1290	2345	2660	-8605	10190
16	71.28	1305	1765	2175	-7805	9560	1305	1765	2175	-8260	10745	1305	1765	2175	-8760	11990
20	60.63	1330	1415	1915	-13485	26320	1330	1415	1915	-15135	29500	1330	1415	1915	-16870	32850
24	54.19	1360	1175	1765	-19240	35725	1360	1175	1765	-21580	40040	1360	1175	1765	-24045	44625
28	50.16	1390	1000	1675	-24380	45455	1390	1000	1675	-27355	50990	1390	1000	1675	-30490	56825
32	47.64	1430	870	1620	-36090	64340	1430	870	1620	-40465	72165	1430	870	1620	-45075	80410
36	46.13	1470	760	1590	-48450	86245	1470	760	1590	-54225	96735	1470	760	1590	-60395	107795
40	45.31	1515	695	1575	-64565	114030	1515	790	1575	-72185	127895	1515	890	1575	-80220	142510
42	45.11	1535	735	1570	-79395	133455	1535	830	1570	-88740	149650	1535	935	1570	-98590	166720
45	45.00	1570	840	1570	-97390	162765	1570	950	1570	-108835	182490	1570	1065	1570	-120895	203285

Table E-23 - 100 ft Span, Variable Wind Load.

15 psf Dead Load
20 psf Construction Load
No Ground Snow Load

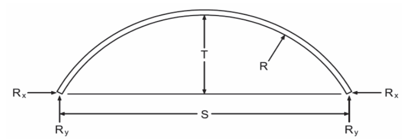

Notes:

All values normalized to C_D = 1.0.
Use ASD design procedure only.

Wind Load

K_{zt} = 1.0
K_d = 0.85

Rise [T] (ft)	Radius [R] (ft)	Basic Wind Speed [V]														
		105 mph					110 mph					115 mph				
		R_y lbs	R_x lbs	F_a lbs	M^- in-lb	M^+ in-lb	R_y lbs	R_x lbs	F_a lbs	M^- in-lb	M^+ in-lb	R_y lbs	R_x lbs	F_a lbs	M^- in-lb	M^+ in-lb
10	130.00	1420	3460	3725	-2750	7510	1420	3460	3725	-3055	7510	1420	3460	3725	-3375	7510
14	96.29	1435	2490	2855	-4230	6915	1435	2490	2855	-4385	6915	1435	2490	2855	-4545	6915
18	78.44	1455	1940	2400	-8045	8590	1455	1940	2400	-8045	8590	1455	1940	2400	-8045	8590
22	67.82	1475	1585	2140	-12765	11590	1475	1585	2140	-12765	11590	1475	1585	2140	-12765	12330
26	61.08	1505	1340	1980	-18390	15655	1505	1340	1980	-18390	15655	1505	1340	1980	-18390	16335
30	56.67	1535	1155	1880	-25020	20730	1535	1155	1880	-25020	20730	1535	1155	1880	-25020	20730
34	53.76	1575	1015	1820	-32740	26815	1575	1015	1820	-32740	26815	1575	1015	1820	-32740	26815
38	51.89	1610	920	1780	-41610	33940	1610	900	1780	-41610	33940	1610	895	1780	-41610	35510
42	50.76	1655	950	1755	-51695	42150	1655	930	1755	-51695	42150	1655	910	1755	-51695	46005
46	50.17	1700	980	1745	-63045	51480	1700	960	1745	-63045	53300	1700	945	1745	-63045	59015
50	50.00	1745	1045	1745	-75720	63275	1745	1030	1745	-75720	70435	1745	1010	1745	-75720	77925

Rise [T] (ft)	Radius [R] (ft)	Basic Wind Speed [V]														
		120 mph					130 mph					140 mph				
		R_y lbs	R_x lbs	F_a lbs	M^- in-lb	M^+ in-lb	R_y lbs	R_x lbs	F_a lbs	M^- in-lb	M^+ in-lb	R_y lbs	R_x lbs	F_a lbs	M^- in-lb	M^+ in-lb
10	130.00	1420	3460	3725	-3710	7510	1420	3460	3725	-4415	7510	1420	3460	3725	-5185	7510
14	96.29	1435	2490	2855	-4720	6915	1435	2490	2855	-5125	6915	1435	2490	2855	-5565	6915
18	78.44	1455	1940	2400	-8045	8590	1455	1940	2400	-8045	8590	1455	1940	2400	-8045	8590
22	67.82	1475	1585	2140	-12765	13590	1475	1585	2140	-12765	16270	1475	1585	2140	-12765	19165
26	61.08	1505	1340	1980	-18390	17995	1505	1340	1980	-18390	21535	1505	1340	1980	-18390	25360
30	56.67	1535	1155	1880	-25020	21705	1535	1155	1880	-25020	26060	1535	1155	1880	-25020	30770
34	53.76	1575	1015	1820	-32740	28690	1575	1015	1820	-32740	34470	1575	1015	1820	-32740	40720
38	51.89	1610	895	1780	-41610	39160	1610	895	1780	-41610	47020	1610	895	1780	-41610	55505
42	50.76	1655	890	1755	-51695	50665	1655	845	1755	-51695	60825	1655	800	1755	-51695	71800
46	50.17	1700	920	1745	-63045	64980	1700	880	1745	-63045	77915	1700	830	1745	-63045	91955
50	50.00	1745	995	1745	-75720	85750	1745	955	1745	-75720	102400	1745	915	1745	-80240	120380

Table E-23 - 100 ft Span, Variable Wind Load.

15 psf Dead Load
20 psf Construction Load
No Ground Snow Load

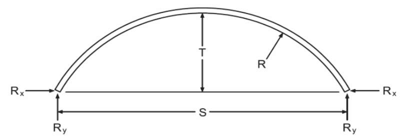

Notes:

All values normalized to C_D = 1.0.
Use ASD design procedure only.

Wind Load

K_{zt} = 1.0
K_d = 0.85

Rise [T] (ft)	Radius [R] (ft)	Basic Wind Speed [V]														
		150 mph					160 mph					170 mph				
		R_y lbs	R_x lbs	F_a lbs	M^- in-lb	M^+ in-lb	R_y lbs	R_x lbs	F_a lbs	M^- in-lb	M^+ in-lb	R_y lbs	R_x lbs	F_a lbs	M^- in-lb	M^+ in-lb
10	130.00	1420	3460	3725	-6030	7510	1420	3460	3725	-6930	7510	1420	3460	3725	-7885	8340
14	96.29	1435	2490	2855	-6040	7165	1435	2490	2855	-6805	8210	1435	2490	2855	-7620	9320
18	78.44	1455	1940	2400	-8425	8590	1455	1940	2400	-8895	9490	1455	1940	2400	-9395	10850
22	67.82	1475	1585	2140	-12765	22270	1475	1585	2140	-13005	25595	1475	1585	2140	-14825	29135
26	61.08	1505	1340	1980	-18390	29465	1505	1340	1980	-18390	33855	1505	1340	1980	-20680	38525
30	56.67	1535	1155	1880	-25020	35825	1535	1155	1880	-25020	41230	1535	1155	1880	-25160	46985
34	53.76	1575	1015	1820	-32740	47430	1575	1015	1820	-32740	54605	1575	1015	1820	-33250	62240
38	51.89	1610	895	1780	-41610	64625	1610	895	1780	-41885	74370	1610	895	1780	-47530	84745
42	50.76	1655	800	1755	-51695	83590	1655	800	1755	-54595	96190	1655	800	1755	-61940	109605
46	50.17	1700	780	1745	-63045	107030	1700	730	1745	-70415	123145	1700	735	1745	-79860	140300
50	50.00	1745	875	1745	-85105	139690	1745	830	1745	-96450	160335	1745	840	1745	-109330	182310

Rise [T] (ft)	Radius [R] (ft)	Basic Wind Speed [V]														
		180 mph					190 mph					200 mph				
		R_y lbs	R_x lbs	F_a lbs	M^- in-lb	M^+ in-lb	R_y lbs	R_x lbs	F_a lbs	M^- in-lb	M^+ in-lb	R_y lbs	R_x lbs	F_a lbs	M^- in-lb	M^+ in-lb
10	130.00	1420	3460	3725	-8900	9295	1420	3460	3725	-9975	10310	1420	3460	3725	-11110	11375
14	96.29	1435	2490	2855	-8485	10500	1435	2490	2855	-9400	11750	1435	2490	2855	-10395	13065
18	78.44	1455	1940	2400	-9930	12295	1455	1940	2400	-10490	13820	1455	1940	2400	-11120	15430
22	67.82	1475	1585	2140	-16755	32885	1475	1585	2140	-18795	36850	1475	1585	2140	-20945	41030
26	61.08	1505	1340	1980	-23360	43480	1505	1340	1980	-26195	48750	1505	1340	1980	-29180	54315
30	56.67	1535	1155	1880	-28440	53085	1535	1155	1880	-31905	59535	1535	1155	1880	-35555	66335
34	53.76	1575	1015	1820	-37575	70340	1575	1015	1820	-42145	78900	1575	1015	1820	-46965	87925
38	51.89	1610	895	1780	-53645	95745	1610	895	1780	-60130	107380	1610	895	1780	-66960	119640
42	50.76	1655	800	1755	-69730	123830	1655	825	1755	-77960	138875	1655	930	1755	-86645	154725
46	50.17	1700	840	1745	-89885	158495	1700	955	1745	-100480	177730	1700	1075	1745	-111645	198005
50	50.00	1745	960	1745	-122990	205735	1745	1085	1745	-137430	230640	1745	1215	1745	-152655	256890

Table E-24 - 110 ft Span, Variable Wind Load.

20 psf Dead Load
20 psf Construction Load
No Ground Snow Load

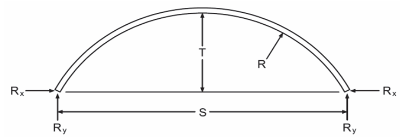

Notes:

All values normalized to C_D = 1.0.
Use ASD design procedure only.

Wind Load

K_{zt} = 1.0
K_d = 0.85

Rise [T] (ft)	Radius [R] (ft)	Basic Wind Speed [V]														
		105 mph					110 mph					115 mph				
		R_y lbs	R_x lbs	F_a lbs	M^- in-lb	M^+ in-lb	R_y lbs	R_x lbs	F_a lbs	M^- in-lb	M^+ in-lb	R_y lbs	R_x lbs	F_a lbs	M^- in-lb	M^+ in-lb
10	156.25	1780	4785	5090	-3125	9820	1780	4785	5090	-3485	9820	1780	4785	5090	-3870	9820
14	115.04	1800	3445	3865	-4725	8440	1800	3445	3865	-4915	8440	1800	3445	3865	-5120	8440
18	93.03	1825	2690	3225	-8745	10000	1825	2690	3225	-8745	10000	1825	2690	3225	-8745	10000
22	79.75	1855	2205	2850	-14060	13165	1855	2205	2850	-14060	13165	1855	2205	2850	-14060	13165
26	71.17	1890	1865	2615	-20365	17575	1890	1865	2615	-20365	17575	1890	1865	2615	-20365	17575
30	65.42	1930	1615	2465	-27785	23130	1930	1615	2465	-27785	23130	1930	1615	2465	-27785	23130
34	61.49	1970	1420	2370	-36430	29825	1970	1420	2370	-36430	29825	1970	1420	2370	-36430	29825
38	58.80	2020	1265	2310	-46375	37685	2020	1265	2310	-46375	37685	2020	1265	2310	-46375	37685
42	57.01	2070	1240	2275	-57700	46760	2070	1220	2275	-57700	46760	2070	1200	2275	-57700	46760
46	55.88	2130	1280	2260	-70485	57095	2130	1260	2260	-70485	57095	2130	1235	2260	-70485	57095
50	55.25	2185	1325	2250	-84795	68750	2185	1305	2250	-84795	68750	2185	1280	2250	-84795	68750
55	55.00	2265	1415	2260	-104925	85260	2265	1395	2260	-104925	85260	2265	1380	2260	-104925	92355

Rise [T] (ft)	Radius [R] (ft)	Basic Wind Speed [V]														
		120 mph					130 mph					140 mph				
		R_y lbs	R_x lbs	F_a lbs	M^- in-lb	M^+ in-lb	R_y lbs	R_x lbs	F_a lbs	M^- in-lb	M^+ in-lb	R_y lbs	R_x lbs	F_a lbs	M^- in-lb	M^+ in-lb
10	156.25	1780	4785	5090	-4280	9820	1780	4785	5090	-5145	9820	1780	4785	5090	-6075	9820
14	115.04	1800	3445	3865	-5330	8440	1800	3445	3865	-5810	8440	1800	3445	3865	-6420	8440
18	93.03	1825	2690	3225	-8745	10000	1825	2690	3225	-8745	10000	1825	2690	3225	-9190	10000
22	79.75	1855	2205	2850	-14060	14490	1855	2205	2850	-14060	17420	1855	2205	2850	-14060	20580
26	71.17	1890	1865	2615	-20365	18780	1890	1865	2615	-20365	22575	1890	1865	2615	-20365	26670
30	65.42	1930	1615	2465	-27785	23130	1930	1615	2465	-27785	27525	1930	1615	2465	-27785	32620
34	61.49	1970	1420	2370	-36430	29825	1970	1420	2370	-36430	32945	1970	1420	2370	-36430	39155
38	58.80	2020	1265	2310	-46375	37685	2020	1265	2310	-46375	42340	2020	1265	2310	-46375	50350
42	57.01	2070	1175	2275	-57700	46955	2070	1130	2275	-57700	56520	2070	1130	2275	-57700	67005
46	55.88	2130	1215	2260	-70485	59420	2130	1165	2260	-70485	71515	2130	1115	2260	-70485	84685
50	55.25	2185	1260	2250	-84795	74595	2185	1210	2250	-84795	89755	2185	1160	2250	-84795	106165
55	55.00	2265	1360	2260	-104925	102015	2265	1315	2260	-104925	122570	2265	1270	2260	-107365	144770

Table E-24 - 110 ft Span, Variable Wind Load.

20 psf Dead Load
20 psf Construction Load
No Ground Snow Load

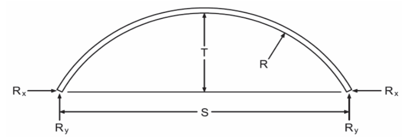

Notes:

All values normalized to C_D = 1.0.
Use ASD design procedure only.

Wind Load

K_{zt} = 1.0
K_d = 0.85

Rise [T] (ft)	Radius [R] (ft)	Basic Wind Speed [V] 150 mph					160 mph					170 mph				
		R_y lbs	R_x lbs	F_a lbs	M^- in-lb	M^+ in-lb	R_y lbs	R_x lbs	F_a lbs	M^- in-lb	M^+ in-lb	R_y lbs	R_x lbs	F_a lbs	M^- in-lb	M^+ in-lb
10	156.25	1780	4785	5090	-7080	9820	1780	4785	5090	-8150	9820	1780	4785	5090	-9310	10185
14	115.04	1800	3445	3865	-7255	8440	1800	3445	3865	-8190	9565	1800	3445	3865	-9190	10860
18	93.03	1825	2690	3225	-9740	10000	1825	2690	3225	-10325	10735	1825	2690	3225	-10945	12290
22	79.75	1855	2205	2850	-14060	23980	1855	2205	2850	-14060	27610	1855	2205	2850	-15935	31475
26	71.17	1890	1865	2615	-20365	31070	1890	1865	2615	-20365	35775	1890	1865	2615	-21825	40785
30	65.42	1930	1615	2465	-27785	38090	1930	1615	2465	-27785	43940	1930	1615	2465	-27785	50170
34	61.49	1970	1420	2370	-36430	45825	1970	1420	2370	-36430	52960	1970	1420	2370	-36430	60550
38	58.80	2020	1265	2310	-46375	58955	2020	1265	2310	-46375	68150	2020	1265	2310	-46375	77940
42	57.01	2070	1130	2275	-57700	78400	2070	1130	2275	-57700	90580	2070	1130	2275	-58650	103545
46	55.88	2130	1060	2260	-70485	99075	2130	1020	2260	-70485	114455	2130	1020	2260	-74660	130830
50	55.25	2185	1100	2250	-84795	124175	2185	1040	2250	-84795	143430	2185	980	2250	-94205	163925
55	55.00	2265	1225	2260	-113365	168610	2265	1175	2260	-119780	194100	2265	1120	2260	-133640	221230

Rise [T] (ft)	Radius [R] (ft)	Basic Wind Speed [V] 180 mph					190 mph					200 mph				
		R_y lbs	R_x lbs	F_a lbs	M^- in-lb	M^+ in-lb	R_y lbs	R_x lbs	F_a lbs	M^- in-lb	M^+ in-lb	R_y lbs	R_x lbs	F_a lbs	M^- in-lb	M^+ in-lb
10	156.25	1780	4785	5090	-10545	11310	1780	4785	5090	-11855	12505	1780	4785	5090	-13230	13760
14	115.04	1800	3445	3865	-10245	12230	1800	3445	3865	-11365	13680	1800	3445	3865	-12540	15210
18	93.03	1825	2690	3225	-11605	13945	1825	2690	3225	-12305	15695	1825	2690	3225	-13430	17535
22	79.75	1855	2205	2850	-18050	35570	1855	2205	2850	-20285	39905	1855	2205	2850	-22640	44475
26	71.17	1890	1865	2615	-24705	46095	1890	1865	2615	-27750	51710	1890	1865	2615	-30960	57650
30	65.42	1930	1615	2465	-30345	56775	1930	1615	2465	-34095	63755	1930	1615	2465	-38050	71115
34	61.49	1970	1420	2370	-36645	68600	1970	1420	2370	-41195	77110	1970	1420	2370	-45995	86080
38	58.80	2020	1265	2310	-47240	88320	2020	1265	2310	-52990	99295	2020	1265	2310	-59150	110865
42	57.01	2070	1130	2275	-66125	117295	2070	1130	2275	-74035	131830	2070	1130	2275	-82425	147150
46	55.88	2130	1020	2260	-84160	148195	2130	1020	2260	-94200	166555	2130	1020	2260	-104785	185910
50	55.25	2185	925	2250	-106165	185660	2185	995	2250	-118805	208640	2185	1125	2250	-132130	232860
55	55.00	2265	1060	2260	-150505	250005	2265	1165	2260	-168330	280425	2265	1315	2260	-187120	312490

Table E-25 - 120 ft Span, Variable Wind Load.

20 psf Dead Load
20 psf Construction Load
No Ground Snow Load

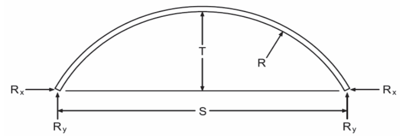

Notes:

All values normalized to C_D = 1.0.
Use ASD design procedure only.

Wind Load

K_{zt} = 1.0
K_d = 0.85

Rise [T] (ft)	Radius [R] (ft)	Basic Wind Speed [V] 105 mph					110 mph					115 mph				
		R_y lbs	R_x lbs	F_a lbs	M^- in-lb	M^+ in-lb	R_y lbs	R_x lbs	F_a lbs	M^- in-lb	M^+ in-lb	R_y lbs	R_x lbs	F_a lbs	M^- in-lb	M^+ in-lb
12	156.00	1950	4765	5130	-3920	9570	1950	4765	5130	-4325	9570	1950	4765	5130	-4755	9570
16	120.50	1965	3595	4075	-6350	9510	1965	3595	4075	-6575	9510	1965	3595	4075	-6810	9510
20	100.00	1990	2885	3475	-11080	11715	1990	2885	3475	-11080	11715	1990	2885	3475	-11080	11715
24	87.00	2020	2405	3105	-16860	15365	2020	2405	3105	-16860	15365	2020	2405	3105	-16860	15940
28	78.29	2055	2060	2870	-23655	20200	2055	2060	2870	-23655	20200	2055	2060	2870	-23655	20200
32	72.25	2095	1800	2715	-31570	26160	2095	1800	2715	-31570	26160	2095	1800	2715	-31570	26160
36	68.00	2140	1600	2610	-40695	33235	2140	1600	2610	-40695	33235	2140	1600	2610	-40695	33235
40	65.00	2185	1430	2540	-51110	41465	2185	1430	2540	-51110	41465	2185	1430	2540	-51110	41465
44	62.91	2235	1330	2495	-62885	50875	2235	1310	2495	-62885	50875	2235	1290	2495	-62885	50875
48	61.50	2290	1370	2470	-76085	61530	2290	1345	2470	-76085	61530	2290	1320	2470	-76085	61530
52	60.62	2345	1410	2460	-90775	73470	2345	1390	2460	-90775	73470	2345	1365	2460	-90775	73470
56	60.14	2405	1485	2455	-107025	86750	2405	1465	2455	-107025	86750	2405	1445	2455	-107025	91830
60	60.00	2470	1540	2465	-124890	101415	2470	1520	2465	-124890	101415	2470	1500	2465	-124890	112305

Rise [T] (ft)	Radius [R] (ft)	Basic Wind Speed [V] 120 mph					130 mph					140 mph				
		R_y lbs	R_x lbs	F_a lbs	M^- in-lb	M^+ in-lb	R_y lbs	R_x lbs	F_a lbs	M^- in-lb	M^+ in-lb	R_y lbs	R_x lbs	F_a lbs	M^- in-lb	M^+ in-lb
12	156.00	1950	4765	5130	-5205	9570	1950	4765	5130	-6165	9570	1950	4765	5130	-7200	9570
16	120.50	1965	3595	4075	-7065	9510	1965	3595	4075	-7650	9510	1965	3595	4075	-8280	9510
20	100.00	1990	2885	3475	-11080	11715	1990	2885	3475	-11080	11715	1990	2885	3475	-11425	11715
24	87.00	2020	2405	3105	-16860	17610	2020	2405	3105	-16860	21165	2020	2405	3105	-16860	25005
28	78.29	2055	2060	2870	-23655	20945	2055	2060	2870	-23655	25305	2055	2060	2870	-23655	30015
32	72.25	2095	1800	2715	-31570	26850	2095	1800	2715	-31570	32370	2095	1800	2715	-31570	38335
36	68.00	2140	1600	2610	-40695	33235	2140	1600	2610	-40695	37560	2140	1600	2610	-40695	44615
40	65.00	2185	1430	2540	-51110	41465	2185	1430	2540	-51110	47420	2185	1430	2540	-51110	56355
44	62.91	2235	1290	2495	-62885	51625	2235	1290	2495	-62885	62110	2235	1290	2495	-62885	73680
48	61.50	2290	1295	2470	-76085	64290	2290	1245	2470	-76085	77345	2290	1185	2470	-76085	91650
52	60.62	2345	1340	2460	-90775	79500	2345	1285	2460	-90775	95630	2345	1225	2460	-90775	113195
56	60.14	2405	1425	2455	-107025	101435	2405	1375	2455	-107025	121865	2405	1325	2455	-107025	143935
60	60.00	2470	1475	2465	-124890	124010	2470	1430	2465	-124890	148925	2470	1380	2465	-128675	175835

Table E-25 - 120 ft Span, Variable Wind Load.

20 psf Dead Load
20 psf Construction Load
No Ground Snow Load

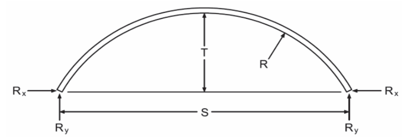

Notes:

All values normalized to C_D = 1.0.
Use ASD design procedure only.

Wind Load

K_{zt} = 1.0
K_d = 0.85

Rise [T] (ft)	Radius [R] (ft)	Basic Wind Speed [V]														
		150 mph					160 mph					170 mph				
		R_y lbs	R_x lbs	F_a lbs	M^- in-lb	M^+ in-lb	R_y lbs	R_x lbs	F_a lbs	M^- in-lb	M^+ in-lb	R_y lbs	R_x lbs	F_a lbs	M^- in-lb	M^+ in-lb
12	156.00	1950	4765	5130	-8315	9620	1950	4765	5130	-9500	10875	1950	4765	5130	-10775	12250
16	120.50	1965	3595	4075	-8955	10230	1965	3595	4075	-10005	11755	1965	3595	4075	-11165	13375
20	100.00	1990	2885	3475	-12080	11715	1990	2885	3475	-12775	13220	1990	2885	3475	-13520	15155
24	87.00	2020	2405	3105	-16860	29130	2020	2405	3105	-16890	33540	2020	2405	3105	-19295	38230
28	78.29	2055	2060	2870	-23655	35075	2055	2060	2870	-23655	40485	2055	2060	2870	-23655	46240
32	72.25	2095	1800	2715	-31570	44740	2095	1800	2715	-31570	51585	2095	1800	2715	-31570	58870
36	68.00	2140	1600	2610	-40695	52190	2140	1600	2610	-40695	60285	2140	1600	2610	-40695	68905
40	65.00	2185	1430	2540	-51110	65950	2185	1430	2540	-51110	76210	2185	1430	2540	-51110	87130
44	62.91	2235	1290	2495	-62885	86175	2235	1290	2495	-62885	99535	2235	1290	2495	-64145	113750
48	61.50	2290	1170	2470	-76085	107190	2290	1170	2470	-76085	123805	2290	1170	2470	-80355	141490
52	60.62	2345	1165	2460	-90775	132370	2345	1100	2460	-90775	152865	2345	1065	2460	-99880	174685
56	60.14	2405	1270	2455	-112110	167635	2405	1210	2455	-118235	192970	2405	1150	2455	-132050	219945
60	60.00	2470	1330	2465	-135945	204735	2470	1270	2465	-143720	235630	2470	1210	2465	-162095	268515

Rise [T] (ft)	Radius [R] (ft)	Basic Wind Speed [V]														
		180 mph					190 mph					200 mph				
		R_y lbs	R_x lbs	F_a lbs	M^- in-lb	M^+ in-lb	R_y lbs	R_x lbs	F_a lbs	M^- in-lb	M^+ in-lb	R_y lbs	R_x lbs	F_a lbs	M^- in-lb	M^+ in-lb
12	156.00	1950	4765	5130	-12140	13705	1950	4765	5130	-13585	15245	1950	4765	5130	-15110	16870
16	120.50	1965	3595	4075	-12400	15090	1965	3595	4075	-13705	16910	1965	3595	4075	-15080	18825
20	100.00	1990	2885	3475	-14305	17205	1990	2885	3475	-15140	19370	1990	2885	3475	-16285	21655
24	87.00	2020	2405	3105	-21845	43210	2020	2405	3105	-24540	48470	2020	2405	3105	-27380	54015
28	78.29	2055	2060	2870	-26365	52345	2055	2060	2870	-29630	58800	2055	2060	2870	-33070	65605
32	72.25	2095	1800	2715	-35555	66600	2095	1800	2715	-39940	74770	2095	1800	2715	-44555	83385
36	68.00	2140	1600	2610	-41660	78045	2140	1600	2610	-46825	87710	2140	1600	2610	-52270	97900
40	65.00	2185	1430	2540	-52645	98715	2185	1430	2540	-59165	110960	2185	1430	2540	-66040	123865
44	62.91	2235	1290	2495	-72320	128830	2235	1290	2495	-81070	144775	2235	1290	2495	-90425	161575
48	61.50	2290	1170	2470	-90580	160245	2290	1170	2470	-101390	180070	2290	1170	2470	-112780	200970
52	60.62	2345	1065	2460	-112560	197825	2345	1065	2460	-125965	222285	2345	1160	2460	-140095	248070
56	60.14	2405	1085	2455	-148730	248550	2405	1130	2455	-166370	278790	2405	1275	2455	-184955	310930
60	60.00	2470	1145	2465	-182530	303395	2470	1300	2465	-204135	340270	2470	1465	2465	-226905	379195

Table E-26 - 130 ft Span, Variable Wind Load.

20 psf Dead Load
20 psf Construction Load
No Ground Snow Load

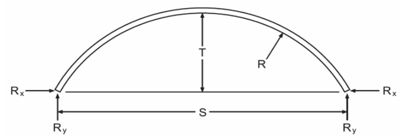

Notes:

All values normalized to C_D = 1.0.
Use ASD design procedure only.

Wind Load

K_{zt} = 1.0
K_d = 0.85

Rise [T] (ft)	Radius [R] (ft)	Basic Wind Speed [V]														
		105 mph					110 mph					115 mph				
		R_y lbs	R_x lbs	F_a lbs	M^- in-lb	M^+ in-lb	R_y lbs	R_x lbs	F_a lbs	M^- in-lb	M^+ in-lb	R_y lbs	R_x lbs	F_a lbs	M^- in-lb	M^+ in-lb
12	182.04	2105	5595	5960	-4520	10640	2105	5595	5960	-5005	10640	2105	5595	5960	-5515	10640
16	140.03	2125	4215	4695	-6600	10100	2125	4215	4695	-6870	10100	2125	4215	4695	-7150	10100
20	115.63	2145	3380	3975	-10865	12065	2145	3380	3975	-10865	12065	2145	3380	3975	-10865	12065
24	100.02	2175	2825	3530	-16655	15550	2175	2825	3530	-16655	15550	2175	2825	3530	-16655	15550
28	89.45	2205	2420	3235	-23410	20250	2205	2420	3235	-23410	20250	2205	2420	3235	-23410	20645
32	82.02	2245	2120	3035	-31245	26060	2245	2120	3035	-31245	26060	2245	2120	3035	-31245	26060
36	76.68	2285	1880	2900	-40250	32970	2285	1880	2900	-40250	32970	2285	1880	2900	-40250	32970
40	72.81	2330	1685	2805	-50495	40995	2330	1685	2805	-50495	40995	2330	1685	2805	-50495	40995
44	70.01	2375	1525	2745	-62045	50170	2375	1525	2745	-62045	50170	2375	1525	2745	-62045	50170
48	68.01	2425	1440	2700	-74965	60540	2425	1415	2700	-74965	60540	2425	1390	2700	-74965	60540
52	66.63	2480	1480	2675	-89320	72145	2480	1455	2675	-89320	72145	2480	1425	2675	-89320	72145
56	65.72	2540	1520	2665	-105170	85035	2540	1495	2665	-105170	85035	2540	1470	2665	-105170	85035
60	65.21	2600	1600	2660	-122570	99255	2600	1575	2660	-122570	99255	2600	1550	2660	-122570	106520

Rise [T] (ft)	Radius [R] (ft)	Basic Wind Speed [V]														
		120 mph					130 mph					140 mph				
		R_y lbs	R_x lbs	F_a lbs	M^- in-lb	M^+ in-lb	R_y lbs	R_x lbs	F_a lbs	M^- in-lb	M^+ in-lb	R_y lbs	R_x lbs	F_a lbs	M^- in-lb	M^+ in-lb
12	182.04	2105	5595	5960	-6045	10640	2105	5595	5960	-7180	10640	2105	5595	5960	-8405	10640
16	140.03	2125	4215	4695	-7480	10100	2125	4215	4695	-8170	10100	2125	4215	4695	-9030	10220
20	115.63	2145	3380	3975	-10865	12065	2145	3380	3975	-11390	12065	2145	3380	3975	-12120	12065
24	100.02	2175	2825	3530	-16655	15550	2175	2825	3530	-16655	15550	2175	2825	3530	-16655	15550
28	89.45	2205	2420	3235	-23410	22840	2205	2420	3235	-23410	27510	2205	2420	3235	-23410	32555
32	82.02	2245	2120	3035	-31245	28790	2245	2120	3035	-31245	34625	2245	2120	3035	-31245	40925
36	76.68	2285	1880	2900	-40250	33960	2285	1880	2900	-40250	40965	2285	1880	2900	-40250	48535
40	72.81	2330	1685	2805	-50495	40995	2330	1685	2805	-50495	47495	2330	1685	2805	-50495	56395
44	70.01	2375	1525	2745	-62045	50170	2375	1525	2745	-62045	58795	2375	1525	2745	-62045	69845
48	68.01	2425	1390	2700	-74965	62860	2425	1390	2700	-74965	75595	2425	1390	2700	-74965	89680
52	66.63	2480	1400	2675	-89320	76950	2480	1340	2675	-89320	92535	2480	1280	2675	-89320	109660
56	65.72	2540	1440	2665	-105170	93635	2540	1380	2665	-105170	112585	2540	1320	2665	-105170	133285
60	65.21	2600	1530	2660	-122570	117630	2600	1475	2660	-122570	141275	2600	1420	2660	-122570	166805

Table E-26 - 130 ft Span, Variable Wind Load.

20 psf Dead Load
20 psf Construction Load
No Ground Snow Load

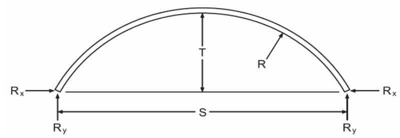

Notes:

All values normalized to C_D = 1.0.
Use ASD design procedure only.

Wind Load

K_{zt} = 1.0
K_d = 0.85

Rise [T] (ft)	Radius [R] (ft)	Basic Wind Speed [V]														
		150 mph					160 mph					170 mph				
		R_y lbs	R_x lbs	F_a lbs	M^- in-lb	M^+ in-lb	R_y lbs	R_x lbs	F_a lbs	M^- in-lb	M^+ in-lb	R_y lbs	R_x lbs	F_a lbs	M^- in-lb	M^+ in-lb
12	182.04	2105	5595	5960	-9720	11245	2105	5595	5960	-11125	12700	2105	5595	5960	-12620	14275
16	140.03	2125	4215	4695	-10205	11835	2125	4215	4695	-11500	13570	2125	4215	4695	-12880	15410
20	115.63	2145	3380	3975	-12900	13130	2145	3380	3975	-13735	15170	2145	3380	3975	-14625	17345
24	100.02	2175	2825	3530	-16655	15550	2175	2825	3530	-17370	16855	2175	2825	3530	-18235	19390
28	89.45	2205	2420	3235	-23410	37975	2205	2420	3235	-23410	43770	2205	2420	3235	-25110	49940
32	82.02	2245	2120	3035	-31245	47690	2245	2120	3035	-31245	54925	2245	2120	3035	-33400	62625
36	76.68	2285	1880	2900	-40250	56660	2285	1880	2900	-40250	65345	2285	1880	2900	-40250	74590
40	72.81	2330	1685	2805	-50495	65960	2330	1685	2805	-50495	76180	2330	1685	2805	-50495	87060
44	70.01	2375	1525	2745	-62045	81715	2375	1525	2745	-62045	94405	2375	1525	2745	-62045	107915
48	68.01	2425	1390	2700	-74965	104850	2425	1390	2700	-74965	121070	2425	1390	2700	-77970	138335
52	66.63	2480	1270	2675	-89320	128210	2480	1270	2675	-89320	148045	2480	1270	2675	-95975	169150
56	65.72	2540	1250	2665	-105170	155810	2540	1175	2665	-105170	179890	2540	1165	2665	-117340	205525
60	65.21	2600	1360	2660	-128485	194230	2600	1295	2660	-135525	223545	2600	1225	2660	-152725	254755

Rise [T] (ft)	Radius [R] (ft)	Basic Wind Speed [V]														
		180 mph					190 mph					200 mph				
		R_y lbs	R_x lbs	F_a lbs	M^- in-lb	M^+ in-lb	R_y lbs	R_x lbs	F_a lbs	M^- in-lb	M^+ in-lb	R_y lbs	R_x lbs	F_a lbs	M^- in-lb	M^+ in-lb
12	182.04	2105	5595	5960	-14230	15950	2105	5595	5960	-15940	17715	2105	5595	5960	-17735	19580
16	140.03	2125	4215	4695	-14340	17365	2125	4215	4695	-15880	19430	2125	4215	4695	-17510	21610
20	115.63	2145	3380	3975	-15610	19650	2145	3380	3975	-17130	22090	2145	3380	3975	-18735	24660
24	100.02	2175	2825	3530	-19150	22075	2175	2825	3530	-20120	24910	2175	2825	3530	-21140	27905
28	89.45	2205	2420	3235	-28425	56480	2205	2420	3235	-31925	63395	2205	2420	3235	-35615	70680
32	82.02	2245	2120	3035	-37785	70795	2245	2120	3035	-42420	79425	2245	2120	3035	-47310	88530
36	76.68	2285	1880	2900	-44990	84400	2285	1880	2900	-50530	94765	2285	1880	2900	-56370	105695
40	72.81	2330	1685	2805	-52570	98600	2330	1685	2805	-59075	110800	2330	1685	2805	-65930	123660
44	70.01	2375	1525	2745	-65145	122240	2375	1525	2745	-73200	137385	2375	1525	2745	-81695	153350
48	68.01	2425	1390	2700	-87895	156650	2425	1390	2700	-98515	176010	2425	1390	2700	-109865	196415
52	66.63	2480	1270	2675	-108175	191540	2480	1270	2675	-121070	215210	2480	1270	2675	-134660	240160
56	65.72	2540	1165	2665	-132230	232710	2540	1165	2665	-147970	261450	2540	1270	2665	-164560	291745
60	65.21	2600	1155	2660	-172010	287855	2600	1220	2660	-192395	322845	2600	1380	2660	-213885	360145

Table E-27 - 140 ft Span, Variable Wind Load.

20 psf Dead Load
20 psf Construction Load
No Ground Snow Load

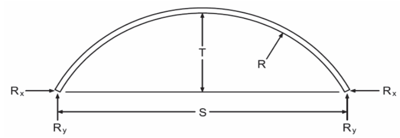

Notes:

All values normalized to C_D = 1.0.
Use ASD design procedure only.

Wind Load

K_{zt} = 1.0
K_d = 0.85

Rise [T] (ft)	Radius [R] (ft)	Basic Wind Speed [V]														
		105 mph					110 mph					115 mph				
		R_y lbs	R_x lbs	F_a lbs	M^- in-lb	M^+ in-lb	R_y lbs	R_x lbs	F_a lbs	M^- in-lb	M^+ in-lb	R_y lbs	R_x lbs	F_a lbs	M^- in-lb	M^+ in-lb
12	210.17	2265	6485	6850	-5175	11800	2265	6485	6850	-5745	11800	2265	6485	6850	-6340	11800
16	161.13	2280	4890	5370	-6880	10745	2280	4890	5370	-7195	10745	2280	4890	5370	-7550	10745
20	132.50	2300	3920	4515	-10645	12450	2300	3920	4515	-10645	12450	2300	3920	4515	-10860	12450
24	114.08	2330	3275	3980	-16455	15775	2330	3275	3980	-16455	15775	2330	3275	3980	-16455	15775
28	101.50	2360	2810	3625	-23190	20340	2360	2810	3625	-23190	20340	2360	2810	3625	-23190	22525
32	92.56	2390	2455	3380	-30970	26020	2390	2455	3380	-30970	26020	2390	2455	3380	-30970	26100
36	86.06	2430	2180	3210	-39875	32785	2430	2180	3210	-39875	32785	2430	2180	3210	-39875	32785
40	81.25	2470	1960	3090	-49975	40640	2470	1960	3090	-49975	40640	2470	1960	3090	-49975	40640
44	77.68	2515	1775	3005	-61340	49610	2515	1775	3005	-61340	49610	2515	1775	3005	-61340	49610
48	75.04	2565	1620	2945	-74030	59730	2565	1620	2945	-74030	59730	2565	1620	2945	-74030	59730
52	73.12	2615	1550	2905	-88105	71050	2615	1520	2905	-88105	71050	2615	1495	2905	-88105	71050
56	71.75	2670	1590	2880	-103615	83605	2670	1560	2880	-103615	83605	2670	1530	2880	-103615	83605
60	70.83	2730	1630	2870	-120620	97445	2730	1600	2870	-120620	97445	2730	1575	2870	-120620	98720

Rise [T] (ft)	Radius [R] (ft)	Basic Wind Speed [V]														
		120 mph					130 mph					140 mph				
		R_y lbs	R_x lbs	F_a lbs	M^- in-lb	M^+ in-lb	R_y lbs	R_x lbs	F_a lbs	M^- in-lb	M^+ in-lb	R_y lbs	R_x lbs	F_a lbs	M^- in-lb	M^+ in-lb
12	210.17	2265	6485	6850	-6960	11800	2265	6485	6850	-8285	11800	2265	6485	6850	-9715	11800
16	161.13	2280	4890	5370	-7935	10745	2280	4890	5370	-8955	10745	2280	4890	5370	-10215	11735
20	132.50	2300	3920	4515	-11235	12450	2300	3920	4515	-12030	12450	2300	3920	4515	-12885	12840
24	114.08	2330	3275	3980	-16455	15775	2330	3275	3980	-16455	15775	2330	3275	3980	-16580	15775
28	101.50	2360	2810	3625	-23190	24880	2360	2810	3625	-23190	29890	2360	2810	3625	-23190	35305
32	92.56	2390	2455	3380	-30970	28905	2390	2455	3380	-30970	34875	2390	2455	3380	-30970	41320
36	86.06	2430	2180	3210	-39875	36075	2430	2180	3210	-39875	43415	2430	2180	3210	-39875	51350
40	81.25	2470	1960	3090	-49975	42065	2470	1960	3090	-49975	50755	2470	1960	3090	-49975	60145
44	77.68	2515	1775	3005	-61340	49610	2515	1775	3005	-61340	58765	2515	1775	3005	-61340	69765
48	75.04	2565	1620	2945	-74030	59730	2565	1620	2945	-74030	71555	2565	1620	2945	-74030	84975
52	73.12	2615	1485	2905	-88105	75340	2615	1485	2905	-88105	90560	2615	1485	2905	-88105	107435
56	71.75	2670	1500	2880	-103615	90885	2670	1440	2880	-103615	109245	2670	1370	2880	-103615	129470
60	70.83	2730	1540	2870	-120620	109070	2730	1480	2870	-120620	131085	2730	1410	2870	-120620	155210

Table E-27 - 140 ft Span, Variable Wind Load.

20 psf Dead Load
20 psf Construction Load
No Ground Snow Load

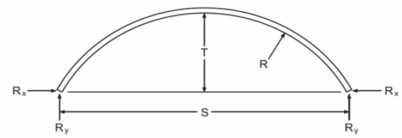

Notes:

All values normalized to C_D = 1.0.
Use ASD design procedure only.

Wind Load

K_{zt} = 1.0
K_d = 0.85

Rise [T] (ft)	Radius [R] (ft)	Basic Wind Speed [V] 150 mph R_y lbs	150 mph R_x lbs	150 mph F_a lbs	150 mph M^- in-lb	150 mph M^+ in-lb	160 mph R_y lbs	160 mph R_x lbs	160 mph F_a lbs	160 mph M^- in-lb	160 mph M^+ in-lb	170 mph R_y lbs	170 mph R_x lbs	170 mph F_a lbs	170 mph M^- in-lb	170 mph M^+ in-lb
12	210.17	2265	6485	6850	-11245	13000	2265	6485	6850	-12890	14660	2265	6485	6850	-14635	16455
16	161.13	2280	4890	5370	-11620	13560	2280	4890	5370	-13135	15520	2280	4890	5370	-14745	17600
20	132.50	2300	3920	4515	-13805	14975	2300	3920	4515	-14790	17265	2300	3920	4515	-16070	19700
24	114.08	2330	3275	3980	-17480	16430	2330	3275	3980	-18440	19070	2330	3275	3980	-19465	21880
28	101.50	2360	2810	3625	-23190	41115	2360	2810	3625	-23750	47330	2360	2810	3625	-27100	53945
32	92.56	2390	2455	3380	-30970	48240	2390	2455	3380	-30970	55640	2390	2455	3380	-31870	63520
36	86.06	2430	2180	3210	-39875	59865	2430	2180	3210	-39875	68970	2430	2180	3210	-41895	78665
40	81.25	2470	1960	3090	-49975	70225	2470	1960	3090	-49975	81005	2470	1960	3090	-49975	92480
44	77.68	2515	1775	3005	-61340	81575	2515	1775	3005	-61340	94200	2515	1775	3005	-61340	107645
48	75.04	2565	1620	2945	-74030	99390	2565	1620	2945	-74030	114800	2565	1620	2945	-74030	131200
52	73.12	2615	1485	2905	-88105	125575	2615	1485	2905	-88105	144965	2615	1485	2905	-93300	165605
56	71.75	2670	1365	2880	-103615	151325	2670	1365	2880	-103615	174690	2670	1365	2880	-113130	199560
60	70.83	2730	1335	2870	-120620	181390	2730	1260	2870	-120620	209370	2730	1260	2870	-136375	239160

Rise [T] (ft)	Radius [R] (ft)	Basic Wind Speed [V] 180 mph R_y lbs	180 mph R_x lbs	180 mph F_a lbs	180 mph M^- in-lb	180 mph M^+ in-lb	190 mph R_y lbs	190 mph R_x lbs	190 mph F_a lbs	190 mph M^- in-lb	190 mph M^+ in-lb	200 mph R_y lbs	200 mph R_x lbs	200 mph F_a lbs	200 mph M^- in-lb	200 mph M^+ in-lb
12	210.17	2265	6485	6850	-16505	18360	2265	6485	6850	-18490	20375	2265	6485	6850	-20585	22495
16	161.13	2280	4890	5370	-16450	19810	2280	4890	5370	-18255	22140	2280	4890	5370	-20160	24600
20	132.50	2300	3920	4515	-17755	22280	2300	3920	4515	-19535	25010	2300	3920	4515	-21410	27890
24	114.08	2330	3275	3980	-20550	24855	2330	3275	3980	-21695	28005	2330	3275	3980	-22975	31325
28	101.50	2360	2810	3625	-30660	60960	2360	2810	3625	-34420	68375	2360	2810	3625	-38380	76190
32	92.56	2390	2455	3380	-36070	71875	2390	2455	3380	-40510	80705	2390	2455	3380	-45195	90015
36	86.06	2430	2180	3210	-47395	88945	2430	2180	3210	-53210	99810	2430	2180	3210	-59335	111270
40	81.25	2470	1960	3090	-55730	104650	2470	1960	3090	-62590	117510	2470	1960	3090	-69820	131070
44	77.68	2515	1775	3005	-64935	121900	2515	1775	3005	-72955	136970	2515	1775	3005	-81410	152855
48	75.04	2565	1620	2945	-79160	148600	2565	1620	2945	-88925	166990	2565	1620	2945	-99225	186375
52	73.12	2615	1485	2905	-105165	187495	2615	1485	2905	-117855	210640	2615	1485	2905	-131420	235035
56	71.75	2670	1365	2880	-127495	225935	2670	1365	2880	-142680	253820	2670	1365	2880	-158690	283210
60	70.83	2730	1260	2870	-153665	270755	2730	1260	2870	-171940	304155	2730	1380	2870	-191210	339355

Table E-28 - 150 ft Span, Variable Wind Load.

20 psf Dead Load
20 psf Construction Load
No Ground Snow Load

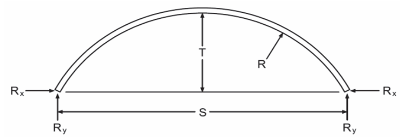

Notes:

All values normalized to C_D = 1.0.
Use ASD design procedure only.

Wind Load

K_{zt} = 1.0
K_d = 0.85

Rise [T] (ft)	Radius [R] (ft)	Basic Wind Speed [V]														
		105 mph					110 mph					115 mph				
		R_y lbs	R_x lbs	F_a lbs	M^- in-lb	M^+ in-lb	R_y lbs	R_x lbs	F_a lbs	M^- in-lb	M^+ in-lb	R_y lbs	R_x lbs	F_a lbs	M^- in-lb	M^+ in-lb
14	207.89	2430	6400	6820	-6150	11700	2430	6400	6820	-6775	11700	2430	6400	6820	-7430	11700
18	165.25	2450	4995	5535	-8840	11895	2450	4995	5535	-9225	11895	2450	4995	5535	-9650	11895
22	138.84	2470	4095	4750	-13240	14275	2470	4095	4750	-13240	14275	2470	4095	4750	-13240	14275
26	121.17	2495	3470	4235	-19505	18105	2495	3470	4235	-19505	18105	2495	3470	4235	-19505	18105
30	108.75	2525	3010	3885	-26720	23115	2525	3010	3885	-26720	23670	2525	3010	3885	-26720	26300
34	99.72	2560	2655	3640	-34990	29215	2560	2655	3640	-34990	29215	2560	2655	3640	-34990	30190
38	93.01	2600	2375	3460	-44395	36380	2600	2375	3460	-44395	36380	2600	2375	3460	-44395	37330
42	87.96	2640	2145	3335	-54985	44625	2640	2145	3335	-54985	44625	2640	2145	3335	-54985	44625
46	84.14	2685	1950	3240	-66835	53975	2685	1950	3240	-66835	53975	2685	1950	3240	-66835	53975
50	81.25	2730	1790	3175	-79990	64460	2730	1790	3175	-79990	64460	2730	1790	3175	-79990	64460
54	79.08	2780	1645	3130	-94515	76125	2780	1645	3130	-94515	76125	2780	1645	3130	-94515	76125
58	77.49	2835	1675	3100	-110450	89005	2835	1645	3100	-110450	89005	2835	1615	3100	-110450	89005
60	76.88	2860	1695	3090	-118970	95915	2860	1665	3090	-118970	95915	2860	1635	3090	-118970	96055

Rise [T] (ft)	Radius [R] (ft)	Basic Wind Speed [V]														
		120 mph					130 mph					140 mph				
		R_y lbs	R_x lbs	F_a lbs	M^- in-lb	M^+ in-lb	R_y lbs	R_x lbs	F_a lbs	M^- in-lb	M^+ in-lb	R_y lbs	R_x lbs	F_a lbs	M^- in-lb	M^+ in-lb
14	207.89	2430	6400	6820	-8110	11700	2430	6400	6820	-9560	11700	2430	6400	6820	-11125	13000
18	165.25	2450	4995	5535	-10085	11895	2450	4995	5535	-11020	11895	2450	4995	5535	-12235	13960
22	138.84	2470	4095	4750	-13620	14275	2470	4095	4750	-14535	14275	2470	4095	4750	-15525	15175
26	121.17	2495	3470	4235	-19505	18105	2495	3470	4235	-19505	18105	2495	3470	4235	-19505	18105
30	108.75	2525	3010	3885	-26720	29045	2525	3010	3885	-26720	34885	2525	3010	3885	-26720	41195
34	99.72	2560	2655	3640	-34990	33420	2560	2655	3640	-34990	40300	2560	2655	3640	-34990	47725
38	93.01	2600	2375	3460	-44395	41265	2600	2375	3460	-44395	49630	2600	2375	3460	-44395	58660
42	87.96	2640	2145	3335	-54985	47640	2640	2145	3335	-54985	57435	2640	2145	3335	-54985	68010
46	84.14	2685	1950	3240	-66835	53975	2685	1950	3240	-66835	65030	2685	1950	3240	-66835	77165
50	81.25	2730	1790	3175	-79990	64750	2730	1790	3175	-79990	78305	2730	1790	3175	-79990	92950
54	79.08	2780	1645	3130	-94515	81470	2780	1645	3130	-94515	97970	2780	1645	3130	-94515	116195
58	77.49	2835	1585	3100	-110450	97280	2835	1520	3100	-110450	116890	2835	1520	3100	-110450	138610
60	76.88	2860	1605	3090	-118970	106105	2860	1535	3090	-118970	127495	2860	1465	3090	-118970	151110

Table E-28 - 150 ft Span, Variable Wind Load.

20 psf Dead Load
20 psf Construction Load
No Ground Snow Load

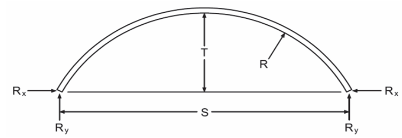

Notes:

All values normalized to C_D = 1.0.
Use ASD design procedure only.

Wind Load

K_{zt} = 1.0
K_d = 0.85

Rise [T] (ft)	Radius [R] (ft)	Basic Wind Speed [V]														
		150 mph					160 mph					170 mph				
		R_y lbs	R_x lbs	F_a lbs	M^- in-lb	M^+ in-lb	R_y lbs	R_x lbs	F_a lbs	M^- in-lb	M^+ in-lb	R_y lbs	R_x lbs	F_a lbs	M^- in-lb	M^+ in-lb
14	207.89	2430	6400	6820	-12805	14865	2430	6400	6820	-14600	16880	2430	6400	6820	-16515	19055
18	165.25	2450	4995	5535	-13850	16180	2450	4995	5535	-15585	18550	2450	4995	5535	-17435	21075
22	138.84	2470	4095	4750	-16585	17730	2470	4095	4750	-17720	20460	2470	4095	4750	-18930	23365
26	121.17	2495	3470	4235	-20545	19330	2495	3470	4235	-21660	22440	2495	3470	4235	-22840	25750
30	108.75	2525	3010	3885	-26720	47970	2525	3010	3885	-27665	55215	2525	3010	3885	-31560	62925
34	99.72	2560	2655	3640	-34990	55700	2560	2655	3640	-34990	64225	2560	2655	3640	-36730	73300
38	93.01	2600	2375	3460	-44395	68365	2600	2375	3460	-44395	78735	2600	2375	3460	-47785	89780
42	87.96	2640	2145	3335	-54985	79375	2640	2145	3335	-54985	91515	2640	2145	3335	-55575	104445
46	84.14	2685	1950	3240	-66835	90195	2685	1950	3240	-66835	104125	2685	1950	3240	-66835	118955
50	81.25	2730	1790	3175	-79990	108680	2730	1790	3175	-79990	125490	2730	1790	3175	-79990	143385
54	79.08	2780	1645	3130	-94515	135770	2780	1645	3130	-94515	156700	2780	1645	3130	-100490	178975
58	77.49	2835	1520	3100	-110450	161965	2835	1520	3100	-110450	186930	2835	1520	3100	-120595	213505
60	76.88	2860	1465	3090	-118970	176570	2860	1465	3090	-118970	203785	2860	1465	3090	-131845	232755

Rise [T] (ft)	Radius [R] (ft)	Basic Wind Speed [V]														
		180 mph					190 mph					200 mph				
		R_y lbs	R_x lbs	F_a lbs	M^- in-lb	M^+ in-lb	R_y lbs	R_x lbs	F_a lbs	M^- in-lb	M^+ in-lb	R_y lbs	R_x lbs	F_a lbs	M^- in-lb	M^+ in-lb
14	207.89	2430	6400	6820	-18545	21360	2430	6400	6820	-20720	23800	2430	6400	6820	-23010	26370
18	165.25	2450	4995	5535	-19390	23755	2450	4995	5535	-21465	26585	2450	4995	5535	-23650	29570
22	138.84	2470	4095	4750	-20820	26445	2470	4095	4750	-22875	29700	2470	4095	4750	-25040	33135
26	121.17	2495	3470	4235	-24095	29265	2495	3470	4235	-25420	32975	2495	3470	4235	-26910	36890
30	108.75	2525	3010	3885	-35690	71100	2525	3010	3885	-40060	79750	2525	3010	3885	-44660	88860
34	99.72	2560	2655	3640	-41560	82925	2560	2655	3640	-46665	93105	2560	2655	3640	-52050	103830
38	93.01	2600	2375	3460	-54040	101490	2600	2375	3460	-60655	113865	2600	2375	3460	-67625	126915
42	87.96	2640	2145	3335	-62885	118155	2640	2145	3335	-70605	132650	2640	2145	3335	-78750	147930
46	84.14	2685	1950	3240	-71710	134680	2685	1950	3240	-80555	151305	2685	1950	3240	-89880	168830
50	81.25	2730	1790	3175	-86440	162370	2730	1790	3175	-97100	182435	2730	1790	3175	-108335	203585
54	79.08	2780	1645	3130	-113370	202600	2780	1645	3130	-127250	227580	2780	1645	3130	-141880	253905
58	77.49	2835	1520	3100	-135910	241695	2835	1520	3100	-152095	271490	2835	1520	3100	-169385	302900
60	76.88	2860	1465	3090	-148575	263475	2860	1465	3090	-166260	295960	2860	1465	3090	-184900	330195

Appendix F: Connection Tables

Appendix F displays tables showing design connection strength values of bolts for varying connection skew angles. Linear interpolation is allowed to find values for skews between those shown.

Table F-1 - 19° Skew Angle Lamella Shear Connection Strength [Z] (lbs/bolt)								
Wood Specific Gravity [G]	Bolt Diameter							
	1/4"	5/16"	3/8"	1/2"	5/8"	3/4"	7/8"	1"
0.31	135	165	210	300	335	365	395	425
0.35	150	180	230	355	400	435	470	505
0.36	155	185	235	370	415	455	490	525
0.37	155	190	240	385	430	475	510	545
0.38	160	190	245	400	450	490	530	570
0.39	165	195	250	410	465	510	550	590
0.40	165	200	255	420	485	530	575	615
0.41	170	200	255	430	500	550	595	635
0.42	170	205	260	435	520	570	615	660
0.43	175	210	265	445	535	590	635	680
0.44	180	215	270	450	555	610	660	705
0.45	180	215	275	460	575	630	680	725
0.46	185	220	280	465	595	650	700	750
0.47	185	225	285	470	610	670	725	775
0.48	190	225	290	480	630	690	745	800
0.49	190	230	295	485	650	710	770	825
0.50	195	235	300	495	670	735	795	850
0.51	200	240	300	500	690	755	815	870
0.52	200	240	305	510	710	775	840	895
0.53	205	245	310	515	730	800	865	920
0.54	205	250	315	525	750	820	885	950
0.55	210	250	320	530	770	845	910	975
0.56	210	255	325	535	790	865	935	1000
0.57	215	260	330	545	805	890	960	1025
0.58	220	260	330	550	815	910	985	1050
0.67	240	290	370	610	905	1125	1215	1295
0.68	245	295	375	620	915	1145	1240	1325
0.71	250	305	385	640	945	1220	1320	1410
0.73	260	310	390	650	965	1270	1375	1470

Table F-2 - 20° Skew Angle Lamella Shear Connection Strength [Z] (lbs/bolt)								
Wood Specific Gravity [G]	Bolt Diameter							
	1/4"	5/16"	3/8"	1/2"	5/8"	3/4"	7/8"	1"
0.31	135	165	210	305	345	375	405	435
0.35	150	180	230	365	410	450	485	520
0.36	155	185	235	380	425	470	505	540
0.37	155	190	240	395	445	485	525	565
0.38	160	190	245	405	460	505	545	585
0.39	165	195	250	410	480	525	570	605
0.40	165	200	255	420	500	545	590	630
0.41	170	200	255	430	515	565	610	655
0.42	170	205	260	435	535	585	635	675
0.43	175	210	265	445	555	605	655	700
0.44	180	215	270	450	570	625	675	725
0.45	180	215	275	460	590	645	700	750
0.46	185	220	280	465	610	670	720	770
0.47	185	225	285	470	630	690	745	795
0.48	190	225	290	480	650	710	770	820
0.49	190	230	295	485	670	735	790	845
0.50	195	235	300	495	690	755	815	870
0.51	200	240	300	500	710	775	840	895
0.52	200	240	305	510	730	800	865	925
0.53	205	245	310	515	750	820	890	950
0.54	205	250	315	525	770	845	910	975
0.55	210	250	320	530	785	865	935	1000
0.56	210	255	325	535	795	890	960	1030
0.57	215	260	330	545	805	915	985	1055
0.58	220	260	330	550	815	935	1010	1080
0.67	240	290	370	610	905	1155	1250	1335
0.68	245	295	375	620	915	1180	1275	1365
0.71	250	305	385	640	945	1255	1355	1450
0.73	260	310	390	650	965	1310	1415	1510

Table F-3 - 21° Skew Angle
Lamella Shear Connection Strength [Z] (lbs/bolt)

Wood Specific Gravity [G]	Bolt Diameter							
	1/4"	5/16"	3/8"	1/2"	5/8"	3/4"	7/8"	1"
0.31	135	165	210	315	355	390	420	450
0.35	150	180	230	375	420	465	500	535
0.36	155	185	235	390	440	480	520	555
0.37	155	190	240	395	460	500	540	580
0.38	160	190	245	405	475	520	565	605
0.39	165	195	250	410	495	540	585	625
0.40	165	200	255	420	515	560	610	650
0.41	170	200	255	430	530	585	630	675
0.42	170	205	260	435	550	605	650	695
0.43	175	210	265	445	570	625	675	720
0.44	180	215	270	450	590	645	700	745
0.45	180	215	275	460	610	665	720	770
0.46	185	220	280	465	630	690	745	795
0.47	185	225	285	470	650	710	770	820
0.48	190	225	290	480	670	735	790	845
0.49	190	230	295	485	690	755	815	875
0.50	195	235	300	495	710	780	840	900
0.51	200	240	300	500	730	800	865	925
0.52	200	240	305	510	750	825	890	950
0.53	205	245	310	515	765	845	915	980
0.54	205	250	315	525	775	870	940	1005
0.55	210	250	320	530	785	895	965	1030
0.56	210	255	325	535	795	915	990	1060
0.57	215	260	330	545	805	940	1015	1085
0.58	220	260	330	550	815	965	1045	1115
0.67	240	290	370	610	905	1190	1285	1375
0.68	245	295	375	620	915	1215	1315	1405
0.71	250	305	385	640	945	1295	1400	1495
0.73	260	310	390	650	965	1325	1455	1560

Table F-4 - 22° Skew Angle Lamella Shear Connection Strength [Z] (lbs/bolt)								
Wood Specific Gravity [G]	Bolt Diameter							
	1/4"	5/16"	3/8"	1/2"	5/8"	3/4"	7/8"	1"
0.31	135	165	210	325	365	400	435	465
0.35	150	180	230	380	435	480	515	555
0.36	155	185	235	390	455	500	540	575
0.37	155	190	240	395	475	520	560	600
0.38	160	190	245	405	490	540	585	625
0.39	165	195	250	410	510	560	605	645
0.40	165	200	255	420	530	580	630	670
0.41	170	200	255	430	550	600	650	695
0.42	170	205	260	435	570	625	675	720
0.43	175	210	265	445	590	645	695	745
0.44	180	215	270	450	610	665	720	770
0.45	180	215	275	460	630	690	745	795
0.46	185	220	280	465	650	710	770	825
0.47	185	225	285	470	670	735	795	850
0.48	190	225	290	480	690	760	820	875
0.49	190	230	295	485	710	780	845	900
0.50	195	235	300	495	730	805	870	930
0.51	200	240	300	500	740	825	895	955
0.52	200	240	305	510	755	850	920	985
0.53	205	245	310	515	765	875	945	1010
0.54	205	250	315	525	775	900	970	1040
0.55	210	250	320	530	785	925	1000	1065
0.56	210	255	325	535	795	950	1025	1095
0.57	215	260	330	545	805	975	1050	1125
0.58	220	260	330	550	815	1000	1080	1150
0.67	240	290	370	610	905	1230	1330	1420
0.68	245	295	375	620	915	1255	1360	1450
0.71	250	305	385	640	945	1300	1445	1545
0.73	260	310	390	650	965	1325	1505	1610

Table F-5 - 22.5° Skew Angle Lamella Shear Connection Strength [Z] (lbs/bolt)								
Wood Specific Gravity [G]	Bolt Diameter							
	1/4"	5/16"	3/8"	1/2"	5/8"	3/4"	7/8"	1"
0.31	135	165	210	330	370	410	440	470
0.35	150	180	230	380	445	485	525	560
0.36	155	185	235	390	465	505	550	585
0.37	155	190	240	395	480	530	570	610
0.38	160	190	245	405	500	550	595	635
0.39	165	195	250	410	520	570	615	660
0.40	165	200	255	420	540	590	640	685
0.41	170	200	255	430	560	615	660	710
0.42	170	205	260	435	580	635	685	735
0.43	175	210	265	445	600	655	710	760
0.44	180	215	270	450	620	680	735	785
0.45	180	215	275	460	640	700	760	810
0.46	185	220	280	465	660	725	785	835
0.47	185	225	285	470	680	745	810	865
0.48	190	225	290	480	705	770	835	890
0.49	190	230	295	485	720	795	860	915
0.50	195	235	300	495	730	820	885	945
0.51	200	240	300	500	740	840	910	970
0.52	200	240	305	510	755	865	935	1000
0.53	205	245	310	515	765	890	960	1030
0.54	205	250	315	525	775	915	990	1055
0.55	210	250	320	530	785	940	1015	1085
0.56	210	255	325	535	795	965	1040	1115
0.57	215	260	330	545	805	990	1070	1145
0.58	220	260	330	550	815	1015	1095	1170
0.67	240	290	370	610	905	1245	1350	1445
0.68	245	295	375	620	915	1260	1380	1475
0.71	250	305	385	640	945	1300	1470	1575
0.73	260	310	390	650	965	1325	1530	1635